# Role of Implant Stability and Local Inflammatory Responses on the Development and Progression of Infection Associated with Internal Fixation Devices

---

**Dissertation**

**zur**

**Erlangung der naturwissenschaftlichen Doktorwürde**
**(Dr. sc. nat.)**

**vorgelegt der**

**Mathematisch-naturwissenschaftlichen Fakultät**

**der**

**Universität Zürich**

**von**

**Marina Sabaté Brescó**

aus Spanien

**Promotionskommission**

Prof. Dr. med. Cezmi Akdis (Vorsitz)

Dr. Fintan T. Moriarty (Leitung der Dissertation)

PD Dr. Liam O'Mahony (Leitung der Dissertation)

Prof. Dr. Roland H. Wenger

Prof. Dr. Georgios N. Belibasakis

**Zürich, 2017**

*Als meus pares i a la meva família, per ser el meu far*
*To my parents and family, for being my lighthouse*

*A tu, Isaac, perquè aquest repte també ha estat teu*
*To Isaac, because this was also his challenge*

**Publications:**

1. **Pathogenic Mechanisms and Host Interactions in *Staphylococcus epidermidis* Device-Related Infection (Review)**
   Front Microb., 2017 Aug 2; 8:1401 (published)

2. **Influence of Fracture Stability on *Staphylococcus epidermidis* and *S. aureus* Infection in a Murine Femoral Fracture Model.**
   Eur Cell Mater., 2017 Nov 21; 34:321-340 (published)

3. **Immune Responses in a Murine Fracture Model upon Staphylococcal Infection and Role of IL-17A in Infection Clearance.**
   Manuscript in preparation to be submitted to Bone

4. **Bone Healing and Infection in a Femoral Fracture model in Histamine Receptor 2 Deficient Mice.**
   Manuscript in preparation

5. **Subcutaneous Pre-exposure to *S. epidermidis* does not Influence Subsequent Infection Rate in a Murine Fracture-related Infection Model.**
   Manuscript in preparation

# Table of Contents

# 1. Common abbreviations

| | |
|---|---|
| AAALAC | Association for Assessment and Accreditation for Laboratory Animal Care |
| AMP | Antimicrobial Peptide |
| AO | Arbeitsgemeinschaft für Osteosynthesefragen / Association for the Study of Internal Fixation |
| APC | Antigen Presenting Cell |
| BA | Blood Agar |
| BMP | Bone Morphogenetic Protein |
| CFU | Colony Forming Unit |
| CoNS | Coagulase-Negative Staphylococci |
| DC | Dendritic Cell |
| DNA | Deoxyribonucleic Acid |
| DRI | Device-Related Infection |
| ECM | Extracellular Matrix |
| FRI | Fracture-Related Infection |
| G-CSF | Granulocyte Colony-Stimulating Factor |
| GE | Giemsa/Eosin |
| H(1/2/3/4)R | Histamine 1/2/3/4 Receptor |
| HIF | Hypoxia Inducible Factor |
| HSC | Hematopoietic Stem Cell |
| IFN-γ | Interferon gamma |
| Ig | Immunoglobulin |
| IL | Interleukin |
| KC | Keratinocyte Chemoattractant |
| KO | Knock-out |
| LOD | Limit of Detection |
| LTA | Lipoteichoic Acid |
| M-CSF | Macrophage Colony-Stimulating Factor |
| MCP-1 | Monocyte Chemotactic Protein 1 |
| MDSC | Myeloid-Derived Suppressor Cell |
| MMP | Matrix Metalloproteinase |
| MPO | Myeloperoxidase |
| MSC | Mesenchymal Stem Cell |
| ODRI | Orthopaedic Device-Related Infection |

| | |
|---|---|
| PBS | Phosphate Buffered Saline |
| PCR | Polymerase Chain Reaction |
| PDG | Peptidoglycan |
| PJI | Peri-prosthetic Joint Infection |
| PMA | Phorbol 12-myristate 13-acetate |
| (P)MMA | (Poly)methylmetacrylate |
| PMN | Polymorphonuclear cells |
| PRR | Pattern-Recognition Receptor |
| PSM | Phenol Soluble Modulin |
| RAPD | Random Amplification of Polymorphic DNA |
| RNA | Ribonucleic Acid |
| SD | Standard Deviation |
| SE | Scanning Electron |
| SEM | Standard Error of the Mean |
| SPF | Specific Pathogen Free |
| TGF | Transforming Growth Factor |
| Th | T helper cell |
| TLR | Toll-Like Receptor |
| TNF-α | Tumour Necrosis Factor alpha |
| Treg | T regulatory cell |
| TSA | Tryptone Soy Agar |
| TSB | Tryptone Soy Broth |
| UV | Ultraviolet |
| WT | Wild-type |

# 2. Summary

The subject matter of the present thesis is fracture-related infections (FRI), which represent one of the most common and challenging complications in orthopaedic trauma surgery. These infections delay fracture healing, can result in permanent loss of function or even amputation of the affected limb, and are associated with significant socio-economic costs. The leading etiologic agents for such infections are *Staphylococcus aureus* and *S. epidermidis*, which account for 50-75% of cases. *S. epidermidis* is responsible of 20-30% of these infections, increasing to 50% in late developing infections. Despite the clear clinical importance, the study of *S. epidermidis* has lagged behind that of *S. aureus*, with comparatively fewer experimental studies described in the literature.

In the first part of the thesis, a new *S. epidermidis* fracture-related infection (FRI) model was established and characterized. The model was established using the MouseFix$^{TM}$ system, a standardized internal fixator system for mice. After successfully establishing this infection model, a follow-up study was performed in order to investigate the role of fracture stability in the development and progression of FRI. The working hypothesis at the start of this thesis was that unstable fractures result in a higher infection incidence. The MouseFix$^{TM}$ system is available with two types of implants that provide either mechanically stable or unstable fracture fixation and so, it served as an ideal system with which to test this hypothesis. This work was performed with both *S. epidermidis* and *S. aureus* and in two mouse strains (C57BL/6 and BALB/c). The study showed that C57BL/6 mice with rigid implants (stable fixation) cleared *S. epidermidis* infection at a higher rate compared to mice with flexible implants, thus providing evidence that stability can have an influence on infection progression. This finding, however, was not repeated for BALB/c mice, for which no differences were observed. The fact that the stability effect was dependent on the mouse strain used, highlights the role of host factors on infection progression. This then prompted the deeper investigation of immune responses in the model. We observed that instability was often associated with a higher tissue inflammation (e.g. higher mRNA levels of interleukin (IL)-33 or IL-6), and the combination of instability plus infection with *S. epidermidis* significantly increased such markers. Due to the fact that infection with *S. aureus* resulted in rapid and extensive osteolysis, we were unable to maintain stability in these animals, so the hypothesis could not be reliably tested in this model for *S. aureus*. We were able, however, to compare the immune responses to *S. epidermidis* and *S. aureus* infection, with significantly higher secretion of pro-inflammatory cytokines (IL-6 or tumour necrosis factor (TNF)-α) and increased cell recruitment in the popliteal lymph node and spleen of mice infected with *S. aureus*.

In subsequent studies, we used our model of *S. epidermidis* FRI to test different hypotheses arising from these initial observations. The first such study involved investigating the role of IL-17A on FRI. We initially found that IL-17A mRNA expression and protein secretion from local cells was increased in experimental mice after inoculation with *S. epidermidis*. A follow-up study was then performed in IL-17A knock-out (KO) mice in an attempt to further elucidate the role of this cytokine in the development and progression of infection. Consistent with our first observations, we observed that IL-17A KO mice showed a reduced ability to clear infection, although differences did not reach statistical significance. In summary, these findings suggest an important role for IL-17A in FRI, although additional compensatory mechanisms may exist that play a similar role in KO mice. In our initial studies, we also found that histamine 2 receptor ($H_2R$) mRNA expression was elevated in *S. epidermidis* inoculated mice and so we used $H_2R$ KO mice in an attempt to elucidate the role of this receptor in the development and progression of infection. Although differences were observed in cytokine and antibody production levels, these did not translate into different bacterial clearance rates suggesting that $H_2R$ is not involved in the infection response in our model. Finally, we aimed to evaluate the impact of previous existing immunity to *S. epidermidis* in our model. Experimental animals (e.g. specific-pathogen free (SPF) mice) do not have any pre-existing immunity to *S. epidermidis*, which contrasts with the human situation where a specific humoral immunity to *S. epidermidis* is observed. After subcutaneous inoculation of non-viable whole *S. epidermidis* cells, we demonstrated that specific adaptive immunity was present, however, this did not influence the infection rate, bacterial burden, or immune responses in our model compared to saline-treated controls.

In conclusion, a *S. epidermidis* fracture-related infection mouse model was successfully established and characterized, representing one of the first models available in the literature. We provide evidence that stability is beneficial for bacterial clearance, supporting those clinical beliefs that stability should be maintained during FRI treatment. Immune responses associated to *S. epidermidis* and *S. aureus* infections were studied in this model, which depicted *S. aureus* as an agent of elevated inflammatory mediators and rapid osteolysis, whilst *S. epidermidis* was revealed to display signs of a sub-acute infection with few elevated markers of inflammation. This closely reflects clinical observations of patients with infection caused by these microorganisms. In addition, we used this model to understand the roles of IL-17A, $H_2R$ and pre-existing immunity in the infection progression, with some immune markers showing significant differences, but ultimately none of these single factors was found to be solely responsible for the development of FRI in this model.

# 3. Zusammenfassung

Das Thema der vorliegenden Doktorarbeit sind Fraktur-bezogene Infektionen, welche eine der häufigsten und herausforderndsten Komplikationen in der Trauma Chirurgie darstellen. Diese Infektionen verzögern die Knochenbruchheilung, was zu einem permanenten funktionalen Verlust oder sogar zur Amputation des betroffenen Körperglieds führen kann und mit signifikanten sozioökonomischen Kosten verbunden sind. Führende Krankheitserreger solcher Infektionen sind *Staphylococcus aureus* und *S. epidermidis*, welche für 50-75% dieser Infektionen verantwortlich sind. Alleine *S. Epidermidis* verursacht 20-30% dieser Infektionen und sogar 50% der Spätinfektionen. Studien an *S. epidermidis* hinken trotz hoher Prävalenz und klinischen Bedeutung hinter jenen von *S. aureus* her. Zudem sind in der Literatur nur wenige etablierte Tiermodelle beschrieben.

In der vorliegenden Doktorarbeit wurde ein neues *S. epidermidis* Fraktur-bezogenes Infektionsmodell etabliert und charakterisiert. Für das Tiermodell wurde das "MouseFix$^{TM}$"-System verwendet, ein standarisiertes internes Fixateur-System für Mäuse. Es stehen zwei verschiedene Implantate zur Verfügung, welche unterschiedliche mechanische Eigenschaften (stabil und unstabil) haben. Nachdem mit diesem Infektionsmodell eine fortschreitende subklinische Infektion nachgewiesen und etabliert werden könnte, wurde anschliessend eine Studie durchgeführt, um den Einfluss der Frakturstabilität auf die Entwicklung und Fortschreitung der Infektion zu untersuchen. Diese Arbeit wurde mit *S. epidermidis* und *S. aureus* in Mäusen der Stämme C57BL/6 und BALB/c durchgeführt. Die Studie zeigte, dass C57BL/6 Mäuse mit "rigid" Implantaten (stabile Fixierung) eine *S. epidermidis* Infektion besser eliminierten als Mäuse mit "flexible" Implantaten. Dies lieferte den Beweis, dass die Stabilität einen Einfluss auf die Infektion hat. Die Tatsache, dass der Stabilitätseffekt vom verwendeten Mausstamm abhängig war, weist darauf hin, dass der Wirt einen Einfluss auf die Infektionsentwicklung hat. In beiden Stämmen, wurde eine höhere Entzündung (z.B. höhere mRNA-Level von Interleukin (IL)-33 oder IL-6) bei Instabilität nachgewiesen. Die Infektion mit *S. Aureus* führte in beiden Systemen ("rigid" und "flexible") zu einer schnellen und extensiven Osteolyse. Daher war ein Vergleichen der Fraktur Stabilität nicht möglich. Jedoch waren wir in der Lage, die Immunantwort von *S. epidermidis* und *S. aureus* zu vergleichen. Einige der untersuchten Immunparameter zeigten signifikante Unterschiede, wie zum Beispiel erhöhte Sekretion der proinflammatorischen Zytokine (IL-6 oder Tumor Nekrosis Faktor(TNF)-α) oder erhöhte Zell Rekrutierung in dem Kniekehlenganglion und in der Milz. Ebenfalls waren ersichtlich signifikante Unterschiede bei Gewichtsverlust und Osteolyse.

In darauffolgenden Studien wurden verschiedene Hypothesen mit unserem Tiermodell untersucht. Eine davon analysierte den Einfluss von IL-17A auf Infektionen. Wir hatten festgestellt, dass in den Mäusen nach einer Inokulation mit *S. epidermidis*, IL-17A mRNA und Protein Spiegel erhöht waren. Mit IL-17A knock-out (KO) Mäusen wurde daraufhin der Einfluss von Zytokinen auf die Entwicklung einer Infektion untersucht. Es konnte gezeigt werden, dass IL-17A KO Mäuse eine Infektion weniger gut eliminierten, jedoch war der Unterschied nicht signifikant. Dies deutet jedoch darauf hin, dass ein kompensatorischer Mechanismus existieren muss. Ebenfalls haben wir in unseren anfänglichen Studien festgestellt, dass die mRNA-Expression des Histamin 2 Rezeptors ($H_2R$) nach einer *S. epidermidis* Inokulation erhöht war. Daher wurde mit $H_2R$ KO Mäusen der Einfluss des Rezeptors auf die Entwicklung einer Infektion untersucht. Unterschiedliche Konzentration an Zytokin- und Antikörper-Produktion wurde beobachtet, wobei dies keinen Einfluss auf die bakterielle Bekämpfung hatte. Dies deutet darauf hin, dass $H_2R$ bei der Infektionsantwort in unserem Modell nicht involviert ist. Zum Schluss wollten wir mit unserem Modell herausfinden, welchen Einfluss eine bereits bestehende *S. epidermidis* Immunität hat. Im Gegensatz zu Menschen, welche eine *S. epidermidis* spezifische humorale Immunität aufweisen, haben Labortiere keine. Nachdem subkutan den Mäusen abgetötete *S. Epidermidis* verabreicht wurden, konnte eine spezifische adaptive Immunität beobachtet werden. Jedoch hatte diese in unserem Modell,verglichen mit den Kontrolltieren, welchen Kochsalzlösung verabreicht wurde, keinen Einfluss auf die Infektionsrate, bakterielle Belastung und Immunantwort.

Zusammenfassend kann gesagt werden, dass ein *S. epidermidis* Fraktur-bezogenes Infektionsmausmodell erfolgreich etabliert und charakterisiert wurde, welches eines der ersten Tiermodelle in der Literatur darstellt. Mit diesem Modell haben wir gezeigt dass, die Frakturstabilität mit einer höheren bakteriellen Eliminierung verbunden war. Die Immunantwort auf *S. epidermidis* und *S. aureus* Infektionen wurde untersucht, wobei signifikante Unterschiede auf klinischer, zellulärer und molekularer Ebene beobachtet wurden. Zudem wurde dieses Modell verwendet, um den Einfluss von IL-17A, $H_2R$ und eine bereits vorhandene Immunität auf die Infektionsentwicklung zu untersuchen.

# 4. Introduction

## 4.1 Bone biology and principles of fracture treatment

### 4.1.1 History of fracture management and the AO Principles

Bone fractures, as may result from road-traffic accidents or falls, occur with an average global incidence of approximately 16 cases/1000/year; with higher rates in developing countries [1-4]. Bone is one of the few tissues in the human body that is able to heal throughout life without scar formation, although fractures can result in permanent disability if not treated appropriately. When a bone fracture occurs, there is a loss of structural continuity of the cortical bone resulting in a loss of function. Without any intervention, the bone would heal spontaneously by callus formation; however, under such conditions, healing is likely to be imperfect, particularly if the respective bone fragments are incorrectly aligned. The surgical treatment of fractured bones via the implantation of fracture fixation devices was developed to restore bone anatomy and function in a more reliable manner [5].

The earliest evidence of fracture management was discovered in Naga-ed-Der, Egypt (300 BC) and consists of rudimentary splints [6]. Splinting, with immobilization in plaster, bracing and traction, remained the main approaches to fracture management until the second half of the 19$^{th}$ century [7, 8]. These early methods of fracture management restrict limb movement during the healing process and require patient immobilization for prolonged periods. These treatments, therefore, routinely lead to progressive weakening of bone, joint stiffness, muscle atrophy, poor functional outcome and prolonged periods of time to achieve fracture healing (from 6-8 weeks to 3-6 months) [9, 10]. Three major medical developments in the second half of 19$^{th}$ century allowed for important advances in the field of surgical treatment of fractures [7]. These key innovations were anaesthesia, antisepsis and radiology. With them, the development of surgical fracture care steadily proceeded. The most important early innovations made regarding the surgical treatment of fractures included external fixation by Albin Lambotte (1886-1956), internal fixation by Lambotte and William Arbuthnot Lane (1856–1943) and the intramedullary nail by Gerhard Küntscher (1900-1972). However, their ideas were not widely or rapidly adopted due to scepticism within the surgical community at that time and technical limitations [8, 9].

In 1958, inspired by Robert Danis (1880-1962), the father of modern osteosynthesis, the AO group (Arbeitsgemeinschaft für Osteosynthesefragen/ Association for the Study of Internal Fixation) was born. It was established with the aim of overcoming the limitations in bone fracture management by providing a better understanding of bone biology and by improving available instruments and

surgical protocols for their use. By doing so, it was expected that the surgical fixation of fractured bones would become a widely adopted revolution in trauma surgery. From this early work, the AO Principles for fracture fixation were established (Table 4-1), which remains to this day the basis of bone fracture management.

**Table 4-1** Description of the AO Principles for fracture management. Adapted from Rüedi *et al.*[9].

| Principle | Description |
|---|---|
| **Fracture reduction** | Realignment of bone fragments to restore the anatomy |
| **Fracture fixation** | Ensures the maintenance of fragment alignment and provides stability (absolute or relative) to the construct |
| **Blood Supply** | Preservation of blood supply |
| **Early mobilization** | Early mobilization of the limb and patient |

## 4.1.2 The bone healing process

Bone tissue can heal through primary healing (also known as direct) or secondary (indirect) healing. The type of healing is dictated by the distance between the bone fragments and the mechanical environment at the fracture site. In general terms, a fixation that provides absolute stability will result in primary bone healing, while a fixation that provides relative stability will result in secondary bone healing.

### Primary bone healing

Primary bone healing is a process of osteonal bone remodelling and/or intramembranous ossification (direct bone formation by osteoblasts with no cartilage formation). Primary bone healing requires absolute stability (a rigid fixation) and reduction of the bone fragments. When these conditions are present, primary bone healing can occur through two processes: contact healing or gap healing (Figure 4-1).

Contact healing happens when mechanical continuity between bone fragments is achieved (gap between bone ends is less than 0.01 mm) [11]. In this situation, healing occurs via osteonal remodelling, i.e. new bone forms directly across the fracture line by direct extension of the osteons (or Haversian system, the functional unit of bone). In brief, the osteons extend through the formation of a cutting cone, which contains osteoclasts in the tip of the cone and osteoblasts at the rear of the cutting cone. Osteoclast drill a tunnel through the dead bone (directing the cutting cone across the fracture line), and at the other side the osteoblasts deposit new bone (osteoid) (Figure 4-1, A).

Gap healing occurs if fracture gap is between 0.25-0.5 mm, although is suggested that it can occur with fracture gaps up to 0.8 mm [11]. In such cases, osteoblasts migrating from the periosteum or resulting from mesenchymal stem cell (MSC) differentiation directly produce osteoid, which is deposited along the fracture line (Figure 4-1, B). In this way, the fracture gap is first filled with woven and lamellar bone, a process that takes 3 to 8 weeks. Subsequently, the bone undergoes a remodelling process resembling the contact healing cascade with cutting cones.

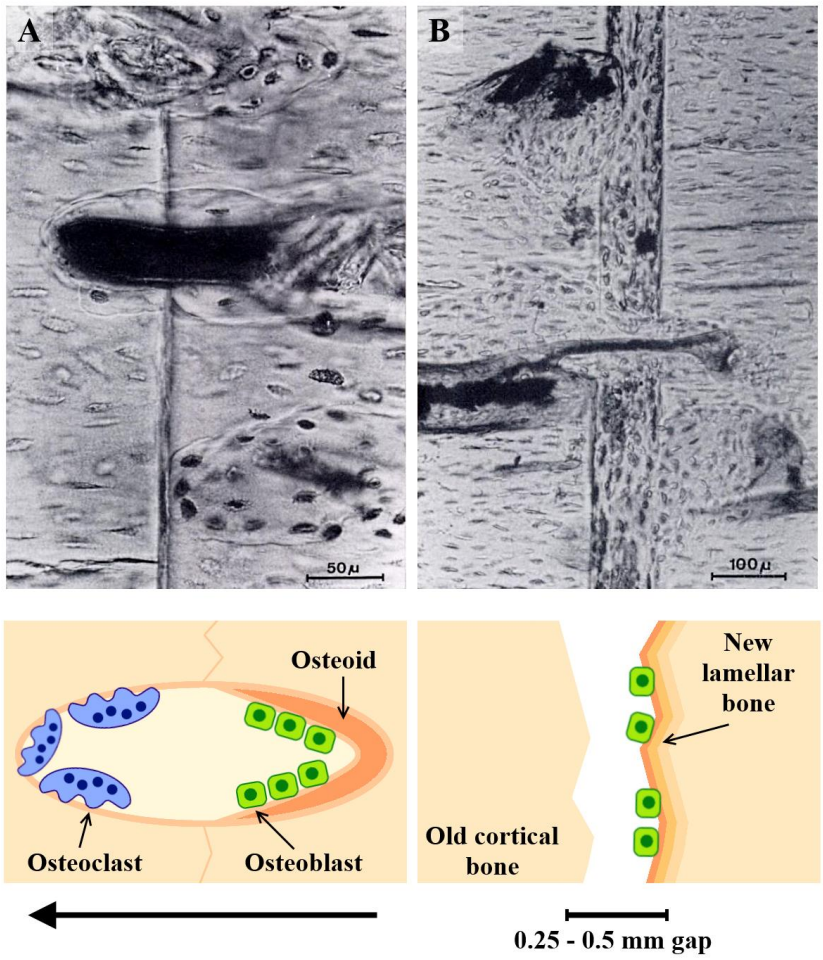


**Figure 4-1** Histological sections of rabbit femurs showing primary bone healing A) by contact healing (with a schematic image below of a cutting cone crossing the fracture gap, with an arrow showing the direction of progression of the cutting cone), or B) by gap healing (with a schematic image below of a fracture gap closing with new lamellar bone formation by osteoblasts). Histology images from Rahn *et al.* [12]

## Secondary bone healing

Secondary bone healing is the most common form of fracture healing. It consists of a mixture of intramembranous ossification and endochondral ossification, which together are the two essential processes occurring during foetal development of the skeletal system. In endochondral ossification,

MSCs differentiate into chondroblasts that form a stabilizing cartilaginous callus, which is further replaced with mineralized bone. Contrary to primary bone healing, it does not require anatomical reduction and absolute stability.

Secondary bone healing consists of consecutive but overlapping phases (Figure 4-2), which could be summarized in: inflammatory phase, soft callus phase, hard callus phase and remodelling phase. As our knowledge of bone healing progresses, more elaborate classifications have been proposed. For example: hematoma formation, inflammation, neovascularization and granulation tissue formation, fibrous tissue formation, fibrocartilage, hyaline cartilage (soft callus), cartilage mineralization, woven bone (hard callus), and finally remodelling [13].

The first phase is the acute inflammatory phase and it occurs during the first hours/days after fracture. At this stage, an hematoma is formed due to vessel disruption and several inflammatory mediators (such as tumour necrosis factor (TNF)-α, interleukin (IL)-6 or CCL2) and growth factors are released to attract cells into the fracture site and to induce angiogenesis [10]. Although the role of hematoma is not completely understood, it has been observed that its removal can lead to non-union, highlighting its functional role in the healing cascade [13, 14]. Neutrophils are the first cells recruited into the fracture site where they clear dead cells and debris [15], and secrete cytokines, chemokines or extracellular matrix (ECM) proteins such as fibronectin [16]. Macrophages have also been observed to be recruited in this early phase and they are believed to play an essential role in bone healing. Macrophages contribute to tissue debridement and secrete a broad range of cytokines, chemokines and growth factors. These secreted factors lead to MSC recruitment from the periosteum, bone marrow and surrounding soft tissue, that further differentiate into osteoblasts and chondroblasts [17]. One to two weeks post-fracture, a soft cartilaginous callus is formed by proliferating chondrocytes (soft callus phase). Afterwards, the soft callus starts to mineralize and become woven bone, stiffening the healing tissue (hard callus phase). The last stage, which takes from months to years, is the remodelling phase where woven bone becomes lamellar bone [18-20].

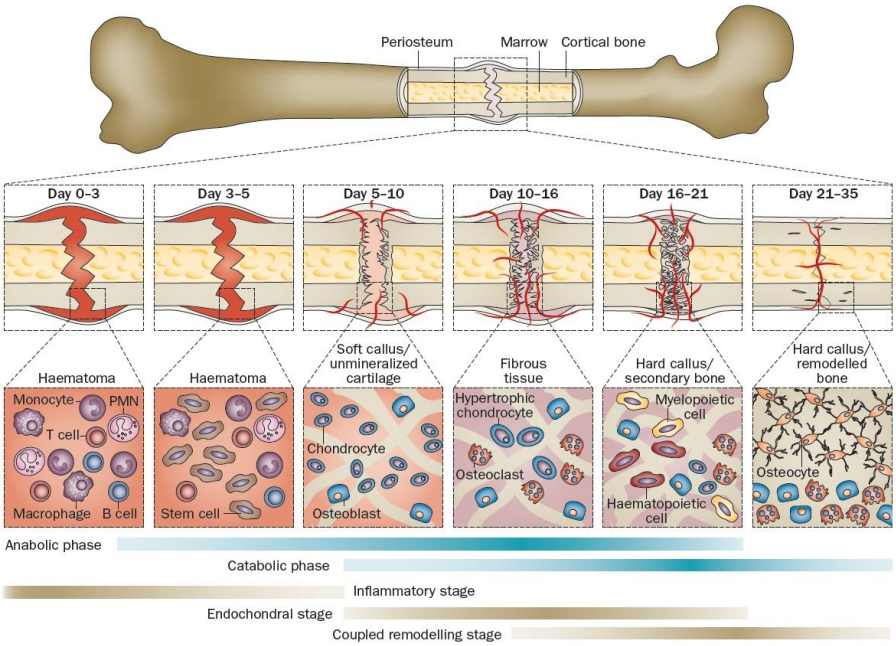


**Figure 4-2** Schematic of secondary bone healing showing the main phases: the inflammatory phase with hematoma formation (days 0-5), the soft callus phase (days 5-16) at the start of the endochondral stage, the hard callus phase (from day 16 on) and finally the remodelling phase, which can take up to several months. Figure from Einhorn and Gerstenfeld [20]

## Factors affecting bone healing

Fracture healing process is a complex and well-orchestrated process influenced by mechanical environment, together with biological factors. The "diamond concept" by Peter Giannoudis (Figure 4-3) summarizes these factors into four specific aspects: osteogenic cells, scaffolds, growth factors and mechanical environment [21]. More recently, the concept has been updated to now also incorporate immune cells and inflammatory mediators as additional essential factors.

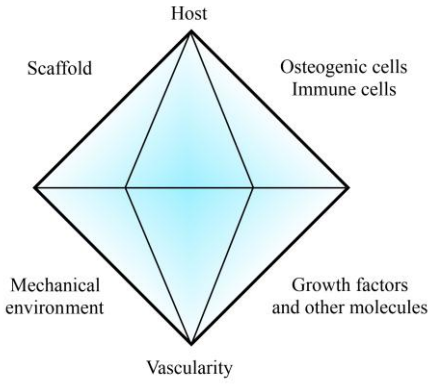


**Figure 4-3** The diamond concept by Peter Giannoudis, showing the main factors influencing bone healing: osteogenic and immune cells, growth factors and other molecules, vascularity, mechanical environment, the scaffold and the host. Adapted from Giannoudis *et al.* [22].

### *Osteogenic and immune cells*

The cells involved in bone healing primarily differentiate from MSCs and hematopoietic stem cells (HSC) (Figure 4-4), although endothelial progenitor cells are also important for bone healing due to the need for re-vascularization throughout the healing process. Osteoblasts are cells derived from MSCs and are responsible for generating the bone ECM. They produce type I collagen, the main organic component of bone ECM, and proteins that stabilize and aid in mineralization of the matrix such as osteopontin or alkaline phosphatase [23, 24]. Over time, a small percentage of osteoblasts get embedded within the bone matrix and develop into osteocytes. Osteocytes are terminally differentiated osteoblasts that form an interconnected network within the mineralized matrix and play a major role in the homeostasis of bone. A second cell type important for bone healing are the chondrocytes, which are also derived from MSCs and are responsible for producing cartilage [25]. When a fracture occurs, MSCs are recruited into the fracture site and differentiate into chondrocytes and osteoblasts that are actively involved in fracture repair. The source of these MSCs is not completely known but most of the data suggests that they are derived from surrounding soft tissues and bone marrow [11]. Equally important to bone homeostasis and bone repair, are the cells that degrade bone, osteoclasts. Osteoclasts are multinucleated cells that are derived from HSCs and belong to the monocyte/macrophage lineage. They are the main bone resorbing cells, through the generation of proteolytic enzymes and acids [23].

The role of immune cells in fracture healing has received increasing attention over the past years. Recent studies have shown that macrophages are essential for bone healing, by initiating the healing cascade and by supporting the transition from the soft callus into a hard callus [26, 27]. The role of lymphocytes is not entirely clear at the present time. Mice lacking an adaptive immune system have been shown to result in accelerated [28] but also delayed [29] bone healing. This apparent contradiction could be due to the effect of different lymphocyte subsets in the final outcome: while CD8+ T cells have been associated with delay in bone healing [30], B and T regulatory (Treg) cells seem to be beneficial [31]. Similarly, the role of γδ T cells is controversial at the present time, with contradictory findings also present in the literature [32, 33].

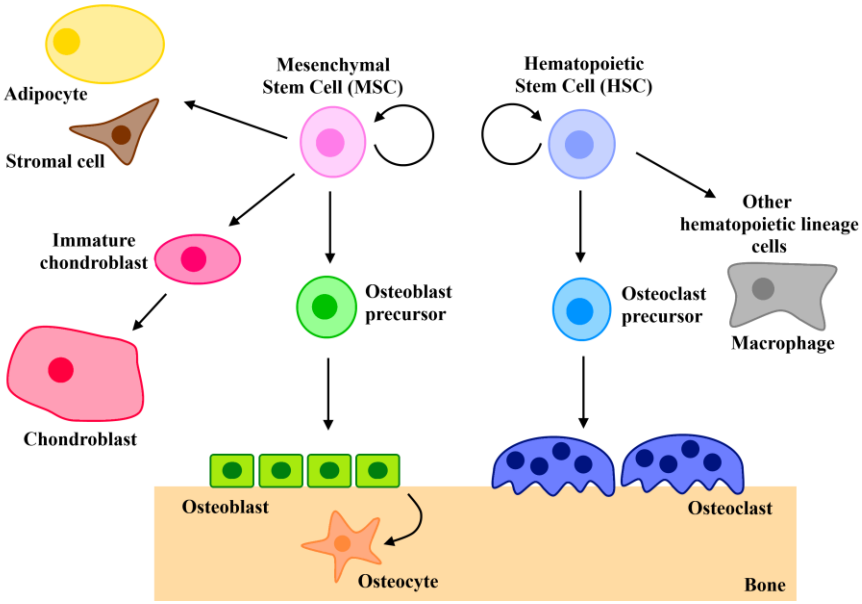


**Figure 4-4** Scheme with the main cell types involved in bone homeostasis/healing: osteoblasts and chondrocytes, which together with adipocytes and other cell types differentiate from MSCs; and osteoclasts and cells from the immune system (e.g. macrophages), which originate from HSCs.

### *Scaffolds*

The scaffold referred to in the diamond concept describe the extracellular matrix of bone that provides a natural support for cells. In a fracture situation, it may be considered that the hematoma (consisting mostly of fibrin) is the first scaffold. Over time, the hematoma evolves into granulation tissue and provisional connective tissue. In clinical practice, scaffold may also refer to different synthetic or natural biomaterials used as bone void fillers to enhance bone formation [34].

### *Growth Factors and other molecules*

Fracture repair is finely regulated by a broad range of growth factors and other molecules such cytokines and chemokines. In the hematoma phase, several pro-inflammatory cytokines (such as IL-1β, IL-6 or TNF-α), macrophage colony-stimulating factor (M-CSF) and members of the transforming growth factor (TGF)-β superfamily (such as bone morphogenetic protein (BMP)-2) are secreted to recruit cells into the fracture site [35, 36]. Angiogenic factors are also induced at early stages. Among the cells recruited there will be MSCs, which get licensed to exert their immunosuppressive functions. MSCs secrete molecules like TGF-β2 and 3, which have been shown to peak at the end of the inflammatory phase, to reduce inflammation in the tissue and to initiate the repair cascade. From that stage on, BMPs and other growth factors orchestrate the generation of soft callus and the further transition into hard callus and the remodelling phase. Some of the most relevant factors are described in Table 4-2.

**Table 4-2** Summary of relevant molecules involved in bone healing. Adapted from selected reviews [35-38].

| Molecule | Role | Comments |
|---|---|---|
| **Tumour necrosis factor (TNF)-α** | Homing of lymphocytes, monocytes/macrophages and MSCs during inflammatory phase. Licensing of MSCs to perform immunosuppressive functions in order to reduce inflammation. In a later phase, aids the transition of cartilage into bone. | High sustained release can lead to bone destruction but in low doses might have a beneficial effect |
| **Interleukin-6** | Homing of lymphocytes and monocytes/macrophages during inflammatory phase (induced within first 24 hours). Enhances osteoclastogenesis and osteoblastogenesis. | Its effect seems to be limited to the early phase. |
| **Interleukin-1β** | Homing of lymphocytes and monocytes/macrophages during inflammatory phase. | |
| **CC chemokine ligand (CCL)2 / Monocyte Chemotactic Protein (MCP)-1** | Recruitment of macrophages into the fracture site. | In CCL2 knock-out (KO) mice there is a significant impairment in bone fracture healing. |
| **Stromal cell-derived factor-1 (SDF-1)** | Recruitment and homing of MSCs to the site of trauma during hematoma phase. | |
| **Fibroblast Growth Factor (FGF)** | Secreted during the early stages. Induces fibroblast, osteoblast and chondrocyte proliferation as well as angiogenesis. | |
| **Platelet-derived growth factor (PDGF)** | Promote the proliferation and the chondrogenic differentiation of MSCs as well as deposition of collagen. Important in the soft callus phase. | |
| **Transforming growth factor (TGF)-β family** | Secreted at the end of the inflammatory phase, probably in order to control inflammation and initiate repair cascade. | |
| **Bone morphogenetic proteins (BMPs)** | Secreted throughout the bone healing process at different time-points, suggesting specific roles of the different BMPs in different phases of bone healing. BMP-2 is secreted from early time-points until the remodelling phase, suggesting a regulatory and essential role for this BMP. | BMP-2 and 7 are clinically approved for non-union treatment, with BMP-2 being the most widely used. |

### *Mechanical environment*

The importance of mechanics in bone healing has been described for many decades and constitutes one of the AO principles. It is well defined that less stable implants lead to a more endochondral bone formation, with the presence of a stabilizing callus, while high stability leads to intramembranous ossification as described above.

The effects of mechanics in bone healing are explained by the strain theory. In brief, strain is the deformation of a material when a given force is applied. Normal strain is the change in length ($\Delta$ l) in comparison to original length (l), and is expressed as a percentage. In a fracture, bone is

generated when the local strain is less than the strain that forming woven bone can tolerate. Thus, when the movement between the fragments is too great (meaning that there is big deformation of the tissue and thus a greater strain), no bone is generated. Nature deals with this by developing a soft callus (cartilage) that leads to less deformation and thus allows bone to be formed [9]. Starting in 1960 with Friedrich Pauwels, who developed a theory for the tissue differentiation in response to local mechanical stresses, several biomechanical models have been proposed to explain the connection between physical forces and cell behaviour in a tissue. Most of them are based on shear strain and hydrostatic forces. As an example (Figure 4-5), Damien Lacroix *et al.* have described a model based on shear strain and fluid flow forces. The model proposed shows that with low strains, MSC differentiate into osteoblasts, while higher strains progressively led to chondrocyte differentiation, fibrous tissue or no differentiation [39]. These findings provide a basis to understand how the mechanical load can drive to different types of bone healing and are of great importance in order to develop treatment opportunities in tissue regeneration [40-42].

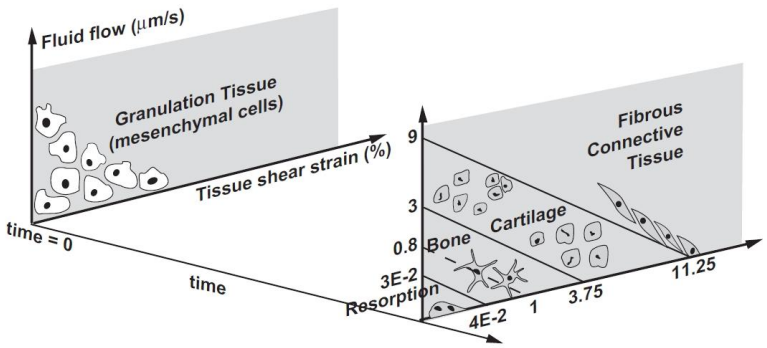


**Figure 4-5** Mechano-regulation concept forces influencing cell differentiation to form fibrous connective tissue, fibro-cartilage or bone. The model is based on two mechanical stimuli: the tissue strain and the interstitial fluid flow. Figure from Lacroix and Prendergast [39].

## 4.1.3 Fracture fixation and stability

Stability is the quality of being firmly fixed, or not likely to move or change. In the surgical field, stability is considered as a spectrum that ranges from absolute stability to instability. Fracture stability will be determined by the fracture pattern (simple facture versus multiple fragments), the type of fixation used, the surgical procedure and the quality of the bone. A stable fracture is defined as a fracture that does not visibly displace under physiological load. This stability can be absolute, when there is no "micromotion" at the fracture site, in contrast to relative stability, which is achieved when certain displacement can occur between the fragments [9]. At the other end of the spectrum one can find instability, with high deformation and thus high strain on the repair tissue that can lead to non-union, as described by the mechano-regulation model.

Absolute stability is achieved through techniques that compress the fragments towards each other (interfragmentary compression). Amongst the range of implants available, certain implants and application techniques provide interfragmentary compression, and these include lag screws, axial compression or tension bands (see examples in Figure 4-6). Absolute stability is more easily achieved in simple fractures and is specially required for intra-articular fragments, as callus formation is not desired within the articulating surface. Relative stability is achieved when "micromotion" can occur between the fragments. As mentioned above, it involves a combination of intramembranous and endochondral ossification with the subsequent formation of a callus [34, 43, 44]. For some type of fractures (e.g. multi-fragmentary fractures) only relative stability can be attained. Techniques that provide relative stability include external splinting, such as conservative techniques or external fixation, and some type of internal splinting like intramedullary nailing or bridging plate (see examples in Figure 4-6).

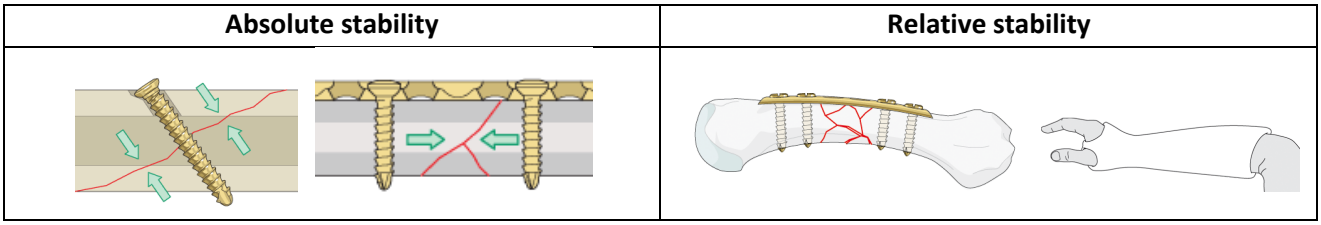


**Figure 4-6** Example of fixation techniques and the type of stability that they provide to the fracture site. On the left side, a lag screw and a plate for axial compression are shown, which provide absolute stability by compressing the bone fragments against each other. On the right side, a plate bridging several fragments and a cast, which provide relative stability. Images from AO Surgery Reference (http://www.aosurgery.org).

## Fracture fixation complications

Upon fracture treatment, certain complications can occur. The most challenging ones include delayed bone-healing or non-union, and implant-related infection.

As this thesis is focused on implant related infection, a more detailed description will be provided of fracture related infection. The main etiologic agents are staphylococci, especially *Staphylococcus aureus* and *S. epidermidis* and other coagulase-negative staphylococci (CoNS), which together account for 50-75% of the isolates [45]. The following section describes the bacteria that have been the focus of this thesis, *S. epidermidis* and has been recently accepted for publication.

## 4.2 Pathogenic Mechanisms and Host Interactions in *Staphylococcus epidermidis* Device-Related Infection

### 4.2.1 Introduction

*Staphylococcus epidermidis* is a permanent member of the normal human microbiota, commonly found on the skin and mucous membranes. By adhering to tissue surface moieties of the host via specific adhesins, *S. epidermidis* is capable of establishing a lifelong commensal relationship with humans that begins early in life. Although commensal *S. epidermidis* isolates display high rates of resistance to antibiotics of clinical relevance [46], their default status as commensal bacteria renders this phenomenon largely irrelevant for the healthy human host. However, with the advent of implanted medical devices such as prosthetic joints and fracture fixation devices, *S. epidermidis* has emerged as an important opportunistic pathogen [47a, 48]. In fact, the implanted medical device may actually facilitate infection since any *S. epidermidis* inadvertently introduced into the surgical site are capable of rapidly adhering to, and accumulating on, the surface of the device. This surface-associated bacterial growth is known as biofilm formation and appears to be the key factor enabling invasive, device-related infection (DRI) for an otherwise largely non-pathogenic microorganism. The ubiquitous presence of *S. epidermidis* on human skin has enabled *S. epidermidis* infection to emerge as a significant complication when using medical devices [49-51]. With the increasing use of such devices, coupled with high antibiotic resistance rates, *S. epidermidis* DRI will likely remain a clinical problem for generations to come.

The following paragraphs describe the host interactions with *S. epidermidis* under both normal healthy commensal conditions, and under conditions of an invasive DRI. This includes describing how this microorganism has adapted to life on human skin, including biofilm formation, and how the same adaptations have enabled invasive DRI. Particular attention will be paid to the impact of *S. epidermidis* in orthopaedic device-related infection (ODRI) since these infections are amongst the most burdensome and expensive to treat [52]. Finally, since the impact of ODRI on bone tissue is a critical feature of these infections, interactions between *S. epidermidis* and bone will be also be described.

### 4.2.2 *S. epidermidis* as a member of commensal human microbiota

Under healthy conditions, the skin commensal microbiota is believed to be beneficial to humans through aiding in nutrition, outcompeting pathogens and educating the immune system [53]. Humans are believed to first encounter *S. epidermidis* in utero, as evidenced by their presence in the

amniotic fluid [54]. The first faeces (meconium) has also been shown to harbour a predominance of *S. epidermidis* [55] and the skin of the new-born will be colonized by *S. epidermidis* within a few days [56]. Thereafter, *S. epidermidis* becomes part of the "normal" resident human skin microbiota, being predominant in moist sites such as nares or fossae, but also present in sebaceous areas such as the facial skin [57] and mucosal tissues such as the gastrointestinal and the lower reproductive tracts [58, 59].

In order to persist on human skin, *S. epidermidis* has evolved diverse mechanisms to sense and overcome the physical and chemical features of host antimicrobial defence. Such mechanisms include surface adhesins enabling attachment to the host [60], systems to sense host antimicrobial peptides (AMPs) and communication molecules (e.g. hormones) [61, 62], mechanisms against AMPs [63] (e.g. *S. epidermidis* derived protease SepA is induced by and directed against the human AMP dermicidin [64]), and survival strategies against desiccation and osmotic stress [65, 66].

*S. epidermidis* has also been shown to influence host colonization by other species, as shown for *S. aureus* [67, 68]. Negative correlations between these two species have been reported in humans, insinuating an antagonism between at least some strains [69, 70]. This effect is at least partially due to the secretion of factors that impact on the viability or colonization capacity of other microorganisms [71, 72]. Phenol soluble modulins (PSMs) are a family of multifunctional amphipathic, alpha-helical peptides that are produced by *S. epidermidis* isolates [73]. They are believed to act on host cells, are important for biofilm maturation [74] and could play a role in the competition between microorganisms on human skin. In particular, PSM-γ and PSM-δ produced by *S. epidermidis* have been shown to selectively reduce survival of *Streptococcus pyogenes* on mouse skin, but did not affect *S. epidermidis* itself [75, 76]. Both PSM-γ and PSM-δ cause membrane leakage in target bacteria (*S. aureus* and *S. pyogens*) [76], which indicate that they function like host-derived AMPs, with whom they share structural similarities. Host-derived AMPs and *S. epidermidis* PSMs have even been shown to act synergistically against bacterial pathogens [75]. In contrast, the closely related δ-toxin of *S. aureus* only seems to possess a very limited antimicrobial activity [77, 78] suggesting that the cooperative effect with host AMPs is not a widespread phenomenon. In addition, many strains of *S. epidermidis* also produce bacteriocins, which are antimicrobial peptides that act against other species or strains (often closely related to the producing bacteria). Gram-positive bacteria usually produce two types of bacteriocins: lanthionine-containing antibacterial peptides (lantibiotics) and class-II bacteriocins [79, 80]. For *S. epidermidis*, examples include the lantibiotics epidermin [81], Pep5, epilancin K7 [82] and epilancin 15X [83], with further examples recently described [72, 84, 85]. Another mechanism employed by *S. epidermidis* to compete with other skin microorganisms involves the degradation of biofilms

from other bacterial species. The serine protease Esp is able to mediate *S. aureus* biofilm degradation by targeting several proteins involved in biofilm assembly [68, 86]. It has been observed that the presence of Esp-secreting *S. epidermidis* in the nose correlates with the absence of *S. aureus* in healthy human volunteers [68]. This activity has been supported experimentally with the finding that the intranasal application of an Esp-secreting strain was able to decrease *S. aureus* colonization in mice and humans [67, 68]. Finally, metabolic products may also serve to counteract other microorganisms. *S. epidermidis* has been shown to ferment glycerol into short chain fatty acids, which have displayed inhibitory activity against *Propionibacterium acnes* (implicated in acne vulgaris) *in vitro* and in mice [87].

### 4.2.3 *S. epidermidis* as a pathogen

In contrast to its standard role as a commensal microorganism, *S. epidermidis* and other CoNS have been found to cause invasive infections in selected groups of patients. These higher risk groups include preterm neonates, immunocompromised individuals and patients with indwelling medical devices [52, 88, 89]. Unlike *S. aureus*, which typically produces numerous extracellular enzymes and toxins that enable invasive infections in otherwise healthy hosts, *S. epidermidis* seems to retain a limited number of virulence factors [90] and normally is unable to cause invasive infection in healthy hosts [91].

#### *S. epidermidis* as a pathogen of the musculoskeletal system

*S. epidermidis* is second only to *S. aureus* as the most prevalent species encountered in ODRIs [92, 93]. *S. epidermidis* causes approximately 20-30% of ODRIs [45, 49, 93] and the prevalence may even increase to 50% in late-developing infections [94]. These late-developing infections may be linked to the sub-acute nature of *S. epidermidis* infections, which may present many months after surgery with subtle signs of infection. This differs from the acute and often obvious nature of *S. aureus* infections and may be partially explained by the lack of virulence factors retained by *S. epidermidis* in comparison with *S. aureus* [95-97]. An illustrative case of a chronic *S. epidermidis* infection is shown in Figure 4-7, detailing the fact that these infections may become apparent many months after the presumptive initial colonization event and they result in prolonged healing times and a poor functional outcome for the patient.

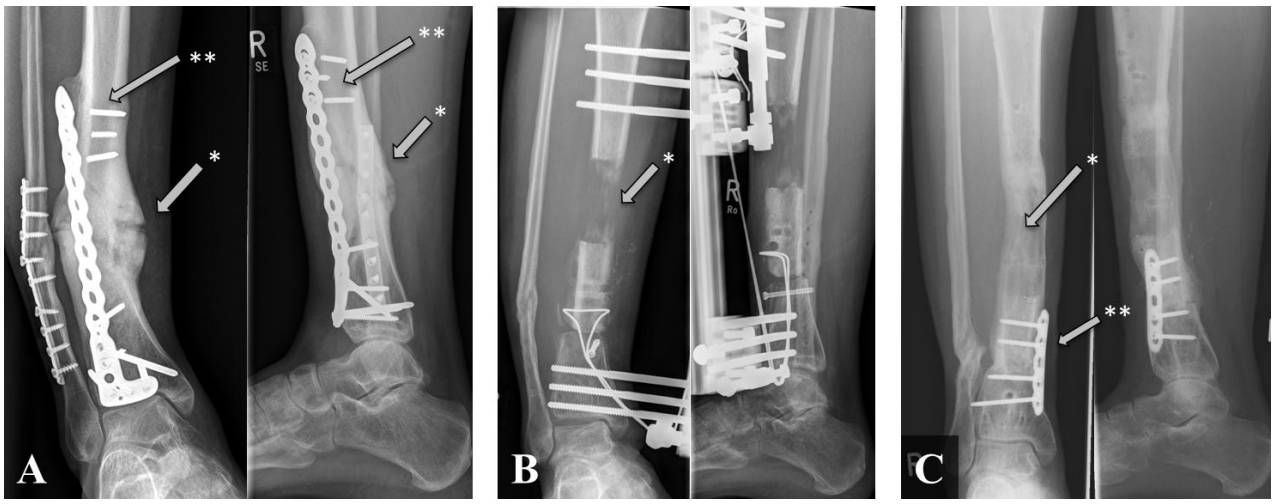


**Figure 4-7** Radiographic documentation of a surgically fixed fracture of the lower leg that failed to heal due to *S. epidermidis* infection. A) Plain x-rays (anterior-posterior and lateral view) show the non-union of the fracture (*) due to *S. epidermidis* infection with secondary displacement and screw failure (**) 10 months after surgery. B) The infection and non-union required plate removal and resection of necrotic bone leaving a 4cm defect in the bone (*). The defect was treated with segmental bone transport using an external fixator. C) Complete consolidation of transport segment (*) and docking site (**) required multiple surgeries and an overall treatment period of three years. Anonymized radiographs from a patient with *S. epidermidis* FRI obtained from Trauma Center BGU Murnau (Germany).

The diagnosis of ODRI is based on the combination of clinical presentation, biopsy culture, histological analysis and clinical diagnostic criteria, such as high C-reactive protein [98]. Diagnosis may be particularly challenging for sub-acute infections due to the lack of obvious clinical signs of infection. Therefore, microbiological culture results are often the most critical diagnostic criteria. Since the microbes grow in biofilms on the foreign material and in necrotic bone tissue, cultivation and identification of the disease-causing pathogens may require the culture of several intraoperative tissue samples and removal of the implant for appropriate sampling [99, 100]. To increase the yield of positive cultures, it is advised to terminate antibiotic therapy before sampling, acquire at least three tissue biopsies, and to perform sonication of removed hardware to remove biofilm-associated bacteria from the surface [93, 98, 101-104]. In suspected *S. epidermidis* infections, where the pathogen is also a skin commensal that could contaminate the biopsy if aseptic techniques are not followed, the same indistinguishable microorganism must be cultured from at least two separate biopsies in order to differentiate a relevant infection from skin contamination. In contrast, in virulent species such as *S. aureus* or *Escherichia coli*, a single positive biopsy may be sufficient to determine the presence of an infection [105, 106].

The treatment of *S. epidermidis* ODRI will depend on patient-specific factors, but will possibly require implant removal and a minimum of 6 weeks antibiotic therapy [45, 92, 93]. Despite such

prolonged and comprehensive therapy, infection recurs in approximately one third of the cases and up to one fifth of cases cannot achieve a cure with restoration of limb function [107-110]. Morgenstern *et al.* investigated the clinical course and outcome of staphylococcal ODRIs in elderly patients and could show *S. epidermidis* was associated with prolonged infections and was associated with lower cure rates (75%) than *S. aureus* (84%), although *S. aureus* related infections were associated with a five-fold higher mortality rate [109]. This data therefore supports clinical beliefs that *S. epidermidis* is an agent of sub-acute infection with significantly worse treatment outcomes, although those infections may be less life-threatening than *S. aureus* infections.

## *S. epidermidis* virulence factors

### *Adhesion to host proteins*

As a commensal microorganism, *S. epidermidis* retains the ability to specifically adhere to host proteins in the skin. In a surgical wound, the bacterium utilises these adhesion mechanisms in order to adhere to the deeper tissues and to the implanted device, or more specifically, the conditioning layer of host proteins deposited on the device. Initial adhesion of bacteria to implant surfaces is mediated by non-specific interactions such as hydrophobic interactions [111], and then as shown schematically in Figure 4-8, by specific adhesins such as autolysin (AtlE) [112], extracellular DNA (eDNA) [113, 114], and staphylococcal surface protein 1 and 2 (SSP-1, SSP-2) [115]. AtlE, SSP-1 and SSP-2 have been primarily associated with adhesion to native surfaces [112, 115], whilst eDNA is generated in *S. epidermidis* through an AtlE-mediated lysis of a subpopulation of the bacteria, promoting biofilm formation within the remaining population [113]. In the context of medical devices, the surface of the device becomes coated with host-derived plasma proteins, ECM proteins and coagulation products (platelets and thrombin) immediately following implantation [116]. Cell-wall-anchored (CWA) proteins/adhesins, such as the microbial surface components recognizing adhesive matrix molecules (MSCRAMMs) [117] bind bacteria like *S. epidermidis* directly to these molecules Figure 4-9. In *S. epidermidis*, adhesins for fibrinogen (as serine-aspartate repeat protein G (SdrG/Fbe) [118, 119]), fibronectin (extracellular matrix-binding protein (Embp) [120]), collagen (SdrF/GehD [121, 122]), vitronectin (AtlE or autolysin/adhesin (Aae) [123]) and elastin (elastin-binding protein (EbpS)) have all been identified. Peptidoglycan-bound wall teichoic acids (WTA) are an essential part of the *S. epidermidis* cell wall and also play an important role in bacterial adhesion. WTA enhances the initial adhesion of *S. epidermidis* to medical devices by binding to adsorbed fibronectin [124] and fibrin clots [125].

### *Biofilm formation*

The ability to adhere to a surface represents the first step in biofilm formation, commonly believed to be the most important virulence factor possessed by *S. epidermidis* (Figure 4-8), particularly for DRI. Biofilm development facilitates resistance against host defence mechanisms [126-129], and confers antibiotic resistance [130, 131]. Biofilm formation also complicates medical and surgical treatment protocols because implant removal is often required to remove the biofilm.

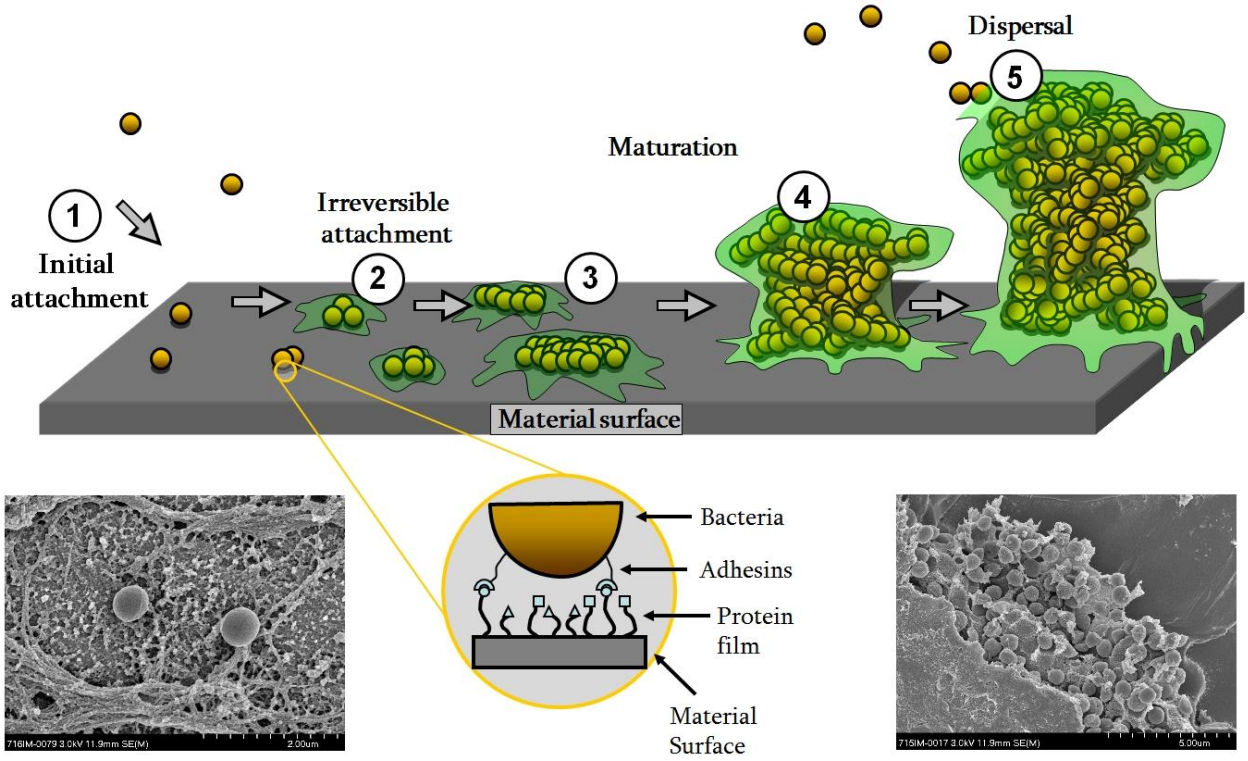


**Figure 4-8** Biofilm formation scheme with scanning electron micrographs of *S. epidermidis* single cells (lower left) or in biofilm community surrounded by EPS (lower right) on a titanium surface. Image adapted with permission from Rochford *et al.* 2011 [132].

Biofilms are defined as complex communities of adherent bacteria encased in a matrix of self-produced extracellular polymeric substances (EPS) [133] (Figure 4-8). The accumulation and maturation of the *S. epidermidis* biofilm occurs via a number of mechanisms. Polysaccharide intercellular adhesin (PIA, or poly-N-acetyl-glucosamine (PNAG)), synthesized by *icaADBC* encoded proteins [134, 135] is responsible for biofilm formation in the majority of *S. epidermidis* isolates [136] and was believed to be the most common molecule associated with biofilm formation [134, 135]. This was endorsed by the observation that the *ica* operon was absent in most commensal *S. epidermidis* strains [137, 138]. However, not all *S. epidermidis* have the *icaADBC* genes [134, 139] and these isolates mediate biofilm formation by proteinaceous factors, such as the accumulation associated protein (Aap) [140] that contributes to biofilm formation upon cleavage by extracellular or host proteases. The *aap* gene has been observed in both pathogenic and commensal

isolates, more frequently than the *ica* operon [139, 141, 142]. Other PIA-independent mechanisms include biofilm associated homologue protein (Bhp) [143, 144], Embp [145, 146], and *S. epidermidis* surface protein (Ses)C [147] and SesE [139]. Interestingly, Rohde *et al.*[148] suggested that PIA-dependent biofilms are more robust than those formed by proteinaceous factors, and another study found they result in a different morphotype or biofilm substructure [139]. WTA have also been linked with *S. epidermidis* biofilm formation. *TagO* encodes the first enzymatic step in WTA biosynthesis and a *tagO* mutant has been shown to have a biofilm negative phenotype. This is partly attributed to an increase in cell surface hydrophobicity, impairing its initial adhesion to the surface, and a decreased production of PIA by activating the *icaADBC* repressor, *icaR* [149]. Both CWA proteins and biofilm formation mechanisms are regulated by several global regulators, such as the accessory gene regulator (*agr*), staphylococcal accessory homologous *sar* genes, sigma factor B ($\sigma^B$), and *luxS* [150-153].

As already mentioned, biofilms play a role in immune evasion, primarily by providing a barrier to immune cells. PIA may contribute to innate immune system evasion by promoting generation of complement C5a fragment [154, 155], inhibiting phagocytes and neutrophil killing [156, 157], and reducing the activity of AMPs [156, 158]. Recently, other studies have reported slightly opposite findings, with PIA-producing bacteria inducing greater inflammatory responses and enhanced phagocytosis [159, 160], although Spiliopoulou *et al.* did observe reduced killing in PIA-producing strains as discussed elsewhere recently [161]. *S. epidermidis* also produces a second exopolymer, the poly-γ-glutamic acid (PGA), although at comparatively lower levels. Synthesized by the gene products of the *cap* locus, PGA is important in mediating *S. epidermidis* resistance to neutrophil phagocytosis and AMPs, and promoting growth at high salt concentrations (PGA is induced under such conditions) [162].

It has yet to be elucidated if WTA has a direct role in *S. epidermidis* immune system evasion. However, like *S. aureus*, *S. epidermidis* contains the genes for D-alanylation of WTA, a modification known to protect the bacteria from the activity of AMPs [163].

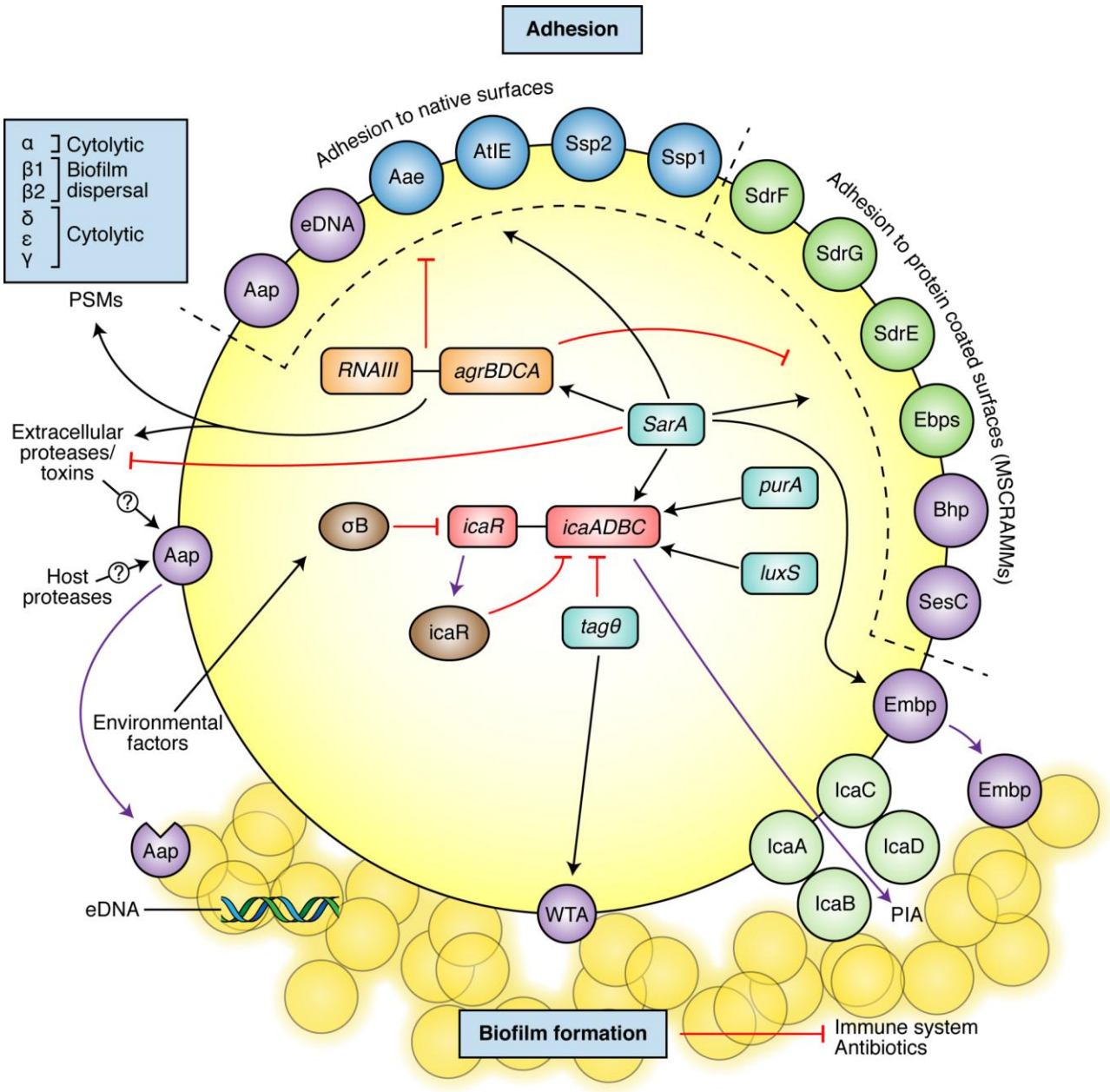


**Figure 4-9** Scheme of the main *S. epidermidis* pathogenic mechanisms, which include adhesion molecules and biofilm formation. The most well described adhesins involved in adhesion to native surfaces or protein-coated surfaces are shown in the upper part (molecules also involved in biofilm formation shown in purple). The main described biofilm components are shown at the bottom of the figure (PIA, cleaved Aap, eDNA, WTA and Empb). The figure also presents some of the most important regulators of biofilm and adhesion molecules (black arrows: activation/positive signalling, red lines: inhibition/negative signalling).

### *Antibiotic resistance*

Although the majority of *S. epidermidis* strains remain susceptible to the newer antibiotics such as daptomycin, tigecycline, linezolid and dalbavancin [164, 165], high endemic antimicrobial resistance within this species represents a significant challenge in the treatment of *S. epidermidis* infections, especially DRI [166]. Methicillin resistance in *S. epidermidis* (MRSE) is an important

characteristic of infecting isolates as it is often associated with additional antibiotic resistance mechanisms. Resistance to other antibiotics, such as erythromycin (encoded by *erm* genes), ciprofloxacin, clindamycin, aminoglycosides (encoded in *aacA/aphD* gene) or trimethoprim-sulfamethoxazole, are also often observed, especially in MRSE [167]. Methicillin resistance is encoded by *mecA*, an alternative penicillin binding protein with decreased affinity to β-lactam based antibiotics such as penicillin, methicillin and oxacillin [168]. It is carried on the mobile genetic element, staphylococcal cassette chromosome *mec* (SCC*mec*), of which several types have been identified for *S. epidermidis* [169]. MRSE have been found to be common in infection-causing isolates (70-87% of all *S. epidermidis* isolates) [110, 167, 170, 171], and even higher (90%) in specific patient cohorts [109]. MRSE prevalence in healthy individuals is low (3-18% of *S. epidermidis* commensal isolates) [167, 170, 172], although prevalence is increased for individuals exposed to the healthcare system, as observed in hospitalized patients or in healthcare workers [46, 173b, 174]. The specific causes of the increased prevalence of resistant isolates in the hospital environment is unknown, although is likely associated with high antibiotic exposure and direct or indirect interpersonal transmission.

It remains unclear whether infection with resistant organisms results in a worse clinical outcome in comparison with susceptible counterparts. In a recent study of patients with *S. epidermidis* ODRIs, methicillin resistance status did not influence the clinical course and outcome of treatment [110], although further studies are required to confirm this finding. In any case, clear therapeutic guidelines are available for the treatment of both MRSE and MSSE, with a high likelihood of treatment success in both cases when guidelines are followed closely.

***Phenol soluble modulins***

Until relatively recently it was thought that *S. epidermidis* did not produce toxins. However, the identification and characterisation of the PSMs have now changed that concept [175]. The PSMs are a family of genome-encoded peptides, and like the CWA proteins/adhesins, are under the strict regulation of the *agr* quorum sensing system (Figure 4-9) [175-177]. In *S. epidermidis*, the PSM family consists of PSMα, PSMβ1, PSMβ2, PSMδ, PSMε, and PSMγ/δ-toxin [175-177]. PSMβ peptides are the primary PSMs produced by *S. epidermidis*, are expressed at high levels during biofilm formation, and have been shown to have a role in the structuring and dispersal of the biofilm [74, 177]. They are specifically associated with the formation of channels observed between the biofilm layers, which are considered important for nutrient uptake [74]. *S. epidermidis*-derived PSMδ is strongly cytolytic against neutrophils, similar to *S. aureus*. However *S. epidermidis* culture filtrates were observed to have a very low cytolytic potential *in vitro* [178]. As growing conditions

are likely to have an influence on PSM production, the role of *S. epidermidis* PSMδ *in vivo* needs to be further addressed.

Finally, certain *S. epidermidis* strains have been shown to produce PSM-mec, a PSM encoded in the mobile genetic element SCC*mec*, in contrast to the other PSMs that are chromosomal encoded [179]. PSM-mec has cytolytic potential against neutrophils *in vitro* and its presence has been associated with decreased bacterial clearance and higher mortality rates in a murine model of sepsis [180].

***Other pathogenic mechanisms***

Small colony variants (SCVs), a colony phenotype characterized by small size, slow growth and downregulation of virulence genes, are recognized as a pathogenic mechanism for several bacterial species, including *S. epidermidis*, and are often associated with chronic infections [181, 182]. SCVs seem to be less susceptible to antibiotics and to the immune system, potentially by being able to survive intracellularly and inducing a more anti-inflammatory environment due to increased secretion of IL-10 [183].

Finally, internalization and intracellular persistence in non-professional phagocytes (e.g. osteoblasts) is a described evasion mechanism for *S. aureus* [184, 185]. A number of internalization mechanisms have been described for *S. epidermidis*, involving AtlE [186] and SdrG [187]. This represents a potentially new pathogenic mechanism for *S. epidermidis* and a location where bacteria could survive to cause persistent/relapsing infections; however its relevance *in vivo* has not yet been proven.

### 4.2.4 Host interaction with *S. epidermidis*

The interaction between *S. epidermidis* as a commensal and the host immune system is thought to play a role in the development of immunological tolerance. That is, to induce immune responses in the host that control aberrant inflammatory responses to non-pathogenic molecules such as those found in food but also in commensal bacteria. This question was assessed in recent murine studies with the topical application of *S. epidermidis* [188, 189] (*S. epidermidis* is typically not a major representative of the normal mouse skin microbiota [190]). Scharschmidt *et al.* reported that the application of *S. epidermidis* to the skin within the first weeks of life established antigen-specific tolerance to the bacteria, by generating CD4+ regulatory Treg cells, which homed into neonatal skin [188]. Mice that were not colonized during the neonatal period presented with higher inflammation and neutrophil recruitment compared to colonized mice, when challenged with the same strain of *S. epidermidis* in a skin-abrasion model. The use of the sphingosine-1-phosphate receptor

antagonist FTY720 during neonatal period, which blocked the egression of Tregs into skin, suppressed the tolerogenic effect indicating that there may a critical period when Treg mediated tolerance can be acquired [188]. On the other hand, Naik *et al.* showed that *S. epidermidis* application induced cutaneous interferon (IFN)-α and IL-17A producing T cells [189]. In this case, IL-17A$^{+}$CD8$^{+}$ T cells were shown to home to the mouse epidermis specifically after *S. epidermidis* application, but not with other tested species. This was mediated through the action of a skin-resident dendritic cell subset and was not associated with the induction of inflammation [189]. More importantly, when an epicutaneous infection model with *Candida albicans* was used, the application of the fungus in mice pre-treated with topical *S. epidermidis* resulted in decreased *C. albicans* CFU counts compared to not pre-treated ones. The effect was lost when either anti-CD8 or anti-IL-17A antibodies were co-administered, which highlights the relevance of the adaptive immune responses generated. Altogether, the study suggested that resident bacteria in the skin (*S. epidermidis*) can modulate the immune system, generating adaptive immune responses that in turn may help in promoting protective innate immune responses and controlling inflammation. The effect seemed to be tissue-specific, since *S. epidermidis* failed to induce IL-17A-producing cells when administered in the lung or gut. In two other studies, *S. epidermidis* lipoteichoic acid (LTA) has been shown to decrease skin inflammation [191], for example by inducing regulatory microRNAs in a *Pseudomonas aeruginosa* skin infection model [192]. However, the true nature of these observations needs to be clarified, as LTA purity even from commercial preparations has been questioned [161].

Overall, these experimental data reveal the capacity of "commensal" *S. epidermidis* to specifically shape cutaneous immunity (innate and adaptive responses) and consequently decrease infection burden in the host. The capacity of *S. epidermidis* to induce similar effects in humans remains to be proven. Nevertheless, this idea can be somewhat supported by *in vitro* findings, whereby human monocytes, monocyte-derived dendritic cells (moDC) and T lymphocytes stimulated with *S. epidermidis* displayed an anti-inflammatory profile, with high production of IL-10 [193]. Further *in vivo* and human microbiome studies may provide a deeper understanding of the complex nature of this microorganism-host interaction.

## Innate immune response during infection

### *Recognition*

Innate immune responses are triggered by the detection of microbial structures through pattern-recognition receptors (PRRs) on immune cells and tissue cells. The most studied PRRs are toll-like receptors (TLRs), which recognize a broad range of bacterial derived macromolecules [194].

*S. epidermidis* triggers immune responses partly via TLR-2 (which often forms heterodimers with TLR-1 and TLR-6 [195]), similar to *S. aureus* [196, 197], which can recognize different bacterial cell wall molecules including lipoproteins, LTA and peptidoglycan (PDG) (Figure 4-10) [195, 198], although some of its ligands are still controversial [199]. Secreted components can also be recognized and activate the immune system, as it was shown for *S. epidermidis* PSM, which is recognized by TLR-2/TLR-6 heterodimers [200].

Recognition of *S. epidermidis* via TLR-2 has been shown for keratinocytes [201, 202], endothelial cells [203], or human fibroblasts [204], and has also been demonstrated in TLR-2 transfected human embryonic kidney (HEK)293 cell line [205]. Furthermore, in preclinical models of *S. epidermidis* bacteraemia or subcutaneous/soft tissue foreign-body infection, an up-regulation of TLR-2 and the adaptor molecule MyD88 has been observed upon infection [206-208]. The use of TLR-2 KO in bacteraemia models with neonatal and adult mice resulted in delayed clearance, especially at early time-points after infection [205, 209, 210]. These data suggest that TLR-2 is involved in the early responses to *S. epidermidis* infections although is not essential for clearance of the infection [210].

Responses towards *S. epidermidis* can also occur independently of TLR-2, as it was shown in the models using TLR-2 KO mice [209]. Other PRRs that may potentially be involved in *S. epidermidis* sensing are NOD-like receptors, as they recognize *S. epidermidis*-derived PDG [211]. CD14, expressed mostly in monocytes and macrophages, is a TLR-2 co-receptor that may contribute to *S. epidermidis* recognition in some cell subsets [204]. PSMs produced by *S. epidermidis* can be sensed by formyl peptide receptor 2 (FPR2/ALX) [212, 213], expressed in neutrophils and involved in their recruitment to the infection site [214]. To date, the contribution of these receptors *in vivo* has not been addressed.

***Induction of antimicrobial peptides (AMPs)***

Human AMPs are a heterogeneous group of amphipathic peptides, which may be subdivided depending on their structure and function. AMPs functions include rapid, direct killing of microbes and activation/modulation of immune responses, such as cell recruitment or chemokine production. One of the most effective early responses of the host to pathogenic insults is mediated through human β-defensins (hBD). *In vitro* experiments with keratinocytes or skin explants have shown that *S. epidermidis* or its culture supernatants can elicit high levels of hBD-2 and hBD-3 but not hBD-1 [202, 215-218], and RNase7 and cathelicidin LL-37 in epithelial cells [219]. This AMP induction may be beneficial under healthy conditions to counteract more pathogenic species [217, 218] but can be also expected to contribute to host defence in *S. epidermidis* superficial or ocular infections.

Of relevance, some of them (hBD-2, hBD-3, LL-37 and human alpha defensin (HNP)-1) have been proven, to different extents, to be effective against *S. epidermidis in vitro* [220-223], although no data is available from *in vivo* studies. Nevertheless, the studies mentioned above showed some discrepancies in terms of AMP killing capacity, which could be explained by differences in strains used, as some of them may possess mechanisms against AMPs. More relevant in the context of *S. epidermidis* DRI, other cell types including neutrophils and monocytes can produce AMPs. These AMPs will often be located in the phagolysosomes, where they can contribute to bacteria killing. Of interest, hBD-3, LL-37 and hepcidin 20, a liver-derived AMP, have been shown to reduce *S. epidermidis* attachment and/or biofilm formation *in vitro* [224-226]. The mechanisms of action is currently unknown, although for hBD-3 a decrease in icaA and icaD expression and increase of icaR were associated with the observations [226].

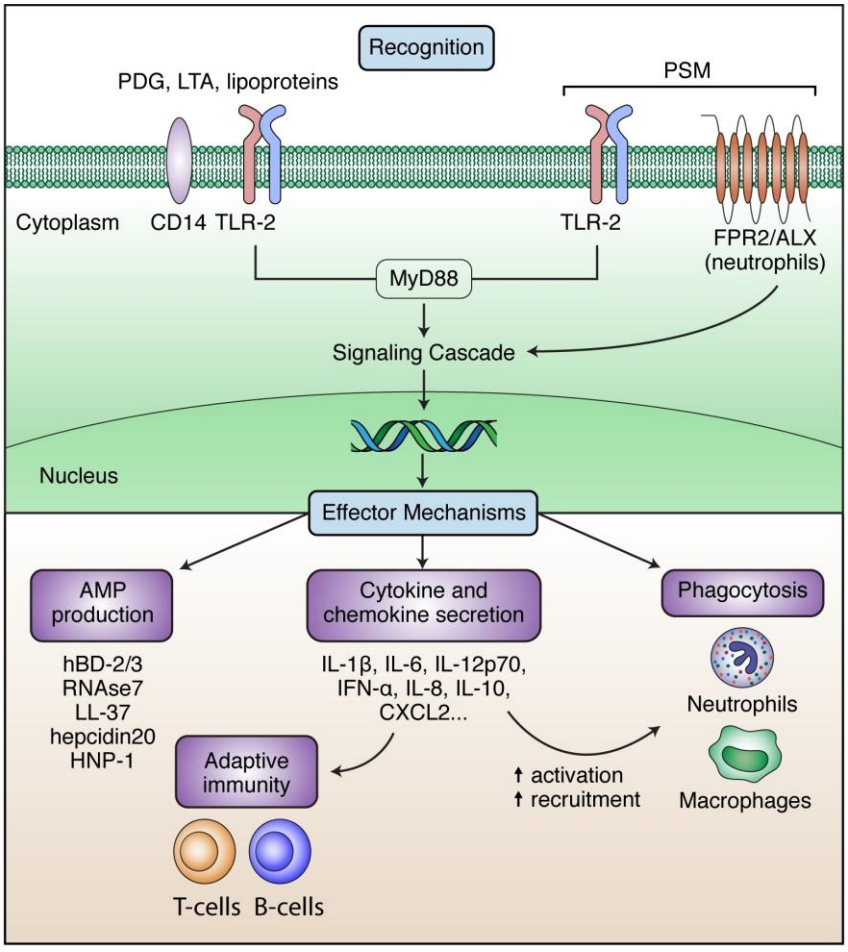


**Figure 4-10** Summary of *S. epidermidis* recognition and subsequent effector mechanisms. Recognition of *S. epidermidis* or its secreted proteins can occur via TLR-2 (in red), which forms heterodimers with TLR-1 and TLR-6 and can also associate with other non-TLR molecules (unspecified partner coloured in blue). Other receptors recognizing *S. epidermidis* include CD14 and FPR2/ALX. Upon recognition, downstream signalling and effector mechanisms are triggered, including secretion of AMPs, phagocytosis by neutrophils and macrophages and secretion of cytokines and chemokines from numerous cell types, which will orchestrate additional innate and adaptive immune responses.

***Phagocytosis/killing by neutrophils and macrophages***

Phagocytosis by neutrophils is one of the most important mechanisms for elimination of contaminating or infecting bacteria. Neutrophils migrate to the site of infection, following host signals (e.g. chemokines, AMPs) or sensing bacterial components as mentioned above. At the infection site, neutrophils will internalize opsonized bacteria forming a phagosome and, finally, bacteria will be destroyed in the phagolysosome by the action of reactive oxygen species (ROS), proteases and AMPs. An additional mechanism to kill bacteria has been described for neutrophils: the generation of neutrophil extracellular traps (NETs) or NETosis. Nuclear and mitochondrial DNA is released to the extracellular space to form NETs, which contain high local concentrations of intracellular antimicrobial proteins. Although literature is still limited, *S. epidermidis* biofilms have been shown to induce DNA release and NETosis *in vitro* [227, 228]. Macrophages are also able to phagocytose and destroy *S. epidermidis* [229] with similar mechanisms, and further present antigens to T cells. Phagocytosis of *S. epidermidis* by macrophages is enhanced following stimulation with IFN-γ *in vitro* [183] and *in vivo* [230].

Phagocytes will also act against biofilms. It has been shown that neutrophils can bind to opsonized but also non-opsonized biofilms, partly by recognizing EPS [228]. Nevertheless, it is generally accepted that the biofilm mode of growth will protect bacteria from phagocytosis, despite some discrepancies in the literature that have been discussed elsewhere [161]. Furthermore, biofilm mode of growth, most often studied in PIA-producing strains, has been shown to decrease killing efficiency in macrophages and neutrophils [127, 131, 157, 160].

Interesting observations were made when comparing the phagocytosis of *S. epidermidis* and *S. aureus* biofilms, with the latter being more likely infiltrated and engulfed [231]. However, although *S. aureus* was more likely phagocytosed, this does not always correlate with the capacity of neutrophils to kill the bacteria. In fact *S. aureus* has several mechanisms to avoid lysis by neutrophils and to persist intracellularly [232]. *S. epidermidis* does not appear to possess similar mechanisms. However, some strains are killed less efficiently, potentially by having a low capacity to prime the oxidative response of neutrophils [233], or as described before by their biofilm mode of growth. These observations, together with lower induction of neutrophil apoptosis, may lead to intracellular survival and could partially explain the low inflammatory nature and chronicity often associated with *S. epidermidis* infections.

***Cytokine and chemokine secretion***

Cytokines are a broad group of secreted proteins that play a role in intercellular communication, with a broad range of functions within the immune system as cell recruitment, differentiation and

activation. Interleukins and other factors play an essential role in leukocyte communication and differentiation, while chemokines are mainly involved in cell recruitment. *In vitro* stimulation of peripheral blood mononuclear cells with different staphylococcal species showed a rapid release of pro-inflammatory cytokines such as IL-1β, IL-6, IL-12p70 or IFN-α [234]. Of note, *S. epidermidis* induced lower levels of pro-inflammatory cytokines compared to *S. aureus* [234]. Studies with monocytes/macrophages have also observed IL-6, TNF-α and IL-1β release after *S. epidermidis* stimulation [235, 236]. Laborel-Préneron *et al.* reported that stimulation of moDC with commensal *S. epidermidis* induced a more anti-inflammatory profile in contrast to stimulation with commensal strains of *S. aureus*, with high levels of IL-10 being a key differentiator. Nevertheless, pro-inflammatory cytokines such as IL-6 and TNF-α were also detected [193]. Similar observations have been made from *in vivo* studies: IL-6, TNF-α and IL-1β are typically observed in serum in the first hours post-challenge with live or inactivated *S. epidermidis* [159, 180, 209, 237, 238], or in tissue exudates/homogenates from experimental DRI models [207, 239]. The regulatory cytokine IL-10 is also present *in vivo* [159] and it has been shown that *S. epidermidis* inoculation result in higher IL-10 levels compared to *P. aeruginosa* in an intradermal infection model [240]. In a *S. epidermidis* DRI mouse model it was shown that IL-10 was involved in reducing infection-associated morbidity, with higher levels of pro-inflammatory cytokines and greater weight loss in IL-10 KO animals. Interestingly, bacterial counts were the same in both wild-type and KO strains, suggesting that IL-10 does not impact bacterial clearance [241]. Overall, despite differences due to different *S. epidermidis* strains and its effect in different tissues, it can be hypothesized that lower induction of pro-inflammatory cytokines together with high IL-10 production, can contribute to the sub-acute nature of *S. epidermidis* infections.

Multiple chemokines are also released upon *S. epidermidis* infection. Secretion of IL-8, important for neutrophil recruitment, has been described *in vitro* and in the first hours post-infection in *in vivo* studies [207, 237-239]. CXCL-1 and CXCL-2, mostly produced by macrophages (via TLR-2 recognition but also by other mechanisms), have also been observed in bacteraemia and peritonitis models [159, 180, 205, 209]. Additionally, a murine peritonitis model revealed increasing levels of numerous chemokines upon challenge with *S. epidermidis* supernatants [242].

***Platelet activation/aggregation***

The aggregation and activation of platelets in the presence of bacteria was first described over 25 years ago [243] and yet the nature of this interaction has only recently been elucidated. Platelets and bacteria can interact in three ways: the indirect binding of bacteria to a plasma protein (which is a ligand of a platelet receptor), the direct recognition of bacteria by platelet receptors and the binding of secreted bacterial products to platelets [244]. Only the first type has been described for

*S. epidermidis*, where the SdrG has been described to bind platelets in a fibrinogen and Ig-dependent manner; an interaction that leads to platelet aggregation [118]. *S. aureus* or *Streptococcus* have been shown to interact with platelets in other ways, which can lead to sepsis or thrombosis but also can play a role in internalization of bacteria by platelets or release of antimicrobial components and immunomodulatory factors [244]. Future studies will be required to elucidate if *S. epidermidis*-platelets interaction is limited to SdrG or if, like other bacteria, possess multiple mechanisms.

## Adaptive immune response during infection

Adaptive immunity refers to antigen-specific and long-lasting immune responses that are mediated by lymphocytes. Adaptive immunity can be broadly divided in cellular responses, represented by T helper (Th) and cytotoxic T lymphocytes, and humoral responses, represented by B lymphocytes and antibodies. Classically, extracellular bacterial infections have been shown to trigger mostly Th1 cell responses, but more recently Th17 responses have also been linked to the clearance of bacterial infections. Of relevance, an *in vivo* model using immunocompromised mice have shown a higher susceptibility for *S. epidermidis* DRI in mice lacking T cells or T and B cells [245], highlighting a role for adaptive immune responses in infection clearance.

Arising from its status as a commensal microorganism, *S. epidermidis* is expected to elicit adaptive immune responses in humans from early in life. This has been proposed to be largely triggered by a pattern of transient self-resolving infections due to micro-invasions, rather than resulting from local response due to colonization [246], but the latter cannot be excluded. These life-long interactions will lead to the generation of an antibody repertoire and a set of memory T and B cells that may confer partial protection from infection. Generation of adaptive immune responses require the presentation of antigens to T cells by antigen presenting cells (APCs), primarily dendritic cells (DC), which will also contribute to T cell polarization. It has previously been shown that CD103 skin-resident DC, after interaction with commensal *S. epidermidis,* generates CD8+IL-17A+ T cells with the capacity to enhance protective responses in the skin [189]. Upon infection, it can also be expected that certain DC subtypes, already present in the tissue or that will migrate there, will shape adaptive immune responses. Data available for *S. epidermidis* interaction with DCs is very limited but it has been observed, *in vitro* and *in vivo,* that *S. epidermidis* can lead to DC activation with an increase in co-stimulatory molecules such as CD86 or CD80 and antigen presenting molecules such as MHC-II [193, 247-249]. Studies describing cytokine secretion by DCs stimulated with *S. epidermidis* (whole bacteria or its secreted proteins) have yielded somewhat inconsistent results. For example, IL-10 was not highly secreted when bone-marrow DCs were stimulated with

*S. epidermidis* [247], but the stimulation of moDCs with *S. epidermidis* secreted proteins led to high IL-10 secretion [193]. The inconsistency between these reports may be due to the different sources of DC and stimuli used, which can lead to different outcomes by activating distinct pathways. The relevance of the stimuli is further highlighted in a series of experiments from Durantez *et al.* [250]. *S. epidermidis* PSM-derived peptides combined with ovalbumin were able to trigger cytotoxic T cell responses, however, this was only observed after those peptides were presented via APCs together with stimuli specific for TLR-3, TLR-7 and TLR-9 [250]. Further experiments are required to clarify the exact role of APCs and different DC subsets in priming and polarizing the T cell response.

With regards to humoral responses, antibodies against *S. epidermidis* proteins have been detected in serum and saliva of healthy individuals [251, 252], but levels are generally lower compared to *S. epidermidis* infected patients [252]. Antibodies against biofilm components and cytoplasmic proteins have been found to be predominant [251].

To assess the potential use of antibody titters in diagnosis of infection, serum antibody titters against staphylococcal proteins have been measured in patients with *S. aureus* or *S. epidermidis* infections (such as wound infections, bacteraemia or DRI). Recently, a multiplex antibody detection-based immunoassay was evaluated for the diagnosis of prosthetic joint infections (PJI). The assay included protein antigens from several strains: diverse staphylococci, *Streptococcus agalactiae* and *P. Acnes* [253]. The test showed a slightly lower sensitivity than C-reactive protein and erythrocyte sedimentation rate, however was able to diagnose around 50% of patients, which were culture positive but presented low systemic inflammation values [253].

Another goal of humoral response studies is to identify immunogenic proteins, which can lead to development of therapeutic and/or prophylactic treatments. Studies employing 2D protein electrophoresis or phage display technology with the aim of identifying *S. epidermidis* immunogenic proteins have been performed in rabbits [254] and humans [255]. Sera of rabbits immunized with live *S. epidermidis* were used to detect relevant immunogens from within a cell wall fraction. Mice were then immunized with several selected proteins, five of whom (Na+/H+ antiporter, Acetyl-CoA C-acetyltransferase, lipoate ligase, cysteine synthase and alanine dehydrogenase) lead to a significant reduction of bacterial loads in a murine infection model [254]. Other proposed immunogenic proteins include AtlE, Staphylococcal conserved antigen B (ScaB), and GehD lipase, which elicited higher antibody titters in infected patients compared to non-infected subjects. Active immunization of mice with these antigens resulted in production of specific antibodies with *in vitro* opsonisation capacity against *S. epidermidis* [255]. An anti-SdrG

antibody was shown to reduce mortality in a neonate bacteraemia rat model and to decrease bacterial counts in a DRI (endocarditis) rabbit model [256], although it failed in a clinical trial to prevent late-onset sepsis in low-birth weight neonates [257]. More recently it was shown that immunization with staphylococcal Major amidase (Atl-AM), a cell wall hydrolase present in some *S. epidermidis* and *S. aureus* strains, increases antibody levels against that protein in mice [258]. In the same study, immunized animals challenged with a lethal intraperitoneal dose of *S. epidermidis* showed a better survival and lower bacterial counts in tissues compared to mock immunized animals [258]. Additionally, immunized mice also presented higher levels of Th1 and Th2 cells, although it did not elucidate which responses were the most relevant for the increased survival. Immunizations with Aap or with antibodies against surface proteins have also been shown to reduce colonization in a murine DRI model by ultimately inhibiting biofilm formation [259, 260]. Despite the fact that their efficacy against *S. epidermidis* infections has not been tested *in vivo*, antibodies against poly-β-1,6-N-acetylglucosamine (PNAG/PIA) and phosphonate ABC transporter substrate binding protein (PhnD) have shown efficacy against *S. epidermidis* biofilm formation *in vitro* [261, 262]. A recent study focused on staphylococcal adhesion proteins, which contain long stretches of Sdr, and are key virulence factors for *S. epidermidis* and also *S. aureus*. The study led to the discovery of two novel bacterial glycosyltransferases, SdgA and SdgB, which can modify all Sdr-proteins to protect them from cleavage by cathepsin G (a neutrophil protein). Neutralization of these enzymes may be the next opportunity for an effective anti-staphylococcal approach [263]. To date, all anti-staphylococcal antibodies tested against *S. epidermidis* and other CoNS (Altastaph, INH A-2 and Pagibaximab) have been found to be ineffective in reducing bacteraemia in neonates [264]. Although there is still much work to be done to fully understand effective immune responses against *S. epidermidis*, on-going research offers several candidates and strategies to develop new therapeutic products.

Additionally, there are also T cell-mediated immune responses to *S. epidermidis* although they are poorly characterized. Based on *in vitro* studies, it has been suggested that *S. epidermidis* opsonisation with IgG promotes Th17 responses [265], although the role of this phenomenon *in vivo* has not been shown. On the other hand, in an *in vivo* model of foreign-body infection, a beneficial effect of IFN-γ injections has been shown, suggesting a protective role of Th1 dominated responses in bacterial infections [230]. Based on cytokines induced by *S. epidermidis* in the different studies (e.g. IL-6, IFN-γ or IL-12), a Th1/Th17 polarization may be expected in such infections. This goes in line with the findings of Ferreirinha *et al.*, who observed that injection of PNAG-producing *S. epidermidis* in mice lead to IFN-γ and IL-17A producing T cells [159]. Also, as mentioned above, immunization of mice with Atl-AM led to an increase in Th1 and Th2 cells

(Th17 cells were not evaluated on that study). Immunization also led to a higher survival; however, direct effect of T cell responses in that finding was not further addressed [258].

### Bone system interactions

The usual chronic nature of *S. epidermidis* osteomyelitis will eventually lead to an inflammatory environment within the bone system, which is of special relevance in the context of ODRIs. Bone as an organ is particularly sensitive to chronic inflammation, due to its continuous remodelling process that is influenced by different components of the immune system and inflammatory pathways [266]. Due to their potent capacity to stimulate the formation and activity of bone resorbing osteoclasts, pro-inflammatory cytokines such as TNF-α, IL-1β and IL-6 [267-269] are powerful drivers of osteolysis. Conversely, the function of the bone matrix-producing cells, osteoblasts, is also negatively affected by pro-inflammatory cytokines, such as TNF-α [270-272] or IL-1β [273] (Figure 4-11). Therefore, persistently elevated levels of pro-inflammatory cytokines in the local bone microenvironment frequently result in marked osteolysis, driven by enhanced osteoclast activity at the site of infection (Figure 4-11) [274], which is likely compounded by a diminished capacity of osteoblasts to produce new bone matrix.

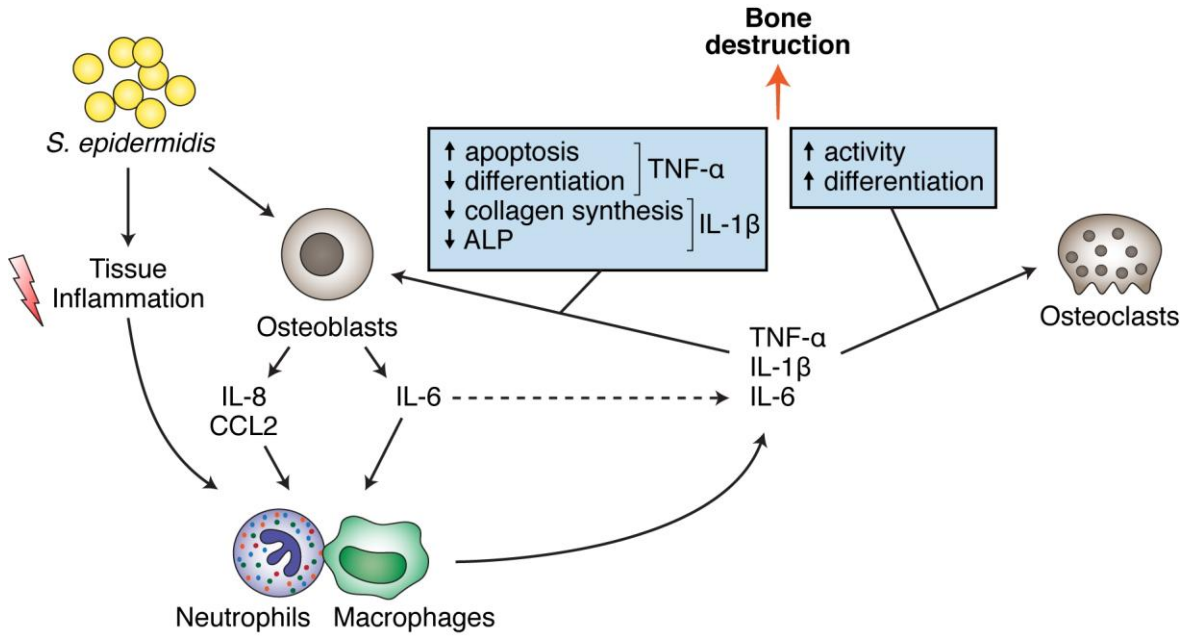


**Figure 4-11** *S. epidermidis* direct and indirect effects on bone cells (osteoblasts and osteoclasts), leading to bone destruction. ALP: Alkaline Phosphatase.

Despite the importance of *S. epidermidis* as a causative agent in ODRI, relatively little information exists about the interactions of *S. epidermidis* with resident bone cells, in particular the molecular mechanisms underlying the bone loss observed in *S. epidermidis*-induced osteomyelitis. The production of cytokines by innate and/or adaptive immune cells in response to *S. epidermidis* is

undoubtedly an important contributor to the enhanced bone resorption observed at the site of infection, however it is becoming apparent that the osteoblast itself may also directly contribute to the production of pro-inflammatory cytokines and therefore further perturb the balance of bone formation and resorption in favour of bone destruction. A recent study has shown the induction *in vitro* of IL-6 by primary human osteoblasts stimulated with *S. epidermidis* [223]. *S. epidermidis* infection also induced chemokines, such as IL-8/CXCL8 and CCL2/MCP-1, suggesting that osteoblasts may be capable of further recruiting immune cells following an encounter with *S. epidermidis*. Interestingly, the authors also demonstrated that osteoblasts were activated not only by the planktonic form of *S. epidermidis* but also by components of *S. epidermidis* biofilms. This suggests that, rather than the relatively simplistic view of the osteoblast for producing bone matrix and regulating osteoclast activity, osteoblasts may also serve an important role as sensors and initiators of immune responses directed against bacteria resident in the local bone microenvironment.

Additionally, *in vitro* studies have observed a decrease in osteoblast viability when co-cultured with *S. epidermidis* [275, 276]. *S. epidermidis* products (resulting from washing bacteria) have been suggested to induce bone destruction as they increased calcium release from murine bones *in vitro* [277]. This is in stark contrast to *S. aureus*, which has been extensively studied in this context and is capable of influencing the behaviour of both osteoblasts and osteoclasts. For example, *S. aureus* has been demonstrated to induce TRAIL-dependent apoptosis in osteoblasts [278-281] and can stimulate expression of osteolytic factors [282] or reduce the expression of its inhibitors [281], exacerbating the osteolytic effect. Furthermore, specific bacterial proteins have been identified as responsible for some of these effects on osteoblasts such as *S. aureus* protein A, which has been demonstrated to bind directly to TNF receptor 1, resulting in an inhibitory effect on proliferation, the induction of apoptosis, and the stimulation of RANKL expression [283, 284].

Regarding the effects of bacterial infection on osteoclasts, a number of studies have reported the effects of inactivated *S. aureus*, or specific *S. aureus* components, for affecting osteoclast formation and/or activity [285-288]. Conversely, staphylococcal LTA inhibits osteoclastogenesis through stimulation of TLR-2 activity [285]. Such conflicting data strongly argues for the use of (preferably live) intact bacteria in such osteoclastogenesis assays rather than purified bacterial components. When the effect of intact bacteria on osteoclastogenesis was recently investigated, *S. aureus* was demonstrated to have both direct and indirect stimulatory effects on osteoclasts *in vitro* [289]. By inducing activation of macrophages and thereby stimulating the production of pro-inflammatory cytokines, *S. aureus* indirectly enhanced the formation of osteoclasts from precursor cells. Additionally, *S. aureus* could also directly infect mature osteoclasts, resulting in increased cell

fusion and enhanced bone resorbing capacity. Much less is known regarding direct interaction of *S. epidermidis* and osteoclasts, although it is expected that induction of pro-inflammatory cytokines will enhance bone destruction in similar ways.

Given the multitude of different effects of *S. aureus* on osteoblast and osteoclast function, it is likely that *S. epidermidis* can also negatively affect the capacity of osteoblasts to produce bone matrix and/or enhance osteoclast formation and function, although much further work is necessary to clarify if this is indeed the case.

Lastly, the interaction of *S. epidermidis* with bone cells could provide a location where bacteria can persist and prolong ODRIs. Both *S. aureus* and *S. epidermidis* are capable of invading osteoblasts *in vitro* [290, 291], however the mechanism underlying this phenomenon appears to differ between these two species. *S. aureus* requires binding to the ECM protein fibronectin, mediated by $\alpha_5\beta_1$ integrin [292], whereas *S. epidermidis* internalization by osteoblasts is not affected by interfering with fibronectin binding or blocking, suggesting a different mechanism [291]. This is supported by the findings of a recent study that reported SdrG mediates the binding of *S. epidermidis* to osteoblasts *in vitro*, an effect likely mediated through SdrG binding to $\alpha_V\beta_3$ integrin [187]. However, this immune evasion mechanism may be of more importance for *S. aureus* rather than *S. epidermidis per se*, since the capacity of *S. epidermidis* for invading osteoblasts *in vitro* does not appear to differ between commensal strains and clinical isolates of *S. epidermidis* obtained from infected orthopaedic devices [293]. This is reinforced by a recent *in vitro* study demonstrating that *S. epidermidis* as well as other opportunistic pathogens such as *S. lugdunensis* and *Enterococcus faecalis* were incompetent at being internalized by MG63 human osteoblastic cells, being internalized at a level approximately three orders of magnitude lower than that observed with *S. aureus* [294]. Osteoclasts are also able to internalize, at least, *S. aureus.* Given the inherent phagocytic capacity of osteoclasts, it may be that internalization of *S. aureus* by osteoclasts relies on such a phagocytic mechanism of uptake. This raises the possibility that *S. epidermidis* may also be the object of uptake by osteoclasts. Together with the previously stated ability of *S. epidermidis* to bind to $\alpha_V\beta_3$ integrin, which is highly expressed by osteoclasts [295], this further suggests that *S. epidermidis* may bind to and be internalized by osteoclasts, although this and the subsequent phenotypical changes resulting from such an interaction requires to be validated experimentally. Taken together, this suggests that while the persistence of orthopaedic implant-associated *S. aureus* infections *in vivo* may well stem from its enhanced ability to invade osteoblasts, and potentially osteoclasts, other mechanisms, such as biofilm formation, may underlie the persistence of *S. epidermidis* in implant-related infection.

Finally, the integration of immune responses within the bone system in the context of *S. epidermidis* infection has been largely unexplored. The number of models described for *S. epidermidis* bone infection is limited (Table 4-3) and none have really focused on host immune responses. Most of the data available is based on *S. aureus* models, where a combination of Th1/Th17 responses has been observed [296, 297], although it is not clear if this response is beneficial or detrimental to the host as no bacterial clearance was achieved [298, 299]. The observation that anti-IL-12p40 conferred protection in *S. aureus* infected C57BL/6 mice supported the hypothesis that skewed Th1/Th17 responses may be harmful [299], as IL-12/IL-23p40 plays a role in polarization of these cell types. This observation, however, could be due to a decrease in myeloid-derived suppressor cells (MDSC) that otherwise would impair immune responses in the vicinity of an implant, as described by Heim *et al.* [300]. The use of different murine strains, inoculum dose and models are factors contributing to the disparity in the available data. Furthermore, the differences between *S. aureus* and *S. epidermidis* are quite significant, and so further work focused on *S. epidermidis* is required to provide a proper understanding of adaptive immune responses to *S. epidermidis* bone infection.

**Table 4-3** Bone-related infection models with *S. epidermidis* as infective agent

| Species | Gender, Age/weight | Strain | CFU dose | Inoculation Method | Study Purpose | Findings | Comments | Ref. |
|---|---|---|---|---|---|---|---|---|
| Mouse | ND | ND | $10^8$ CU | Bacteria inoculated at the end of the wire (joint area) | Protocol available only | NA | Prosthetic joint infection model | [301] |
| Wistar rat | Males, 250-300 g | IDRL-8883 clinical isolate (MRSE strain) | $10^7$ CFU and colonized wire | Bacteria injected (0.1ml) into the tibia and a pre-colonized wire was implanted | Established a model of foreign body-associated osteomyelitis to test Tedizolid treatment and to compare with standard treatment | Tedizolid alone presented better results than vancomycin monotherapy. Addition of rifampin to both treatments increased effectivity of therapy | No fracture. Addition of sclerosing agent | [302] |
| Wistar rat | Males, 12-week old | Clinical isolate (MRSE strain) | $10^3$, $10^5$ and $10^8$ CFU | Bacteria injected (0.03 ml) into femoral defect | Establish a model to study *S. epidermidis* non-unions | Low-grade *S. epidermidis* contamination can prevent bone healing, even in the absence of infectious signs | Bone osteotomy performed. Self-clearance in some animals from low dose group (33%) | [303] |
| Wistar rat | Males, 12-week old | Clinical isolate (MRSE strain) | $10^5$ CFU | Bacteria injected (0.03 ml) into femoral defect | Test systemic and local administration of vancomycin or MSC on infection | | Bone osteotomy performed | [304] |
| Wistar rat | ND, 350 - 450 g | *S. epidermidis* ATCC 35984 | $10^4$ CFU | Bacteria injected into surgical site before wound closure (calvarial defect reconstituted with different materials) | Compare silicon nitride implants with titanium and PEEK implants in terms of bone formation and prevention of infection | Silicon nitride implants showed higher osseointegration and lower presence of live bacteria | Only histological findings with a very small group size | [305] |
| Sprague-Dawley rat | Male, adult 425 ± 37 g | Clinical isolates of *S. epidermidis* and *S. aureus* | $1.5x10^7$ (*S. epidermidis*) $1.5x10^4$ (*S. aureus*) | Bacteria injected (0.05 ml) through a PTFE catheter into tibia medullary canal. Catheter left on place | To test $^{68}$Ga-DOTA-Siglec-9 PET/CT imaging in *S. aureus* and *S. epidermidis* infection | $^{68}$Ga-DOTA-Siglec-9 PET/CT was able to detect tissue inflammation but not able to distinguish *S. aureus* from *S. epidermidis* infections | No fracture. 5% sodium morrhuate added before inoculation in *S. epidermidis* group but not in *S. aureus* or control group | [306] |
| New Zealand White rabbit | ND, 2.5 - 3.5 kg | *S. epidermidis* ATCC 35984 | $10^3$, $10^4$ and $10^5$ CFU (pilot study) $10^4$ CFU (main study) | Bacteria injected (in 1 ml) into knee joint, near inserted implants (stainless-steel screw and UHMWPE washer) | To study the effect of Allicin (antibacterial principle of garlic) in biofilm formation in a prosthetic joint infection model | Allicin alone and in combination with Vancomycin were effective in reducing biofilm formation | Prosthetic joint infection model | [307] |
| New Zealand White rabbit | Female, adult 2.46 ± 0.23 kg | Clinical isolate (MRSE strain) | $10^7$ CFU | Bacteria injected (in 0.1 ml of saline) into tibia medullary cavity. Afterwards, a bone cement cylinder was inserted | To test effectivity of chitosan loaded PMMA bone cements *in vivo* | Quaternized chitosan-loaded PMMA was able to reduce scoring and CFU counts when compared to sole, gentamicin or chitosan loaded PMMAs | No fracture | [308] |
| New Zealand White rabbit | Male, skeletally mature 3.2 ± 0.37 kg | Clinical isolates and *S. epidermidis* ATCC 35983 | $10^8$ CFU (*S. epidermidis*) $10^4$ CFU (*S. aureus*) | Bacteria injected (in 0.1 ml) into tibia medullary space next to a cement block | To test $^{18}$F-FDG PET/CT imaging in *S. aureus* and *S. epidermidis* infection | *S. epidermidis* infection presented low $^{18}$F-FDG uptake due to limited leukocyte infiltration | No fracture. 5% sodium morrhuate added in medullary canal in *S. epidermidis* groups only | [309] |

| | | | | | | | | |
|---|---|---|---|---|---|---|---|---|
| New Zealand White rabbit | Male, 2.5 - 3.5 kg | *S. epidermidis* Xen 43, bioluminescent strain derived from a clinical isolate | $10^4$ CFU | Bacteria injected (in 0.1 ml of saline) into tibia medullary cavity where an intramedullary electrode was placed | To compare the electricidal effect with an antibiotic treatment | Electrical current was as effective as intravenous doxycycline treatment in a foreign-body infection model | No fracture | [310] |
| New Zealand White rabbit | Male, 4.0 ± 0.5 kg | *S. epidermidis* RP-62A Clinical isolate? | - | Commercially-pure titanium implants were exposed to a $10^6$ CFU/ml solution for 1h at 37°C. Implant placed into the lateral femoral condyle | To study the effectivity of cross-linked albumin coating in infection prevention | The albumin coated implants presented a lower infection rate | No fracture Not clear results: animals where bacteria were detected with gram stain counted as not infected | [311] |
| New Zealand White rabbit | Female, adult, 3.5 – 4 kg | Clinical isolate of *S. epidermidis* | $5x10^7$ CFU | Bacteria were injected into femoral medullary canal and drill hole was closed with a stainless steel screw | To test vancomycin and minocycline alone or in combination with rifampin in an orthopaedic device related infection model | Vancomycin plus rifampin was the most effective treatment, followed by minocycline plus rifampin. No clearance or very low was used with antibiotics alone | No fracture | [312] |
| New Zealand White rabbit | Male, ND | *S. epidermidis* G109-83 and *Bacteroides thetaiotaomicron* N54-83 and clinical isolate N1660-75B | $10^7$ CFU of each strain | Barium-impregnated silicone rubber catheter was introduced into medullary canal and bacteria were injected into it (0.1ml for each) together or separately. Second group was injected directly into medullary canal without a foreign body | Observe influence of foreign-body in a model of osteomyelitis with *S. epidermis* and *B. thetaiotaomicron*, alone or in combination | Both strains, alone or in combination were able to cause osteomyelitis, however in the presence of a foreign-body the severity of osteomyelitis was higher | No fracture 5% sodium morrhuate added | [313] |
| New Zealand White rabbit | Male, ND | *S. epidermidis* G109-83 and clinical isolate *Bacteroides fragilis* N17-85 | $10^7$ CFU of each strain (alone or combined) | Barium-impregnated silicone rubber catheter was introduced into medullary canal and bacteria were injected into it (0.1ml for each) together or separately | Establish a foreign-body-associated osteomyelitis model with *B. fragilis*, *S. epidermidis* or combination of both | Both strains, alone or in combination were able to cause osteomyelitis, however *S. epidermidis* appeared less pathogenic than *B. fragilis* | No fracture 5% sodium morrhuate added | [314] |
| New Zealand White rabbit | Male, ND | *S. epidermidis* G109-83 and *Bacteroides thetaiotaomicron* N54-83 | $10^7$ CFU of each strain | Barium-impregnated silicone rubber catheter was introduced into medullary canal and bacteria were injected into it (0.1 ml for each) | Study ciprofloxacin efficacy in polymicrobial osteomyelitis | Ciprofloxacin showed little efficacy in a polymicrobial device-related osteomyelitis | No fracture 5% sodium morrhuate added | [315] |
| Dog | ND, 10 - 15 kg | *S. epidermidis, S. aureus* and *E. coli* | $10^2$ to $10^8$ CFU? | Bacterial suspension was introduced into femoral canal, with or without implants | Study influence of different implants on infection incidence (materials tested) | All materials increased likelihood of *S. aureus* infection, and only PMMA polymerized *in vivo* increased *S. epidermidis* and *E. coli* infection risk | No fracture | [316] |
| Goat | ND | Clinical isolate *S. epidermidis* | $3x10^5$ CFU | Bacterial suspension inoculated (0.1ml) into wounds around pins placed on tibia | To study the effectivity of electrical current on stainless steel fixator in preventing infection | Small current applied to external fixators decreased the infection percentage | No fracture | [317] |

| | | | | | | | | |
|---|---|---|---|---|---|---|---|---|
| Ile-de-France sheep | ND,<br>4 - 9 years | Clinical isolate *S. epidermidis* | 1-3x10$^{8}$ CFU | Bacteria injected (in 1 ml of PBS) into femur medullary canal.<br>Afterwards, a stainless steel implant was inserted (uncoated, hydroxyapatite-coated or PMMA cemented) | To study the effect of hydroxyapatite and PMMA implant coatings on infection progression | Higher infection rate in animals with an hydroxyapatite-coated implant | No fracture | [318] |

**Abbreviations:** CFU = Colony forming units; PEEK= poly(ether ether ketone); PTFE = polytetrafluoroethylene; $^{68}$Ga-DOTA = $^{68}$Ga-labeled 1,4,7,10-tetraazacyclododecane-1,4,7,10-tetraacetic acid; Siglec-9 = Sialic acid-binding immunoglobulin-like lectin 9; 18F-FDG = 2-deoxy-2-[fluorine-18]fluoro-D-glucose; PMMA = polymethylmetacrylate; NA= Not applicable; ND = Not described; UHMWPE = ultra-high molecular weight polyethylene

# 5. Results

## 5.1 Influence of fracture stability on *Staphylococcus epidermidis* and *S. aureus* infection in a murine femoral fracture model

M. Sabaté Brescó[1, 2], L. O'Mahony[2], S. Zeiter[1], K. Kluge[1], M. Ziegler[2], C. Berset[3], D. Nehrbass[1], R. G. Richards[1], T. F. Moriarty[1]*

[1] AO Research Institute Davos, Davos, CH; [2] Swiss Institute of Asthma and Allergy Research, Davos, CH; [3]AO Foundation, Davos, CH

*Corresponding author:
T F Moriarty, AO Research Institute Davos, AO Foundation, Clavadelerstrasse 8, Davos Platz, CH7270, CH. Phone: +41 81 414 2397, E-mail: fintan.moriarty@aofoundation.org

Running Title: Infection and implant stability

*This manuscript has been published in European Cell and Materials (eCM) journal.*
Eur Cell Mater., 2017 Nov 21; 34:321-340

## Abstract

Fracture related infection (FRI) is a major complication in surgically fixed fractures. Instability of the fracture after fixation is considered a risk factor for infection; however, little experimental data is available confirming this belief. To study our hypothesis that stable fractures lead to higher infection clearance, mouse femoral osteotomies were fixed with either stable or unstable fixation and the surgical site was contaminated with either *Staphylococcus epidermidis* or *S. aureus* clinical isolates. Infection progression was assessed at different time-points by quantitative bacteriology, total cell counts in spleen and lymph node, and histological analysis. Non-inoculated mice were operated as controls. Two inbred mouse strains (C57BL/6N and BALB/c) were included in the study to determine the influence of different host background in the outcome. Stable fixation allowed a higher proportion of C57BL/6N mice to clear *S. epidermidis* inoculation in comparison with equivalents with unstable fixation. No difference associated with fixation type was observed for BALB/c mice. Inoculation with *S. aureus* resulted in a more severe infection for both stable and unstable fractures in both mouse strains; however, significant osteolysis around the screws rendered the stable group functionally unstable. Our results suggest that fracture stability can have an influence on *S. epidermidis* infection, although host factors also play a role. No differences were observed when using *S. aureus*, probably due to a more severe infection which lead to substantial bone destruction. Further studies are required in order to address the biological features underlying the differences observed.


## Introduction

Fracture related infection (FRI) remains one of the most significant complications in the surgical treatment of fractured bones. FRI is often associated with prolonged antibiotic treatment, repeated surgical debridement, implant removal, high healthcare costs and poor functional outcome for affected patients [98, 319]. The prevalence of FRI ranges from 0.5-3% for closed fractures, but can increase up to 30% in open fractures [98, 320]. *S. aureus* and the coagulase-negative staphylococci (CoNS), in particular *S. epidermidis,* are the most prevalent species in FRI, accounting together for 50-75% of all cases [93, 321].

The risk of developing an infection associated with any implanted device is increased by the presence of the device itself [322, 323]. This is because the device acts as a foreign-body that provides a surface for adhesion and biofilm formation to any microorganism entering the wound. Other risk factors for implant associated infections include patient characteristics such as advanced age, smoking or co-morbidities such as diabetes or obesity [319, 324, 325]. One additional factor that is specific to surgically fixed fractures is the biomechanical properties of the fixation. It is

widely known that healing of fractures is influenced by biomechanics [326-328]: when fracture fixation provides absolute stability, the fragments are compressed together with little strain under loading, leading to primary bone healing. In contrast, when the fixation is less rigid, displacement may occur under load and the fracture tends to heal due to secondary bone healing with callus formation [36, 329]. The stability of the fixation is also considered to be a critical factor in FRI [330, 331]. A few preclinical experimental studies [331-334] have provided supportive evidence for the association between stable fixation and reduced infection risk. However, there was poor standardization of the stability of the fractures within these models and no studies to date have investigated this phenomenon for *S. epidermidis* FRI. FRI caused by *S. aureus* has been intensively studied in both clinical and basic science literature, with numerous preclinical *in vivo* models available [296, 335-339]. However, the literature describing *S. epidermidis* FRI is comparatively scarce and fewer *in vivo* preclinical models are available [340].

The aim of our study was therefore to study FRI progression under different mechanical environments (stable and unstable fixation). We used an established model developed with two types of implants (rigid and flexible) that lead to different types of bone healing [329, 341, 342]. This model has shown that under rigid fixation, bone healing occur via a mixture of intramembranous and some endochondral ossification, while with flexible fixation, healing occurs mainly via endochondral ossification with the formation of a large stabilizing callus observed at day 14 [329, 342]. Mechanical testing data also confirmed that in vertical plane, the flexible plate was only ¼ of the stiffness of the rigid plate, when bridging two fragments separated by a 0.45 mm gap [329]. These implants were therefore used in our study to determine the role of fracture stability in infection rate for both *S. epidermidis* and *S. aureus.* Two well-characterized inbred mouse strains, C57BL/6N and BALB/c. C57BL/6N mice were selected as they have been previously used in previous studies with MouseFix$^{TM}$ implants. As the strain is T helper (Th)-1 skewed, we added a Th2-skewed strain (BALB/c) to determine if the observations are consistent across different host backgrounds.

## Materials and methods

### Animals

The study was approved by the ethical committee of the canton of Graubünden in Switzerland (TVB 11/2013) and was carried out in a research facility accredited by Association for Assessment and Accreditation for Laboratory Animal Care (AAALAC) International. Skeletally mature (20-28 weeks old, average weight ± SD: 24.34±2.12 g), female, specific pathogen free (SPF) C57BL/6N and BALB/c mice (Charles River, Germany), were used in this study. All animals were allowed to acclimatize to experimental conditions for at least two weeks prior to the start of the study. Mice were randomly housed in individually ventilated cages (XJ, Allentown) under a 12 hour dark/light cycle in groups of three to six. Cages were changed weekly and mice were re-housed in the same groups post-surgery. Cages were randomly assigned to the different groups and all animals within the same cage were assigned to the same treatment group. Animals were fed with a standard diet (3436, Provimi Kliba) and had free access to sterile water at all times. Any animal excluded from the experiment due to fracture or implant failure was replaced unless stated otherwise.

### Study design

The study was performed using groups of mice with rigid fixation to those with flexible fixation according to the scheme outlined in Figure 5-1. The first series of experiments compared C57BL/6N (Figure 5-1A) and BALB/c (Figure 5-1B) mice with rigid fixation to those with flexible fixation under aseptic (non-inoculated) conditions. This was repeated for mice inoculated with *S. epidermidis* (See Figure 5-1A, B for time-points and group size). The second series of experiments involved inoculation with *S. aureus*, which was performed at the standard dose in C57BL/6N mice, but that series was discontinued due to rapid onset of osteolysis leading to unstable fractures in both groups. Therefore, the experiment was repeated in C57BL/6N and BALB/c mice at lower inoculation (See Figure 5-1C-D for time-points and group size). Age-matched C57BL/6N and BALB/c mice (N=6-8), without any surgical intervention, were euthanized as controls to obtain baseline levels of cell counts.

### Bacteria and inoculum preparation

The two test microorganisms were *S. epidermidis* Epi 103.1 and *S. aureus* JAR06.01.31, both of which are clinical isolates. *S. epidermidis* Epi 103.1 was obtained from a patient with chronic implant-related bone infection (Trauma Center BGU Murnau, Germany), has a weak *in vitro* biofilm formation capacity according to the scoring system of Stepanovic [343] and is resistant to benzylpenicillin and fusidic acid. *S. aureus* JAR06.01.31, was originally cultured from an infected

hip prosthesis (University Hospital Basel, Switzerland) [344, 345], belongs to sequence type (ST) 15, displays weak biofilm formation capacity, and is resistant only to benzylpenicillin. Both strains are deposited in the Culture Collection of Switzerland (CCOS): *S. epidermidis* Epi 103.1 (awaiting number) and *S. aureus* JAR06.01.31 (CCOS 890).

For inocula preparation, a single colony was resuspended in 40 ml of tryptone soy broth (TSB) (Oxoid) and cultured overnight at 37°C, 100 rpm. On the day of the surgery, the bacteria were sub-cultured into pre-warmed TSB and incubated at 37°C and 100 rpm for at least 2 hours to obtain a log-phase culture. When a pre-defined optical density corresponding to $4.6x10^7$ Colony Forming Units (CFU)/ml was reached, the culture was centrifuged at 8500 g for 5 minutes and resuspended in the same volume of phosphate buffered saline (PBS) (Sigma-Aldrich). Finally, the suspension was further diluted, as required, in PBS to prepare the inoculum, which was used within 1 hour of preparation. The target inoculum was set to $1 \times 10^4$ CFU for the standard *S. epidermidis* and *S. aureus* dose, and $1x10^3$ for the low *S. aureus* dose.

**Implants and surgery**

Commercially pure Titanium (CpTi) 4-hole rigid and CpTi 4-hole flexible MouseFix™ implants (Figure 5-2) and Titanium Aluminium Niobium alloy (Ti6Al4Nb (TAN)) screws were used in this study (RiSystem AG). The side bars of the flexible implant are composed of Nitinol. Prior to use, all implants were cleaned and sterilized as previously described [296].

Surgery was performed as previously described [296]. Briefly, under general anaesthesia with isoflurane (2-3% isoflurane in 100% $O_2$, 1 l/min) (Isofluran Baxter®, Baxter AG), the animal was placed in prone position and a skin incision was made from tail base to left stifle. The subcutaneous Fascia lata was cut and the tissue plane between the quadriceps and the biceps femoris muscle was bluntly dissected. A Teflon foil was placed around the femur to protect the soft tissue from contamination. The implant was then fixed to the bone using four self-tapping, angular stable screws. Screw holes were predrilled with a 0.31 mm drill bit (RISystem AG). Once the implant was in place, a 0.44 mm defect osteotomy was performed using a jig and a Gigli wire. In the inoculated groups, 2.5 µl of bacteria suspension was injected in the osteotomy site. The foil was then removed and the Fascia lata and the skin were closed with continuous sutures (5-0 Vicryl rapide, Ethicon, Belgium). Following surgery, a lateral radiograph of the femur was taken to confirm proper positioning of the implant. Analgesia was provided in the form of subcutaneous injections of buprenorphine (0.1 mg/kg, Bupaq®, Streuli Pharma AG), pre-operatively and post-operatively every 6-8 hours for 16 hours. Additionally, a palatable form of acetaminophen (2 mg/ml, as Dafalgan® Syrup for Children, Bristol-Myers Squibb SA) was added to the drinking water for 5

days. Animals were monitored twice daily for 5 days post-operatively and subsequently once a day, using a detailed numerical scoring system that takes into account general behaviour, external appearance, wound status and animal movement (scale 0-18, outlined in Supplementary Table 5-1). Weights and radiographs of the operated limb were taken weekly.

**Gait analysis**

Gait analysis was performed in a subset of non-inoculated animals in order to compare weight bearing between animals receiving different implant types. Mice (N=5 per group) were run through the Catwalk XT system (Noldus Information Technology) [346] for the detection of paw footprints (camera gain was set to 20 and the detection threshold to 0.1). Three runs with a speed variance lower than 60% were recorded per animal pre-operatively and 6, 9, 12, 24, 48 and 72 hours after surgery. Footprint area ($cm^2$) and light intensity (arbitrary units) of detected paw footprints were the selected outcome measures.

**Euthanasia and post-mortem sample processing**

At each scheduled time-point, the animals were euthanized by cervical dislocation after inducing general anaesthesia in an induction box (5% isoflurane in 100% $O_2$, 1 l/min). A lateral radiograph of the left femur with implant in place was acquired post-mortem. The operated femur, the implant and the surrounding soft tissue were harvested separately in sterile containers with cold PBS. The soft tissue and the bone were mechanically homogenized (Omni Tissue Homogenizer and Hard Tissue Homogenizing tips, Omni International). The number of bacteria associated with the implant was determined by sonicating the implant and screws in PBS for 3 minutes (BandelinSonorex at 40 KHz) and vortex mixing for 10 seconds. Viable bacterial counts were performed by plating serial dilutions of each sample on 5% horse blood agar (BA) (Oxoid). All BA plates were incubated at 37°C for bacterial counts at 24 and 48 hours. Mice were considered as infected when at least one sample (bone, soft tissue or implant) was culture positive. Bacteria recovered from each animal were confirmed to be *S. epidermidis* Epi 103.1 by Random Amplification of Polymorphic DNA (RAPD) test [347], or to be *S. aureus* with latex agglutination assay (Staphaurex, Thermo Scientific). Spleen and popliteal lymph node were harvested in cold PBS and processed to obtain total cell counts in each organ as a measure of lymphocyte infiltration as previously described [296]. Animals with osteosynthesis or implant failure were excluded from final analysis and replaced when considered necessary (see comments Figure 5-1)

**Histology and Scanning electron microscopy**

Samples for histology were largely processed as described previously [296]. Immediately after euthanasia, the entire operated femur and surrounding musculature underwent fixation with 70% (v/v) methanol for polymethylmethacrylate (PMMA) or paraffin embedding. PMMA samples were dehydrated through an ascending series of ethanol, transferred to xylene, and finally infiltrated with and embedded in PMMA [329]. The polymerized blocks were cut using an annular blade saw (Leica SP1600 saw microtome, Leica AG). Two sections were glued with cyanoacrylate onto opaque Plexiglas slides, ground and polished down to approximately 100 µm using a microgrinding system (Exact®) and stained with Giemsa/Eosin (GE). GE sections were blindly analysed by a certified pathologist. For paraffin embedding, the implant was removed and samples were decalcified in a 12.5% EDTA 1.25% sodium hydroxide (NaOH) solution. Finally, samples were cut longitudinally and both halves were embedded together in paraffin (McCormick). Paraffin blocks were cut using a microtome HM 355S (Microm, ThermoFisher Scientific) and sections were collected on Superfrost Plus slides (ThermoFisher). Slides were stained with Brown and Brenn (BB) for bacteria staining. The removed implants and selected paraffin sections (after deparaffinization) were taken for scanning electron (SE) microscopy for observation of any bacteria. Afterwards, the samples were dehydrated in an ascending series of ethanol (50-100%, 2 x 5 minutes). Implants and sections were then left to air dry overnight in a sterile flow hood. Samples were sputter coated with 10 nm gold palladium using a BAL-TEC MED 020. Representative SE micrographs of the surfaces were acquired using a Hitachi FESEM 4700 (3 kV, 40 µA).

**Statistical analysis**

Statistical analysis was performed with GraphPad Prism 7. Fisher Exact Test was used for proportions of infected animals and Mann-Whitney test for quantitative CFU data. Weight change and cell counts were compared over time between groups with 2-way ANOVA with Sidak or Dunnett post hoc tests. Differences were considered statistically significant with a $p$-value < 0.05.

# Results

## Animal monitoring

In total, 255 C57BL/6N mice and 135 BALB/c mice were operated throughout the entire study. There were 38 (9.78%) osteosynthesis/implant failures resulting in early euthanasia. Additionally, there were 10 exclusions (2.57%) due to post-operative complications not related to the fracture model (lameness, secondary infection, or exitus) and 10 animals (2.57%) excluded due to intra-operative complications (such as implant misplacement, implant failure or anaesthetic fatality). These animals were excluded from analysis and replaced as deemed necessary (details in Figure 5-1). No differences were observed between mouse strains or implant type in terms of susceptibility to failure. *S. aureus* inoculated animals presented a higher rate of exclusion (17.14%) compared to *S. epidermidis* inoculated animals (10.15%) although the difference was not statistically significant.

In general, there was no consistent difference for either C57BL/6N or BALB/c mice with regard to weight change between groups (rigid versus flexible and non-inoculated versus *S. epidermidis* inoculated). In general, *S. aureus* inoculated C57BL/6N and BALB/c mice lost more weight than *S. epidermidis* inoculated and non-inoculated counterparts. For standard *S. aureus* dose (C57BL/6N mice), the differences between groups were statistically significant at day 7 for animals with a rigid implant, and at all time-points for animals with a flexible implant. For *S. aureus* low dose (C57BL/6N and BALB/c) differences were statistically significant at day 14 for C57BL/6N with flexible implant groups, and at all time-points for C57BL/6N rigid implant groups and BALB/c mice (both implants) ($p<0.05$, Supplementary Figure 5-13). The clinical score did not show significant differences between groups.

## Gait analysis

Gait analysis revealed that there was an observable difference in the footprint area of the operated limb for mice fixed with rigid and flexible implants during the first 9-12 post-operative hours (Figure 5-3). This returned to baseline levels after this time. Of note, there was no significant difference between the rigid and flexible groups, although for mice with a flexible device the decrease was significant and returned to baseline level with a slight delay compared to rigidly fixed equivalents. There was a trend for increased values for the contralateral limb for the first 24 hours, remaining high up to 72 hours post-operatively, which most likely was to compensate for the effect on the operated limb.

**Bacteriology**

Quantitative bacteriological analysis of the inocula prepared for the surgeries confirmed that they were within the target range. For *S. epidermidis,* the average inoculum was $1.35x10^4$ CFU (SD: $5.69x10^3$) in C57BL/6N and $1.95x10^4$ CFU (SD: $5.02x10^3$) in BALB/c. For the *S. aureus* study the inoculum was $1.13x10^4$ CFU (SD: $4.28x10^3$) for the high dose study, and $1.98x10^3$ CFU (SD: $3.83x10^2$) for the low dose study. No significant differences were observed between the inocula administered to the rigid and flexible implant groups.

Post-mortem, mice were confirmed as infected or not-infected on the basis of quantitative bacteriological evaluation of bone, soft tissue and implant from the operated limb. The results of the bacteriological assessment for the C57BL/6N mice receiving the *S. epidermidis* inoculum are shown in Figure 5-4. On day 3, all *S. epidermidis* inoculated C57BL/6N mice were found to be culture positive for Epi 103.1. The total number of bacteria at day 3 had increased approximately ten-fold relative to the initial inoculated dose. From day 7 onwards the total CFU count reduced in all groups and in all compartments (bone, soft tissue and implant), and some mice in both rigid and flexible implant groups were culture negative in all compartments. Importantly, the proportion of animals that cleared the infection in the rigid implant group (14/28) was significantly greater than the number of mice that cleared the infection in the flexible implant group (6/28) when all data points were considered ($p$=0.049, Fisher Exact Test, 2-tailed). The quantitative bacteriology data revealed that mean CFU counts were often higher in mice with flexible implants, although this only reached statistical significance in soft tissue at day 7 (Figure 5-4c).

Results for BALB/c mice inoculated with *S. epidermidis* are shown in Figure 5-5. All BALB/c mice were infected 7 and 14 days post-operatively, and CFU counts were ten to one hundred fold higher in bone and implant samples compared to equivalent measurements for C57BL/6N mice (significant differences between total CFU counts at day 7, Kruskal Wallis test with Dunn's post hoc: $p$=0.0093). Clearance of the infection in BALB/c mice was first observed at day 30, with no differences observed between the rigid and flexible groups. With all time-points included, the proportion of mice that cleared the bacterial infection in the rigid implant group (4/17) did not differ from the flexible group (3/18). Similarly, there were no differences for CFU counts between mice with flexible or rigid implants, except at day 14 when soft tissue had significantly higher levels of bacteria in the flexible implant group (Figure 5-5c).

In the *S. aureus* study 100% of C57BL/6N mice from both groups were found infected at all time-points at the standard dose (Figure 5-6). The number of bacteria cultured from the tissues and the implant on day 3 was 2-3 orders of magnitude higher than CFU counts from *S. epidermidis*-infected

mice. At days 7 and 14, the mean number of bacteria decreased in all compartments in both implant groups, however it maintained an average CFU burden of $10^6$ -$10^7$ CFU per sample, with no clearance of bacteria being observed. In addition, the mean CFU counts between the rigid and flexible implant groups were very similar across the experiment. At all time-points, *S. aureus* total CFU counts were significantly higher compared to *S. epidermidis* total CFU counts in C57BL/6N mice (Kruskal-Wallis test with Dunn's post hoc: $p<0.0001$). As no clearance was observed in C57BL/6N strain, together with severe osteolysis and tissue damage observed, experiments were not performed in BALB/c background.

As the initial *S. aureus* inoculum dose resulted in a 100% infection rate for the entire study period, we could not identify any impact of fixation type on infection. Thus, we repeated the experiment at a lower dose in both mice strains, where we anticipated the animals may have a better chance of clearing the infection and a role for fracture stability may emerge. However, even when the initial dose was reduced 10-fold, neither mouse strain cleared the infection by day 14 and CFU counts were similar to those measured for the *S. aureus* standard dose group (Figure 5-7). Total *S. aureus* CFU counts in those animals were significantly higher compared to *S. epidermidis* total CFU counts in both C57BL/6N and BALB/c mice at day 14 (Mann-Whitney test, $p<0.0001$ for both comparisons).

**Spleen and popliteal lymph node cell counts**

Total cell counts were performed in lymph node and spleen to evaluate inflammation in local and systemic secondary lymphoid organs respectively. The type of fixation did not have an impact on cell counts from spleens or popliteal lymph nodes of C57BL/6N mice either with or without *S. epidermidis* inoculation (Figure 5-8). Levels were only slightly increased at day 3 compared to day 0, probably due to inflammation caused by surgical procedure, but they returned to baseline levels afterwards. *S. aureus* infection resulted in a significant increase in spleen and lymph node cell counts at days 7 and 14 when compared to the non-inoculated or *S. epidermidis* inoculated equivalents for both rigid and flexible implant groups (Figure 5-8, a and b). Finally, cell counts in the bone samples did not show significant differences (data not shown).

In BALB/c mice, *S. epidermidis* inoculated animals showed an increase in cell numbers at day 7 in spleen and lymph node compared to non-inoculated animals (Figure 5-8, c and d). This higher number of cells in inoculated animals may be linked to the higher percentage of infected animals and higher CFU counts in BALB/c mice compared to C57BL/6N. Levels returned to baseline values from day 14. For femur cell counts, there were again no significant differences between the

groups with regards to implant type or between non-inoculated and *S. epidermidis* inoculated animals.

**Histological evaluation**

Additional animals were used to obtain intact soft tissue and femurs with implant in place for histological samples (Figure 5-1). Representative overview images of the histological features of C57BL/6N mice with rigid and flexible implants at day 14 and 30 are shown in Figure 5-9 (for non-inoculated mice) and Figure 5-10 (for inoculated mice).

Non-inoculated mice with rigid implant fixation were observed to undergo a mixture of intramembranous and endochondral ossification at day 14 (Figure 5-9, a-b), with the osteotomy gap filled with new bone (Figure 5-9, b). At the same time-point, non-inoculated mice fixed with the flexible implant were undergoing endochondral ossification with a large stabilizing, mainly cartilaginous, callus (Figure 5-9, e-f, white asterisk: cartilaginous callus). The osteotomy gap in these mice was filled with mostly fibrin and cartilage (Figure 5-9, f) and a region of fibrous tissue was observed in the bone marrow, in the distal side of the osteotomy (Figure 5-9, f, black asterisk). Early granulation tissue was observed over the screw heads and implant of both groups, often more obvious in flexible group (Figure 5-9, c-d for rigid and g-h for flexible, black arrows: blood vessels), as well as muscle regeneration.

At day 30, the osteotomy gap was completely closed in animals with a rigid implant (Figure 5-9, i-j, black arrow), while the gap was still visible in most of the animals with a flexible implant (Figure 5-9, m-n, black arrow), suggesting a delay in bone healing in the flexible group. The large cartilaginous callus observed at day 14 was under remodelling by day 30, consisting predominantly of woven bone and secondary bone marrow (Figure 5-9, m-n, black asterisk). The granulation tissue overlying the plate at that time-point was only a thin layer of fibrous tissue (Figure 5-9, k-l and o-p, white asterisk).

*S. epidermidis* inoculated animals are shown in Figure 5-10. Inoculation did not seem to impair the progression of bone healing at day 14 in either of the implant groups, when compared to non-inoculated equivalents (Figure 5-10, a-b and e-f), with new bone formation in the osteotomy of animals with a rigid implant and a big cartilaginous callus in the flexible implant group. Higher soft tissue inflammation was observed in inoculated animals at that time-point, as reflected in a higher lymphocyte and granulocyte infiltration in surrounding soft tissue and the presence of fluid filled spaces (Figure 5-10, a,c-d and e,g-h, black arrows). Such signs were often localized to small foci, and not widespread throughout the tissues. In some cases, osteolysis around screws was observed

(Figure 5-10, a and b, white arrows) with more granulocytic infiltrate compared to aseptic osteolysis that occurred in some non-inoculated animals due to instability or stress shielding (Figure 5-11).

By day 30, the osteotomy was mostly closed in inoculated animals with a rigid implant, while in mice with a flexible implant the cartilaginous callus was in a remodelling phase. The soft tissue showed a similar appearance to the non-inoculated animals (Figure 5-10, k-l and o-p). Signs of infection were found as higher bone remodelling, indicated by larger regions with secondary bone marrow (Figure 5-10, i and m). Osteolysis was observed in some inoculated animals, with some granulocyte infiltrates. However, these were not general features and evidence of infection was weak or even absent in both implant groups, which supports the microbiology data that indicates many of the animals had cleared the infection by this time-point.

In BALB/c mice, the histological observations were similar (data not shown) regarding bone healing, with often earlier closure in animals with a rigid implant and a cartilaginous callus, which remodels at day 30 in animals with a flexible implant. Interestingly, a more inconsistent healing was detected, with some animals showing no gap closure at all at day 14. To our knowledge, this is the first study using flexible MouseFix$^{TM}$ plate in BALB/c background and thus, we cannot compare this observation with other authors work. Importantly, this phenomenon was not linked to the presence of bacteria. Signs of infection were also similar to that observed for C57BL/6N mice, only being evident in soft tissue over the plate at day 14 and becoming less pronounced at day 30.

Bacteria were observed on the implants from C57BL/6N and BALB/c mice at day 14 and also in paraffin sections (Figure 5-12).

## Discussion

Despite the prevalence of *S. epidermidis* and other CoNS in orthopaedic implant related infections, the scientific literature in the field is dominated by *S. aureus* [340]. To the best of our knowledge, there has been only one model described for *S. epidermidis* FRI [303, 304], which was performed in rats. In the present study, we have established and characterized an *S. epidermidis* FRI model in mice, and further developed the model to study the influence of fracture stability on infection progression. To overcome the limitations of previous preclinical *in vivo* models assessing the influence of stability on infection [331-334], we have used a standardized femoral fixation system previously described for monitoring fracture healing under different biomechanical conditions [329, 342]. Using gait analysis, we could show that both fixations allowed the mice to return to baseline mobility within a short period after surgery, and histological observations confirmed healing to proceed under mostly intramembranous ossification and endochondral ossification respectively, as expected for the implant fixation used. In terms of the clinical appearance of the infections in this study, and its relevance to clinical FRI in humans, *S. epidermidis* inoculated mice (both mice strains) did not show major differences over time in weight change or cell counts, suggesting a subclinical type of infection. This closely matches the typical clinical picture of *S. epidermidis* infection [94, 98]. Animals infected with *S. aureus* exhibited instead higher weight loss, higher CFU counts in tissues and higher cell numbers in spleen and lymph node, suggesting overall greater inflammation. In addition, it could visually be observed purulent tissue over the plate and osteolysis around the screws, below the implant and in the osteotomy site. This also correlates with clinical observations, whereby *S. aureus* infection is associated with acute onset of symptoms.

The *S. epidermidis* infection was seen to resolve in many animals, which is similar to previous implant associated infection models for this organism [303, 309, 318]. Higher inocula may guarantee a persistent infection, however, as reported recently for *S. aureus*, infectious dose might alter immune responses and has to be considered carefully [348]. Considering our experimental hypothesis that fracture instability predisposes to infection, a low inoculum enabled us to differentiate between the development of infection (or not) rather than merely looking for changes in CFU counts, which would be less indicative of an effect. Of note, even when using a low inoculum, infection persisted in some animals up to 30 days. It was in general difficult to detect bacteria in our histology samples to better characterize persistence sites. We did observe some biofilm-like structures in our SEM images, and located bacteria in locations of difficult access such as bone vessels within the bone. In addition, *S. epidermidis* has been shown to be able to persist intracellularly *in vitro* [183] and *in vivo* [229, 230], although we did not assess intracellular presence.

In testing our hypothesis under controlled conditions, we wished to advance the field from the data provided by early studies [331-334]. Friederich and Klaue [332] showed that stable fractures were associated with a lower *S. aureus* infection rate in rabbits. However, in this study animals were allocated to the stable or unstable group after radiographic observations, with both plate and nail fixation methods present in both arms of the study as pre-allocation based on implant type was evidently unable to provide predictable mechanics. In 1986 Merritt *et al.* performed a study with open fractures in hamsters [333], however they compared a K-wire fixed fracture with a non-fixed fracture and so there was no foreign body in that study, which thereby misses an important fact in device associated infection, i.e. the device itself. Finally, in the most recent experimental study on this topic by Worlock *et al.*[334], the stable construct (plate) showed a lower *S. aureus* infection rate compared with the unstable construct (an intramedullary rod). This study therefore once again has a confounding factor of whether different fixation systems (plate vs. intramedullary rod) may also have influenced infection rates. Our study provides the first standardized model, allowing controlled conditions. We successfully used two similar implant types with reliable healing outcomes, confirming previous observations in C57BL/6 mice regarding bone healing [329, 342] and extending the model into the FRI field. The study provides evidence that *S. epidermidis* infection can, in fact, be influenced by implant stability. After inoculating with *S. epidermidis*, we found that infection clearance was enhanced in C57BL/6N mice fixed with rigid plates over time, and the bacterial burden displayed a trend towards lower numbers. This result does agree in general with all earlier studies that instability is a risk factor for infection or infection progression. Ongoing work is attempting to provide some understanding of this phenomenon by assessing immune markers in samples obtained in this study. Previous publications focusing on bone healing have described different gene and protein expression patterns between both implant types [349, 350] and we would like to extend this knowledge by studying samples from infected animals, where we predict that environment may also differ between both implant types.

The observation that stability influences *S. epidermidis* infection did not hold true for the second mouse strain. Interestingly, BALB/c mice first achieved clearance of infection at day 30, a time-point when the osteotomies in both rigid and flexible groups had already healed. As such, mechanical differences may be low or non-existent between groups at this time. In fact, the clearance of infection was equal between both groups at that time, which may in fact further support to the need for stability to eradicate infection. There was again no difference in infection rate between the groups when inoculated with *S. aureus.* It is important to note however that *S. aureus* displays a virulent behaviour in this model, leading to peri-implant osteolysis six days post-operatively as shown previously in a different model [351]. This osteolysis was observed at both the

standard and low doses, making comparison between groups irrelevant as all animals were effectively "unstable". This data therefore does not discredit the requirement for implant stability, although the effect may be more pronounced under conditions of a low grade infection.

Patient factors such as age or co-morbidities are known to influence infection risk and also need to be considered for treatment management [319, 352, 353]. In our study, when using two different inbred strains, we observed that C57BL/6N mice more rapidly cleared bacteria and presented lower CFU counts at most of the time-points compared to BALB/c animals. A higher bacterial burden was also associated with higher cell counts in draining lymph node. Other studies using *S. epidermidis* foreign-body infection models have shown similar results, with BALB/c mice showing higher CFU counts and/or bigger abscesses compared to C57BL/6 equivalents [354, 355]. Nevertheless, the number of studies is limited and the topic remains controversial when considering studies using *S. aureus*, which have obtained contradictory results [299, 356-359]. It is known that the immune system of C57BL/6 and BALB/c mice have differences [360], with C57BL/6 mice being more T helper (Th)1 polarized and BALB/c mice being more Th2 polarized. Overall, our results support the notion that host genetic background may influence study outcomes, and needs to be considered together with the infecting pathogen. Further analysis into immune system differences between these murine strains could provide valuable data regarding the effective immune responses required to clear *S. epidermidis* infections. Deeper analysis into inflammatory markers at gene and protein level is the subject of ongoing studies in our laboratory to characterize the cell environment in the different mechanical contexts.

## Conclusion

An *S. epidermidis* model of FRI was established, which recapitulates many of the clinical features of this infecting agent such as mild clinical signs and low levels of tissue inflammation. This was especially evident when compared to animals inoculated with *S. aureus*, in terms of weight loss, macroscopic observations or cell counts. This model was used to study the impact of fracture stability on i clearance, with stable fixation resulting in a lower infection rate for *S. epidermidis* but not for *S. aureus*. Detailed understanding of this process is the subject of ongoing studies.

## Acknowledgements

The project was funded by AO Trauma as part of the Clinical Priority Program Bone Infection (grant AR2011_08). The authors would like to acknowledge Tanja Schmid and Iska Dresing for performance of surgery in the *in vivo* study; Iris Keller and Pamela Furlong are acknowledged for the bacteriological work-up and SE microscopy; Nora Goudsouzian and Mauro Bluvol are acknowledged for support with histological processing.

**Figures:**

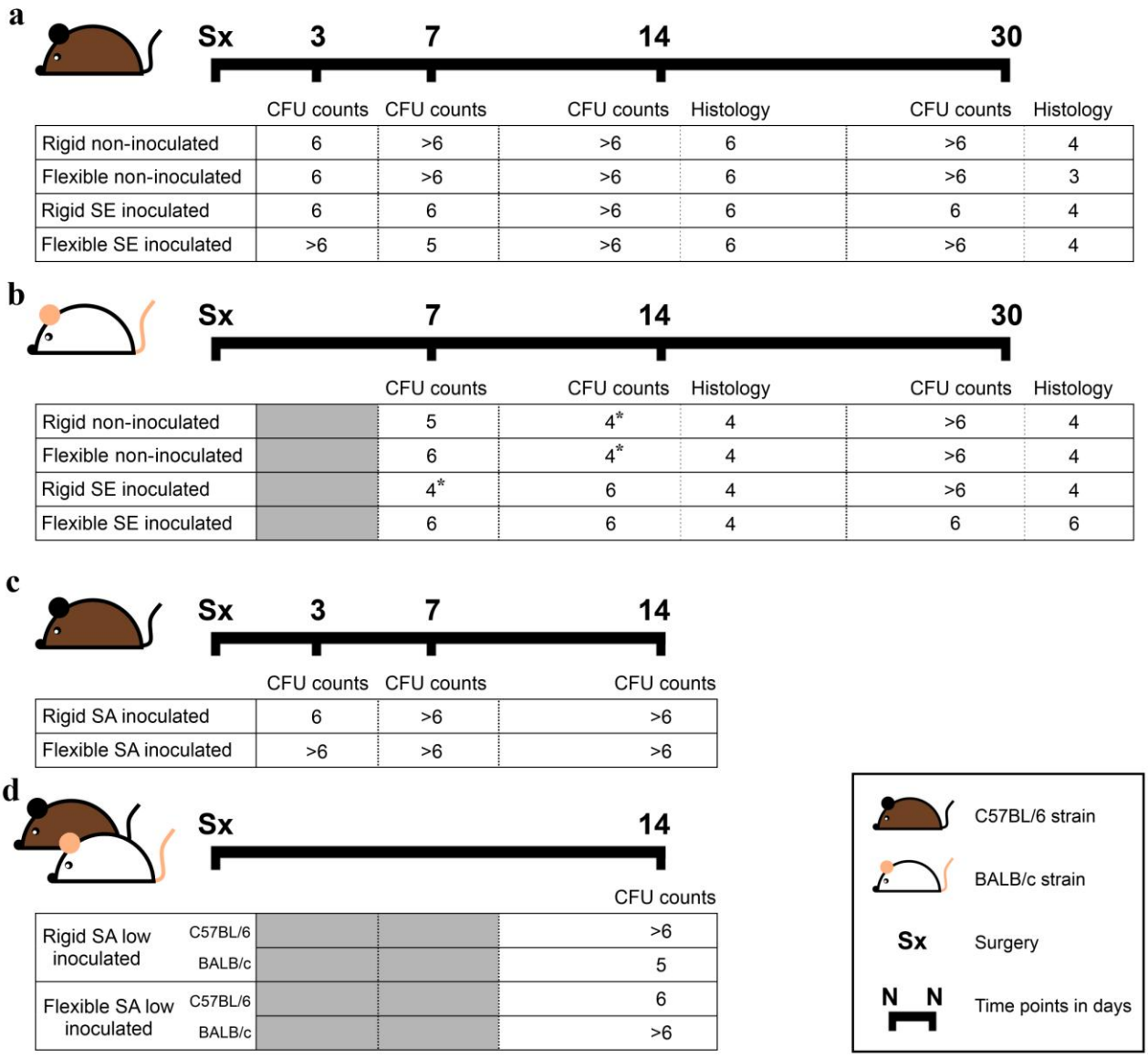


**a**

| | CFU counts | CFU counts | CFU counts | Histology | CFU counts | Histology |
|---|---|---|---|---|---|---|
| Rigid non-inoculated | 6 | >6 | >6 | 6 | >6 | 4 |
| Flexible non-inoculated | 6 | >6 | >6 | 6 | >6 | 3 |
| Rigid SE inoculated | 6 | 6 | >6 | 6 | 6 | 4 |
| Flexible SE inoculated | >6 | 5 | >6 | 6 | >6 | 4 |

**b**

| | | CFU counts | CFU counts | Histology | CFU counts | Histology |
|---|---|---|---|---|---|---|
| Rigid non-inoculated | | 5 | 4* | 4 | >6 | 4 |
| Flexible non-inoculated | | 6 | 4* | 4 | >6 | 4 |
| Rigid SE inoculated | | 4* | 6 | 4 | >6 | 4 |
| Flexible SE inoculated | | 6 | 6 | 4 | 6 | 6 |

**c**

| | CFU counts | CFU counts | CFU counts |
|---|---|---|---|
| Rigid SA inoculated | 6 | >6 | >6 |
| Flexible SA inoculated | >6 | >6 | >6 |

**d**

| | | CFU counts |
|---|---|---|
| Rigid SA low inoculated | C57BL/6 | >6 |
| | BALB/c | 5 |
| Flexible SA low inoculated | C57BL/6 | 6 |
| | BALB/c | >6 |

**Figure 5-1** Graphic scheme of animals per group in the different studies, with C57BL/6 represented as a brown mouse and BALB/c as a white mouse. Surgery (Sx) and time-points in days are indicated in each axis. SE: *S. epidermidis*, SA: *S. aureus*. Note: day 3 was not performed in BALB/c as no differences in clearance were observed neither at day 7 or 14; and thus it was not deemed necessary to evaluate impact on clearance. For the same reason, it was not deemed necessary to replace animals in some groups at day 7 and 14 (marked with an asterisk). For *S. aureus* low dose, only one time-point was performed. Again, as no differences were observed in CFU counts and clearance, earlier time-points were not studied.

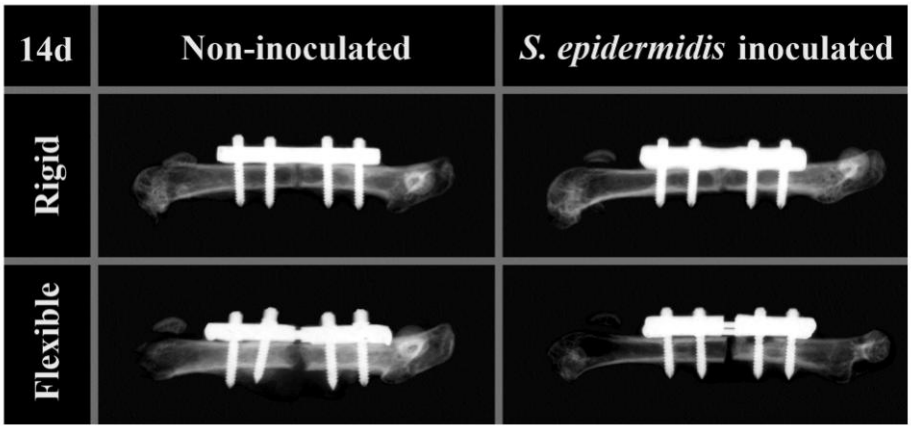


**Figure 5-2** Post-mortem contact radiographs of rigid and flexible plates in non-inoculated (left) and *S. epidermidis* inoculated (right) mice at day 14 post-operatively. Note osteotomy starts to show closure in animals with rigid implant fixation while there is no such closure observed in animals with flexible fixation.

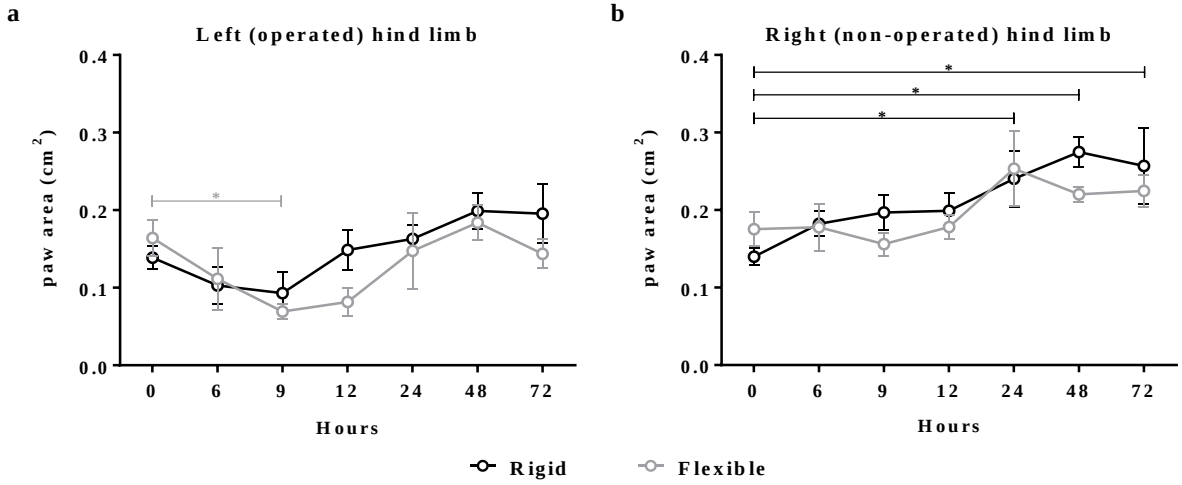


**Figure 5-3** Area ($cm^2$) of left (a) and right (b) hind paws measured in Catwalk XT System, pre-operatively and at 6, 9, 12, 24, 48 and 72 hours post-operatively, for rigid (black) and flexible (grey) implant groups. Mean values with SEM (n=5), * = $p<0.05$). Significant differences were observed between several time-points and baseline values for both implant groups (rigid group in black, flexible group in grey), while no significant differences were observed between animals from rigid or flexible group.

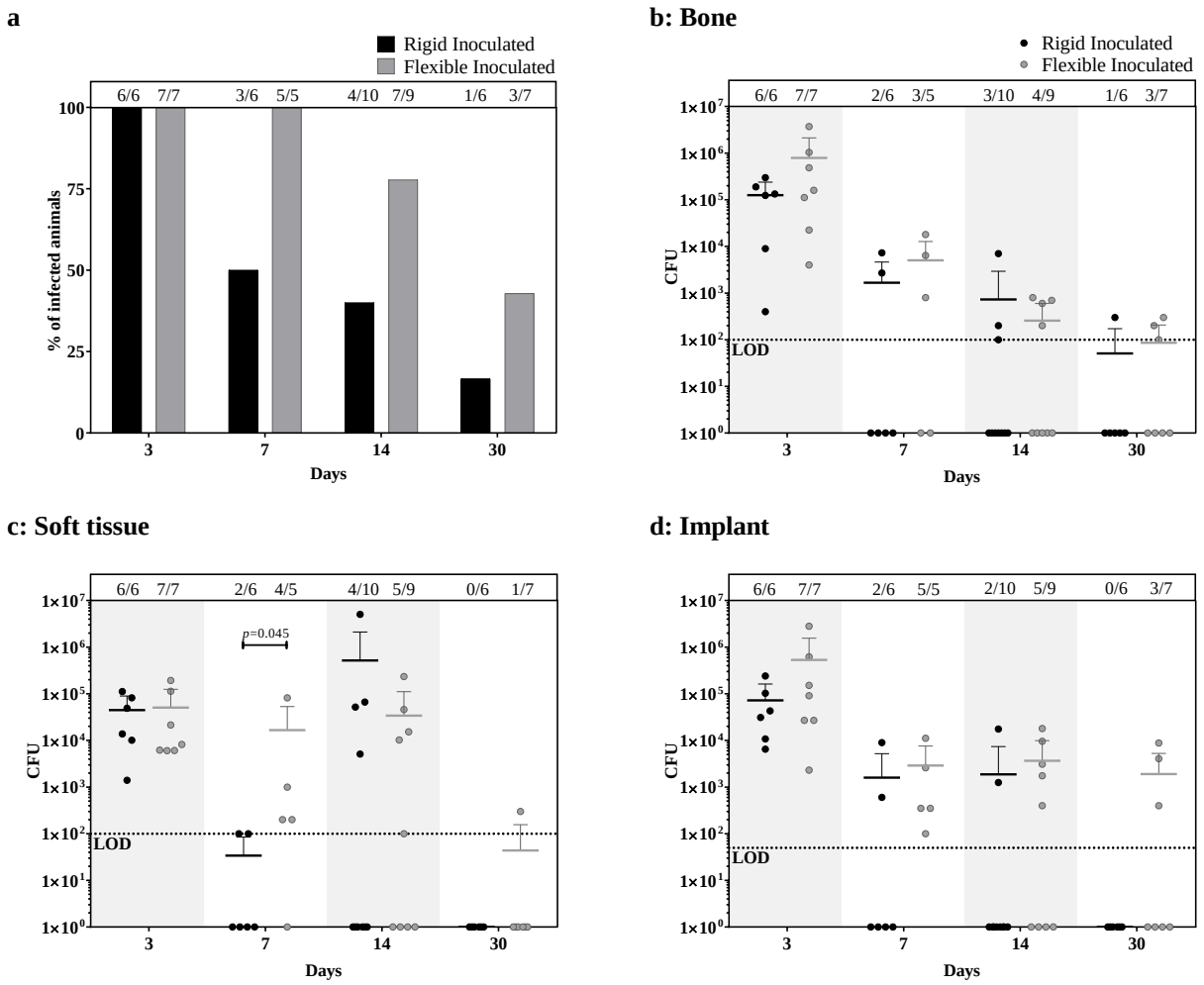


**Figure 5-4** Percentage of *S. epidermidis* infected C57BL/6N mice at each time-point (a) and quantitative bacteriology from each compartment (b, bone; c, soft tissue; d, implant). Upper panel of each graph shows proportion of culture positive animals/ total animals per group. Mean values and SD (n=5-10). LOD = Limit of detection ($1x10^2$ CFU for bone and soft tissue, $0.5x10^2$ CFU for the implant), samples below LOD were represented as 1. It can be observed that animals with a rigid device cleared infection (culture negative for all samples) in a higher percentage when compared to flexible group, at all time-points.

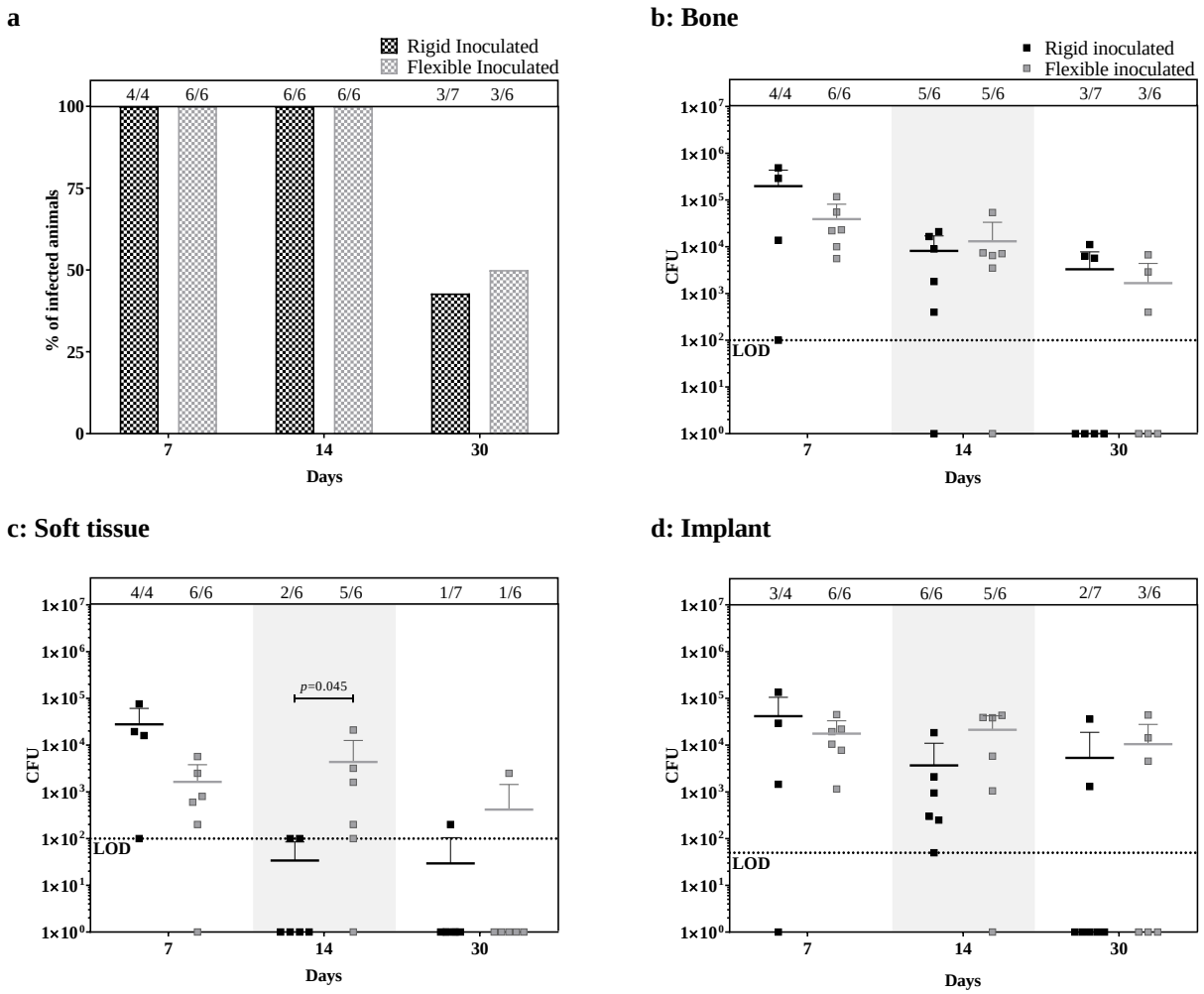


**Figure 5-5** Percentage of *S. epidermidis* infected BALB/c mice at each time-point (a) and quantitative bacteriology from each compartment (b, bone; c, soft tissue; d, implant). Upper panel of each graph shows proportion of culture positive animals/ total animals per group. Mean values and SD (n=4-7). LOD = Limit of detection ($1x10^2$ CFU for bone and soft tissue, $0.5x10^2$ CFU for the implant), samples below LOD were represented as 1. It can be observed that contrary to C57BL/6N mice, BALB/c did not clear infection at 7 or 14 days post-operatively, irrespective of implant type. At day 30, mice from both implant groups cleared the infection.

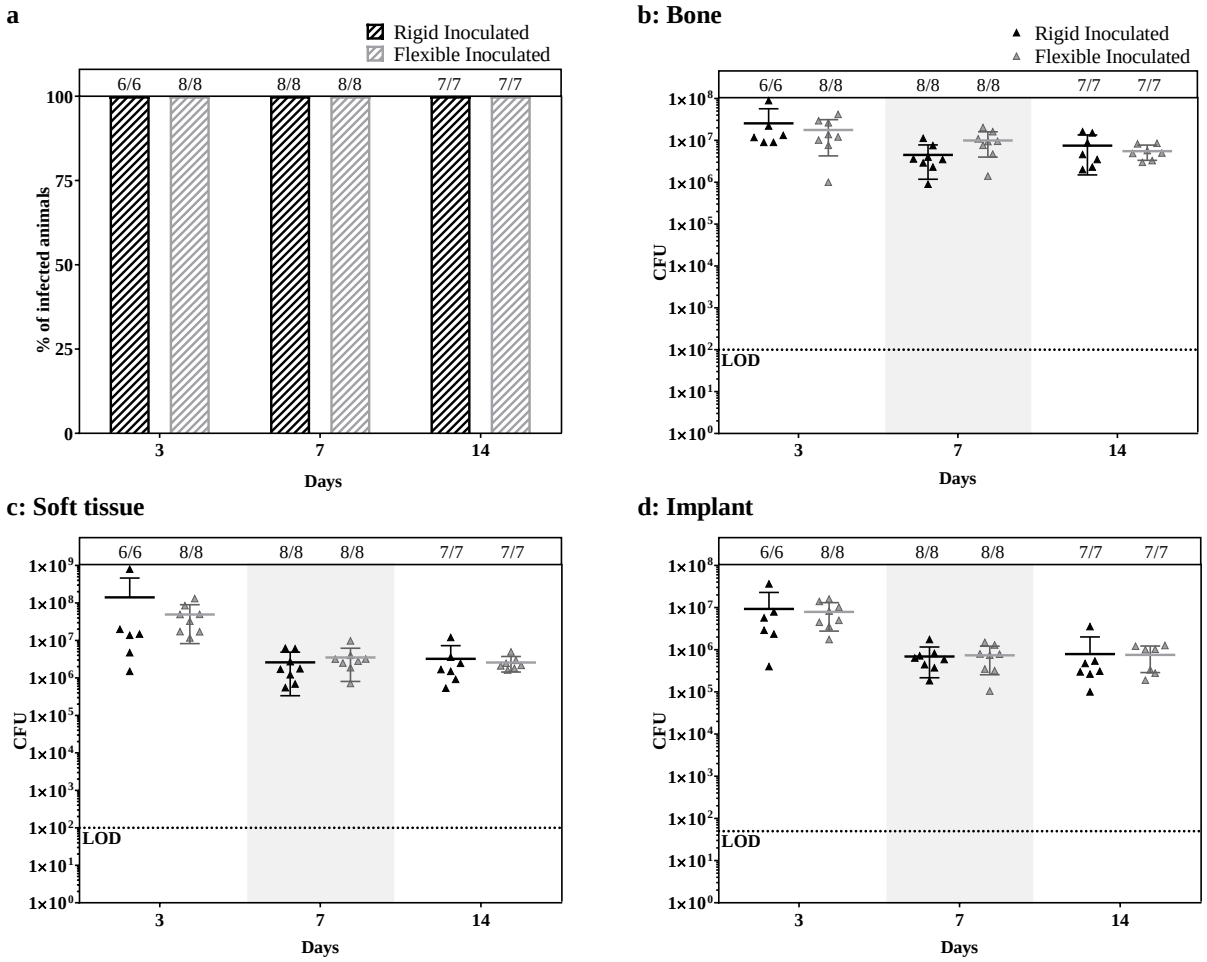


**Figure 5-6** Percentage of *S. aureus* infected C57BL/6N mice at each time-point (a) and quantitative bacteriology from each compartment (b, bone; c, soft tissue; d, implant). Upper panel of each graph shows proportion of culture positive animals/ total animals per group. Mean values and SD (n=6-8). LOD = Limit of detection ($1x10^2$ CFU for bone and soft tissue, $0.5x10^2$ CFU for the implant), samples below LOD were represented as 1. As shown, no animal cleared bacteria at any time-point. In addition, high bacterial counts were recovered from all compartments, being significantly higher compared to *S. epidermidis* counts in C57BL/6N.

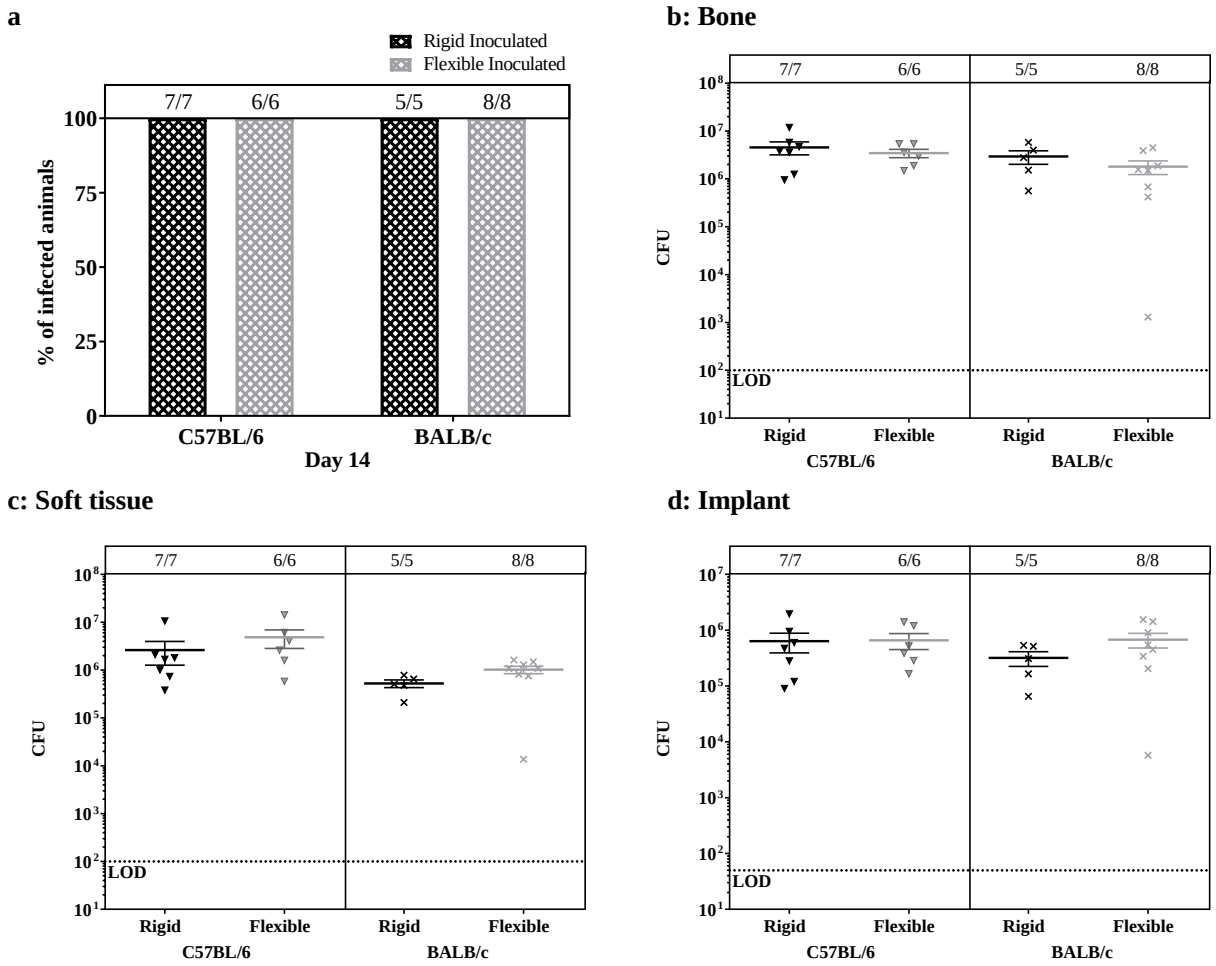


**Figure 5-7** Percentage of low dose *S. aureus* infected C57BL/6N and BALB/c mice at day 14 (a) and quantitative bacteriology from each compartment (b, bone; c, soft tissue; d, implant). Upper panel of each graph shows proportion of culture positive animals/ total animals per group. Mean values and SD (n=5-8). LOD = Limit of detection ($1x10^2$ CFU for bone and soft tissue, $0.5x10^2$ CFU for the implant), samples below LOD were represented as 1. Despite using a 10-times lower dose compared to standard inoculum, all animals remained infected, with high bacterial counts in all compartments.

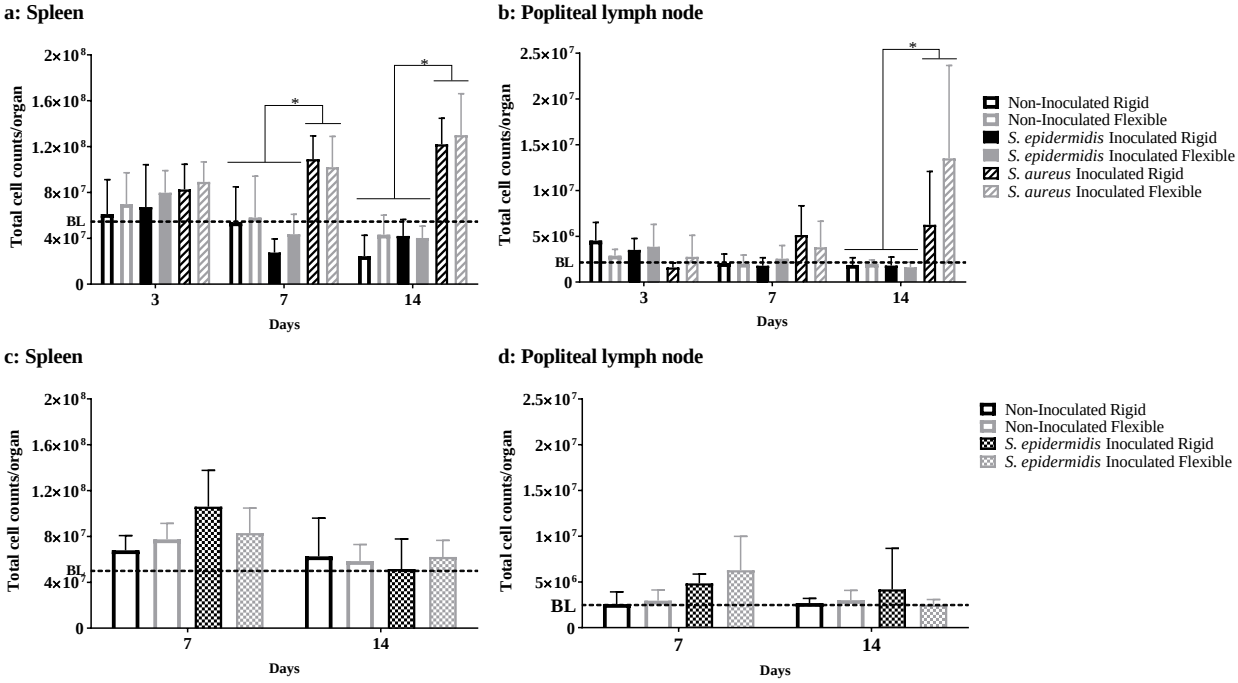


**Figure 5-8** Total cell counts in spleen and popliteal lymph node single cell suspensions of C57BL/6N and BALB/c mice. Total cell counts in spleen and popliteal lymph node of C57BL/6N (a and b) and BALB/c (c and d) mice with a rigid (black) or flexible (grey) implant at 3, 7 and 14 days. BL (dashed line): baseline levels from average values of control animals. Mean and SEM (N=4-10); * = $p<0.05$. All operated animals present an early increase in spleen and lymph node cell counts, probably due to the inflammation induced by surgical procedure. This increase was not significant compared to baseline levels. At later time-points, only *S. aureus* inoculated animals (in C57BL/6N mice) present significantly higher cell counts, which supports a more severe infection process and higher inflammation process.

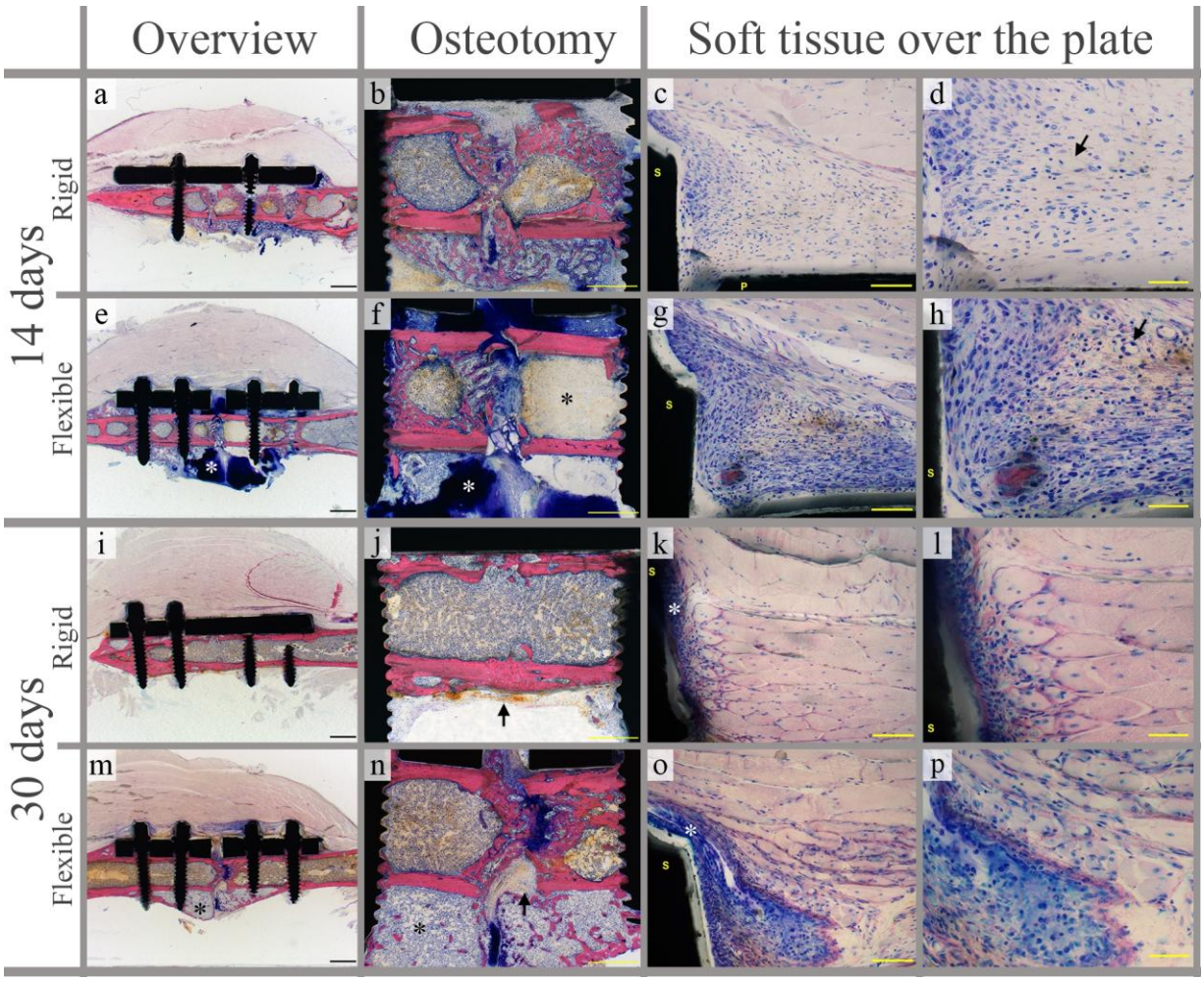


**Figure 5-9** Light microscopic images of GE stained MMA sections, of non-inoculated C57BL/6N mice at days 14 and 30 post-operatively, treated with rigid or flexible implants. First column: overviews of femur with implant in place and surrounding soft tissue (scale bar: 1000 µm). Second column: close-up of the osteotomy site (scale bar: 500 µm). Third column: tissue over the plate (scale bar: 200 µm). Fourth column: higher magnification of an area of third column (scale bar: 100 µm). Screw (S) and plate (P) are indicated in high magnification images to help orienting in the sample, asterisk and arrows are used to point at some of the described details. At day 14, rigid implant group (a) presented periosteal and endosteal new bone closing the osteotomy site (b) while flexible implant group (e) at the same time-point showed non-closure of the osteotomy site but a big cartilaginous callus (e and f, white asterisk). In addition, for animals with flexible implants bone marrow in distal site looked unstained, consisting in fibrotic tissue (e, black asterisk). Early granulation tissue (c-d and g-h) consisting of fibroblasts, new vessels (d and h, black arrows) and leukocyte infiltrate, with different grade of inflammation, was observed over the plate for both implant types. At day 30, in rigid implant group (i) the osteotomy was closed (j, black arrow). In flexible implant group (m) the callus was still remodelling (m and n, black asterisk) with still substantial amounts of cartilage tissue present and full closure of the osteotomy was not achieved (n, black arrow). The inflammation of the tissue over the plate was reduced to a thin layer of fibrous tissue (k and o, white asterisk), especially in the rigid implant group.

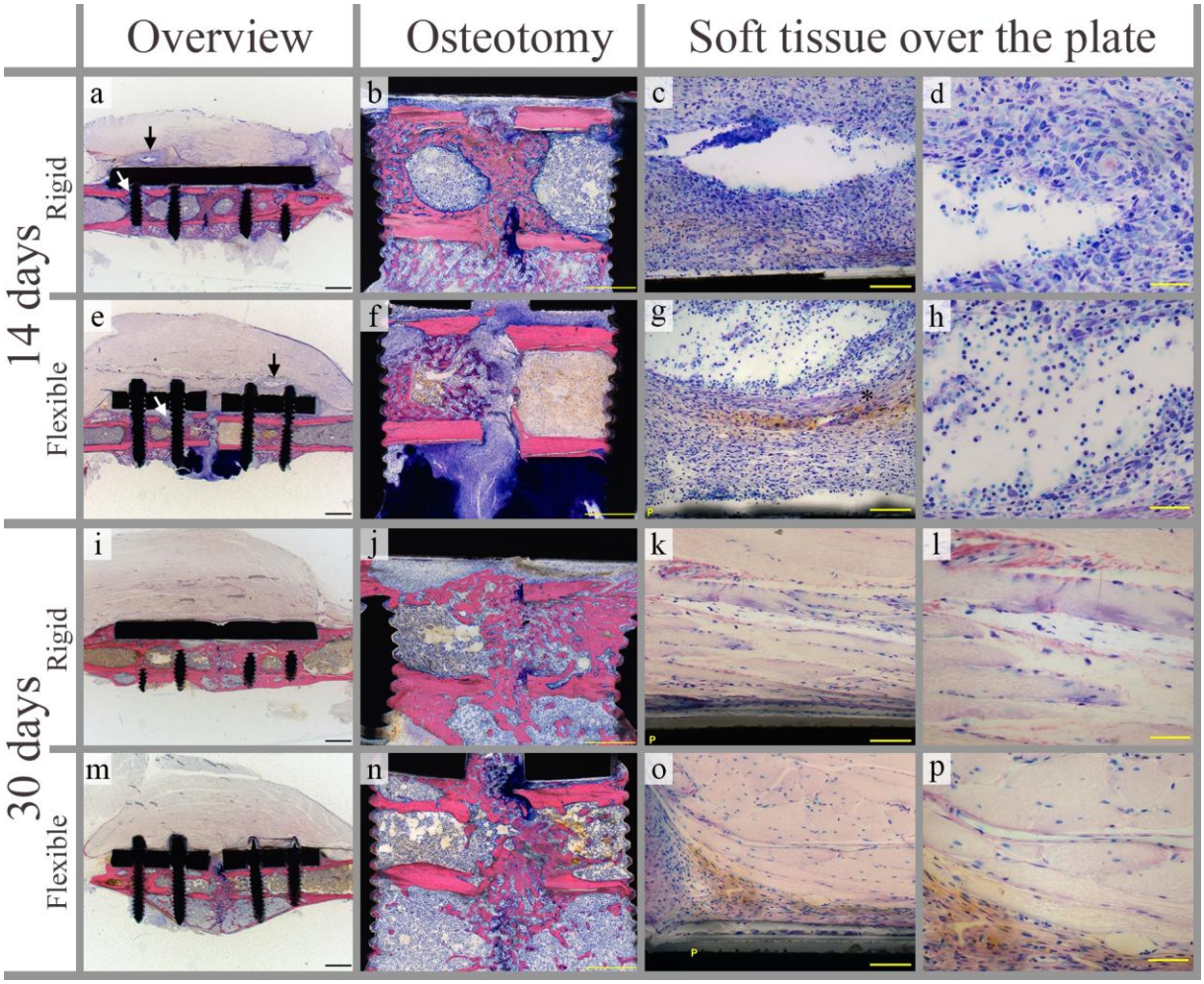


**Figure 5-10** Light microscopic images of GE stained MMA sections of inoculated C57BL/6N mice at day 14 and 30 treated with rigid and flexible implants. First column: overviews of femur with implant in place and surrounding soft tissue (scale bar: 1000 µm). Second column: close-up of osteotomy site (scale bar: 500 µm). Third column: tissue over the plate (scale bar: 200 µm). Fourth column: higher magnification of an area of third column (scale bar: 100 µm). Plate (P) is indicated in high magnification images to help orienting in the sample, asterisk and arrows are used to point at some of the described details. At day 14, once again, the osteotomy site in the rigid group showed a high degree of closure (a and b), while a complete non-closure of the osteotomy site and a large cartilaginous callus was observed in the flexible group (e and f). In both implant groups, the soft tissue presented small foci of inflammatory cell accumulation (a and e, black arrow). These foci, with high infiltrate of polymorphonuclear (PMN) cells, are shown in high magnification images (c and d, g and h). In some cases the presence of a fibrous capsule was observed (g, black asterisk), suggesting that this foci could be defined as a small encapsulated abscess. Bone edges at osteotomy site and near screws shown signs of osteolysis (a and e, white arrows). At day 30, closure of the osteotomy site was advanced in both, rigid and flexible implant groups. In contrast to day 14, inflammation of the tissue above the plate was reduced to a minimal degree (k and l, o and p).

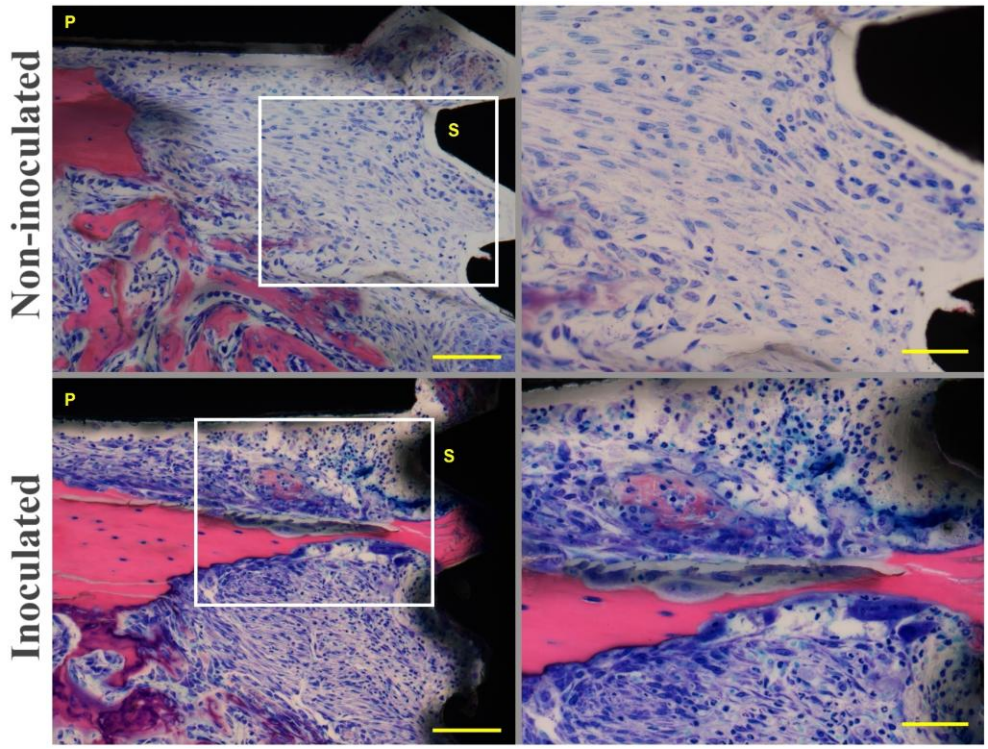


**Figure 5-11** Light microscopic images of GE stained thick-sections at day 14 in C57BL/6N mice with a rigid implant. Note small areas of low osseointegration near screws in both groups. In non-inoculated animals there is new bone formation (callus) and the tissue mainly consist of fibroblasts/-cytes, low number of capillaries and very little inflammatory cells mainly of mononuclear type (late granulation tissue). In contrast, in inoculated animals scalloped bone surface and osteoclasts can be observed (osteolysis), and the inflammatory cell infiltration of the granulation tissue is much higher consisting predominately of PMN cells and tissue debris (microabscess). Scale bar: 100 µm (first column) and 50 µm (second column, magnification images).

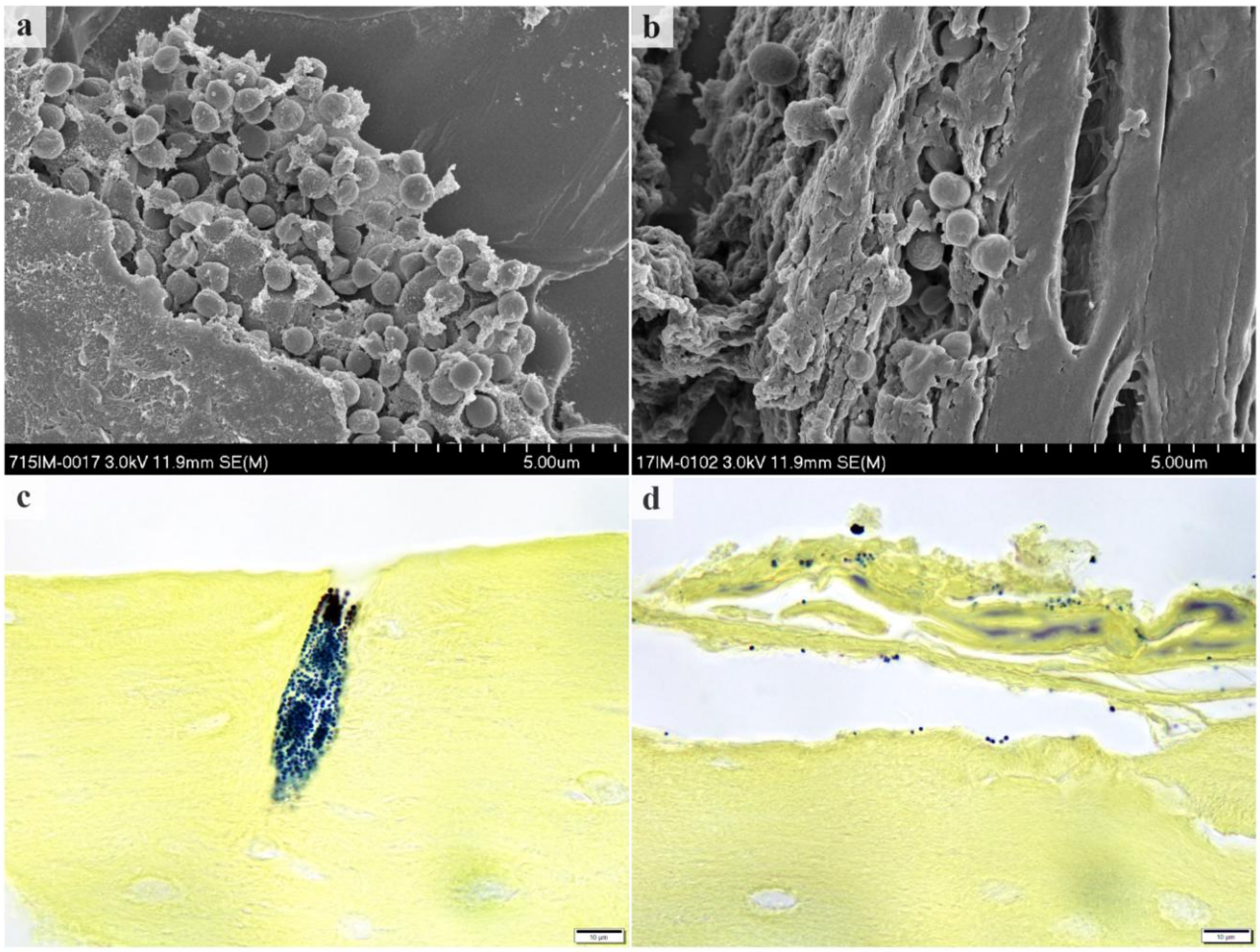


**Figure 5-12** SE micrographs and light microscope images of bacteria on the implant and bone. SE micrograph images show clusters of coccoid bacteria attached to the implant surface (a) and in the periosteum (b). They were also observed in paraffin sections stained with BB (bacteria in blue) in a bone vessel (c) or in the periosteum/delaminated bone fragments (d). Scale bars shown in image: 5 µm (a and b) and 10 µm (c and d).

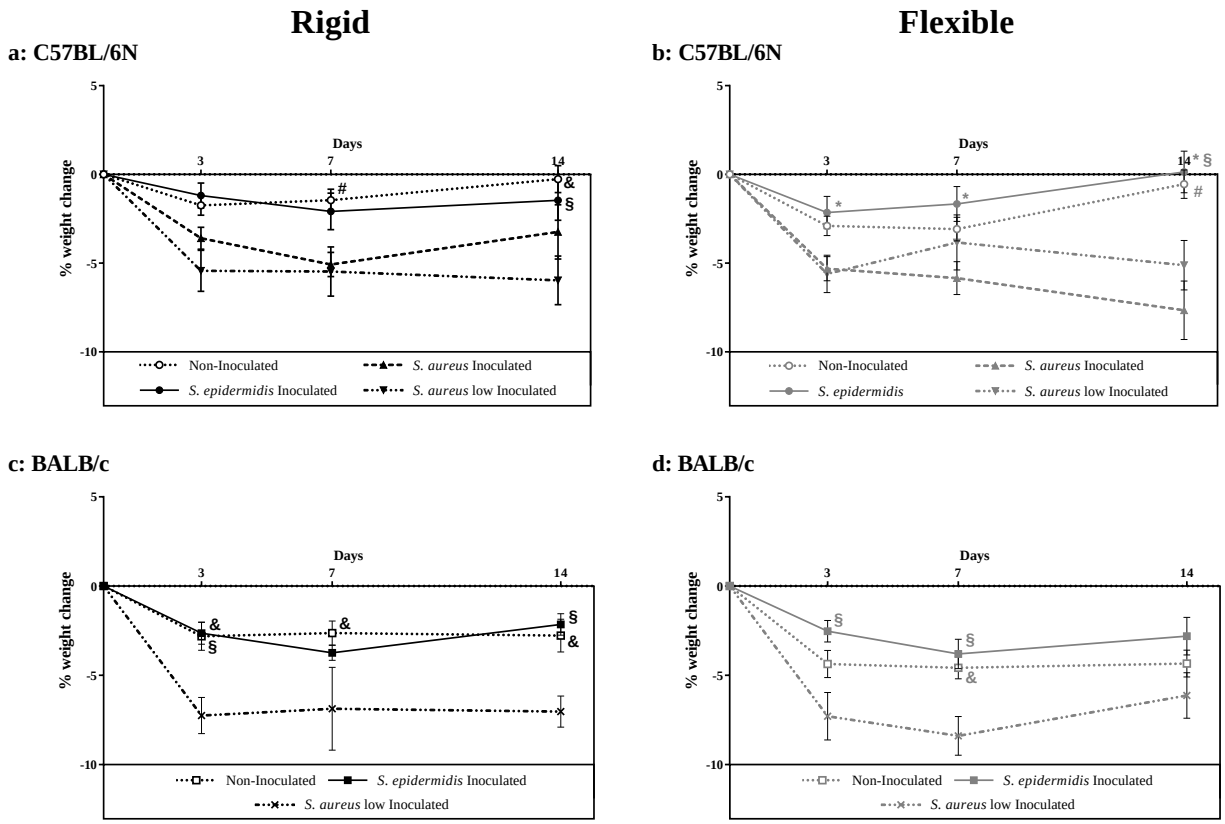


**Supplementary Figure 5-13** Weight change of *S. epidermidis* and *S. aureus* infected C57BL/6N (a and b) and BALB/c mice (c and d). Percentage of weight change (compared to post-operation weight) in a) C57BL/6N mice with a rigid implant, b) C57BL/6N mice with a flexible implant, c) BALB/c mice with a rigid implant and d) BALB/c mice with a flexible implant. Mean and SEM (N=10-43). Repeated measures 2-way ANOVA with Tukey post hoc; #/*/&/§ = $p<0.05$. Statistically significant differences are marked as follows: # for significant differences between non-inoculated and *S. aureus* inoculated, * for significant differences between *S. epidermidis* inoculated and *S. aureus* inoculated, & for significant differences between non-inoculated and *S. aureus* low dose inoculated and § for significant differences between *S. epidermidis* inoculated and *S. aureus* low dose inoculated.

**Supplementary Table 5-1** Self-designed animal scoring system

| Parameter | Scores |
|---|---|
| Behaviour / Overall impression | 0 / 2 / 4 |
| Breathing | 0 / 2 / 3 |
| Fur / Eyes / Skin | 0 / 1 / 3 |
| Movement | 0 / 1 / 2 / 3 |
| Faeces / Urine | 0 / 2 |
| Wound healing | 0 / 1 / 3 |

## 5.2 Immune Responses in a Murine Fracture Model upon Staphylococcal infection and Role of IL-17A in Infection Clearance

Marina Sabaté Brescó[1,2], Liam O'Mahony[2], Corina Berset[3], Stephan Zeiter[1], Barbara Stanic[1], Keith Thompson[1], Mario Ziegler[2], Geoff R. Richards[1], Fintan T. Moriarty[1]*

[1] AO Research Institute Davos, CH; [2] Swiss Institute of Asthma and Allergy Research, CH, [3] AO Foundation, CH

*Corresponding author:
T F Moriarty, AO Research Institute Davos, AO Foundation, Clavadelerstrasse 8, Davos Platz, CH7270, Switzerland. Phone: +41 81 414 2397, E-mail: fintan.moriarty@aofoundation.org

Running Title: Immune response to Staphylococcal bone infection

*This manuscript is in the final phase of preparation and will be submitted to Bone journal.*

**Abstract**

Biomechanical stability plays an important role in fracture healing, with stable fixation being required to achieve optimal conditions for bone repair. Furthermore, the lack of stability has been considered a known risk for failure to treat fracture related infection (FRI), although literature addressing this topic is limited. Infection is one of the major complications in trauma surgery, being associated with increased hospital stays, prolonged treatment, poor functional outcome of the affected limb or even amputation, and high socio-economic costs. Recently, using an experimental model in mice, we have shown that animals with fractures fixed with a rigid implant (stable fixation) cleared infection more frequently than equivalents fixed with a flexible implant (unstable fixation). In this study, we aimed to characterize the immune responses associated with stable and unstable fracture fixation in this model, both under sterile conditions and after inoculation with either *Staphylococcus epidermidis* or *S. aureus*. Under unstable fixation, inflammation markers such as interleukin (IL)-6 were increased, and this was exacerbated by *S. epidermidis* infection. *S. aureus* inoculation led to very high inflammation for both type of implants, but also greater in unstable fixation. We also observed differences in terms of cell recruitment or mRNA levels, with again unstable fixation showing higher levels of inflammatory markers. We observed that IL-17A was upregulated on the presence of *S. epidermidis* infection and that this cytokine was mostly produced by CD4+ and γδ T cells. Using an IL-17A knock out mouse strain, we aim to address the role of IL-17A in infection progression. KO strain cleared infection at a slower rate, although no significant differences were observed, which may be associated to an increase in interferon (IFN)-γ production in those animals.

**Introduction**

Fracture healing is a complex process influenced by several interconnected factors, as summarized in the so called "diamond concept" [21]. Classically, this concept includes osteogenic cells, an osteoconductive scaffold, growth factors and the biomechanical environment. The first stage in the healing cascade is now known to involve acute inflammation [361] and the importance of immune cells in bone healing is now also widely recognised. For example, it has been shown that immune cells, such as T cells [32, 362, 363], B cells [31], macrophages [26, 27, 364, 365] or granulocytes [366], as well as soluble mediators such as pro-inflammatory cytokines or chemokines [367, 368] can contribute to fracture healing. The interaction between skeletal and immune systems (known as osteoimmunology) has been studied increasingly over the last years, including its application to fracture treatment [35, 361, 369, 370].

Fracture related infections (FRI) are a major complication in trauma surgery, and are associated with long hospital stays, long-term antibiotic treatment, multiple revision surgeries, and, overall, a reduced quality of life and high healthcare costs. *S. aureus* and coagulase-negative staphylococci (CoNS) are the leading etiologic agents in such infections accounting for more than 60% of infections. *S. epidermidis* is the most prominent member of the CoNS and causes approximately 20% of orthopaedic device-related infections [93]. However, its prevalence may even increase to 50% in late-developing infections [94], which is often attributed to the sub-acute nature of *S. epidermidis* infections, with patients often only presenting many months after surgery.

Despite its prevalence in orthopaedic device and fracture-related infection, relatively little is known about host defences against *S. epidermidis,* or how these infections progress in humans. Innate immune responses to *S. epidermidis* have been studied outside the context of FRI and are known to involve the secretion of interleukin (IL)-6, IL-1β, tumour necrosis factor (TNF)-α or IL-8, most of which occurs through toll-like receptor (TLR)-2 recognition. This results in the recruitment of neutrophils and macrophages, which will subsequently attempt to phagocytose and kill the bacteria through the production of reactive oxygen species, antimicrobial peptides, or proteases. While these mechanisms are highly effective against planktonic bacteria, the causative bacteria in FRI frequently reside in a biofilm and, as such, are more resistant to host defences [131, 160, 371, 372]. Currently, the specific details concerning adaptive immune responses to *S. epidermidis* are relatively unknown, although the use of immunodeficient mice has shown that mice lacking T and B cells present a delay in infection clearance [245].

Recently, we established a *S. epidermidis* FRI model in mice [373], in order to provide a reliable model to study FRI caused by this pathogen. Using this model, we assessed the influence of fracture fixation stability on infection progression and we observed that different mechanical environments led to different infection outcomes in C57BL/6 mice. Specifically, unstable fractures displayed a delay in clearance of the infection from the tissues. This phenomenon was not observed in BALB/c mice, suggesting that host genetics play a key role in these models. In addition, we examined *S. aureus* infection in the same murine model and observed a more severe infection associated with higher osteolysis, compared to that seen with *S. epidermidis*.

The aim of this study was to characterize the immune responses during fracture healing for stable and unstable constructs, under both sterile conditions and following inoculation with *S. epidermidis* or *S. aureus*. We aimed to determine if the differing infection rates could be linked to features of the immune response impacted by the different mechanical contexts [373].

## Materials and methods

### *Animals*

The study was approved by the ethical committee of the canton of Graubünden in Switzerland (TVB 11/2013 and TVB 2016/03) and was carried out in a research facility accredited by Association for Assessment and Accreditation for Laboratory Animal Care (AAALAC) International. Skeletally mature (20-28 weeks old, average weight ± SD: 25.85 ± 2.79 g), female, specific pathogen free (SPF) C57BL/6 mice, purchased from Charles River (Germany), and C57BL/6 IL-17A knock-out (KO), kindly provided by Prof. Dr. Manfred Kopf (ETH Zürich, Switzerland), were used in this study. All animals were allowed to acclimatize to experimental conditions for at least two weeks prior to the start of the study. Mice were housed under a 12 hour dark/ 12 hour light cycle, in groups of three to six in individually ventilated cages (XJ, Allentown), changed weekly, and they were re-housed in the same groups post-surgery. Animals were fed with a standard diet (3436, Provimi Kliba) and had free access to water at all times.

### *Study design*

Samples for the study of immune responses during fracture healing, with and without infection, were obtained from C57BL/6 and BALB/c SPF mice (females, 20-28 weeks old) (Groups described in Table 5-2). That study was conducted in a similar way as the one described here, although all specific details can be found elsewhere [373].

**Table 5-2** Model characterization study design. Samples were obtained from a previous study using the following set up. NA: Not applicable.

| | **Day 3** | | **Day 7** | | **Day 14** | | **Day 30** | |
|---|---|---|---|---|---|---|---|---|
| **Group** | **C57BL/6** | **BALB/c** | **C57BL/6** | **BALB/c** | **C57BL/6** | **BALB/c** | **C57BL/6** | **BALB/c** |
| Non-inoculated | | | | | | | | |
| Rigid | 6 | NA | ≥ 6 | 5 | ≥ 6 | 4 | ≥ 6 | ≥ 6 |
| Flexible | 6 | NA | ≥ 6 | 6 | ≥ 6 | 3 | ≥ 6 | ≥ 6 |
| *S. epidermidis* Inoculated | | | | | | | | |
| Rigid | 6 | NA | 6 | 4 | ≥ 6 | 6 | 6 | ≥ 6 |
| Flexible | ≥ 6 | NA | 5 | 6 | ≥ 6 | 6 | ≥ 6 | 6 |
| *S. aureus* Inoculated | | | | | | | | |
| Rigid | 6 | NA | ≥ 6 | NA | ≥ 6 | NA | - | - |
| Flexible | ≥ 6 | NA | 5 | NA | ≥ 6 | NA | - | - |

After characterizing the model, we aimed to assess mRNA expression in C57BL/6 with and without *S. epidermidis* infection. Based on data from the previous study, we selected two time-points to observe mRNA expression changes over time (Table 5-3).

**Table 5-3** mRNA expression study design. Final number of animals per group.

| **mRNA expression study groups (C57BL/6 mice)** | | | | | |
|---|---|---|---|---|---|
| | **Day 0** | **Day 7** | | **Day 14** | |
| **Group** | **Non-operated** | **Rigid** | **Flexible** | **Rigid** | **Flexible** |
| Non-inoculated | 7 | 6 | 5 | 6 | 5 |
| *S. epidermidis* inoculated | - | 6 | 6 | 6 | 5 |

Finally, we aimed to determine the role for IL-17A in *S. epidermidis* infection outcome, in C57BL/6 and IL-17A KO C57BL/6 mice (Table 5-4).

**Table 5-4** IL-17A study groups. Final number of animals per group.

| **IL-17A study groups (C57BL/6 mice)** | | | | | |
|---|---|---|---|---|---|
| | **Day 0** | **Day 14** | | **Day 30** | |
| **Group** | **Non-operated** | **Non-inoculated** | ***S. epidermidis* inoculated** | **Non-inoculated** | ***S. epidermidis* inoculated** |
| Wild type | 4 | 9 | 8 | - | 9 |
| IL-17A KO | 3 | 9 | 8 | - | 7 |

*Bacteria and inoculum preparation*

In all studies, the test microorganism was *S. epidermidis* Epi 103.1, obtained from a patient with chronic implant-related bone infection. This strain has a weak *in vitro* biofilm formation capacity (our unpublished observations) according to the scoring system of Stepanovic *et al.* [343]. The inocula were prepared as described before [373]. The administered inoculum was $1x10^4$ Colony Forming Units (CFU).

*Surgery*

Commercially pure Titanium (CpTi) 4-hole rigid and CpTi 4-hole flexible MouseFix™ implants, and Titanium Aluminium Niobium alloy (Ti6Al4Nb (TAN)) screws (RiSystem AG) were used in the mRNA expression study, while in IL-17A KO animals only the rigid plates were used. Prior to use, all implants were cleaned and sterilized as previously described [296].

Surgery was performed as previously described [373]. Briefly, under general anaesthesia with isoflurane (2-3% isoflurane in 100% $O_2$, 1 l/min) (Isofluran Baxter®, Baxter AG), the animal was placed in prone position and a skin incision was made from tail base to left stifle. The subcutaneous Fascia lata was cut and the tissue plane between the quadriceps and the biceps femoris muscle was bluntly dissected. A Teflon foil was placed around the femur to protect the soft tissue from contamination. The implant was then fixed to the bone using four self-tapping, angular stable screws. Screw holes were predrilled with a 0.31 mm drill bit (RISystem AG). Once the implant was

in place, a 0.44 mm defect osteotomy was performed using a jig and a Gigli wire. In the inoculated groups, 2.5 µl of bacteria suspension was injected in the osteotomy site. The foil was then removed and the Fascia lata and the skin were closed with continuous sutures (5-0 Vicryl rapide, Ethicon, Belgium). Following surgery, a lateral radiograph of the femur was taken to confirm proper positioning of the implant.

Analgesia was provided in the form of subcutaneous injections of buprenorphine (0.1 mg/kg, Bupaq®, Streuli Pharma AG), pre-operatively and post-operatively every 6-8 hours for 16 hours. Additionally, a palatable form of acetaminophen (2 mg/ml, as Dafalgan® Syrup for Children, Bristol-Myers Squibb SA) was added to the drinking water for 5 days. Animals were monitored twice daily for 5 days post-operatively and subsequently once a day, using a detailed numerical scoring system that takes into account general behaviour, external appearance, wound status and animal movement (scale 0-18). Weights and radiographs of the operated limb were taken weekly.

*Euthanasia and sample collection*

At each scheduled time-point, the animals were euthanized by cervical dislocation after inducing general anaesthesia in an induction box (5% isoflurane in 100% $O_2$, 1 l/min). Immediately prior to euthanasia, blood was collected via retro-orbital bleeding to prepare serum for subsequent analysis (centrifuged at 5000 rpm for 10 minutes). Post-mortem, a lateral radiograph of the left femur with implant in place was acquired. The operated femur, the implant, and the surrounding soft tissue, were harvested separately in sterile containers with cold phosphate buffered saline (PBS), or RNAlater (Qiagen) for mRNA expression analysis. Some contralateral femurs were also collected as additional controls. The soft tissue and bone samples collected for quantitative bacteriology were mechanically homogenized (Omni Tissue Homogenizer and Hard Tissue Homogenizing tips, Omni International). Aliquots of the tissue homogenate were kept for quantitative bacteriology and for cytokine/chemokine quantification. The remaining sample was filtered through a 70 µm cell strainer (BD Falcon) and finally resuspended in complete RPMI (cRPMI: RPMI 1640 (Gibco)), penicillin (1 U/ml, Sigma-Aldrich), streptomycin (1 µg/ml, Sigma-Aldrich), kanamycin (0.1 µg/ml, Gibco), MEM vitamin (1x, Sigma-Aldrich), L-glutamine (2 mM, Sigma-Aldrich), sodium pyruvate (1 mM, Sigma-Aldrich), non-essential amino acids (1x, Sigma-Aldrich) and heat-inactivated foetal calf serum (10%, Sigma-Aldrich)). Spleen and popliteal lymph node were harvested in cold PBS and cRPMI respectively. To obtain single cell suspensions, samples were mashed with a syringe rod through a 70 µm cell strainer. For the spleen, erythrocytes were haemolysed with $ddH_2O$ for 1 minute. Both single cells suspensions were finally resuspended in cRPMI. Cells were counted in all samples with Scepter™ 2.0 Cell Counter (Millipore) and adjusted to $2x10^6$ cells/ml.

*Quantitative bacteriology*

Viable bacterial counts were determined by plating bone homogenate and soft tissue homogenate on 5% horse blood agar (BA) (Oxoid). The number of bacteria associated with the implant was determined by sonicating the implant and screws in PBS for 3 minutes (Bandelin Sonorex at 40 KHz), vortex mixing for 10 seconds, and finally plating serial dilutions on 5% horse BA. All BA plates were incubated at 37°C for performing bacterial counts at 24 and 48 hours. Mice were considered as infected when at least one sample (bone, soft tissue or implant) was culture-positive. Bacteria recovered from each animal were confirmed to be *S. epidermidis* Epi 103.1 by Random Amplification of Polymorphic DNA (RAPD) test [347].

*Multiplex assays*

Bone homogenates stored at -20°C were thawed, centrifuged (9000 g, 4°C, 10 minutes) and the supernatants collected for cytokine and chemokine quantification. Those were measured using a Milliplex MAP Mouse cytokine/chemokine Magnetic Bead Panel (Merck) for: granulocyte colony-stimulating factor (G-CSF), interferon (IFN)-γ, IL-2, IL-4, IL-6, IL-10, IL-13, IL-17A, keratinocyte chemoattractant (KC), monocyte chemoattractant protein (MCP)-1 and TNF-α. Additionally, spleen single cell suspensions resuspended in cRPMI were plated in 24-well plates ($1x10^6$ cells/well) and were stimulated with phorbol 12-myristate 13-acetate (PMA) (20 ng/ml, Sigma-Aldrich) and ionomycin (200 ng/ml, Sigma-Aldrich) then incubated at 37°C, 5% $CO_2$. Culture supernatants were collected 48 hours later. Using Milliplex MAP Mouse cytokine/chemokine Magnetic Bead Panel (Merck) the following analytes were measured: IFN-γ, IL-2, IL-4, IL-10, IL-17A and TNF-α. Bone homogenates from the IL-17A study were centrifuged (9000 g, 4°C, 10 minutes) and supernatants were collected and stored at -80°C until use. IFN-γ, IL-4, IL-6, IL-17A, IL-17F, IL-22, IL-33 and KC were then measured in those samples using a U-PLEX Biomarker Group 1 (mouse) assay (Mesoscale Discovery), following the manufacturer's instructions. Samples were incubated in the plate at 4°C overnight to improve detection sensitivity.

*Flow cytometry*

Bone single cell suspensions were stained with Fixable Viability Dye eFluor780 (eBioscience) and for surface markers, as described in Supplementary Information Table 5-5. Single cell suspensions from lymph nodes and bones of IL-17A KO animals were stimulated with PMA (50 ng/ml), ionomycin (500 ng/ml) and Brefeldin A (1x, eBioscience) for 4 hours at 37°C, 5% $CO_2$. Cells were subsequently stained with Fixable Dye eFluor780 and for surface markers before fixation and permeabilization using Intracellular Fixation & Permeabilization Buffer (eBioscience). Finally,

samples were stained intracellularly for cytokines, as described in Supplementary Information Table 5-5. All samples were analysed using a Gallios flow cytometer (Beckman Coulter). Gating strategies are shown in Supplementary figures: Figure 5-24, Figure 5-25 and Figure 5-26.

*Myeloperoxidase analysis*

Bone homogenates (from day 3 post-surgery), previously frozen at -80°C, were thawed and the supernatant collected before myeloperoxidase (MPO) levels were measured using a mouse MPO ELISA kit (Boster Biological Technology), according to the manufacturer's instructions.

*RNA extraction and mRNA expression evaluation*

Femoral bone diaphysis from the mRNA expression study groups were collected in RNAlater (Qiagen) and stored at -80°C after 24 hours at 4°C. RNA extraction was performed using a Tissue Lyse kit (Qiagen) following the manufacturer's instructions. RNA amount and quality was quantified using a NanoDrop 1000 Spectrophotometer (Thermo Fisher) and integrity was assessed using P200 Screen Tape (Agilent Technologies). Reverse transcription was performed on 400 ng of RNA/sample using Reaction Buffer (5x), dNTP Mix (10 mM), Random Hexamer Primer (0.2 µg/µl), RiboLock RNase Inhibitor (20 U/µl) and RevertAid Reverse Transcriptase (200 U/µl) (Thermo Scientific). mRNA expression was assessed using 48-gene custom TaqMan® Array Micro Fluidic Cards (Affymetrix/Thermo Fisher), with 100 ng of cDNA loaded into each port (selected genes, representative of bone healing process, tissue regeneration and immune responses are listed in Supplementary Information Table 5-6. mRNA expression in the microfluidic cards were measured using a QuantStudio 7 Flex Real-Time PCR System (Thermo Fisher). To evaluate mRNA level differences, the ΔΔCt method was used, with *18S*, *Eef2* and *Gapdh* as endogenous controls, and a control group (femurs of non-operated mice) was used as a calibrator when possible (otherwise indicated in results section).

*Statistical Analysis*

Statistical analysis was conducted using GraphPad Prism 7 software (GraphPad Software). Statistical tests performed are indicated in each figure legend. Differences were considered significant with $p<0.05$ ($p$-values reported in the figures).

## Results

*Cytokine production locally for non-inoculated and inoculated (C57BL/6 and BALB/c)*

Bone homogenate supernatants were analysed to determine cytokine and chemokine levels at the fracture site of non-inoculated and inoculated C57BL/6 (Figure 5-14) and BALB/c animals (Supplementary Figure 5-27). We assessed innate immune response markers such as G-CSF, KC, MCP-1 and IL-6. Cytokines associated with T cell differentiation/responses were also measured such as IFN-γ, IL-17A, IL-2, IL-4, IL-13 and IL-10. IL-4 and IL-13 were in general not detected, while for IL-2 and IL-10 levels were very low and close to the detection limit.

For non-inoculated C57BL/6 animals, the innate immune response markers (G-CSF, KC, MCP-1 and IL-6) increased at 3 and 7 days post-operatively, and returned to baseline levels between days 14 and 30. There were no statistically significant differences in cytokine levels between non-inoculated animals with flexible or rigid devices, although groups with a flexible device tend to present higher levels.

Inoculation with *S. epidermidis* in C57BL/6 mice resulted in a similar trend in innate immune markers. Values peaked between days 3 and 7 and decreased afterwards, reaching baseline levels between days 14 and 30. Animals with a flexible implant presented with higher levels of cytokines and chemokines, with statistically significant differences at day 3 for G-CSF, KC and IL-6. MCP-1 and IFN-γ did not show differences between implant types, while IL-17A was slightly increased in *S. epidermidis* inoculated compared to non-inoculated animals, although differences were not statistically significant. Interestingly, inflammation markers generally did not differ significantly between non-inoculated and inoculated animals with a rigid device.

Inoculation with *S. aureus* lead to significant changes in innate markers, with G-CSF, KC and IL-6 being significantly higher at all time-points when groups were compared to non-inoculated or *S. epidermidis* inoculated counterparts. IL-17A was highly elevated in *S. aureus* inoculated animals compared to non-inoculated animals. Similar to *S. epidermidis* inoculated animals, mice with a flexible implant displayed higher G-CSF, KC and IL-6 responses to *S. aureus* infection compared to animals with a rigid device.

In the BALB/c animals, similar trends were observed (Supplementary Figure 5-27). Once more, animals with a flexible implant (non-inoculated or *S. epidermidis* inoculated) often presented with higher inflammation markers compared to their counterpart group with a rigid implant (Supplementary Figure 5-27).

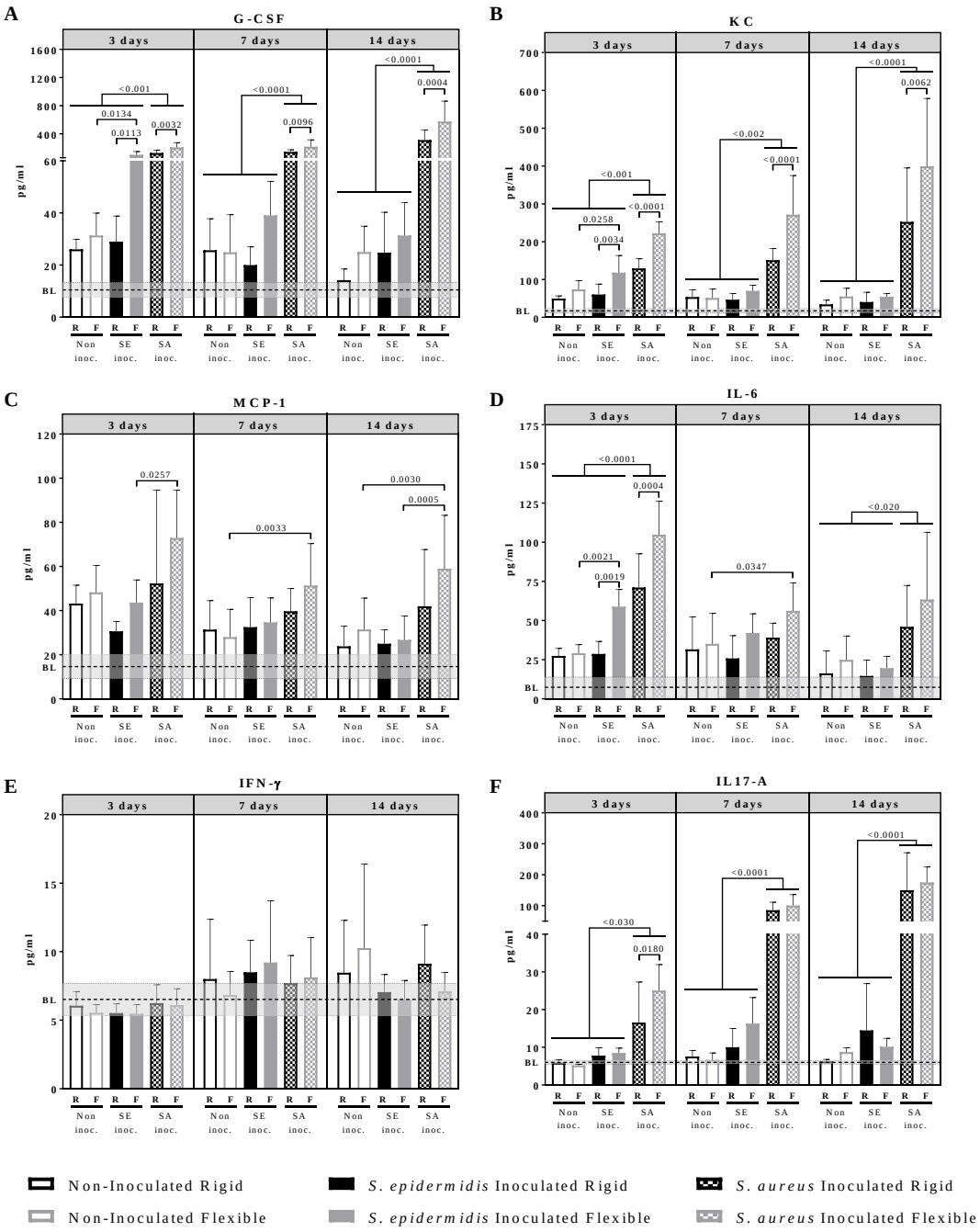


**Figure 5-14** Cytokine levels (pg/ml) in bone homogenate supernatants of C57BL/6 mice at 3, 7 and 14 days post-operatively. Mean values and SD (n=5-11). BL: baseline, mean of the control group; grey area: BL±SD of the control group. 2-way ANOVA per time-point with Tukey or Sidak post hoc correction. Grouped statistics summarizes the following comparisons, with only largest *p*-value reported: Non-inoculated Rigid vs *S. aureus* Inoculated Rigid, *S. epidermidis* Inoculated Rigid vs *S. aureus* Inoculated Rigid, Non-inoculated Flexible vs *S. aureus* Inoculated Flexible, *S. epidermidis* Inoculated Flexible vs *S. aureus* Inoculated Flexible. R: rigid implant; F: flexible implant

*Infection influences immune cell populations within the bone marrow*

Cell populations in the femoral bone marrow were analysed by flow cytometry (gating strategy: Supplementary Figure 5-24). Macrophages (F4/80+Ly6G-), T cells (CD3+CD19-) and B cells (CD19+CD3-), as well as T lymphocyte subclasses (CD4+, CD8+ and CD4-CD8-), were analysed

at day 3, 7 and 14. As no significant differences were observed in total cell counts and viability, results are reported as a proportion of all live cells, or as a percentage of total CD3+ cells. In non-inoculated C57BL/6 mice, macrophage proportions were seen to increase at early time-points and they decreased over time (Figure 5-15A). T cells and B cells reached their peak at day 14, although for T cells the increase was not statistically significant, while B cells experienced a significant increase in proportion (Figure 5-15A). For *S. epidermidis* inoculated animals, similar results were observed, with a significant increase in macrophages at day 3 and B cells at day 14. Finally, for *S. aureus* inoculated animals a significant increase in macrophages was also observed at days 3 and 7, while B cells showed an opposite trend, with a decrease in proportion. Within T cell subclasses, no significant differences were observed for non-inoculated mice. *S. epidermidis* inoculated animals with a flexible device and all *S. aureus* inoculated animals experienced a decrease in CD8+ and CD4+ T cells in favour of double-negative T cells (Figure 5-15B). In BALB/c animals, similar trends were observed, with recruitment of macrophages at early time-points, and a peak in T and B cells at day 14 (Supplementary Figure 5-28).

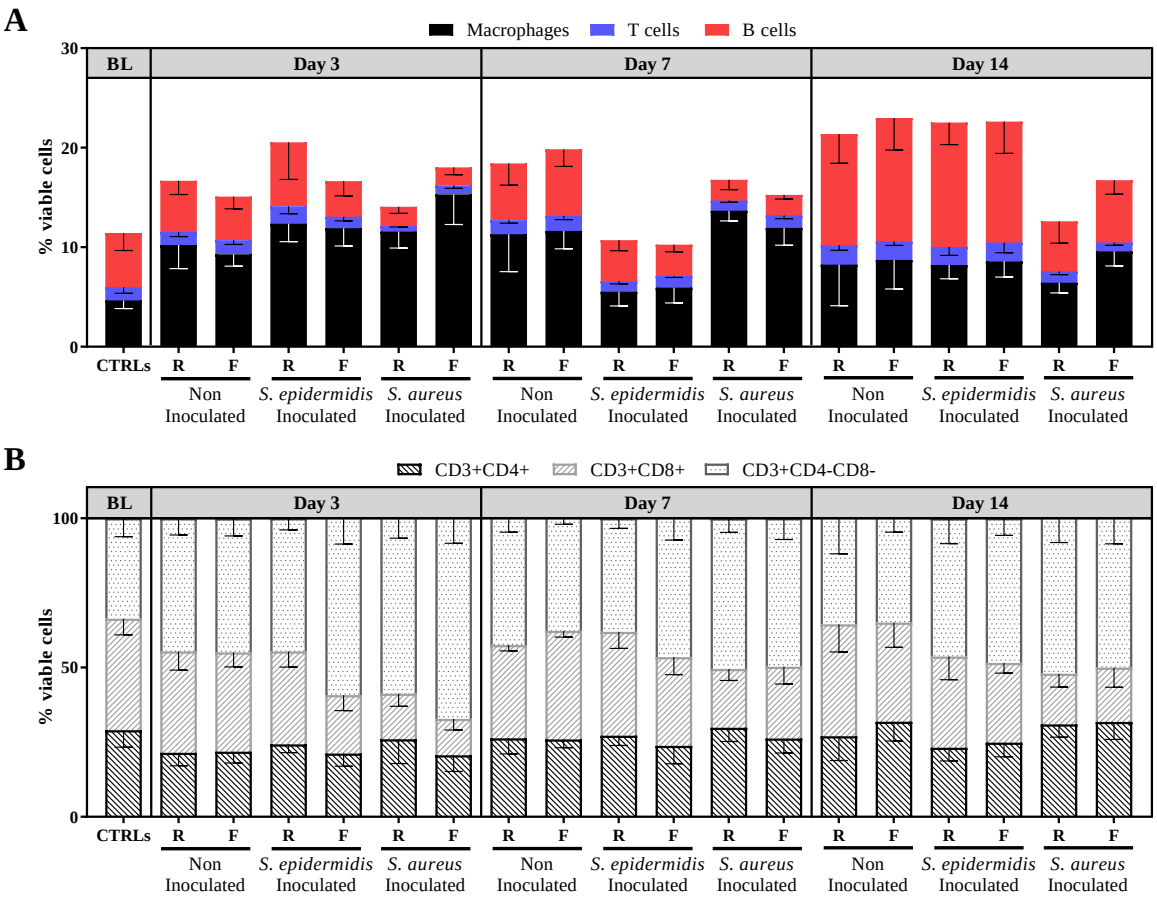


**Figure 5-15** Percentage of macrophages (Ly6G-F4/80+), T cells (CD3+CD19-) and B cells (CD19+CD3-) over viable cells (A), and percentage of CD4+, CD8+ and CD4-CD8- over CD3+ cells (B), in bone single cell suspensions of C57BL/6 mice at days 3, 7 and 14 post-operatively. Mean values and SD (n=5-9). BL: baseline, mean of the control group. R: rigid implant; F: flexible implant

*Early granulocyte infiltration*

Early granulocyte infiltration (day 3 post-operatively) was assessed with MPO measurements in bone homogenates of C57BL/6 mice. Higher levels of MPO were observed after surgery, in all groups, being statistically significant only for animals with a flexible implant. Flexible implant groups tend to have higher levels in comparison to rigid counterparts, although this did not reach statistical significance (Figure 5-16).

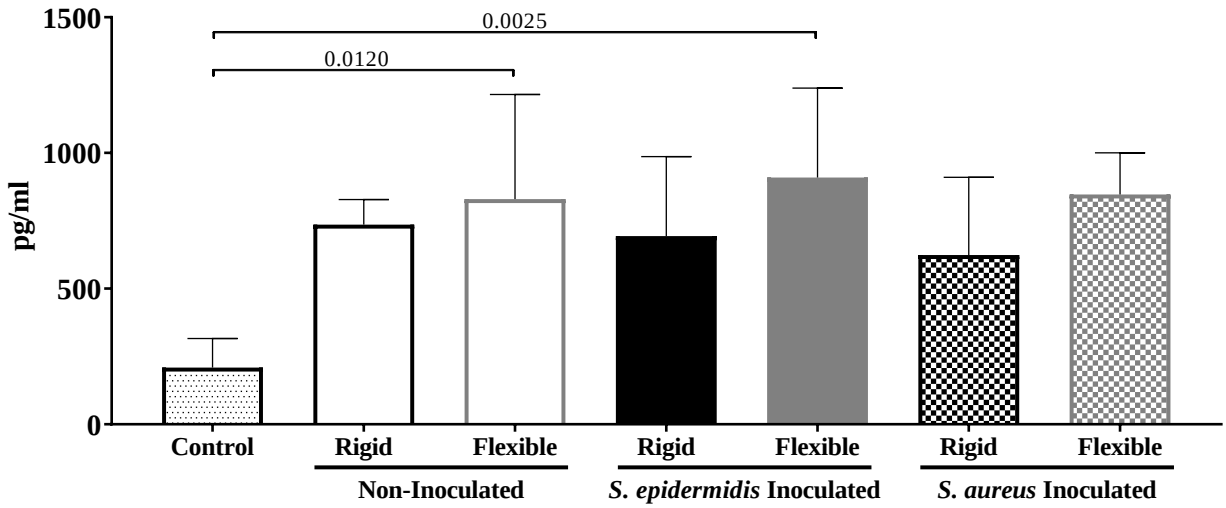


**Figure 5-16** MPO levels (pg/ml) at day 3 in bone homogenate supernatants. Mean values and SD (n=4-7). Control: contralateral femurs. Normality test with Shapiro-Wilk test.1-way ANOVA, Sidak post hoc correction.

*Infection development in C57BL/6*

In additional groups of animals, the experiment was repeated and *S. epidermidis* numbers quantified in both the soft tissue and those associated with the implant. Animals with a rigid device tended to clear the infection more quickly than animals with a flexible implant (Figure 5-17).

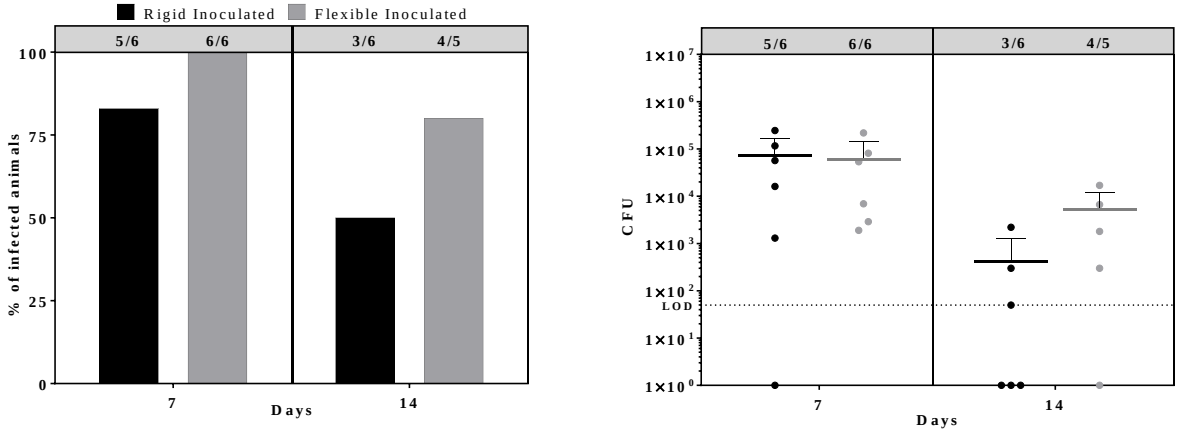


**Figure 5-17** Percentage of C57BL/6 mice infected at days 7 and 14, and total CFU counts (from soft tissue and implant). Number of culture-positive animals/total number of animals per group are shown in the upper panel of each graph. Mean values and SD (n=5-6). LOD: Limit of detection, $0.5x10^2$. Fisher's exact test and Mann-Whitney test. No significant differences observed.

*mRNA expression data in C57BL/6*

mRNA expression within bone homogenates was analysed at days 7 and 14 in C57BL/6 mice (Figure 5-18). All samples analysed had an A230/A260 index greater than 2 and RIN values were bigger than 6. Expression was detected for most of the genes, however, *Col10a1* and *Csf3* were only expressed in operated femurs, while *Csf2*, *Hrh4*, *Il23* and *Il4* appeared only at very late cycle numbers, or were not detected at all. Interestingly, *Il17a* was almost only expressed in the inoculated animals (Figure 5-18).

From the mRNA expression data, several patterns could be observed (Figure 5-18). Some genes, such as *Arg1*, *Ccl2*, *Nos2*, *Il6* and *Hif1a* (Supplementary Figure 5-29), were maximally expressed at day 7 and decreased by day 14, although they were still upregulated compared to control group. Of note, they were often upregulated in flexible groups compared to rigid counterparts, although this was not always statistically significant. Interestingly, a group of genes linked to bone regeneration including *Col1a1*, *Acp5*, *Col10a1* and *Sox9*, showed a continuous increase over time, with highest levels detected at day 14. Both *Col10a1* and *Sox9* were especially increased in animals with a flexible device, probably due to their role in endochondral ossification. We also observed some genes whose expression decreased over time but only in non-inoculated animals, while in inoculated mice they remained slightly upregulated. Genes included in this category are mostly associated to immune responses and pathogen recognition such as *Cd80*, *Tlr2*, *Tlr4*, *Tnf* and *Adgre1*. A gene that was almost exclusively expressed in inoculated animals was *Il17a*, with very low levels in the non-inoculated samples where expression was detected. Finally, some genes were downregulated at all time-points in all operated femurs (e.g. *Casp3*, *Elane*, *Hmgb1* and *Sell*), or

were downregulated at day 14 (*Ccr2*, *Hdc*, *Hrh2*, *Mrc1*, *S100a8*, *S100a9* and *Tgfb1*). Interestingly several of these genes are associated with cell damage signalling or neutrophil products.

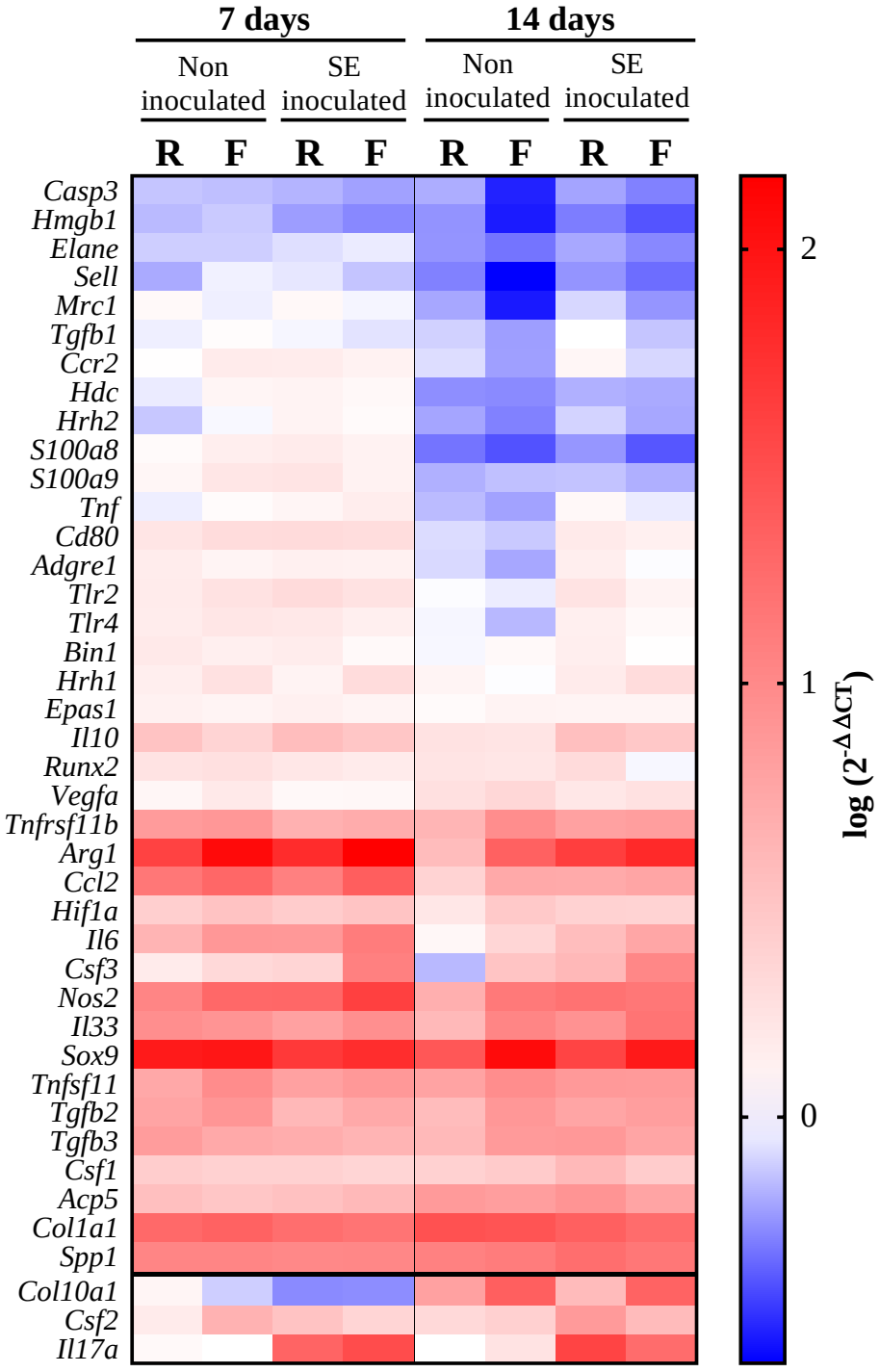


**Figure 5-18** Heatmap of mRNA expression at days 7 and 14. Values represent log ($2^{-\Delta\Delta CT}$), using Control group as a calibrator except for *Col10a1*, *Csf2* and *Il17a* (bottom of the chart) where Non-inoculated Rigid group was used as no mRNA expression was detected in Control group. SE: *S. epidermidis*, R: rigid, F: flexible

*Adaptive immune responses: Lymph node and Spleen*

To evaluate adaptive immune responses, popliteal lymph nodes and spleens were collected. Lymph node single cell suspensions were stimulated for 4 hours with PMA, ionomycin and brefeldin A, and stained with surface and cytokine antibodies (Figure 5-19). In general, an increase of activated cells was observed in all groups after day 3. Some significant differences were observed between the different groups, especially at day 14. Of note, total cell counts in lymph nodes of *S. aureus* inoculated mice were significantly higher at days 7 and 14, when compared to non-inoculated or *S. epidermidis* inoculated animals and thus the differences in percentage at those time-points may mean no differences in cell numbers

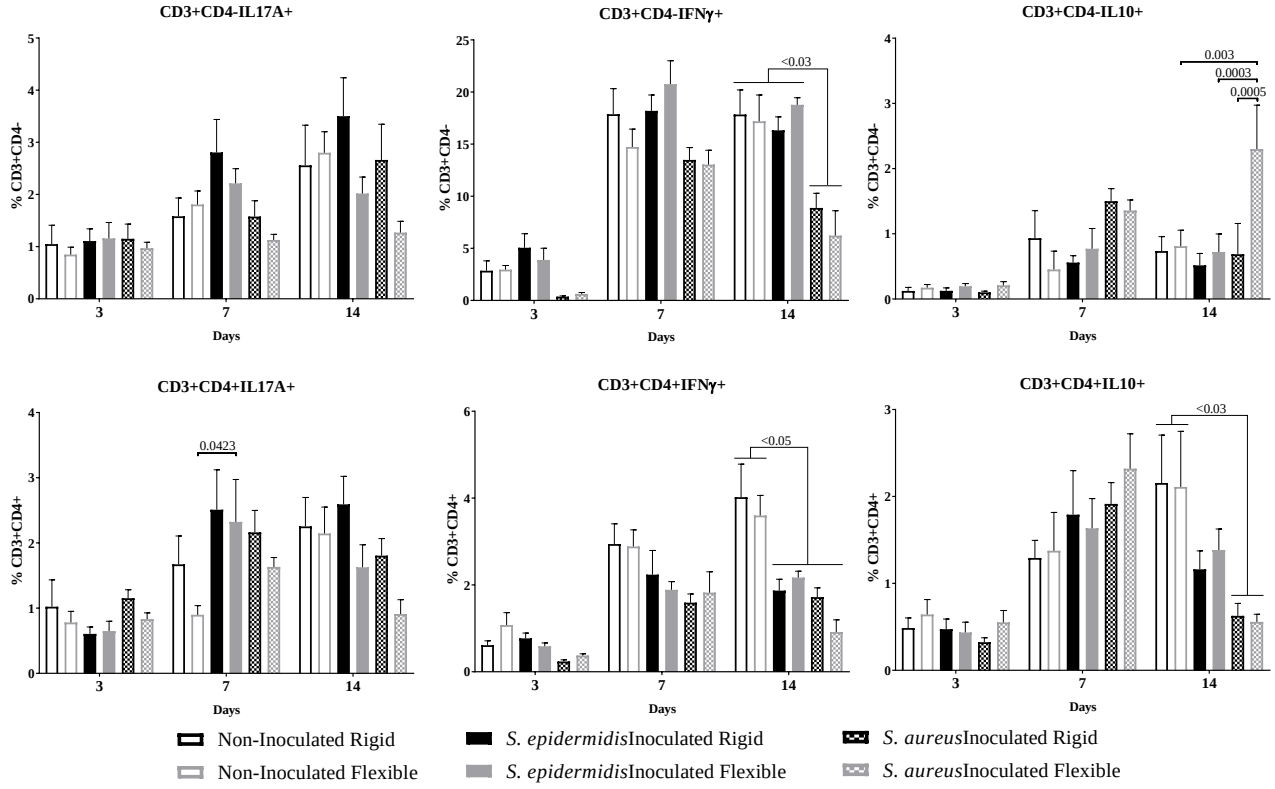


**Figure 5-19** Percentage of IL-17A, IFN-γ and IL-10 producing T cells (CD3+CD4- and CD3+CD4+) in popliteal lymph node of C57BL/6 mice. Mean values and SEM (n=6-9). 2-way ANOVA per time-point, Tukey post hoc test.

Additionally, day 30 spleen samples from non-inoculated and inoculated C57BL/6 and BALB/c mice were stimulated with UV-killed *S. epidermidis*. After 72 hours, secretion of several innate immunity markers were observed for both conditions (non-inoculated versus inoculated). IL-17A was the cytokine more differentially expressed between both groups, being almost only secreted in animals that had been previously inoculated with *S. epidermidis* (Figure 5-20) for both C57BL/6 and BALB/c strains.

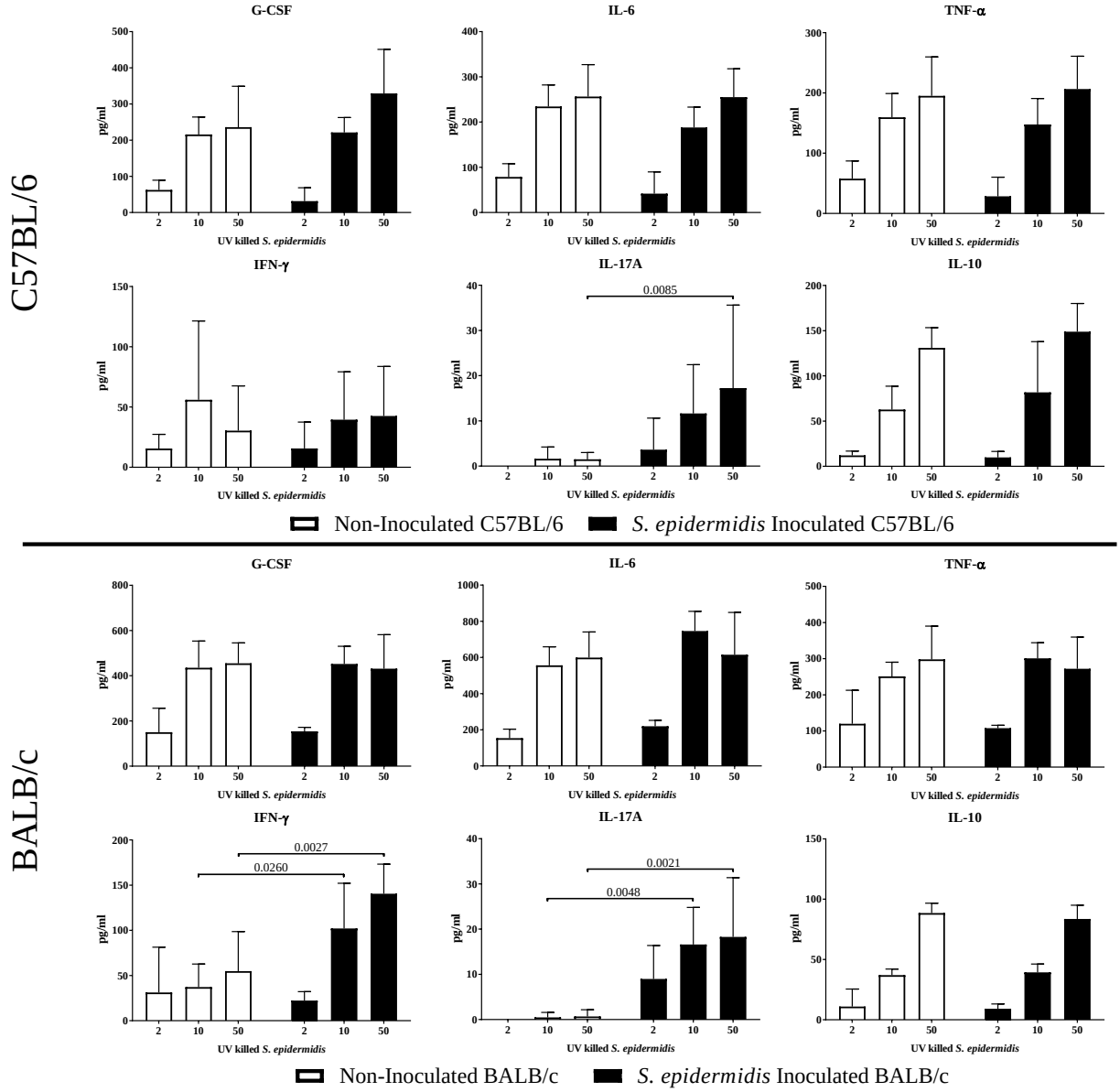


**Figure 5-20** Cytokine production by splenocytes from non-inoculated and *S. epidermidis* inoculated C57BL/6 and BALB/c mice (rigid and flexible samples grouped together) after stimulation with UV-killed *S. epidermidis in vitro* (dose indicated in the x-axis: ratio of bacteria per splenocyte). Mean values and SD (n=5-8). Two-way ANOVA, Sidak post hoc correction.

*IL-17A KO model*

As IL-17A seemed to be selectively induced by the presence of *S. epidermidis*, IL-17A KO mice were used to study the role of IL-17A in infection clearance. As observed above, at day 14 some WT animals had become culture-negative, while none of the IL-17A KO animals cleared the infection at that time-point. However, differences were not statistically significant. At day 30, culture-negative animals were found in both groups, with more WT animals clearing the infection

compared to the KO animals. In terms of bacterial counts, no significant differences were observed at any time-point (Figure 5-21).

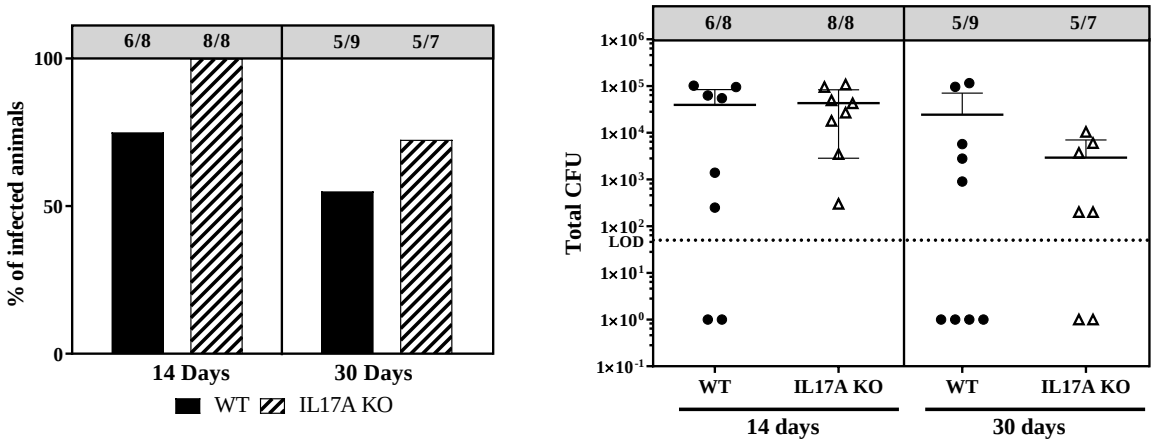


**Figure 5-21** Percentage of WT and IL-17A KO C57BL/6 mice infected at days 14 and 30, and total CFU counts (from bone, soft tissue and implant). Mean values and SD (n=7-9). LOD: Limit of detection, $0.5x10^2$. Fisher's exact test and Mann-Whitney test. No significant differences observed.

We aimed to identify the cellular source of IL-17A, previously detected in bone. From flow cytometric analysis (gating strategy in Supplementary Figure 5-26), we observed several cell types producing IL-17A such as CD4+ T lymphocytes, γδ T lymphocytes, NK cells and lineage-negative cells (negative for all the markers included). Following surgery, there was an increase in IL-17A+ CD4+ and γδ T lymphocytes compared to control groups (Figure 5-22). CD4+IL-17A+ cells were significantly increased in inoculated animals in comparison to non-inoculated or control mice. Of note, animals that were found culture-negative (infection considered cleared), had the lowest levels of IL-17A+ CD4+ and γδ T lymphocytes, suggesting once more that IL-17A seems to be induced on an active infection.

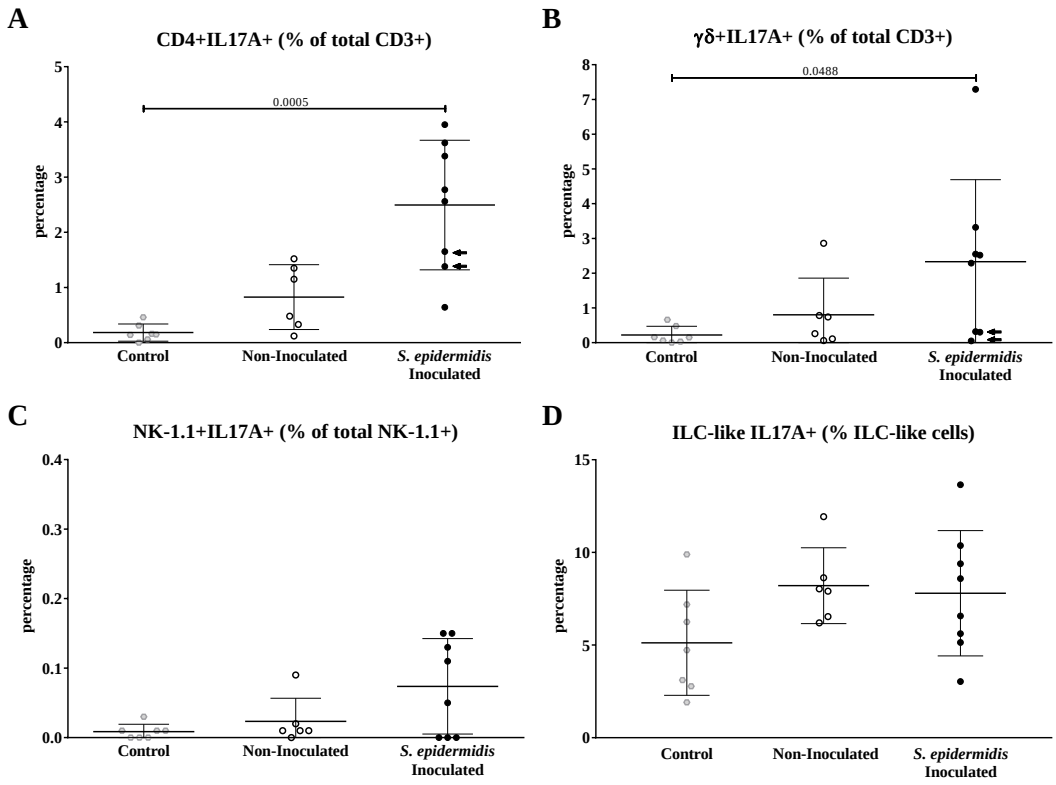


**Figure 5-22** Percentage of IL-17A producing cells in control, non-inoculated *or S. epidermidis* inoculated for WT and IL-17A KO C57BL/6 mice at day 14. Each graph title shows over which population percentage is expressed. Note in A and B, WT mice that were found culture negative are indicated with a black arrow. Mean values and SD (n=7-11). 1 way-ANOVA or Kruskal-Wallis, with Tukey or Dunn's post hoc test.

Cytokines were measured in bone homogenate supernatants (Figure 5-23). Once more, levels for most of the cytokines were quite low when comparing non-inoculated and inoculated animals, with only slightly higher levels of inflammatory markers such IL-33 or IL-6. We could detect IL-17A only in inoculated WT animals, supporting the increase seen in the previous study at the mRNA expression level. IFN-γ was detected in low concentrations in all groups, with both inoculated WT and KO presenting the highest levels. Nevertheless, only the KO inoculated group was significantly different compared to non-inoculated counterpart animals.

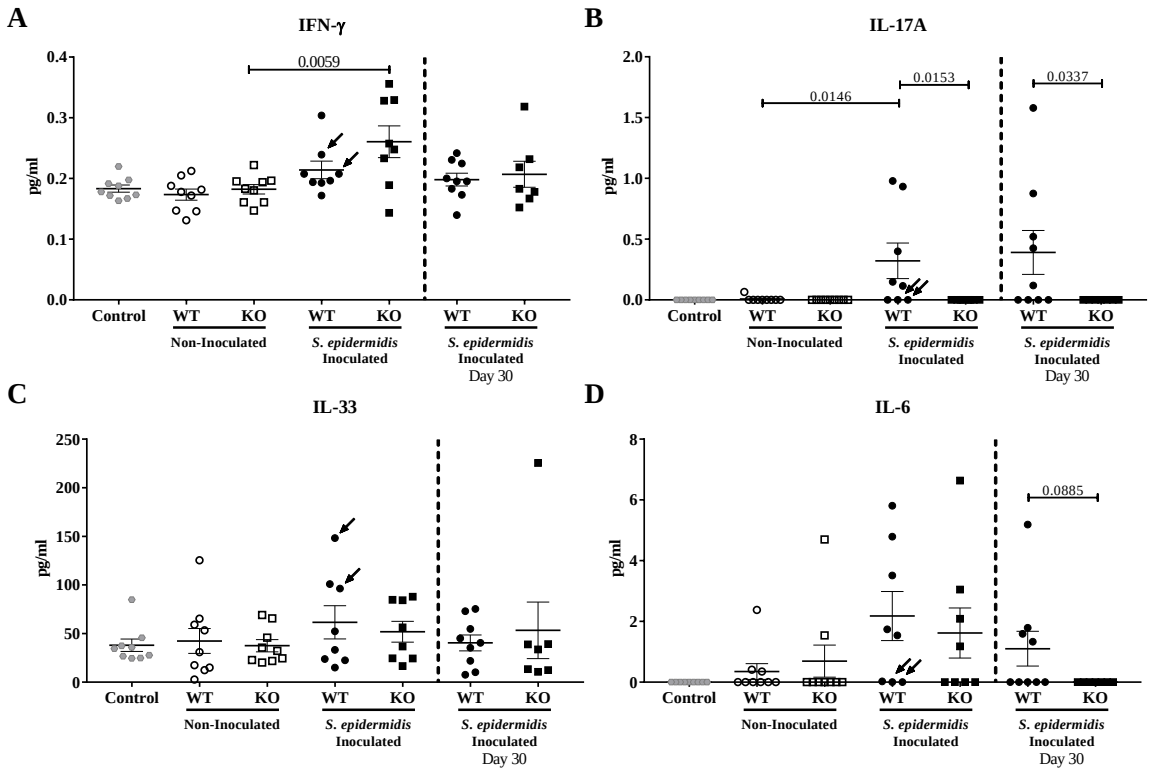


**Figure 5-23** Cytokine levels in bone homogenates of control animals (wilt-type and KO pooled together as no differences were observed), wild-type and IL-17A KO C57BL/6 mice, non-inoculated and inoculated. Mice that were found culture negative are indicated with a black arrow Mean values and SD (n=7-9). 2 way-ANOVA with Tukey post hoc for day 14, Mann-Whitney test for day 30.

## Discussion

In this study we aimed to characterize the immune responses associated with bone fracture, with a focus on *S. epidermidis* and *S. aureus* FRI. Our model included implants with different mechanical properties, which, based on our previous findings [373], can lead to different kinetics of infection clearance. We have previously demonstrated that *S. epidermidis* inoculated C57BL/6 mice were more likely to clear infection when a rigid fixation device was implanted compared to a flexible device. We therefore sought to investigate if differential immunological responses to fixation stiffness could explain the differences observed in our previous study.

The fact that non-inoculated animals with a flexible implant had a tendency for higher inflammatory markers compared to mice with a rigid implant (both in C57BL/6 and BALB/c), suggests that instability leads to a more inflamed local microenvironment. This was also supported by MPO analysis in bone marrow and in mRNA expression analysis. However, differences in levels of individual mediators were often small and did not reach statistical significance in the majority of cases. Similar observations were done in a sheep model of mechanically-induced impaired bone

healing. In that study, Schmidt-Bleek *et al.* reported a higher percentage of cytotoxic T cells and macrophages in the hematoma and bone marrow of less stable fractures, which they associated to a higher/prolonged inflammatory environment [374]. Thus, in non-inoculated conditions, the more inflammatory environment observed in the unstable context could have a negative impact in bone healing. Consistent with this, the link between increased inflammation (acute or chronic) and fracture healing complications has already been proposed [375-380]. In clinics, politrauma patients, who often have high systemic levels of inflammatory cytokines (such as IL-6 or TNF-α) present a high percentage of fracture healing complications [381]. Also, pronounced inflammatory responses were observed in hematomas (at 72 hours) of patients considered immunologically compromised (e.g. patients with autoimmune diseases, cancer or osteoporosis), which often exhibit delayed healing and other complications [382]. While inflammation is required to initiate the healing process, the effective resolution of this inflammation is believed to be necessary for effective healing to occur [361]. Therefore, the prolonged inflammatory microenvironment due to the use of a flexible plate (unstable context) can be a factor contributing to a higher risk of delayed or non-union often associated with fracture instability.

For *S. epidermidis*, differences at cytokine or mRNA expression level between non-inoculated and inoculated animals were often not significant. This data supports the idea that our model closely resembles a low-grade infection, also described in other models [303]. The only exception was mice with flexible implants at early time-points (both for C57BL/6 and BALB/c), which showed significantly higher levels of inflammatory markers such as IL-6, G-CSF or KC. Although we did not specifically identify the cellular sources of these cytokines/chemokines, macrophages recruited into the tissue, and also osteoblasts, have been shown to secrete similar cytokines upon *S. epidermidis* stimulation [235, 236, 383]. At later time-points, cytokine levels decreased to levels observed in control mice (baseline levels). The mRNA expression data in non-inoculated and *S. epidermidis* inoculated C57BL/6 mice are consistent with the cytokine quantification data described above. We again observed a tendency for higher inflammatory/tissue damage markers in animals with a flexible implant compared to rigid counterparts. Furthermore, the combination of flexible implant and *S. epidermidis* led to the highest responses in cytokine/chemokine release (e.g. *Csf3*, *Il6*, *Nos2* or *Ccl2*). Interestingly, the increased expression of *Hif1a* suggests that the instability and/or infection results in a more hypoxic environment, although this did not translate to significant differences in hypoxia-inducible factor (Hif)-1α regulated genes such as *Vegfa*, which could suggest an inadequate adaptation to hypoxia as suggested by Hoff *et al.*[384]. Further studies to investigate the responses of other Hif-1α regulated genes, such as *Ldha* or *Pgk1*, are therefore warranted to elucidate the role of hypoxia in unstable fixation associated with FRI. Taken together, we observed

that the combination of a flexible implant and infection results in higher levels of inflammation, hypoxia and tissue damage markers.

A number of important differences in the immune response were observed following inoculation with *S. epidermidis* compared to *S. aureus*. *S. aureus* inoculation led to a much higher and sustained inflammation in the tissue; in line with the acute nature of *S. aureus* infections and the consequent host immune responses to the infection [373]. Almost all cytokines measured (IL-6, G-CSF, KC, MCP-1) were significantly increased up to day 14, when compared to non-inoculated or *S. epidermidis* inoculated mice. This highly inflamed environment was accompanied with significant bone destruction. Similar to other studies, we observed high levels of IL-17A in the infected tissues [296, 297], which may be relevant for infection clearance but has also been suggested to contribute to pathogenesis due to the stimulatory effects of IL-17A on bone destruction and tissue damage [298, 299].

To summarize, cytokine secretion in full bone homogenates early after surgery depicted an increase for several innate immune markers (such as G-CSF, TNF-α or IL-6) in all groups, often increased in animals with a flexible implant compared to animals with a rigid implant. This was especially evident upon infection with *S. epidermidis* or *S. aureus*. It can be hypothesized that the enhanced inflammatory environment may lead to the delayed bacterial clearance observed in unstable fractures. However, the specific contribution of inflammation *per se* to delayed bacterial clearance is difficult to assess, since inflammatory responses are directly induced by the infection itself. In future, studies involving anti-inflammatory treatments may help to elucidate inflammation requirements for a successful bacteria clearance, although this needs to be carefully addressed. In addition, it would also be interesting to combine the fracture-model presented here with other disease models (such as obesity or diabetes) together with infection, in order to determine how fixation stability influences infection risk and progression in groups of patients known to be at higher risk of post-surgical complications.

At the cellular level, we observed a recruitment of macrophages in the bone marrow/fracture site at early time-points, in line with the peak of innate immunity markers. Despite the fact that we could not detect neutrophils directly, MPO measurements also suggested recruitment of neutrophils at day 3. Macrophage numbers also peaked at early time-points, in line with their role in bone healing [27, 369], and their levels did not return to baseline levels up to day 30 (data not published) suggesting a role throughout the healing process. In general, no significant differences were observed between non-inoculated and inoculated animals except for day 7 in C57BL/6 mice, when *S. epidermidis* inoculated animals presented lower levels. Unfortunately, we could not further characterize

macrophage phenotype so far, which would be interesting to understand if they play a more pro- or anti-inflammatory role. Conversely, the numbers of adaptive immune cells (T and B cells) peaked at day 14. This is consistent with previous observations, where two recruitment waves of T and B cells were observed during bone healing [385]. Regarding immune cell subclasses, an increase in percentage of double negative (CD4-CD8-) cells was noted at day 3; especially in the flexible plate *S. epidermidis* inoculated group, and *S. aureus* inoculated animals (both rigid and flexible implants). The fact that these 3 groups demonstrated higher inflammatory responses suggests that different levels of inflammatory markers may alter the pattern of cells recruited. Of note, γδ T cells, which are frequently CD4-CD8- [386], have been associated with *S. aureus* infection (specifically peritonitis and surgical site infection models) responses, at least in early time-points [387, 388], and could be partly responsible for this observed increase. Currently it is unknown whether γδ T cells play any role in *S. epidermidis* infection.

We observed that within the leukocyte compartment in bone marrow/fracture site, T helper cells and γδ T cells were the main sources of IL-17A. IL-17A producing lymphocytes, which have been proposed to contribute to bone healing [32, 389] but also to bone destruction [390, 391], were also detected in non-inoculated animals. However, in those, cell number and *Il17a*mRNA expression were much lower, which could be linked to time-points studied. Nevertheless, we performed histology in IL-17A KO mice and we did not observe major differences in terms of bone healing when compared to WT (Supplementary Figure 5-30 and [373]). Upon infection, it was observed that IL-17A was induced at both the mRNA and the protein level, as well as in adaptive immune responses, suggesting a role for Th17 responses during infection. Similar observations were previously reported in *S. aureus* FRI [296] and there is evidence that Th17 responses are important for *S. aureus* clearance in other infection models [388, 392, 393], or in reducing *S. aureus* nasal carriage [394]. Concerning a role for Th17 cells in *S. epidermidis* infection, there is currently limited data to support such a role, although it is known that adaptive immunity is required for infection clearance [245]. The importance of IL-17A-associated responses in our model was investigated using IL-17A KO mice. Since IL-17A is involved in neutrophil recruitment and activation, this may indicate a beneficial effect of IL-17A in bacterial infection, although the pro-inflammatory and pro-osteolytic effects of IL-17A in murine models of inflammatory arthritis is suggestive of tissue damaging effects [395]. This has also been proposed for *S. aureus* infections, suggesting that bacteria skew adaptive immunity towards a Th17/Th1 profile in order to evade the immune system [298]. We observed that there was a trend for IL-17A KO animals to clear the *S. epidermidis* infection less effectively than in WT animals, although differences were not statistically significant. While IFN-γ was not significantly increased in WT animals following

infection, we did observe an increase in this cytokine in IL-17A KO animals, suggesting a compensatory mechanism of IFN-γ in the absence of IL-17A. IL-17F, which has a high homology with IL-17A and can signal through the same receptor [396] or IL-22, produced also by Th17, would be other candidates with potential to compensate IL-17A loss of function, however we did not find detectable levels of IL-17F or IL-22 cytokines in WT or KO mice. Moreover, other studies have demonstrated a positive role for IFN-γ in *S. epidermidis* infections [230]. This would suggest a need for both Th1 and Th17 responses, which should be assessed in future studies. Nevertheless, due to the osteolytic effect of cytokines such IL-17A, it may be expected that therapeutic strategies aimed at modulating IL-17-based immunotherapies should be carefully considered. Furthermore, since we only used the rigid plate in the IL-17A KO animals it is currently unknown whether enhanced pro-inflammatory responses using the flexible implant would be again observed, and which influence this would have on the relative efficacy of IL-17A.

**Conclusion**

Our data suggests that fracture instability contributes to inflammatory processes locally. The combination of *S. epidermidis* infection and instability led to a significant increase in several inflammatory markers at early time-points, with the trend being maintained at later time-points. *S. aureus* infections resulted in a much more severe inflammatory response, associated with the higher secretion of pro-inflammatory cytokines. A trend for higher inflammation during *S. aureus* infection was also observed in animals with a flexible implant. However, since all animals remained infected in the *S. aureus* group, it is currently not possible to hypothesize how mechanical stability influences bacteria clearance. Levels of inflammation were associated with different patterns of local immune cell recruitment, but no significant differences were observed systemically. Finally, the role of IL-17A in infection clearance was addressed, with the use of IL-17A KO animals. Bacterial clearance was impaired in the IL-17A KO animals but differences to WT animals were not significant, perhaps due to increases in compensatory IFN-γ or Th1 responses.

**Acknowledgements**

The authors would like to thank Tanja Schmid for its contribution in surgeries; Iris Keller, Pamela Furlong and Noelia Rodriguez for technical assistance; Nora Goudsouzian, Mauro Bluvol and Dirk Nehrbass are acknowledged for support with histological processing; and Elisa Schiavi and Hideaki Morita for their valuable advices.

## Supplementary Tables and Figures:

**Table 5-5** Flow cytometry panels, with antibodies and related products used

| Product | Clone (If applicable) | Reference number | Company |
|---|---|---|---|
| Fixable Viability Dye eFluor780 | NA | 65-0865-14 | eBioscience |
| **Bone panel** | | | |
| FITC anti-mouse Ly6G Antibody | 1A8 | 127605 | Biolegend |
| PE anti-mouse CD8a Antibody | 53-6.7 | 100708 | Biolegend |
| PerCP/Cy5.5 anti-mouse CD19 Antibody | 6D5 | 115534 | Biolegend |
| PE/Cy7 anti-mouse F4/80 Antibody | BM8 | 123114 | Biolegend |
| APC anti-mouse CD138 (Syndecan-1) Antibody | 281-2 | 142506 | Biolegend |
| Pacific Blue anti-mouse CD3ε Antibody | 145-2C11 | 100334 | Biolegend |
| Brilliant Violet 510 anti-mouse CD4 Antibody | RM4-5 | 100553 | Biolegend |
| **Lymph node panel** | | | |
| PE/Cy7 anti-mouse CD3ε Antibody | 145-2C11 | 100320 | Biolegend |
| Pacific Blue anti-mouse CD4 Antibody | RM4-5 | 100531 | Biolegend |
| Alexa Fluor 488 anti-mouse/rat IL-17A Antibody | eBio17B7 | 53-7177-81 | eBioscience |
| PE anti-mouse IL-10 Antibody | JES5-16E3 | 12-7101-81 | eBioscience |
| PerCP-Cy5.5 anti-mouse IFN-γ Antibody | XMG1.2 | 45-7311-80 | eBioscience |
| APC anti-mouse IL-4 Antibody | 11B11 | 17-7041-82 | eBioscience |
| **IL-17A Bone panel** | | | |
| PE anti-mouse CD19 Antibody | 6D5 | 115507 | Biolegend |
| PE anti-mouse TER-119/Erythroid Cells Antibody | TER-119 | 116207 | Biolegend |
| PE anti-mouse Ly-6G/Ly-6C (Gr-1) Antibody | RB6-8C5 | 108407 | Biolegend |
| PE anti-mouse F4/80 Antibody | BM8 | 123109 | Biolegend |
| PE anti-mouse/rat CD61 Antibody | 2C9.G2 (HMß3-1) | 104307 | Biolegend |
| Alexa Fluor® 700 anti-mouse CD45 Antibody | 30-F11 | 103128 | Biolegend |
| PerCP/Cy5.5 anti-mouse NK-1.1 Antibody | PK136 | 108728 | Biolegend |
| PE/Cy7 anti-mouse CD8a Antibody | 53-6.7 | 100722 | Biolegend |
| APC Anti-mouse TCR γ/δ Antibody | GL3 | 118116 | Biolegend |
| Pacific Blue anti-mouse CD3ε Antibody | 145-2C11 | 100334 | Biolegend |
| Brilliant Violet 510 anti-mouse CD4 Antibody | RM4-5 | 100553 | Biolegend |
| Alexa Fluor 488 anti-mouse/rat IL-17A Antibody | eBio17B7 | 53-7177-81 | eBioscience |

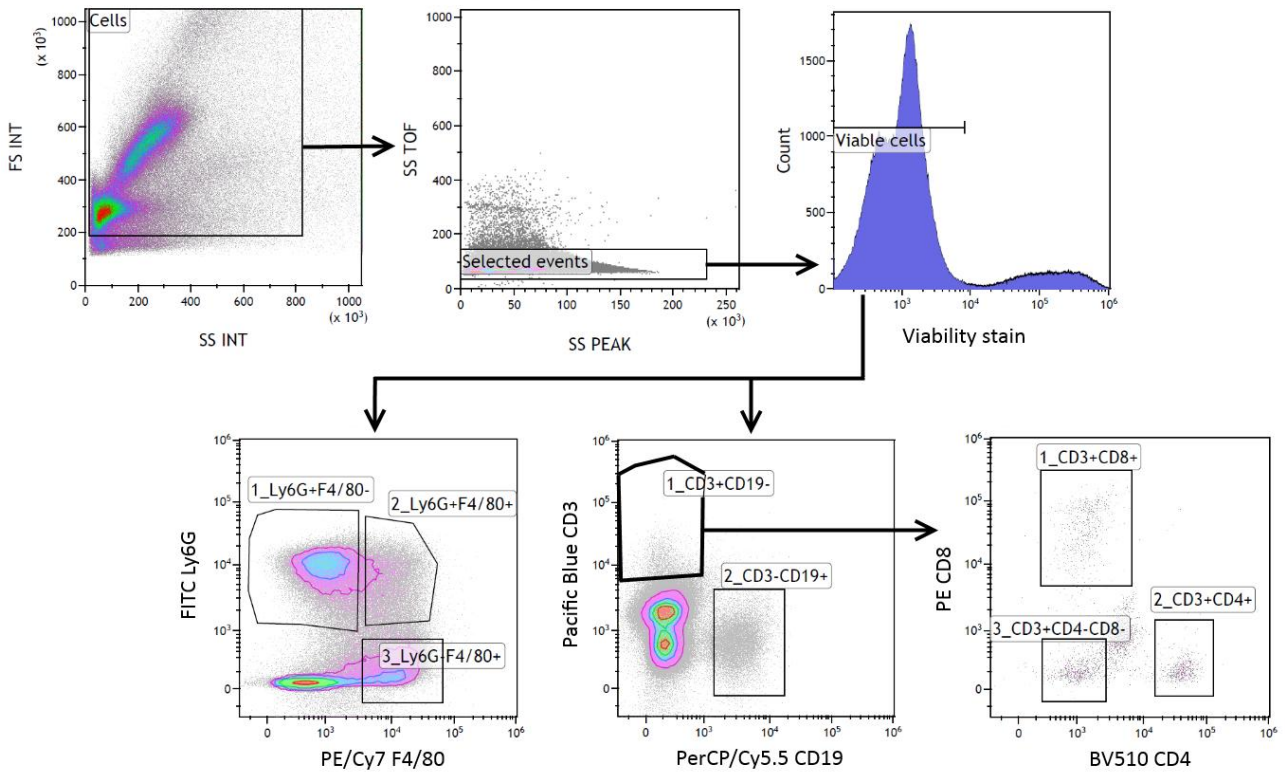


**Figure 5-24** Flow cytometry gating strategy to determine macrophage, T and B cell populations in bone single cell suspensions.

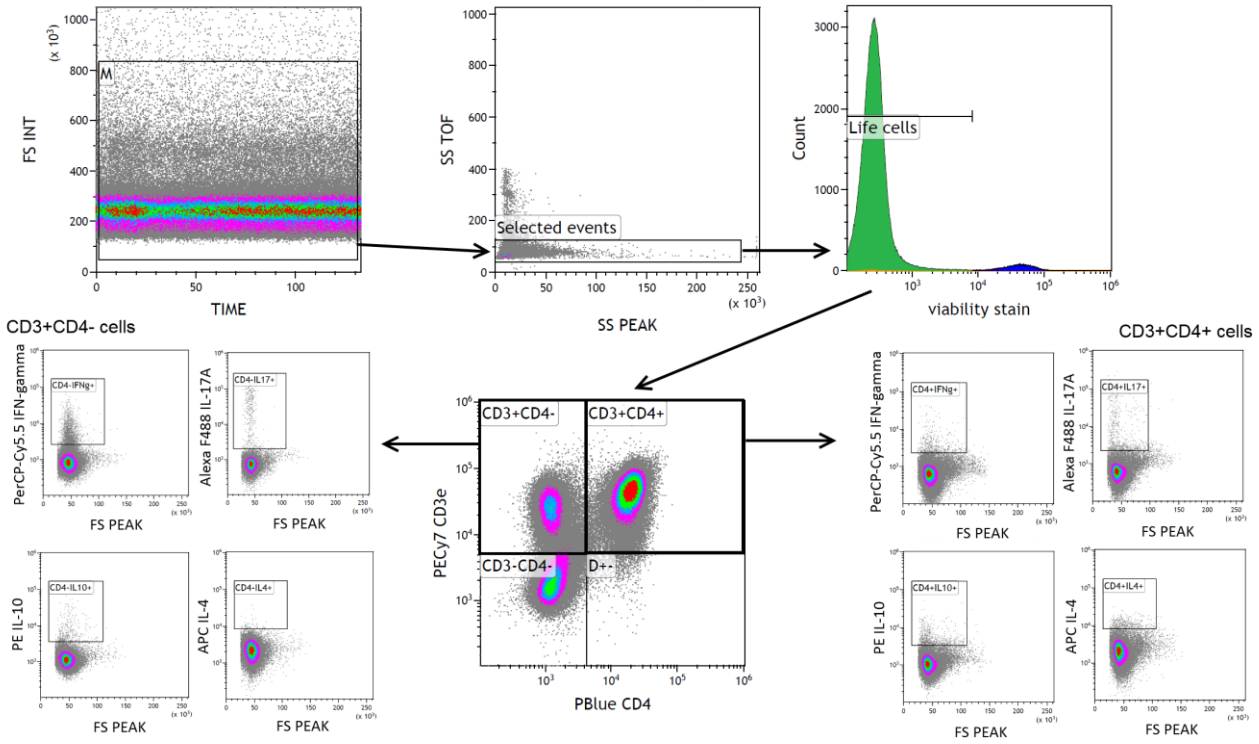


**Figure 5-25** Flow cytometry gating strategy to determine T cell populations and cytokines secreted by those cells in popliteal lymph node cell suspensions.

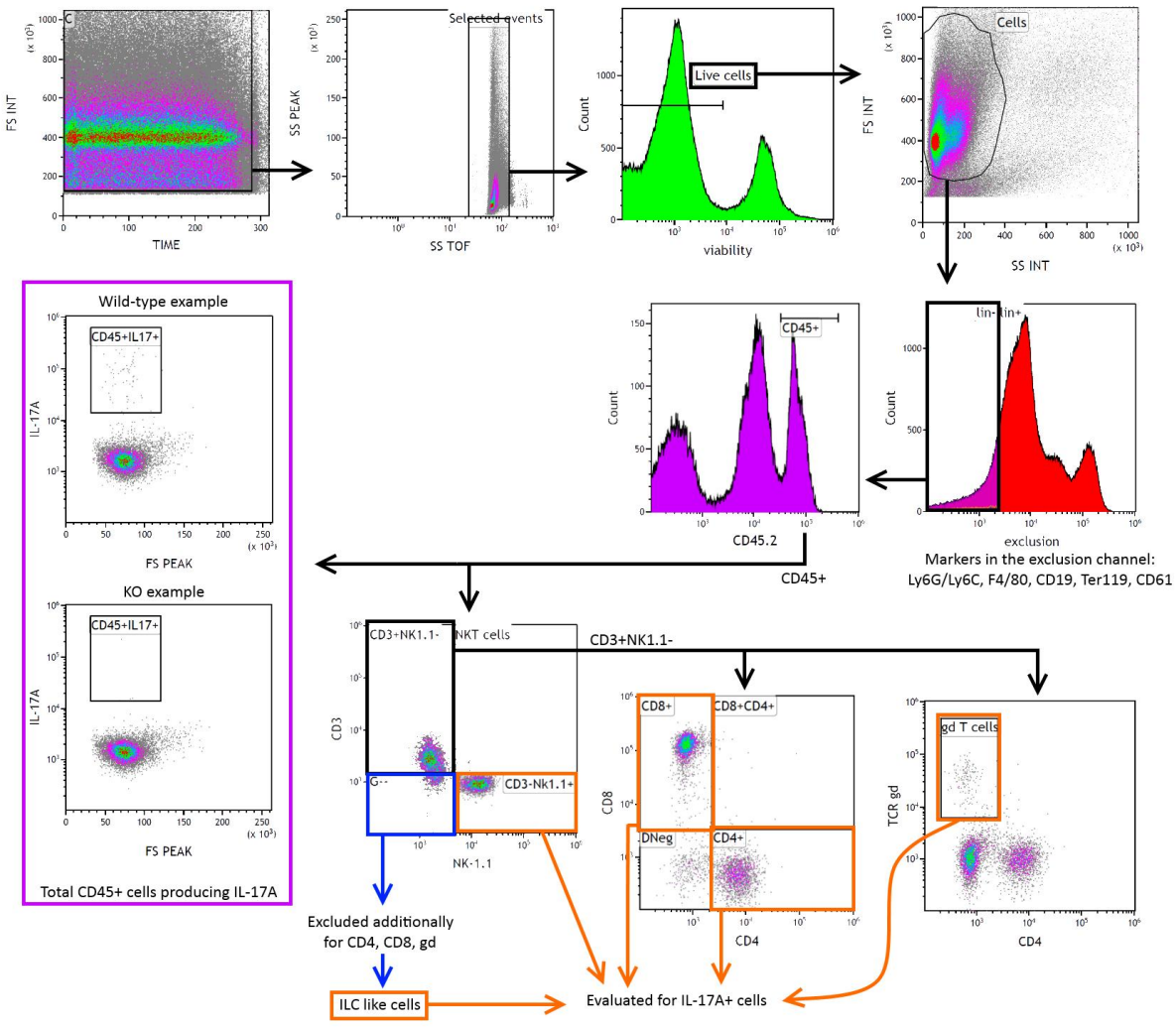


**Figure 5-26** Flow cytometry gating strategy to determine IL-17A source within the leukocyte compartment in the bone marrow. Cells selected for final evaluation were positive for CD45+ and negative for the following lineage markers: Gr-1 (Ly6G/Ly6C), F4/80, CD19, Ter119 and CD61.

**Table 5-6** List of genes included in the microfluidic card

| # | Gene name* (common abbreviation) | Gene symbol* | Gene ID* | Applied Biosystems® Assay ID | Amplicon Length |
|---|---|---|---|---|---|
| **1** | Adhesion G protein-coupled receptor E1 (F4/80) | *Adgre1* | 13733 | Mm00802529_m1 | 92 |
| **2** | Mannose receptor, C type 1 (CD206) | *Mrc1* | 17533 | Mm00485148_m1 | 76 |
| **3** | Arginase, liver (Arg-1) | *Arg1* | 11846 | Mm00475988_m1 | 65 |
| **4** | Nitric oxide synthase 2, inducible (iNos-2) | *Nos2* | 18126 | Mm00440502_m1 | 66 |
| **5** | Elastase, neutrophil expressed | *Elane* | 50701 | Mm01168928_g1 | 69 |
| **6** | Tumour necrosis factor (ligand) superfamily, member 11 (RANKL) | *Tnfsf11* | 21943 | Mm00441906_m1 | 66 |
| **7** | CD80 antigen | *Cd80* | 12519 | Mm00711660_m1 | 117 |
| **8** | Tumour necrosis factor (TNF-α) | *Tnf* | 21926 | Mm00443258_m1 | 81 |
| **9** | Interleukin 4 (IL-4) | *Il4* | 16189 | Mm00445259_m1 | 79 |
| **10** | Interleukin 6 (IL-6) | *Il6* | 16193 | Mm00446190_m1 | 78 |
| **11** | Interleukin 10 (IL-10) | *Il10* | 16153 | Mm00439614_m1 | 79 |
| **12** | Interleukin 17A (IL-17A) | *Il17a* | 16171 | Mm00439618_m1 | 80 |
| **13** | Interleukin 17F (IL-17F) | *Il17f* | 257630 | Mm00521423_m1 | 85 |
| **14** | Interleukin 23, alpha subunit p19 (IL-23) | *Il23a* | 83430 | Mm01160011_g1 | 109 |
| **15** | transforming growth factor, beta 1 (TGF-beta1) | *Tgfb1* | 21803 | Mm01178820_m1 | 59 |
| **16** | transforming growth factor, beta 2 (TGF-beta2) | *Tgfb2* | 21808 | Mm00436955_m1 | 82 |
| **17** | transforming growth factor, beta 3 (TGF-beta3) | *Tgfb3* | 21809 | Mm00436960_m1 | 60 |
| **18** | colony stimulating factor 1, macrophage (M-CSF) | *Csf1* | 12977 | Mm00432686_m1 | 70 |
| **19** | colony stimulating factor 3, granulocyte (G-CSF) | *Csf3* | 12985 | Mm00438335_g1 | 63 |
| **20** | colony stimulating factor 2, granulocyte-macrophage (GM-CSF) | *Csf2* | 12981 | Mm01290062_m1 | 125 |
| **21** | Interleukin 33 (IL-33) | *Il33* | 77125 | Mm00505403_m1 | 83 |
| **22** | Chemokine (C-C motif) ligand 2 (CCL2) | *Ccl2* | 20296 | Mm00441242_m1 | 74 |
| **23** | chemokine (C-C motif) receptor 2 (CCR2) | *Ccr2* | 12772 | Mm01216173_m1 | 88 |
| **24** | Toll-like receptor 2 (TLR-2) | *Tlr2* | 24088 | Mm00442346_m1 | 69 |
| **25** | Toll-like receptor 4 (TLR-4) | *Tlr4* | 21898 | Mm00445273_m1 | 87 |
| **26** | Vascular endothelial growth factor A (VEGF-A) | *Vegfa* | 22339 | Mm01281449_m1 | 81 |
| **27** | Hypoxia inducible factor 1, alpha subunit (HIF1- α) | *Hif1a* | 15251 | Mm00468869_m1 | 75 |
| **28** | Endothelial PAS domain protein 1 (HIF2-α) | *Epas1* | 13819 | Mm01236112_m1 | 63 |
| **29** | Histidine decarboxylase (HDC) | *Hdc* | 15186 | Mm00456104_m1 | 99 |
| **30** | Histamine receptor H1 (H1R) | *Hrh1* | 15465 | Mm00434002_s1 | 70 |
| **31** | Histamine receptor H2 (H2R) | *Hrh2* | 15466 | Mm00434009_s1 | 64 |
| **32** | Histamine receptor H4 (H4R) | *Hrh4* | 225192 | Mm00467634_m1 | 68 |
| **33** | S100 calcium binding protein A8 (S100A8) | *S100a8* | 20201 | Mm00496696_g1 | 131 |
| **34** | S100 calcium binding protein A9 (S100A9) | *S100a9* | 20202 | Mm00656925_m1 | 162 |
| **35** | High mobility group box 1 (HMGB1) | *Hmgb1* | 15289 | Mm00849805_gH | 158 |
| **36** | Caspase 3 | *Casp3* | 12367 | Mm01195084_m1 | 79 |
| **37** | Selectin, lymphocyte (CD62L) | *Sell* | 20343 | Mm00441291_m1 | 101 |
| **38** | Tumour necrosis factor receptor superfamily, member 11b (osteoprotegerin, OPG) | *Tnfrsf11b* | 18383 | Mm01205928_m1 | 75 |
| **39** | Secreted phosphoprotein 1 (OPN) | *Spp1* | 20750 | Mm00436767_m1 | 114 |
| **40** | Collagen, type I, alpha 1 (ColIα1) | *Col1a1* | 12842 | Mm00801666_g1 | 89 |
| **41** | Collagen, type X, alpha 1 (ColXα1) | *Col10a1* | 12813 | Mm00487041_m1 | 77 |
| **42** | Bridging integrator 1 (ALP-1) | *Bin1* | 30948 | Mm00437457_m1 | 72 |
| **43** | Runt related transcription factor 2 (Runx2) | *Runx2* | 12393 | Mm00501584_m1 | 91 |
| **44** | Acid phosphatase 5, tartrate resistant (TRAP) | *Acp5* | 11433 | Mm00475698_m1 | 79 |
| **45** | SRY (sex determining region Y)-box 9 (Sox9) | *Sox9* | 20682 | Mm00448840_m1 | 101 |
| **46** | Eukaryotic translation elongation factor 2 (eEF-2) | *Eef2* | 13629 | Mm01171434_g1 | 74 |
| **47** | Glyceraldehyde-3-phosphate dehydrogenase (GAPDH) | *Gapdh* | 14433 | Mm99999915_g1 | 109 |
| **48** | Ribosomal 18S | *18s* | - | - | - |

** Details according to NCBI*

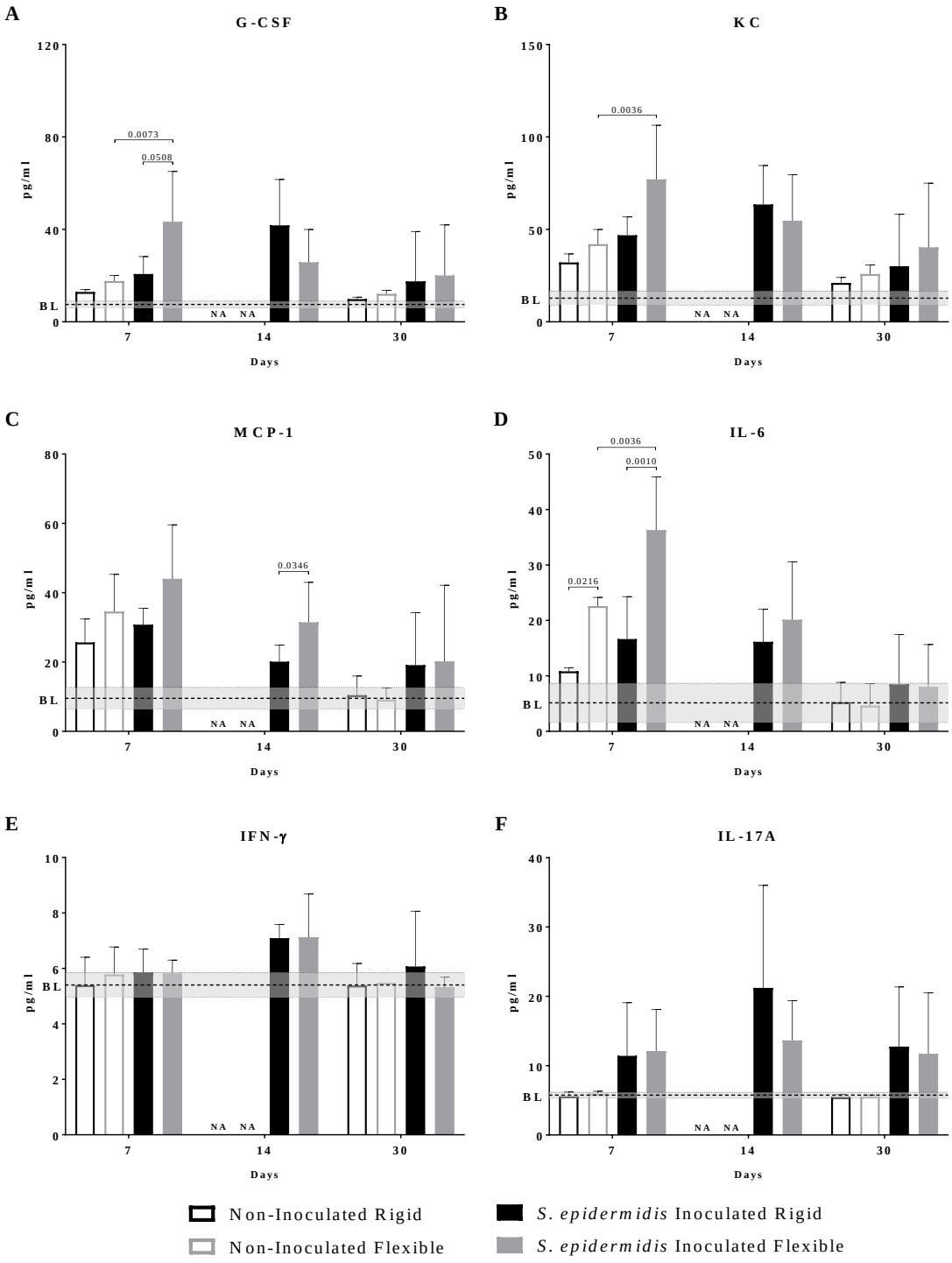


**Figure 5-27** Cytokine levels (pg/ml) in bone homogenate supernatants of BALB/c mice at 7, 14 and 30 days post-operatively. Mean values and SD (n=3-7). BL: baseline, mean of the control group; grey area: BL ± SD of the control group. 2-way ANOVA per time-point, Tukey or Sidak post hoc correction; except day 14 when Rigid and Flexible groups were analysed with Mann-Whitney. NA= Not available.

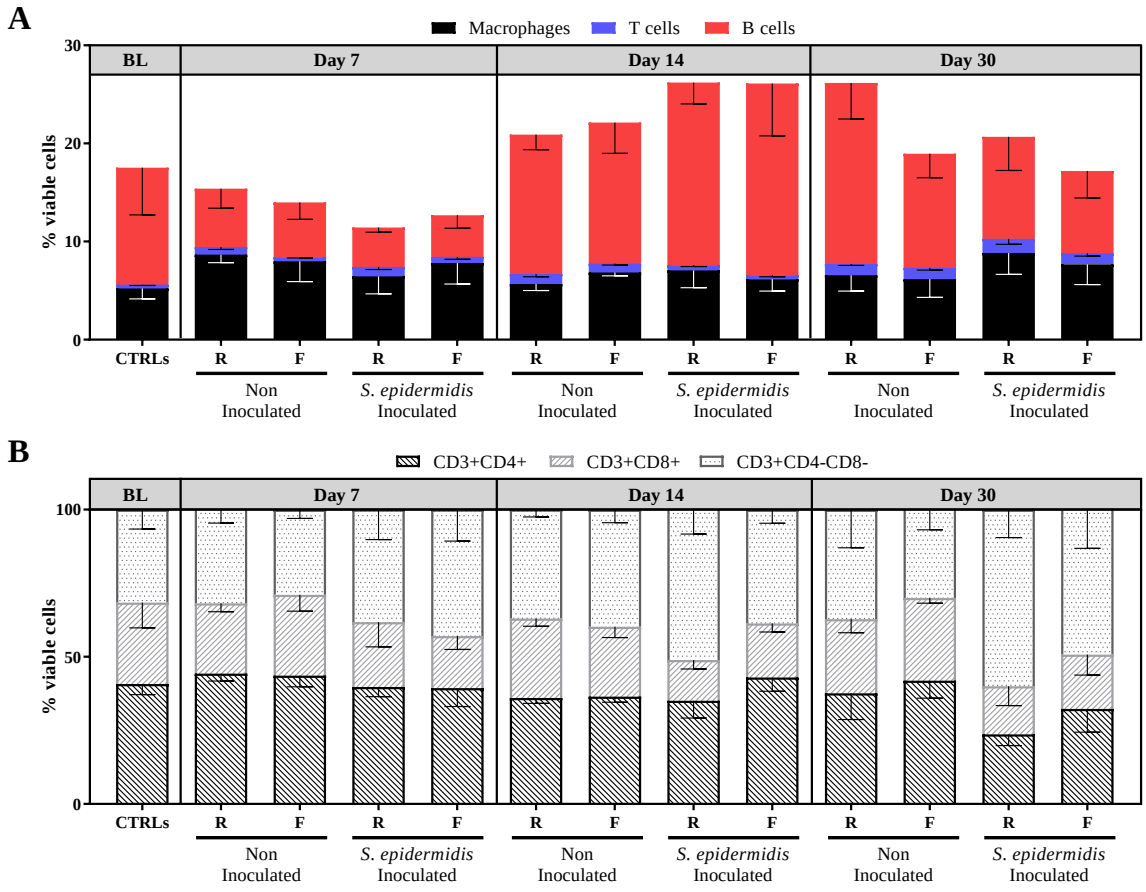


**Figure 5-28** Percentage of macrophages (Ly6G-F4/80+), T cells (CD3+CD19-) and B cells (CD19+CD3-) over viable cells (A), and percentage of CD4+, CD8+ and CD4-CD8- over CD3+ cells (B), in bone single cells suspensions of BALB/c mice at days 7, 14 and 30 post-operatively. Mean values and SD (n=3-8). BL: baseline, mean of the control group.

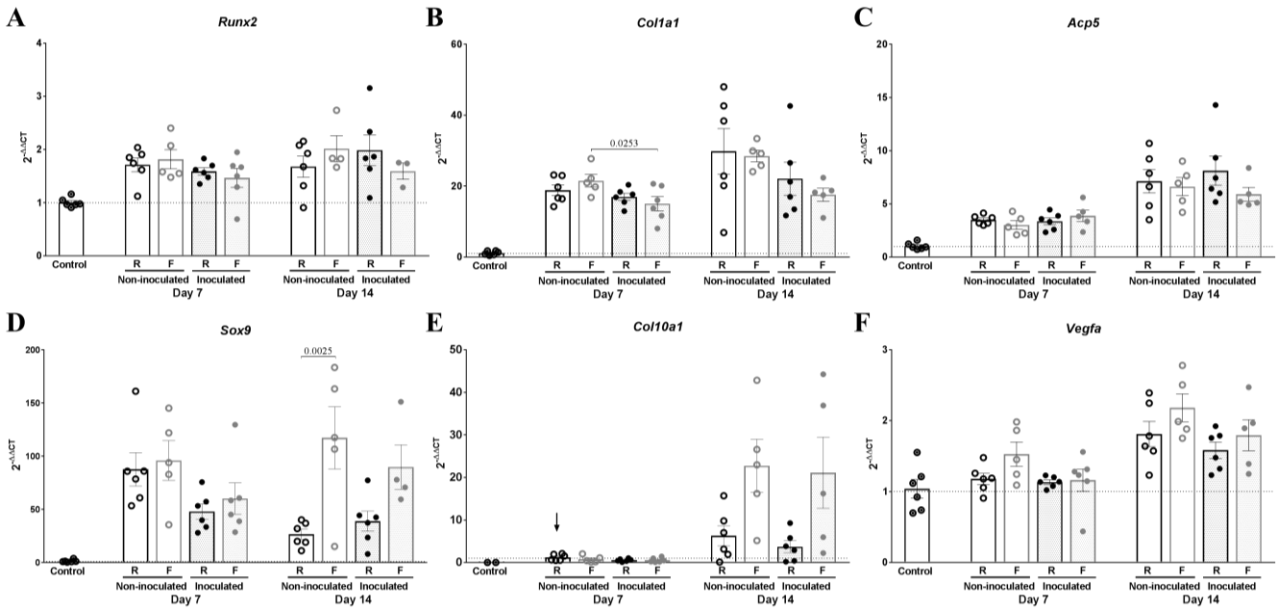


**Figure 5-29** $2^{-\Delta\Delta CT}$ of *Arg1*, *Nos2*, *Ccl2*, *Cd80*, *Il33* and *Hif1a* in mRNA isolated from operated and not operated femurs (controls and contralateral femurs); at 0, 7 and 14 days post-operatively.*18S*, *Eef2* and *Gapdh* used as endogenous controls, control group used as reference group (calibrator). Mean values and SD (n=5-7). 2-way ANOVA per time-point, with Tukey post hoc test. R: rigid implant, F: flexible implant.

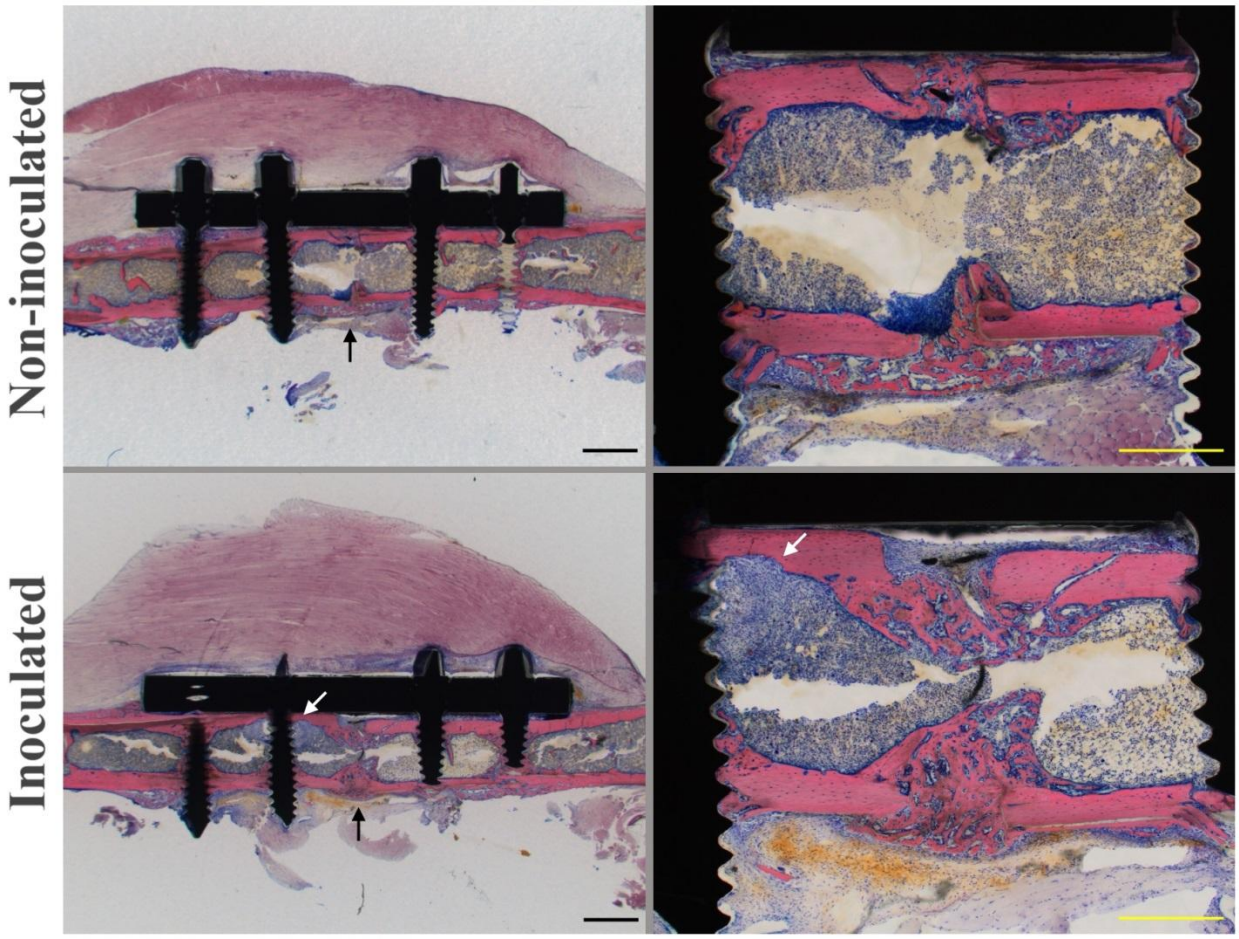


**Figure 5-30** Light microscopic images of Giemsa/Eosin stained MMA sections of C57BL/6 IL-17A KO mice non-inoculated and *S. epidermidis* inoculated at day 14. Scale bar overview images: 1000 µm. Scale osteotomy magnification: 500 µm. Similar observations were done when comparing with WT prior data [373]. The osteotomy gap was filled with new bone in both groups (black arrows). *S. epidermidis* inoculated mice only showed localized signs of infection as osteolytic regions around the screws with granulocyte infiltrate (white arrows). Histology sections were generated as described before [373]

## 5.3 Bone healing and infection in a femoral fracture model in histamine receptor 2 deficient mice

Marina Sabaté Brescó[1,2], Corina Berset[3], Stephan Zeiter[1], Barbara Stanic[1], Geoff R. Richards[1], Liam O'Mahony[2], Fintan T. Moriarty[1]*

[1] AO Research Institute Davos, CH; [2] Swiss Institute of Asthma and Allergy Research, CH; [3] AO Foundation, CH

*****Corresponding author:
T F Moriarty, AO Research Institute Davos, AO Foundation, Clavadelerstrasse 8, Davos Platz, CH7270, Switzerland. Phone: +41 81 414 2397, E-mail: fintan.moriarty@aofoundation.org

Running Title: Histamine 2 receptor in bone healing and infection

*This manuscript is in preparation.*

**Abstract**

Histamine is a biogenic amine produced by numerous cell types and with various immunoregulatory roles. The response to histamine is influenced by which of its four receptors through which the signal is transduced. After a traumatic bone fracture, histamine will be secreted in the fracture site as part of the inflammatory phase responses, leading to higher vascular permeability. In a previous fracture-related infection model in mice, we observe an increase of histamine receptor 2 ($H_2R$) mRNA expression in animals inoculated with *S. epidermidis*. The role of $H_2R$ in infection has been not yet been fully described, with conflicting results reported in the literature in different pre-clinical models. The clinical data from human patients is also not conclusive about $H_2R$ and $H_2R$ antagonists in infection risk.

In this study, we used a $H_2R$ knock-out mouse strain (in BALB/c background) in order to address the role of this receptor in our *S. epidermidis* fracture-related infection model. Despite we observed differences in local immune responses, as shown by cytokines and chemokine secreted in the fracture site (e.g. tumour necrosis factor-alpha), this did not lead to bacteria clearance differences.

**Introduction**

Histamine (2-[4-imidazolyl]-ethylamine) is a short-lived and low-molecular-weight biogenic amine produced by mast cells and basophils, who store histamine in intracellular granules and release them upon activation. Other immune cells, like dendritic cells or T cells, can synthesize histamine *de novo* and release it immediately [397]. Histamine is a potent regulator of the immune system, and is able to act in both a pro-inflammatory and in an anti-inflammatory manner, depending on which cell type and what receptor through what it is signalling [398]. Histamine has been shown to modulate granulocyte function or to alter cytokine secretion by dendritic cells [399, 400] and thereby influence T cell polarization, among other mechanisms [397].

The role of histamine in the antibacterial immune response is to increase the permeability of the capillaries, facilitating access of host defence cells to infected tissues. Nevertheless, the complete role of histamine and its receptors in bacterial infections is not completely clear, with positive and negative effects being reported in different studies [401-403]. We observed an upregulation of histamine 2 receptor (*H2r)* mRNA expression in mice femurs with an implant related bone infection caused by *Staphylococcus epidermidis* (Results 5.2). The infected mice then transitioned to a down-regulation at later time-points, mirroring uninfected controls.

A wide diversity of cells and tissues, including T and B lymphocytes, dendritic cells or smooth muscle cells, express histamine 2 receptor ($H_2R$). $H_2R$ has been shown to regulate immune responses. Signalling through $H_2R$ can inhibit mast cell degranulation, impair neutrophil chemotaxis and reduce oxidative burst in neutrophils and monocytes [404-406]. In the adaptive immune system, $H_2R$ signalling may polarize T cell responses into Th2 and/or Treg phenotype [398, 407]. However, as described above, the role of this receptor in infection is not clear.

It has also been shown that mast cell degranulation (which will lead to the release of histamine) may be involved in mediating acute inflammatory responses to implanted biomaterials [408]. By contrast, histamine secretion nearby the implant may contribute to the immunosuppressive environment suggested to accompany foreign bodies [409].

We hypothesized that histamine secretion in the fracture site, due to tissue damage and bacterial [410] and/or foreign body presence [408, 411], may impair immune responses in the vicinity of the implant through $H_2R$ signalling. We aimed to determine if $H_2R$ deletion could play a beneficial role in our *S. epidermidis* fracture-related infection (FRI) model.

## Materials and methods

### *Animals*

The study was approved by the ethical committee of the canton of Graubünden in Switzerland (TVB 2016/03) and was carried out in a research facility accredited by Association for Assessment and Accreditation for Laboratory Animal Care (AAALAC) International. Skeletally mature (20-28 weeks old, average weight ± SD: 26.46 ± 5.56 g), female, specific pathogen free (SPF) BALB/c mice, purchased from Charles River (Germany), and BALB/c $H_2R$ knock-out (KO), provided by Prof. Takeshi (Watanabe, Osaka, Japan) and bred in our facilities, were used in this study. All animals were allowed to acclimatize to experimental conditions for at least two weeks prior to the start of the study. Mice were housed under a 12-hour dark/ 12-hour light cycle in groups of three to six in individually ventilated cages (XJ, Allentown), changed weekly, and they were re-housed in the same groups post-surgery. Animals were fed with a standard diet (3436, Provimi Kliba) and had free access to water at all times.

Wild-type (WT) and KO mice underwent surgery, as non-inoculated or *S. epidermidis* inoculated (n=8/group). Animals were euthanized 14 days post-operatively.

### *Bacteria and inoculum*

The test microorganism was *S. epidermidis* Epi 103.1, obtained from a patient with chronic implant-related bone infection, which has a weak capacity for *in vitro* biofilm formation according to the scoring system of Stepanovic *et al.* [343]. The inocula were prepared as described previously [373]. The target inoculum was set to $1x10^4$ Colony Forming Units (CFU).

### *Surgery*

Commercially pure Titanium (CpTi) 4-hole rigid and CpTi 4-hole flexible MouseFix$^{TM}$ implants and Titanium Aluminium Niobium alloy (Ti6Al4Nb (TAN)) screws (RiSystem AG) were used to fix a transverse mid femoral osteotomy in mice. Prior to use, all implants were cleaned and sterilized by steam autoclave.

Surgery was performed as previously described [373]. Briefly, under general anaesthesia with isoflurane (2-3% isoflurane in 100% O2, 1 l/min) (Isofluran Baxter®, Baxter AG), the animal was placed in prone position and a skin incision was made from tail base to left stifle. The subcutaneous Fascia lata was cut and the tissue plane between the quadriceps and the biceps femoris muscle was bluntly dissected. A Teflon foil was placed around the femur to protect the soft tissue from

contamination. The implant was then fixed to the bone using four self-tapping, angular stable screws. Screw holes were predrilled with a 0.31 mm drill bit (RISystem AG). Once the implant was in place, a 0.44 mm defect osteotomy was performed using a jig and a Gigli wire. In the inoculated groups, 2.5 µl of bacteria suspension was injected in the osteotomy site. The foil was then removed and the Fascia lata and the skin were closed with continuous sutures (5-0 Vicryl rapide, Ethicon). Following surgery, a lateral radiograph of the femur was taken to confirm proper positioning of the implant.

*Post-operative care and euthanasia*

Analgesia was provided in the form of subcutaneous injections of buprenorphine (0.1 mg/kg, Bupaq®, Streuli Pharma AG), pre-operatively and twice post-operatively every 6-8 hours. Additionally, a palatable form of acetaminophen (2 mg/ml, as Dafalgan® Syrup for Children, Bristol-Myers Squibb SA) was added to the drinking water for 5 days. Animals were monitored twice daily for 5 days post-operatively and subsequently once a day, using a detailed numerical scoring system which takes into account general behaviour, external appearance, wound status and animal movement [373]. Weight was taken pre-operatively and 3, 7 and 14 days post-operatively, while radiographs of the operated limb were taken weekly to ensure no implant/osteosynthesis failure. 14 days post-operatively, mice were euthanized and samples collected as previously described (in Materials and Methods of Results 5.2).

*Quantitative bacteriology*

Viable bacterial counts were performed by plating serial dilutions of bone homogenate and soft tissue homogenate on 5% horse blood agar (BA) (Oxoid). The number of bacteria associated with the implant was determined by sonicating the implant and screws in PBS for 3 minutes (Bandelin Sonorex at 40 KHz), vortex mixing for 10 seconds and finally also plating serial dilutions in 5% horse BA. All BA plates were incubated at 37°C for bacterial counts at 24 and 48 hours. Mice were considered as infected when at least one sample (bone, soft tissue or implant) was culture positive. Bacteria recovered from each animal were confirmed to be *S. epidermidis* Epi 103.1 by Random Amplification of Polymorphic DNA (RAPD) test [347]

*In vitro stimulation of bone*

Bone single cell suspensions were plated in 24-well plate ($1x10^6$ cells/well) with complete RPMI (cRPMI: RPMI 1640 (Gibco), penicillin (1 U/ml, Sigma-Aldrich), streptomycin (1 µg/ml, Sigma-Aldrich), kanamycin (0.1 µg/ml, Gibco), MEM vitamin (1x, Sigma-Aldrich), L-glutamine (2 mM,

Sigma-Aldrich), Na-pyruvate (1 mM, Sigma-Aldrich), non-essential amino acids (1x, Sigma-Aldrich) and heat inactivated foetal calf serum (10%, Sigma-Aldrich)). Cells were left unstimulated or stimulated with phorbol 12-myristate 13-acetate (PMA) (20 ng/ml, Sigma-Aldrich) and ionomycin (200 ng/ml, Sigma-Aldrich). Samples were incubated at 37°C, 5% $CO_2$ and supernatants were collected after 48 hours. Cytokines and chemokines present in supernatants were measured using Milliplex Map Mouse cytokine/chemokine Magnetic Bead Panel (Millipore). The following cytokines were measured: G-CSF, IL-4, IL-6, IL-10, IL-17A, KC/GRO, MCP-1 and TNF-α.

*Flow cytometry*

Bone single cell suspensions were stained with life viability dye (eBioscience) for 30 minutes at 4°C in darkness, followed by staining with the following panel: FITC anti-mouse Ly6G, PE anti-mouse CD8, APC anti-mouse CD138, PerCP-Cy5.5 anti-mouse CD19, PE-Cy.7 anti-mouse F4/80, Pacific Blue anti-mouse CD3ε and Brilliant Violet 510 anti-mouse CD4 (all from Biolegend). At least $0.5x10^6$ cells were acquired in Gallios flow cytometer (Beckman Coulter). Lymph node single cell suspensions were stimulated for 4 hours with PMA (50 ng/ml), ionomycin (500 ng/ml) and Brefeldin A (1x, eBioscience) at 37°C, 5% $CO_2$. Afterwards, cells were stained with life viability dye as described above and stained with the following surface markers: PE/Cy7 anti-mouse CD3ε and Pacific Blue anti-mouse CD4 (all from Biolegened). Cells were fixed and permeabilized with the Intracellular Fixation & Permeabilization Buffer kit (eBioscience) and finally stained for intracellular cytokines: Alexa Fluor 488 anti-mouse/rat IL-17A, PE anti-mouse IL-10, PerCP-Cy5.5 anti-mouse interferon (IFN)-γ and APC anti-mouse IL-4. All samples were measured using a Gallios flow cytometer (Beckman Coulter). *Anti-S. epidermidis antibody ELISA*

UV killed *S. epidermidis* Epi 103.1 in PBS was processed to obtain a lysate for plate coating. The process included 5 cycles of snap-freezing in liquid nitrogen, 1 hour incubation at 37°C with 200 µg/ml of Lysostaphin (Sigma-Aldrich) resuspended in 20 mM Sodium Acetate (Sigma-Aldrich) pH 4.5 at 10 mg/ml and 1 mM of EDTA 0.5 M (Sigma-Aldrich). Subsequently, samples were sonicated 4 times (each step: 10 minutes, 60 Hz, on ice) with sterile glass beads (90-150 µm, VWR). Finally, the sample was centrifuged at 200 rpm for 10 minutes to remove glass beads. Protein in the collected supernatant was quantified and adjusted to 550 µg/ml with PBS before it was aliquoted and frozen at -20°C.

For the ELISA, Maxisorp Nunc 96 flat-bottom well plates (ThermoFisher) were coated with 2.5 µg/ml of *S. epidermidis* Epi 103.1 lysate (overnight, 4°C). Afterwards, wells were blocked with 5% milk powder in PBS 0.05% Tween 20 (Fluka) and incubated with serum dilutions ranging from 1:20 to 1:320. Antibodies against *S. epidermidis* were detected using biotinylated goat anti-mouse

IgG and IgM (Mabtech), HRP-streptavidin (Sigma-Aldrich), tetramethylbenzidine (TMB) mix and 1M $H_2SO_4$ as a stop solution. Plates were read at 450nm in a plate reader (Berthold Technologies).

*Statistical analysis*

Statistical analysis was performed using the software GraphPad Prism 7 software. Test performed are included in figure legend. D'Agostino-Pearson normality test was used to determine if sample distribution was not normal. Differences were considered significant with $p<0.05$.

## Results

*Animal monitoring*

All animals survived the surgical procedure and there was 1 animal euthanized prior to the scheduled time-point. When observing weight change over time (Figure 5-31), we observed a more pronounced weight loss in $H_2R$ knock-out (KO) mice when compared to their wild-type (WT) counterparts. This was again observed for both inoculated and non-inoculated mice, although it only reached statistical significance for the non-inoculated groups at days 7 and 14. The *S. epidermidis* inoculated groups showed a tendency to lose more weight than non-inoculated counterparts for both WT and KO groups, although this did not reach statistical significance. The clinical scoring did not show significant differences between the different groups.

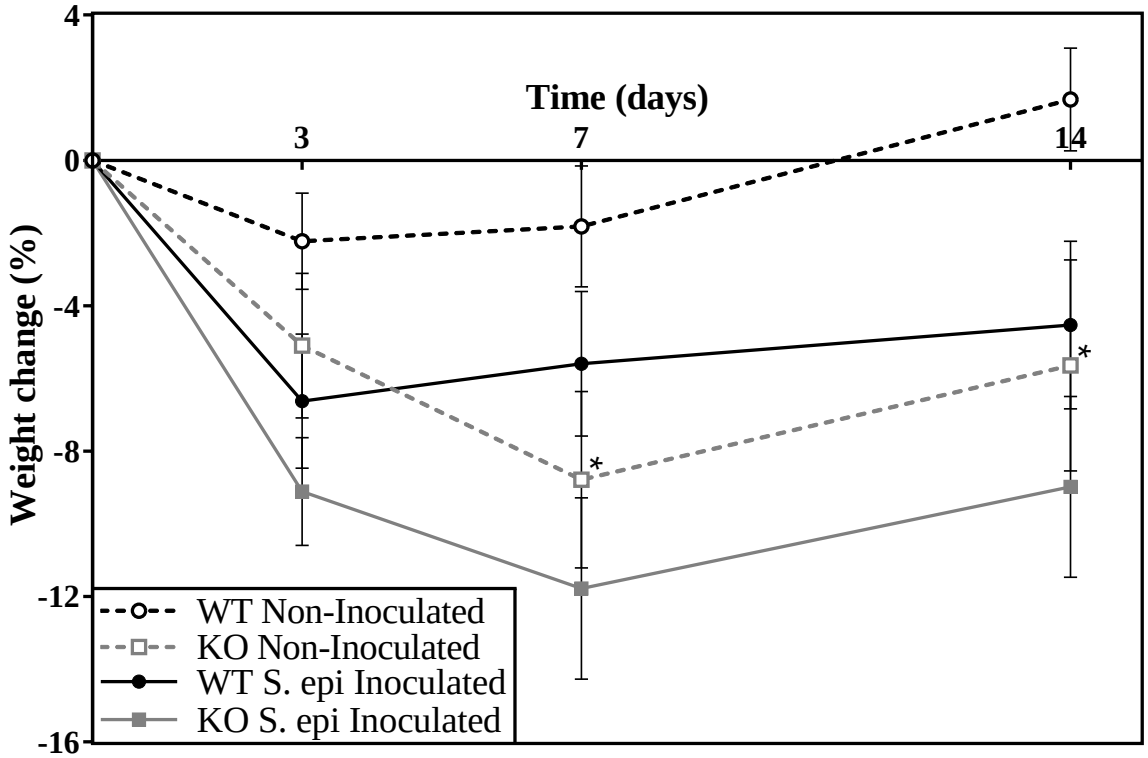


**Figure 5-31** Percentage of weight change compared to time-point 0 at days 3, 7 and 14 post-operatively. Data shown for wild-type (black) and KO animals (grey), non-inoculated (dashed lines) or *S. epidermidis* inoculated (solid lines). Data shown is mean +/- SEM (n=8-9 per group). Repeated measures 2-way ANOVA, * = $p<0.05$. All animals lost weight after surgery, and was more pronounced in $H_2R$ KO mice than in their WT counterparts. Significant differences were observed between non-inoculated WT and KO ($p<0.05$) at days 7 and 14.

*Quantitative bacteriology*

Infection was assessed by total viable bacterial counts in the different compartments (bone, soft tissue and implant) at day 14 (Figure 5-32). All WT and $H_2R$ KO mice were found to be culture positive at euthanasia. The WT group tended to have more culture negative samples (9 culture negative samples in WT versus 6 in KO) although this was not statistically significant. CFU counts were often lower in $H_2R$ KO, although once again this did not reach statistical significance (Figure 5-32).

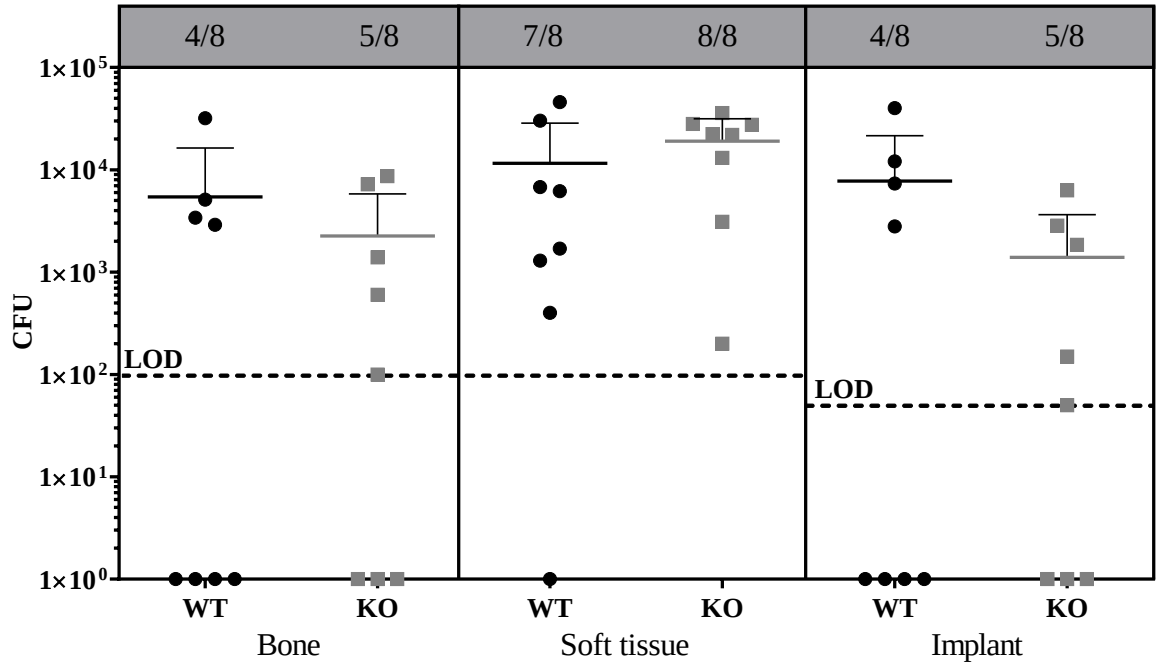


**Figure 5-32** CFU counts for bone, soft tissue and implant, for WT (black) and $H_2R$ KO (grey) mice at day 1 post-operatively. Mean and SD (n=8). Samples found culture negative are represented as 1. LOD: Limit of detection, $1x10^2$ CFU for bone and soft tissue and $0.5x10^2$ CFU for implant. Mann-Whitney test, no significant differences found.

*Cytokine production in bone*

Bone single cell suspensions were prepared from homogenized femurs. Total cell numbers obtained were similar between both groups (Supplementary Figure 5-37). Cells were re-stimulated and cytokine secretion was measured after 48 hours. Secretion of G-CSF, TNF-α and IL-10 (Figure 5-33 A-C) were elevated in KO mice compared with WT in both inoculated and non-inoculated groups, although differences were not always significant (Figure 5-33). IL-17A secretion was only observed in inoculated animals, and was increased in inoculated KO mice compared with inoculated WT mice, although this did not reach statistical significance (Figure 5-33 D).

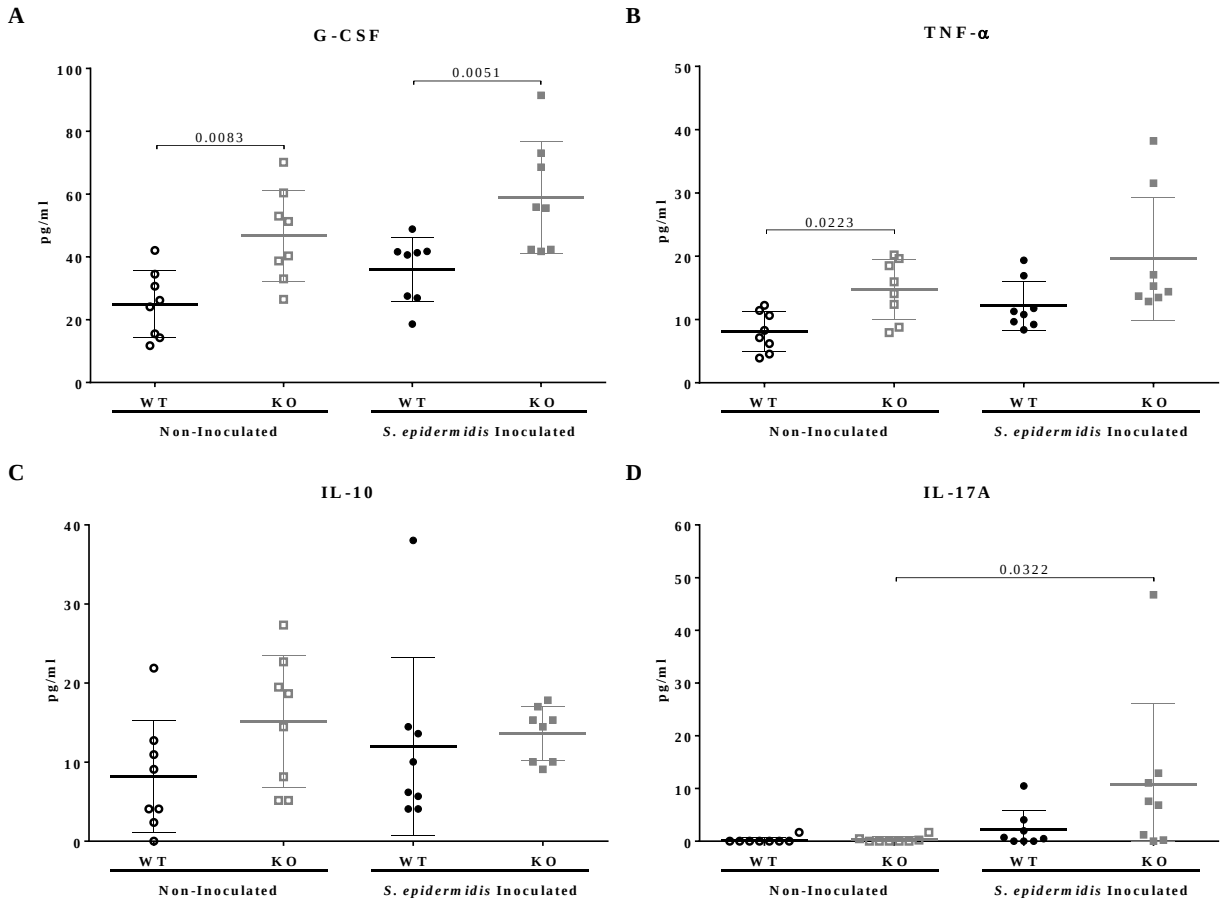


**Figure 5-33** G-CSF (A), TNF-α (B), IL-10 (C) and IL-17A (D) levels (pg/ml) in 48 hours re-stimulated bone single cell suspensions of non-inoculated and *S. epidermidis* inoculated mice. Mean and SD (n=8). One-way ANOVA with Sidak post hoc or Kruskal-Wallis with Dunn's post hoc test, significant *p*-values indicated ($p<0.05$).

### *Flow cytometry of bone single cell suspensions*

We also analysed the percentages of macrophages, T cells and B cells in the bone single cell suspensions (Figure 5-34). Total cell number (Supplementary Figure 5-37) and the relative percentage of macrophages (F4/80+Ly6G-, Figure 5-34 A) was similar between each group. T lymphocytes (CD3+CD19-, Figure 5-34B) were significantly increased in WT mice inoculated with *S. epidermidis* compared to non-inoculated WT equivalents. There was a trend for reduced B cell percentage $H_2R$ KO animals although this did not reach statistical significance.

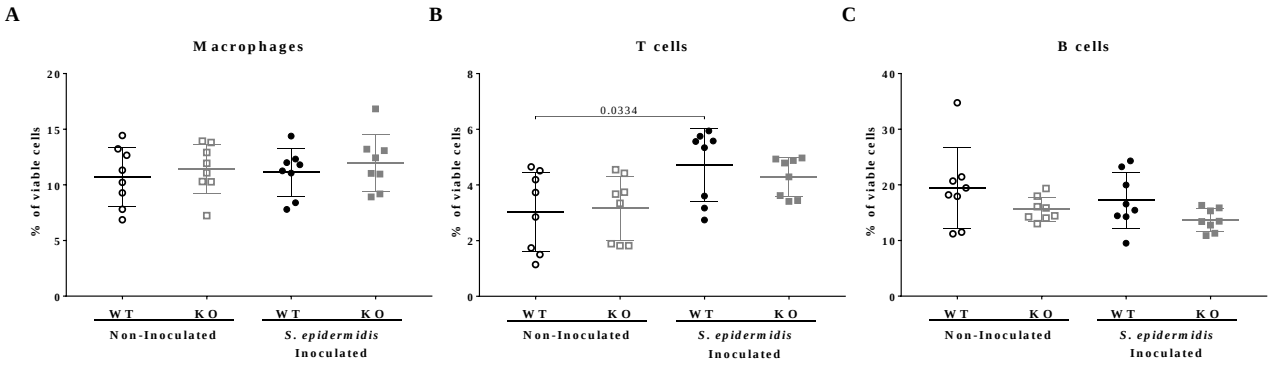


**Figure 5-34** Percentage of macrophages (F4/80+Ly6G-) (A), T cells (CD3+CD19-) (B) and B cells (CD19+CD3-) (C) in all groups, expressed as a percentage of viable cells. Mean and SD (n=8). One-way ANOVA with Sidak post hoc, significant p-values indicated ($p$<0.05).

*Adaptive immune responses in popliteal lymph node*

Popliteal lymph node cells were re-stimulated and treated with Brefeldin A to determine cytokine production. We observed that both KO mice groups (non-inoculated and *S. epidermidis* inoculated) had a slightly reduced CD3+CD4- percentage and significantly lower CD3+CD4+ percentage (Figure 5-35, A and D) compared to WT equivalents. However, KO mice T cells were producing higher levels of IFN-γ and IL-17A (Figure 5-35, B-C and E-F), and although levels were low this was also true for IL-10. No association was found with T cell levels and infection.

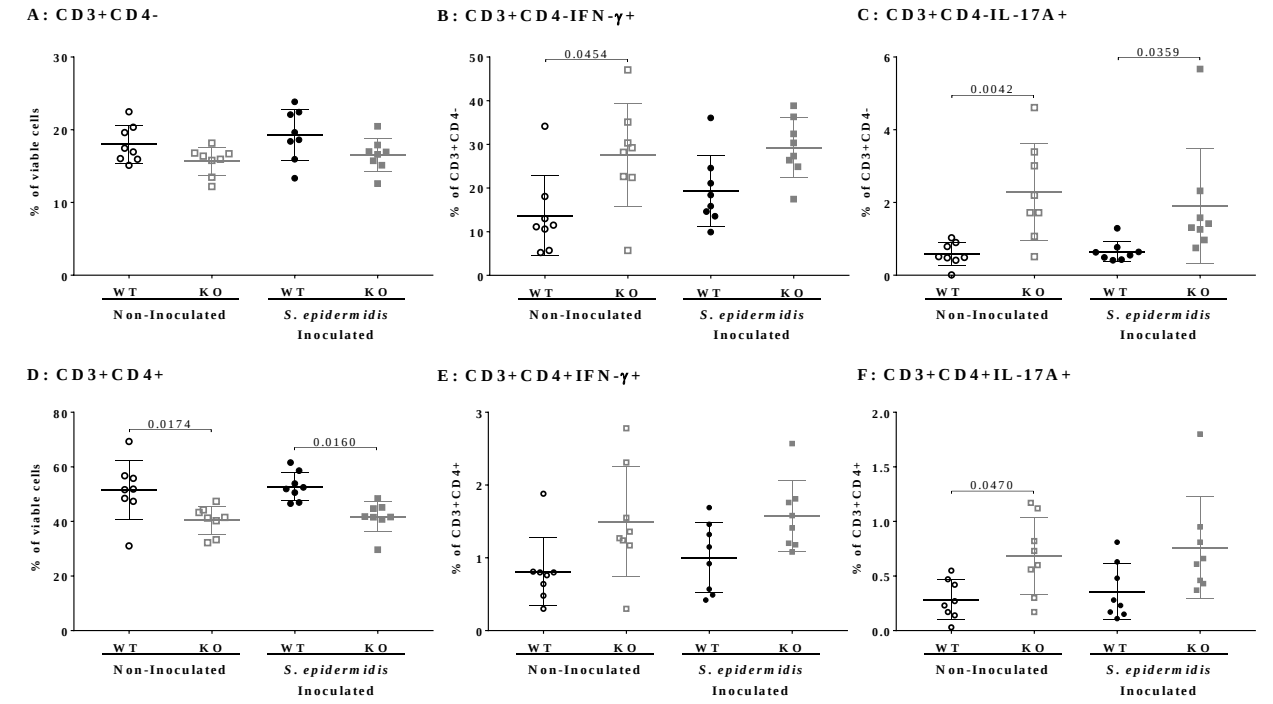


**Figure 5-35** Percentage of total CD3+CD4- and cells producing IFN-γ or IL-17A (A-C), and percentage of total CD3+CD4+ and cells producing IFN-γ or IL-17A (D-F) in popliteal lymph node. Mean and SD (n=8). One-way

ANOVA with Sidak post hoc or Kruskal-Wallis with Dunn's post hoc test, significant p-values indicated in the figure ($p<0.05$).

Anti-*S. epidermidis* IgG levels were measured at day 14 (Figure 5-36). In general, levels were low for all the groups, except for *S. epidermidis* inoculated $H_2R$ KO mice. Nevertheless, values were very variable within the group, with some animals presenting very low antibody levels. In addition, we observed that even non-inoculated $H_2R$ KO had slightly higher levels of antibodies compared to WT counterpart.

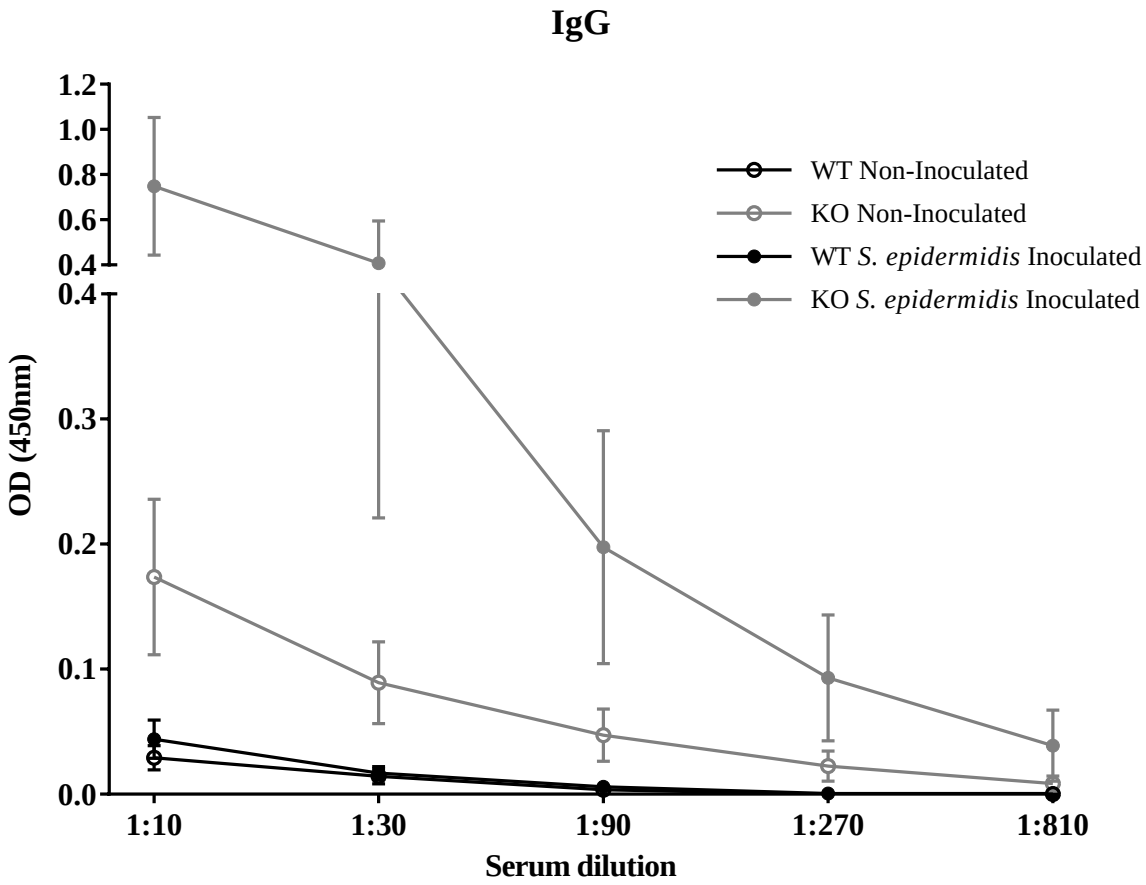


**Figure 5-36** Levels of IgG recognizing *S. epidermidis* proteins (expressed as optical density measured at 450nm) at different serum dilutions. Mean and SEM (n=8-9).

## Discussion

Histamine is a potent biogenic amine with multiple functions. After tissue damage or biomaterial implantation, it is expected that histamine may be released. This will lead to vasodilatation on the site, which will allow cell recruitment in the affected tissue. This study showed that $H_2R$ influenced the immune responses against *S. epidermidis* but this was not related to differences in infection clearance.

$H_2R$ has previously been shown to play a role in infection by gram-negative bacteria, although the data is somewhat inconsistent. Cimetidine ($H_2R$ antagonist) treatment reduced mortality in diabetic mice in a sepsis model (induced by cecum ligation and puncture) and histamine administration lead to a higher survival rate [401]. Contrasting with this, the same antagonist led to an increased mortality in a *Yersinia enterocolitica* infection model [402] and lead to higher morbidity in a peritonitis model [403]. This apparent contradiction has been attributed to the different effects that histamine can have in different cell types and tissues. Furthermore, certain bacteria are capable of producing histamine [412], which is hypothesized that could be used in their benefit to modulate immune system. While the gene used for histamine production (*hdc)* has been found in some *S. epidermidis* strains [413] we could not detect it in our *S. epidermidis* strain (12 different primers tested, data not shown). Thus, in our model, the only source of histamine in the infected bone/soft tissue would be the host.

In this study, differences were observed between WT strains and $H_2R$ KO, with higher post-operative weight loss for KO, higher cytokine levels in the tissues or reduced T lymphocytes numbers in lymph node, which presented greater cytokine secretion compared to WT. Nevertheless, differences in immune responses observed did not lead to significant differences in terms of infection clearance. With regards to bacterial burden, $H_2R$ KO animals often showed lower CFU counts in bone and implant, while for soft tissue the average was higher than WT. Of note, in this FRI model, BALB/c mice have been shown to clear bacteria only late time-points [373] and a longer observation period may provide better evidence to clarify if there is a role for histamine and $H_2R$ in this FRI model.

At our observation point of 14 days, few differences were associated to the presence of infection. However, our *S. epidermidis* FRI model results in a subclinical type of infection and after the first few days, clinical differences (e.g. weight loss or behaviour scoring) between non-inoculated and inoculated animals are minimal [373]. Higher levels of IL-17A and higher percentage of T cells in bone single cell suspensions were the main differences between non-inoculated and *S. epidermidis* inoculated mice.

Finally, in the context of bone, histamine has been associated with rheumatoid arthritis [414], and seems to act by stimulating the production of prostaglandin E and matrix metalloproteinase (MMP)-1, which eventually leads to bone damage and destruction [415]. Similarly, the use of Cimetidine ($H_2R$ antagonist) reduced bone loss by downregulating IL-6, MMP-1 and MMP-9 [416]. Other authors have reported that histamine can directly promote osteoclastogenesis by increasing histamine receptors in osteoclasts and osteoblasts [417]. Although we did not perform

measurements to evaluate bone healing, we did observe a better healing outcome in $H_2R$ KO mice which could be linked to this finding and that would be of interest to evaluate in future.

## Conclusion

Despite significant differences in immune responses observed between wild-type and $H_2R$ knock-out animals, this did not translate in infection clearance differences, with similar percentage of samples found negative and similar CFU counts.

## Acknowledgements

Tanja Schmid, Iris Keller, Pamela Furlong from the AO Research Institute Davos are thanked for technical and surgical assistance. Ruth Ferstl and Remo Frei are thanked for providing the $H_2R$ mice.

## Supplementary Figures

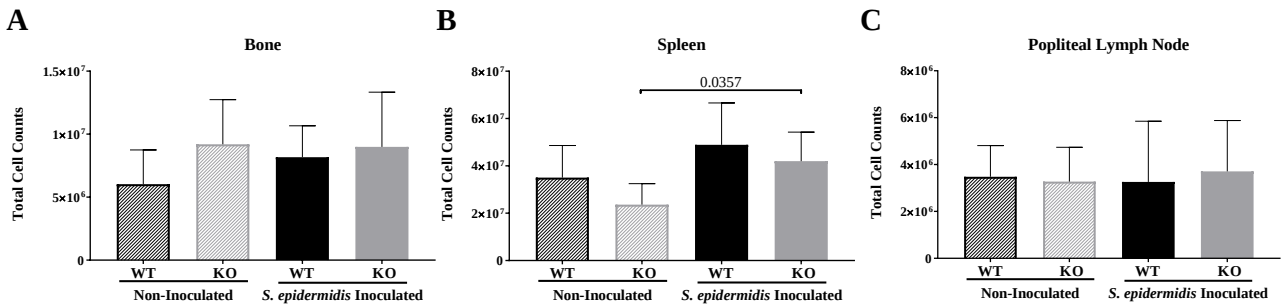


**Figure 5-37** Total cell counts in bone (A), spleen (B) and popliteal lymph node (C) for non-inoculated and *S. epidermidis* inoculated mice. Mean and SD (n=4-9). One-way ANOVA with Sidak's post hoc test, significant values indicated ($p$<0.05).

## 5.4 Subcutaneous pre-exposure to *S. epidermidis* does not influence subsequent infection rate in a murine fracture-related infection model

Marina Sabaté Brescó[1,2], Liam O'Mahony[2], Corina Berset[3], Stephan Zeiter[1], R. Geoff Richards[1], T. Fintan Moriarty[1]*

[1] AO Research Institute Davos, CH; [2] Swiss Institute of Asthma and Allergy Research, CH; [3] AO Foundation, CH

*****Corresponding author:
T F Moriarty, AO Research Institute Davos, AO Foundation, Clavadelerstrasse 8, Davos Platz, CH7270, Switzerland. Phone: +41 81 414 2397, E-mail: fintan.moriarty@aofoundation.org

Running Title: pre-exposure and *S. epidermidis* infection

*This manuscript is in preparation.*

**Abstract**

*Staphylococcus epidermidis* is a common member of the commensal human microbiota. Life-long exposure of this microorganism results in the development of a specific adaptive immune response as revealed by the presence of anti-*S. epidermidis* antibodies in human serum. In an apparent contradiction to its role as a commensal, *S. epidermidis* has also emerged as an important opportunistic pathogen in device related infection (DRI). To date, the influence of pre-existing specific adaptive immunity in the development or progression of *S. epidermidis* DRI remains unclear.

We have recently developed a model for *S. epidermidis* fracture-related infection (FRI) in specific-pathogen free (SPF) mice, although these mice are naïve to *S. epidermidis*. The present study was therefore performed to determine whether pre-existing specific adaptive immunity to *S. epidermidis* can influence infection rate, bacterial burden or immune responses in this model. SPF C57BL/6 male and female mice ($n \geq 8$ per group) were inoculated by subcutaneous injection of UV inactivated *S. epidermidis* and observed for four weeks. Upon confirmation of the presence of specific antibody in these mice, a fracture fixation device was applied to fix femoral osteotomies and the surgical site was contaminated with a clinical strain of *S. epidermidis.* The mice were observed for a further 14 days, at which time quantitative bacteriological evaluation was performed to determine if infection rate, bacterial burden or immune responses were affected by pre-exposure. Mice receiving saline injections were included as controls.

We observed a trend for lower CFU counts in mice pre-exposed to *S. epidermidis*, although no significant differences were observed in overall infection rate. Local and systemic immune responses 14 days after infection establishment showed minor differences between *S. epidermidis* exposed and saline groups. Levels of several cytokines and chemokines (IL-6, G-CSF, IL-17A or VEGF) were increased at the site of infection, and after stimulation with inactivated *S. epidermidis*, secretion of IL-17A and IFN-γ was increased in splenocytes. Thus, it can be concluded that previous humoral immunity has only a limited effect in subsequent infection, with a trend for lower bacterial counts, but no significant impact on infection.

**Introduction**

*S. epidermidis* is part of the normal human commensal microbiota, with life-long colonisation of the skin commencing within a few days after birth [56]. It is predominant in moist areas such as nares or fossae, but also present in sebaceous areas such as the facial skin [57] and mucosal tissues such as the gastrointestinal and the lower reproductive tracts [58, 59]. The presence of *S. epidermidis* at

these locations has been suggested to play a beneficial role for the host by inducing immune maturation [188, 189] and by outcompeting more pathogenic strains [67, 68, 71, 72]. Colonisation will also result in the generation of a specific adaptive immunity that has been proposed to be due to numerous transient self-resolving infections due to micro-invasions, rather than directly from colonization itself [246]. The nature of the adaptive immunity to commensal *S. epidermidis* has not been extensively studied, although antibodies have been detected in serum and saliva of healthy individuals against *S. epidermidis* proteins [251, 252], and experimental studies have shown *S. epidermidis* interaction with CD103+ skin-resident dendritic cells generates CD8+IL-17A+ T cells with the capacity to enhance protective responses in the skin [189].

In contrast to its conventional role as a commensal microorganism, the use of implanted medical devices has resulted in *S. epidermidis* becoming one of the most prominent causes of device related infection (DRI). *S. epidermidis* is not recognised as a highly virulent pathogen, however, the ability to rapidly adhere to and form a biofilm on the implanted device are considered critical to its ability to cause DRI [47a, 48]. How the specific adaptive immune response, that under normal circumstances may be expected to confer partial protection from infection, can influence the development and progression of DRI remains unclear. Antibodies against biofilm components and cytoplasmic proteins have been found to be predominant in patients with confirmed *S. epidermidis* infection [251], and titres are elevated in patients in comparison with healthy volunteers [252]. However, there remains limited understanding of the importance of specific adaptive immunity in this context.

We have previously described a mouse model of FRI. In this model, the device is a fracture fixation device used to fix osteotomies of the mouse femur. Using specific pathogen free (SPF) mice, we established a reliable *S. epidermidis* infection model. The presence of *S. epidermidis* on rodent skin is not well-characterized and has been reported as absent or at very low levels in studies with SPF mice [189, 190]. It may, however be present in wild/feral mice [418] and some inbred strains [419]. Presuming a much-reduced presence of *S. epidermidis* in murine skin, we aimed to generate adaptive immune responses via subcutaneous injection of UV-killed bacteria, to further study the impact of such immunity in a subsequent deep tissue infection. This would resemble a situation where skin commensal bacteria, against which immunity may exist, would colonize deeper tissues and arise as a pathogen. Our aim was to assess the effect of previous systemic exposure to *S. epidermidis* on subsequent infection with the same bacteria in an established mouse fracture model.

## Materials and methods

*Mouse skin bacteria isolation*

Dorsal skin pieces (approximately 1 $mm^2$) of SPF mice kept in our facilities were incubated in tryptone soy broth (TSB) for 48 hours at 37°C in agitation at 100 rpm. Afterwards, serial dilutions of the broth were plated in tryptone soy agar (TSA) (Oxoid), for total counts, and in mannitol-salt agar (MSA) (Oxoid) to identify staphylococcal strains. Single colonies were re-plated to ensure pure strains and sent for identification to Synlab (Luzern, Switzerland).

*Animals*

The study was approved by the ethical committee of the canton of Graubünden in Switzerland (TVB 30E-2015) and was carried out in a research facility accredited by Association for Assessment and Accreditation for Laboratory Animal Care (AAALAC) International. Skeletally mature (24 weeks old), male (average weight ± SD: 36.85 ± 3.44g) and female (28.27 ± 2.78g), SPF C57BL/6N mice, purchased from Charles River (Germany), were used in this study. All animals were allowed to acclimatize to experimental conditions for at least two weeks prior to the start of the study. Mice were housed under a 12 hour dark/ 12 hour light cycle in groups of four to six in individually ventilated cages (XJ, Allentown), changed weekly. Animals were fed with a standard diet (3436, Provimi Kliba) and had free access to water at all times. The study design is summarized in Figure 5-38. It consisted of two subcutaneous injections of either saline or UV killed *S. epidermidis* Epi 103.1 at 30 and 14 days before surgery. Equal groups of mice were blindly allocated in one of the two treatment groups and randomly operated/inoculated ($n \geq 8$ per group). The mice were re-housed in the same groups post-surgery. In addition, non-operated age-matched males and females were used as control group.

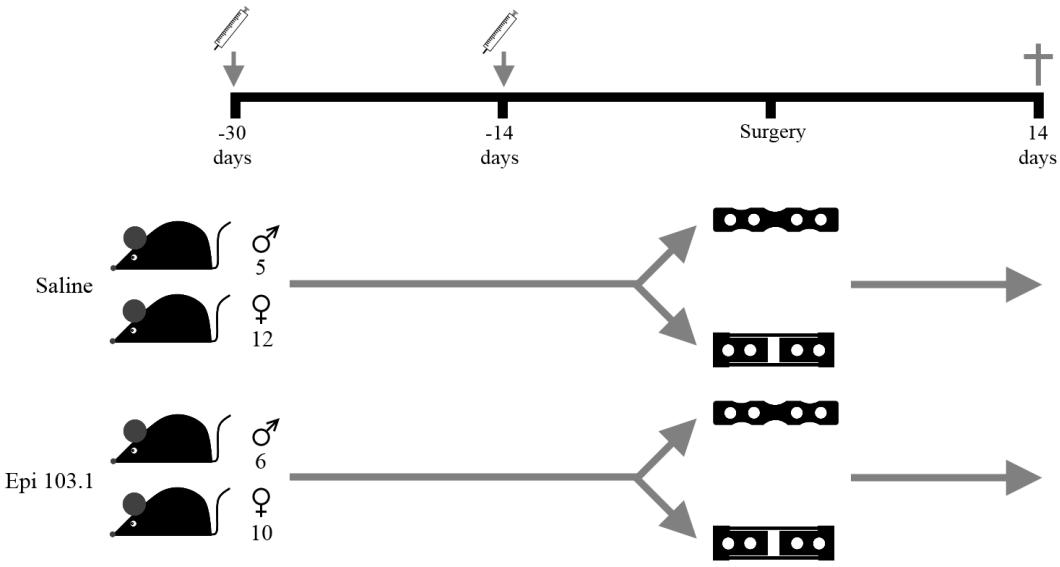


**Figure 5-38** Experimental scheme of the studies, with final number of animals analysed per group. Syringe schemes indicate time of subcutaneous injection of saline or UV-killed *S. epidermidis*.

*Bacteria preparation for subcutaneous injections*

The strain used in this study, *S. epidermidis* Epi 103.1, is a clinical isolate obtained from a patient with chronic implant-related bone infection. UV killed bacteria were prepared for subcutaneous inoculations. Briefly, bacteria were grown in TSB (Oxoid) at 37°C, under agitation (100 rpm), until they reached an optical density corresponding to $9.33x10^8$ CFU/ml. They were washed twice in phosphate-buffered saline (PBS) (Sigma-Aldrich), sonicated for 3 minutes (Bandelin Sonorex at 40 KHz) and exposed to flow-hood UV light (254 nm) for 4 hours. Bacteria were pelleted (3000 g, 15 minutes) and resuspended in sodium chloride (NaCl) 0.9% (B.Braun). One ml of the initial suspension was cultured overnight in TSB (37°C, 100 rpm) to ensure that the inactivation of all bacteria was successful. The suspension obtained was aliquoted and frozen at -20°C. Prior to use, aliquots were thawed and diluted in NaCl 0,9% to a final concentration of $4x10^7$ CFU/ml.

*Subcutaneous exposure and antibody levels*

Thirty and fourteen days before surgery, mice were injected subcutaneously with 100 µl of NaCl 0,9% or 100 µl of bacteria suspension (estimated dose: $4x10^6$ CFU). Injections were performed under general anaesthesia with isoflurane (2-3% isoflurane in 100% $O_2$, 1 l/min) (Isofluran Baxter®, Baxter AG). Dorsal skin was clipped and prepped aseptically (washed with Hibiscrub® soap and then cleaned with Softasept® N (B.Braun) solution) before treatment solution was injected with a 25G needle. Two weeks after the second injection, blood was collected via tail vein for antibody measurements.

*Implants and surgery*

Commercially pure Titanium (CpTi) 4-hole rigid and CpTi 4-hole flexible MouseFix$^{TM}$ implants and Titanium Aluminium Niobium alloy (Ti6Al4Nb (TAN)) screws were used in this study (RiSystem AG). Prior to use, all implants were cleaned and sterilized as previously described [296]. Surgery and inoculum were performed as described previously [373].

*Euthanasia and post-mortem sample processing*

Fourteen days post-operatively, animals were anesthetized in an induction box (5% isoflurane in 100% $O_2$, 1 l/min) and blood was taken from retro-orbital sinus for serum isolation (5000 rpm, 10 minutes). Afterwards, mice were euthanized by cervical dislocation. A lateral radiograph of the left femur with implant in place was acquired post-mortem. The operated femur, the implant and the surrounding soft tissue were harvested separately in sterile containers with cold PBS. Contralateral femurs were collected from some of the operated animals (from both saline and Epi 103.1 pre-exposed groups) as additional controls. The soft tissue and the femurs were mechanically homogenized (Omni Tissue Homogenizer and Hard Tissue Homogenizing tips, Omni International). To determine bacteria associated with the implant, all metal hardware were sonicated in PBS for 3 minutes (BandelinSonorex at 40 KHz) and vortex mixing for 10 seconds. Viable bacterial counts were performed by plating serial dilutions of each sample on 5% horse blood agar (BA) (Oxoid). All BA plates were incubated at 37°C for bacterial counts at 24 and 48 hours.

Aliquots of bone homogenates were also used for cytokine and chemokine quantification. A 700 µl aliquot sample was centrifuged at 9000 g at 4°C, and the supernatant was aliquoted and frozen until measurement. Finally, the remaining sample was filtered through a 70 µm cell strainer (BD Falcon) and resuspended in complete RPMI (cRPMI: RPMI 1640 (Gibco), penicillin (1 U/ml, Sigma-Aldrich), streptomycin (1 µg/ml, Sigma-Aldrich), kanamycin (0.1 µg/ml, Gibco), MEM vitamin (1x, Sigma-Aldrich), L-glutamine (2 mM, Sigma-Aldrich), Na-pyruvate (1 mM, Sigma-Aldrich), non-essential amino acids (1x, Sigma-Aldrich) and heat inactivated foetal calf serum (10%, Sigma-Aldrich)). Spleen and popliteal lymph node were harvested in cold PBS and cRPMI respectively. To obtain single cell suspensions, samples were mashed with a syringe rod through a 70 µm cell strainer. For the spleen, erythrocytes were haemolysed with $ddH_2O$ for 1 minute. Both single cells suspensions were finally resuspended in cRPMI. Cells were counted in all samples with Scepter™ 2.0 Cell Counter (Millipore) and adjusted to $2x10^6$ cells/ml.

*Cell suspension re-stimulation*

Spleen single cell suspensions were plated in 24-well plate ($1x10^6$ cells/well) with cRPMI. Cells were left unstimulated or stimulated with phorbol 12-myristate 13-acetate (PMA) (20 ng/ml, Sigma-Aldrich) and ionomycin (200 ng/ml, Sigma-Aldrich), or UV killed *S. epidermidis* (1:1 and 1:10, cells:bacteria). Samples were incubated at 37°C, 5% $CO_2$ and supernatants were collected after 24 and 72 hours.

*Cytokine and chemokine quantification*

Cytokines and chemokines were quantified in bone homogenates and spleen supernatants using Milliplex Map Mouse cytokine/chemokine Magnetic Bead Panel (Millipore). The following cytokines were measured in supernatants of bone homogenate: G-CSF, IFN-γ, IL-2, IL-4, IL-6, IL-10, IL-13, IL-17A, KC/GRO, MCP-1 and TNF-α. The following cytokines were measured from supernatants of stimulated splenocytes: IFN-γ, IL-2, IL-4, IL-10, IL-17A and TNF-α.

*Flow cytometry*

Bone single cell suspensions were stained with the following antibodies after life viability dye with Fixable Viability Dye eFluor 780 (eBioscience) for 30 minutes at 4°C in darkness: FITC anti-mouse Ly6G, PE anti-mouse CD8, APC anti-mouse, PerCP-Cy5.5 anti-mouse, PE-Cy.7 anti-mouse, Pacific Blue anti-mouse and Brilliant Violet 510 anti-mouse CD4 (all from Biolegend). At least $0.5x10^6$ cells were acquired in Gallios flow cytometer (Beckman Coulter). Lymph nodes were stimulated for 4 hours at 37°C and 5% $CO_2$ in cRPMI with PMA (50 ng/ml), ionomycin (500 ng/ml) and brefeldin A (1x, eBioscience). Afterwards, medium was washed and cells were stained with Fixable Viability Die eFluor 780 as above and with the following antibodies for surface markers: PE/Cy7 anti-mouse CD3 and Pacific Blue anti-mouse CD4 (all from Biolegend). Afterwards cells were fixed and permeabilized with the Intracellular Fixation & Permeabilization Buffer Set (eBioscience) and stained intracellularly with Alexa Fluor 488 anti-mouse/rat IL-17A, PE anti-mouse IL-10, PerCP-Cy5.5 anti-mouse IFN-γ and APC anti-mouse IL-4 (all from eBioscience). Samples were measured in a Gallios (Beckman Coulter) flow cytometer and analysed using the Kaluza software.

*Anti-S. epidermidis antibody ELISA*

UV killed *S. epidermidis* Epi 103.1 in PBS was processed to obtain a lysate for plate coating. The process included 5 cycles of snap-freezing in liquid nitrogen, 1 hour incubation at 37°C with 200 µg/ml of Lysostaphin (Sigma-Aldrich) resuspended in 20 mM Sodium Acetate (Sigma-

Aldrich) pH 4.5 at 10 mg/ml and 1 mM of EDTA 0.5 M (Sigma-Aldrich). Subsequently, samples were sonicated 4 times (each step: 10 minutes, 60 Hz, on ice) with sterile glass beads (90-150 µm, VWR). Finally, the sample was centrifuged at 200 rpm for 10 minutes to remove glass beads. Protein in the collected supernatant was quantified and adjusted to 550 µg/ml with PBS before it was aliquoted and frozen at -20°C.

For the ELISA, Maxisorp Nunc 96 flat-bottom well plates (ThermoFisher) were coated with 2.5 µg/ml of *S. epidermidis* Epi 103.1 lysate (overnight, 4°C). Afterwards, wells were blocked with 5% milk powder in PBS 0.05% Tween 20 (Fluka) and incubated with serum dilutions ranging from 1:20 to 1:320. Antibodies against *S. epidermidis* were detected using biotinylated goat anti-mouse IgG and IgM (Mabtech), HRP-streptavidin (Sigma-Aldrich), tetramethylbenzidine (TMB) mix and 1M $H_2SO_4$ as a stop solution. Plates were read at 450nm in a plate reader (Berthold Technologies).

*Statistical Analysis*

Statistical analysis was conducted using GraphPad Prism 7 software (GraphPad Software). Statistical tests performed are indicated in each figure legend. Differences were considered significant with $p<0.05$.

## Results

*Staphylococcus presence in mouse skin*

At two different times, we collected skin samples from mice euthanized in our facilities for other projects to address if we could isolate *S. epidermidis*. Skin samples were incubated in TSB to allow bacteria to grow and after 48 hours they were plated MSA, a selective medium for staphylococci. From 7 different mice (7 samples), 15 staphylococcal strains were isolated (Supplementary Figure 5-45), which were identified mostly as *S. xylosus* and *S. cohnii*. One mouse was found to be culture positive for *S. aureus* isolate, and none for *S. epidermidis*.

*Weight change and animal welfare in pre-exposure study*

All animals lost weight after each subcutaneous injection and again after surgery. Differences were not statistically significant. After surgery males tended to lose less weight compared to female groups, although this was not significant. No differences in weight regarding implant type were observed (data not shown).

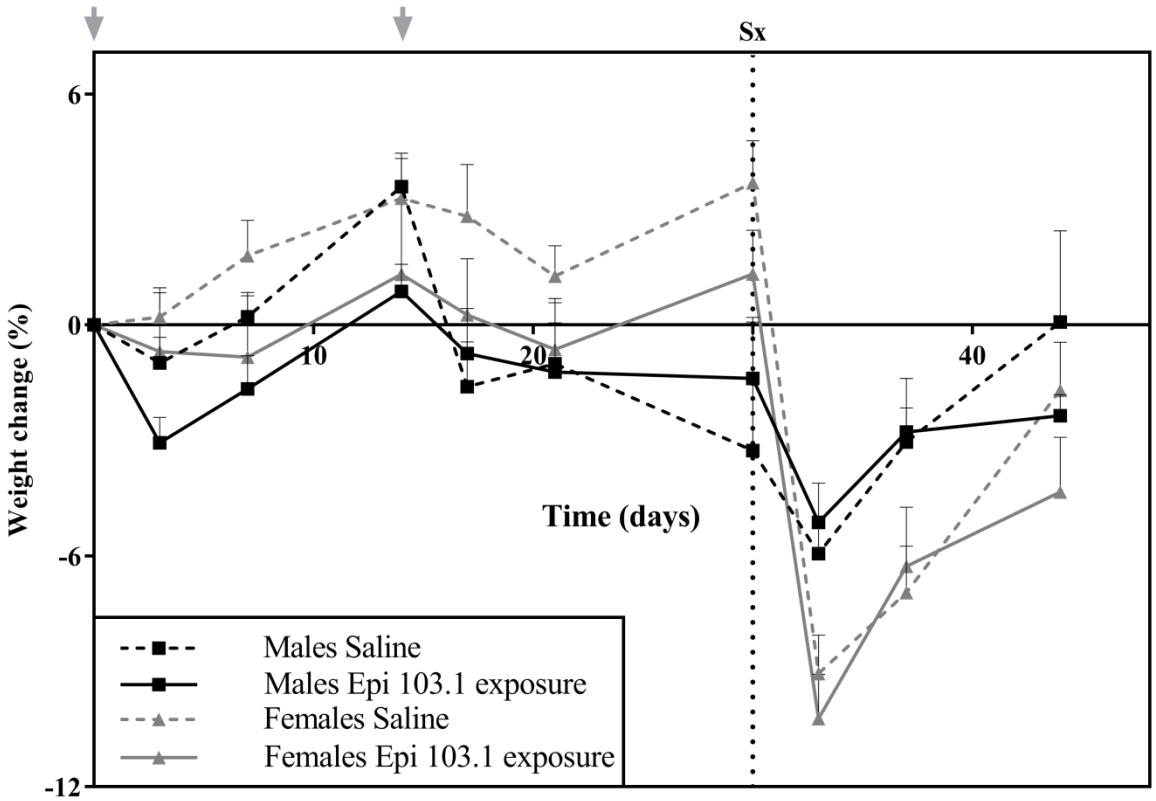


**Figure 5-39** Weight change in percentage during treatment and post-surgery (Sx). Day 0 is used as a reference to calculate weight change before surgery. Pre-operative weight is used as a reference to calculate weight change post-operatively. Mean and SEM (n=5-6 for males / 10-12 for females). Repeated measures 2-way ANOVA with Tukey post hoc test, $p<0.05$.

*Quantitative bacteriology*

Mice were inoculated with an average dose of $1.84x10^4$ CFU (no significant differences between saline and Epi 103.1 pre-exposure groups). At euthanasia (14 days post-operatively), all animals treated with saline were culture positive and 81.25% of the animals previously exposed to Epi 103.1 were culture positive (Figure 5-40). CFU counts were not significantly different at any time-point but did show a trend for lower counts in Epi 103.1 pre-exposure group.

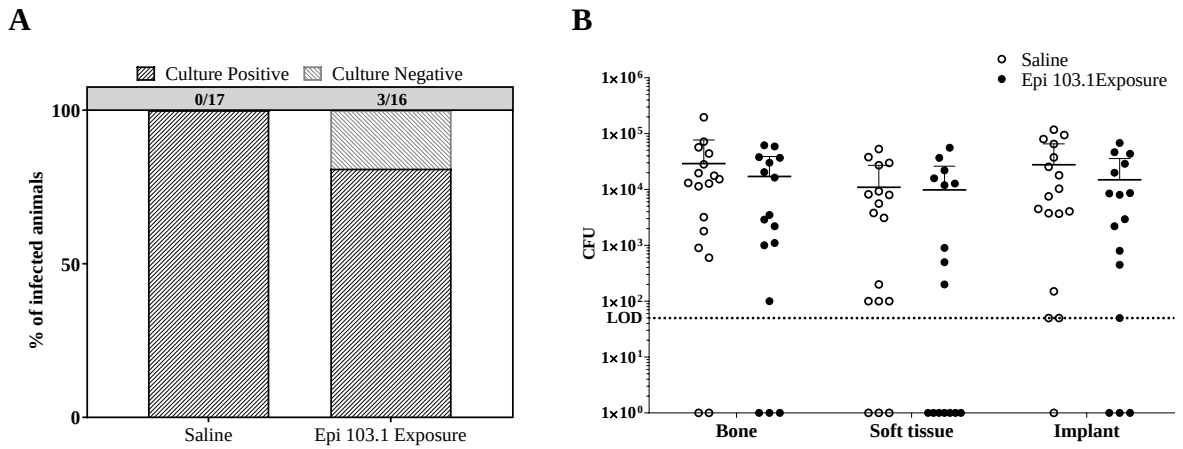


**Figure 5-40** A) Percentage of culture positive and culture negative mice in saline and Epi 103.1 pre-exposed groups. B) CFU counts in the different compartments: bone, soft tissue and implant. LOD: Limit of detection. Fisher Exact test for proportions and Mann-Whitney test for CFU counts. No statistical significant differences observed.

*Local response: cytokine production in bone marrow*

Cytokines in bone homogenate were quantified at euthanasia. Innate immune markers were slightly increased in the operated limb of inoculated and ultimately infected animals (saline and Epi 103.1 pre-exposed groups) compared to non-operated controls or contralateral femurs. This reached statistical significance for G-CSF and KC (Figure 5-41, A and C), whereby both the saline and UV killed *S. epidermidis* pre-exposure resulted in an increased secretion. Pre-exposure significantly increase IL-2, IFN-γ, IL-17A (Figure 5-41, D-F) and VEGF (Supplementary, A) relative to the control group, while in the saline treated animals, only IL-17A was significantly increased compared to controls (Figure 5-41, F). IL-10, MCP-1 and TNF-α presented very low levels in all groups (Supplementary Figure 5-47, B-D). When data was subdivided by gender, still no differences were observed between saline and *S. epidermidis* exposure (Supplementary Figure 5-48). When samples were subdivided by implant type, we could observe a trend for higher inflammatory markers in flexible implant groups, although this was reduced after exposure, being significant for G-CSF (Supplementary Figure 5-49).

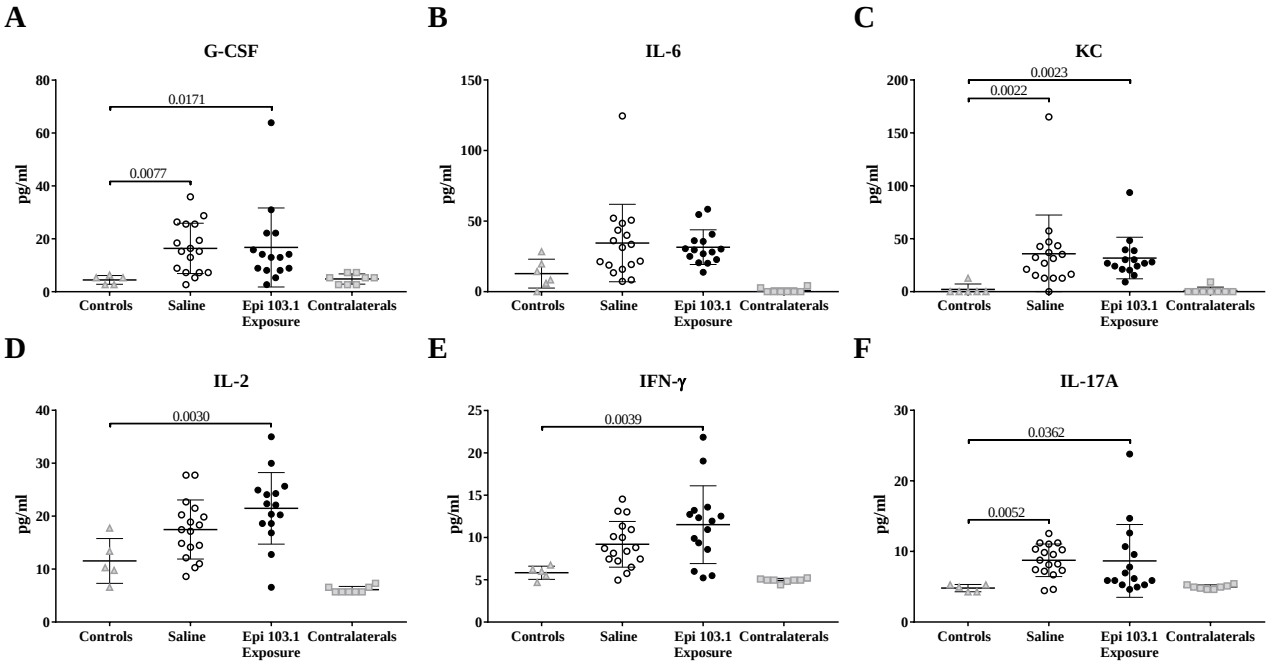


**Figure 5-41** Cytokine and chemokine levels in bone homogenates of C57BL/6N mice, from control (non-operated mice), saline, Epi 103.1 pre-exposed groups and contralateral femurs (for contralateral femurs, no differences were observed between samples from saline or *S. epidermidis* exposed animals and thus, values were pooled together). Mean values and SD (n=5-17 per group). One-way ANOVA with Sidak post hoc or Kruskal-Wallis test with Dunn's post hoc.

*Systemic responses: Spleen and Lymph Node*

Splenocytes were stimulated with *S. epidermidis* Epi 103.1 to measure cytokine secretion (Figure 5-42). We observed that inoculated animals (saline and Epi 103.1 pre-exposed groups) had a greater response compared to the negative control group, with significant differences observed for IL-10, IFN-γ and IL-17A. In general, Epi 103.1 pre-exposed animals had higher levels of cytokines than saline treated animals, although the differences were not statistically significant. IL-4 was also measured but was not detected.

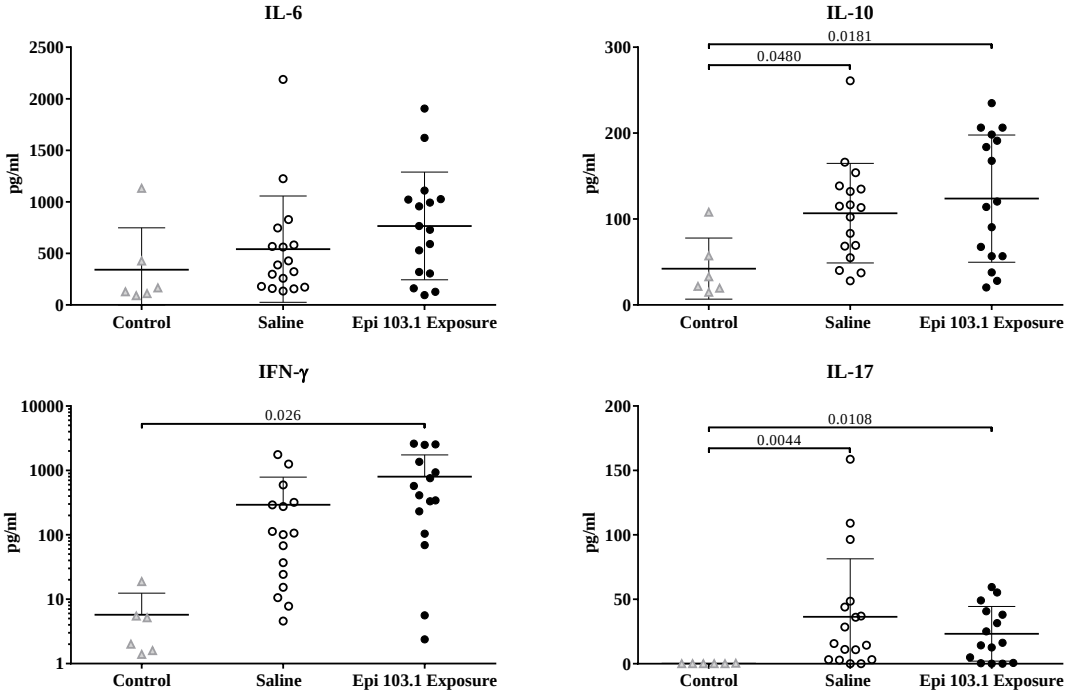


**Figure 5-42** Cytokine levels in splenocytes of C57BL/6N mice, from control, saline, Epi 103.1 pre-exposed groups after 72 hours stimulation with Epi 103.1 (10 bacteria: 1 cell). Mean values and SD (n=6-17). Kruskal-Wallis test with Dunn's post hoc.

Popliteal lymph nodes were also analysed, after stimulation with PMA/ionomycin. We did not observe statistically significant differences between treated groups and controls. A trend towards a decrease in CD3+CD4- and CD3+CD4+ proportions was observed for treated groups (saline and Epi 103.1 pre-exposed) in comparison to control animals. In terms of cytokine production, within the T helper compartment (CD3+CD4+) we did not observe significant differences. Some treated animals (both saline and Epi 103.1 pre-exposed) tended to have higher percentages of IFN-γ and IL-17A T helper cells but values were highly variable across the groups. Animals with high values did not correspond to animals that cleared infection.

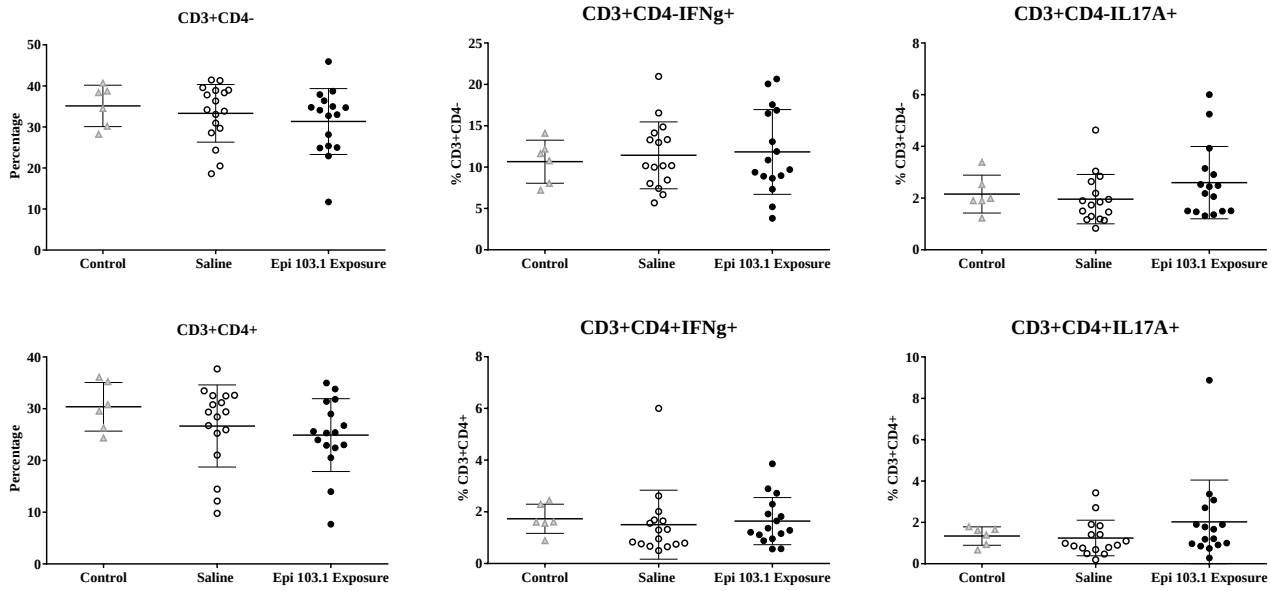


**Figure 5-43** Percentage of T cells (total CD3+CD4- or CD3+CD4-, and positive for IFN-γ or for IL-17A) in popliteal lymph node of C57BL/6N mice, from control, saline, Epi 103.1 pre-exposed groups. Mean values and SD (n=6-17). Kruskal-Wallis test with Dunn's post hoc. No significant differences observed.

### *S. epidermidis specific antibodies*

Specific antibodies against *S. epidermidis* 103.1 were measured pre-operatively and at day euthanasia with an ELISA, where the plate was coated with a *S. epidermidis* 103.1 total lysate. Pre-operatively, we observed that some of the *S. epidermidis* exposed mice had developed IgM or IgG antibodies, although the response was not homogeneous and some animals did not show increased values. At day 14, IgM values had increased, with no significant differences between groups or controls (Figure 5-44). IgG responses seemed to be related to implant-associated *S. epidermidis* infection as control animals had very low levels of *S. epidermidis*–specific IgG. However, no differences were observed between saline and Epi 103.1 pre-exposed groups at euthanasia.

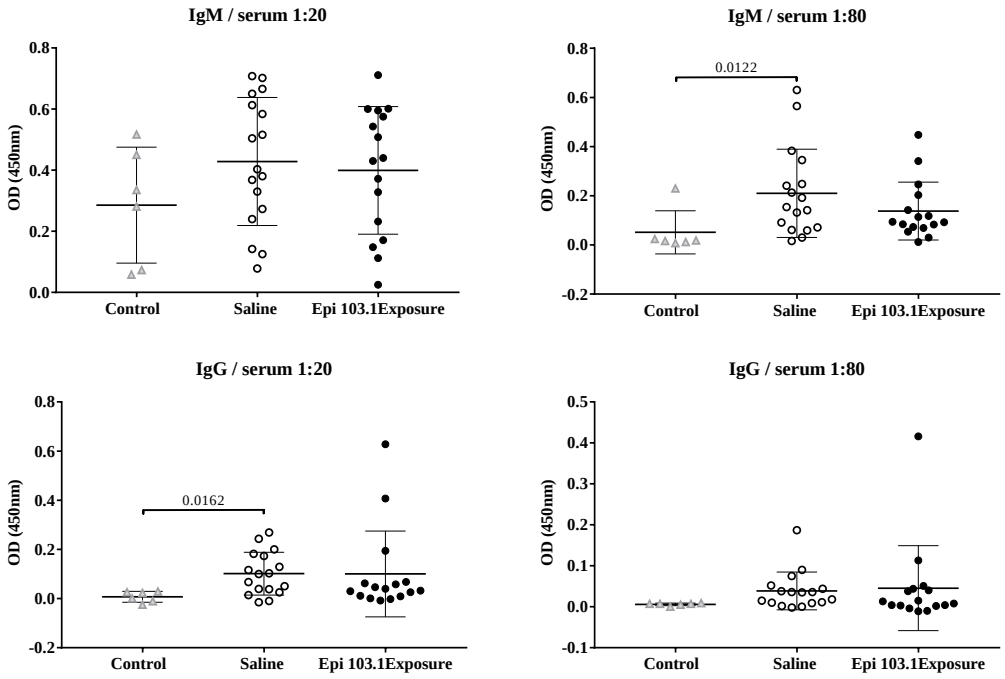


**Figure 5-44** IgG and IgM antibody levels against *S. epidermidis* 103.1 at day 14, two different dilutions (1:20 and 1:80). Mean and SD (n=6-17). Kruskal-Wallis test with Dunn's post hoc test.

## Discussion

The use of SPF mice in DRI studies is widespread, although these mice have limited exposure to *S. epidermidis*. As a result, there is no pre-existing specific adaptive immunity towards these bacteria. On the contrary, in humans *S. epidermidis* represents one of the main colonizers. This raises questions about the use of SPF mice in DRI models with commensal pathogens, as the impact of specific immunity to the pathogen is not replicated in these models. In this study, we compared the infection rate and immune responses in mice with a four-week subcutaneous pre-exposure to inactivated *S. epidermidis* with naïve controls. The aim was to provide an understanding about whether a specific immunity will influence the risk and progression of DRI. Although minor differences were observed in bacterial burden and immune responses, there was no significant impact on infection rate.

The confirmation of the mice as negative for *S. epidermidis* is important to clarify. We attempted to isolate *S. epidermidis* from mice kept in our facilities and, although other staphylococci were present (Supplementary Figure 5-45), *S. epidermidis* could not be isolated. A more comprehensive analysis of murine skin with more specimens and combining different techniques such as 16s sequencing would be possible to provide further confirmation. Nevertheless, we believe that even if some *S. epidermidis* might be present, their limited number would lead to very residual adaptive

immune responses and thus, pre-exposing the animals subcutaneously is still an interesting approach to better understand the role of adaptive immunity. Moreover, other recent studies aiming to elucidate host immune modulation by human commensal bacteria, did not observe significant levels of *S. epidermidis* in mice skin [189].

Presuming that *S. epidermidis* was absent from our mice, we injected the bacteria subcutaneously to simulate the access of the bacteria to the more superficial tissues, which would generate adaptive immune responses. We injected UV-inactivated *S. epidermidis* subcutaneously twice in a 4 week period, as it is expected that adaptive immune responses will be built up within approximately 7 days. In a previous pilot study performed in a small number of animals, we compared the injection of UV-inactivated *S. epidermidis* alone or with Freund's adjuvant (complete and incomplete).Both methods were shown to elicit adaptive immune responses (Supplementary Figure 5-50). For this study, we decided to use the bacteria alone, as Freund's adjuvant resulted in skin irritation in some animals. We already observed at that time that adaptive immune responses were not equally induced in all animals; however, as our aim was not to generate a protective vaccine or strong immunity, we did not modify the exposure protocol. In the main study, we did assess antibody levels before surgery, although we encountered some limitations. On one hand, the amount of blood obtained was very small and was often haemolytic, which could interfere with the readout of the ELISA. In some mice, we could observe anti-*S. epidermidis* IgM and IgG antibodies at the time of surgery, however, results were not homogenous and also some saline group animals showed signal in the ELISA. Of note, we used the whole bacteria lysate to coat the plate, in order to have a broad range of antigenic molecules present. However, these molecules may present cross-reactivity with other antibodies present, which were not specific of *S. epidermidis*. It is also important to note that the study was performed blinded until the euthanasia, and so we could not intervene at that stage and extend the exposure period. Nevertheless, our aim was not to elicit strong adaptive immune responses, which would completely protect animals, instead we aimed to simulate a previous contact with the bacteria as may occur in superficial tissues.

After surgery and infection generation, we observed that the only group with culture negative animals was the *S. epidermidis* pre-exposed group, with also a trend for lower CFU counts in all the different compartments (implant, soft tissue and bone) tested. This was especially evident within soft tissue. Nevertheless, no statistically significant differences were observed. Thus, it seems that the previous exposure to *S. epidermidis* systemically had a very limited effect in our model system.

In terms of immune responses between saline and Epi 103.1 pre-exposed animals, only minor differences were observed. This suggests that the infection process was the major driver behind

immune responses generation, and not the pre-exposure. For cytokine secretion, *S. epidermidis* Epi 103.1 pre-exposure seemed to induce a more IFN-γ-skewed response (higher levels of IFN-γ in bone homogenates and after spleen re-stimulation). This was not dependent on gender or implant type, and thus we believe it is a mild effect of different immunological status in both groups. No significant differences were observed in popliteal lymph node populations. Nevertheless, few animals from the operated groups (both saline and Epi 103.1 pre-exposed) had higher cytokine responses compared to control animals. As we did not stimulate lymph nodes with Epi 103.1, we might be missing differences that could arise due to antigen-specific responses (as was observed in the splenocytes re-stimulation).

Humoral responses were evaluated with an ELISA, using *S. epidermidis* 103.1 lysate to coat the plates. While inoculated animals tend to show higher levels of IgM and IgG, no differences were observed between saline and Epi 103.1 pre-exposed groups. Detectable levels of antibodies against *S. epidermidis* in our control animals (especially for IgM) suggest that cross-reactivity can explain part of the results observed. In the future, it would be interesting to elucidate differential antigen recognition between controls and inoculated groups to identify major immunogenic proteins during the infection process. This has been often addressed in the context of *S. aureus* infection [420-425]. A few studies have reported that the Na+/H+ antiporter, Acetyl-CoA C-acetyltransferase, lipoate ligase, cysteine synthase or alanine dehydrogenase can be important *S. epidermidis* immunogenic proteins [254, 255].

In future, longer-term exposure to live microbes, instead of UV-treated microbes, could be tested. Also, "cutaneous-only" exposure has been successfully performed recently [188, 189] and would be interesting to undergo this approach, although it can induce regulatory responses. Ideally, a better characterization of human immune responses towards commensal strains should be achieved in order to replicate such responses in preclinical models when aiming to simulate clinical scenarios. In addition, infection models with common mouse-skin colonizers (such as *S. xylosus* or *S. cohnii*, based on our isolates) could represent an alternative approach to understand the impact of commensal strains in further infections occurring in the host.

## Conclusion

In contrast to human skin, murine skin does not present *S. epidermidis*. Thus, it is expected that the animals are completely naïve to this bacteria. We aimed to amend this situation, which is never present in humans, to understand the impact of previous immunity, arising from transient contact with the bacteria, in a deep-tissue infection. Although our data is a preliminary approach, we observed that immune responses built up upon infection did not differ significantly between pre-exposed and saline groups. This suggests that the infection process was the main trigger of immune responses and previous exposure just led to minimal differences.

## Acknowledgements

The authors would like to thank Tanja Schmid, Iris Keller and Pamela Furlong for technical assistance.

**Supplementary Figures:**

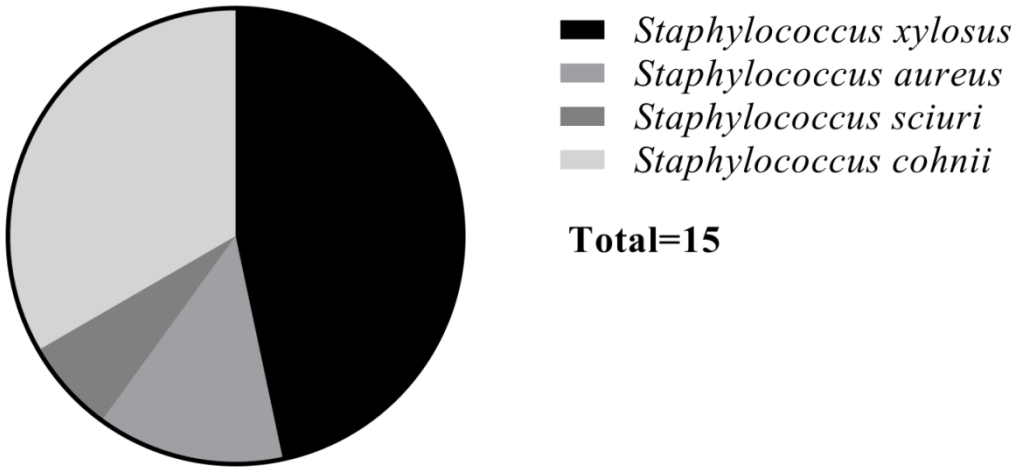


**Figure 5-45** Distribution of staphylococcal isolates (n=15) by species obtained from 7 mice.

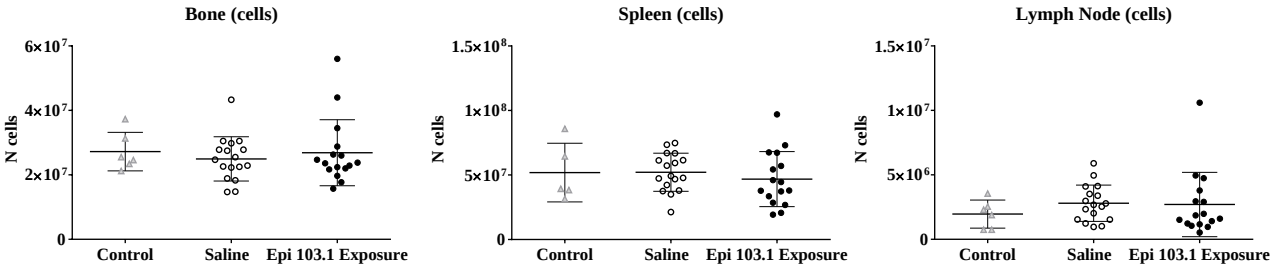


**Figure 5-46** Total cell counts in bone, spleen and lymph node. Mean and SD (n=6-17). 1-way ANOVA with Tukey's post hoc test. No significant differences observed.

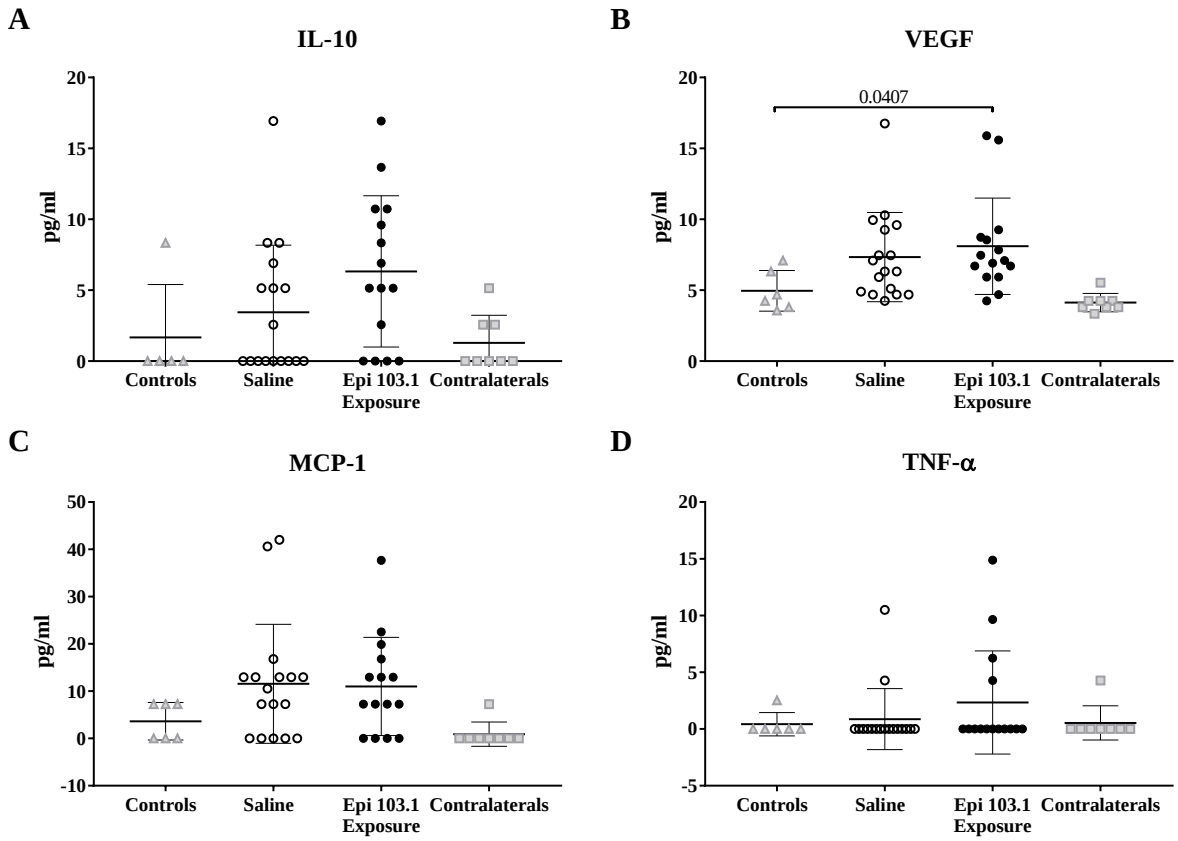


**Figure 5-47** Cytokine and chemokine levels in bone homogenates of C57BL/6N mice. Mean and SD (n=5-12). Kruskal-Wallis with Dunn's post hoc test.

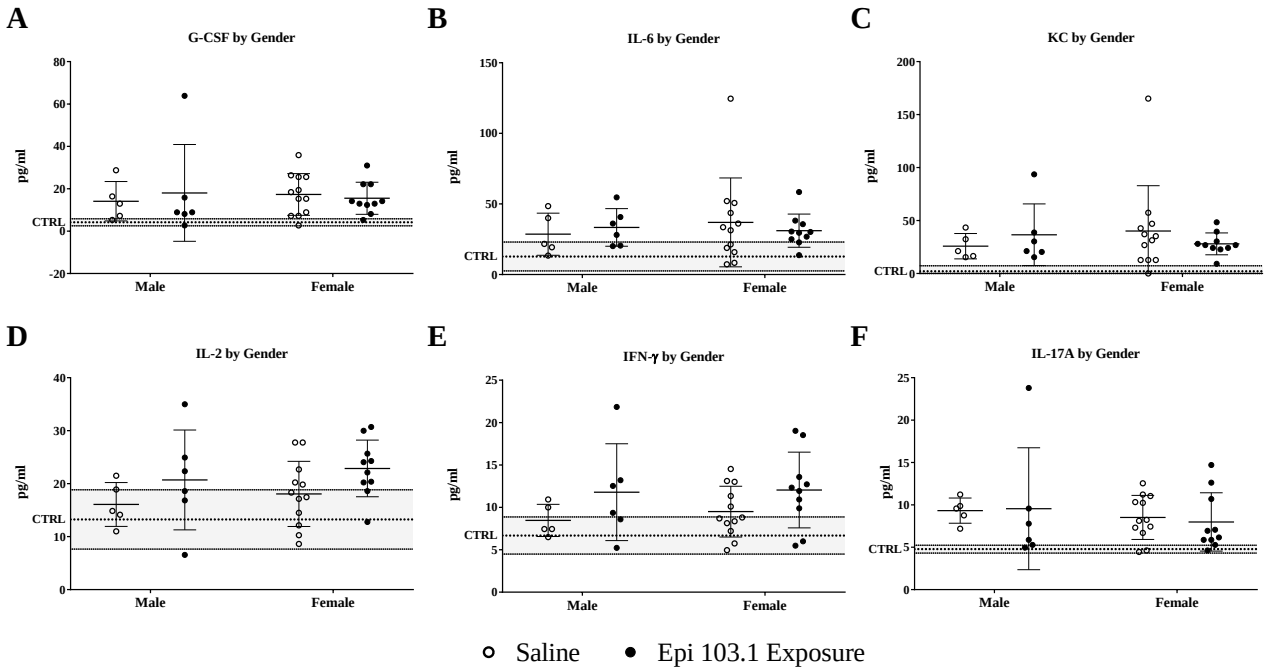


**Figure 5-48** Cytokine and chemokine levels in bone homogenates of C57BL/6N mice (samples subdivided by Gender). CTRL: mean of control values ± SD. Mean and SD (n=5-12). 2-way ANOVA with Sidak's post hoc test.

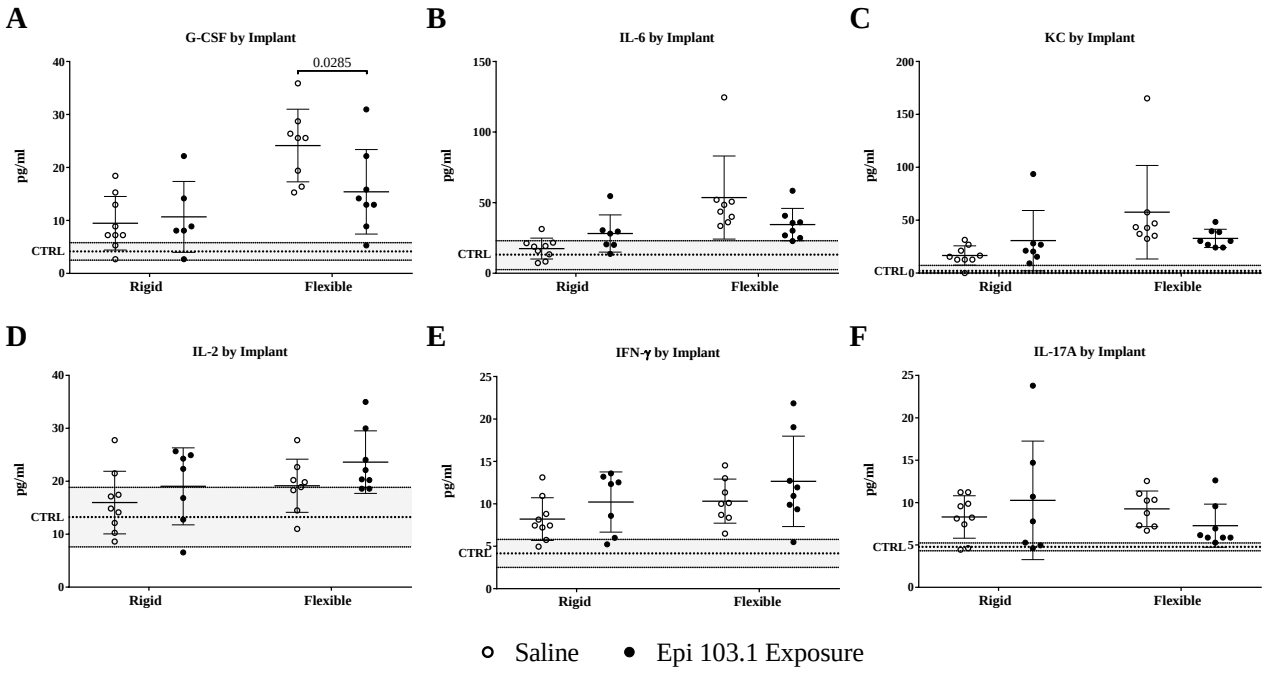


**Figure 5-49** Cytokine and chemokine levels in bone homogenates of C57BL/6N mice (samples subdivided by Implant type). CTRL: mean of control values ± SD. Mean and SD (n=5-12). 2-way ANOVA with Sidak's post hoc test.

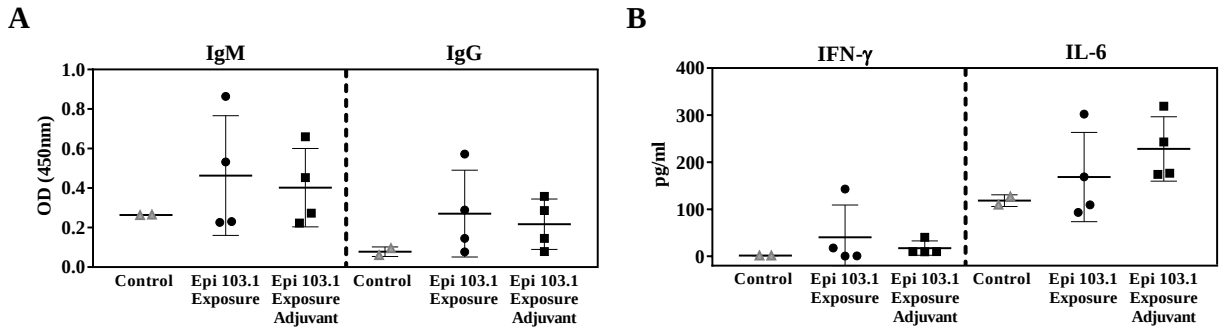


**Figure 5-50** Data from a pilot study were animals were injected subcutaneously with $2x10^6$ CFU of UV-inactivated *S. epidermidis* Epi 103.1, alone or in combination with Freund's adjuvant (complete in the first injection, incomplete in the second). A) anti-*S. epidermidis* antibodies in serum (dilution 1:20) from control mice and pre-exposed mice. Mean values and SD (n=2-4) B) Cytokine levels in splenocytes of C57BL/6N mice from control mice and pre-exposed mice after 72 hours stimulation with Epi 103.1 (10 bacteria: 1 cell). Mean values and SD (n=2-4). No statistical analysis performed.

# 6. General discussion

## 6.1 Clinical and scientific rationale

Fracture-related infection (FRI) is one of the major complications in orthopaedic trauma surgery. It can require prolonged antibiotic treatment, can delay healing, and may result in poor functional outcome for affected patients. *S. epidermidis* causes approximately 20-30% of orthopaedic device-related infections (ODRI) [45, 49, 93] and the prevalence may even reach 50% in late-developing infections [94]. The predominance of this microorganism in late-developing infections may be linked to the sub-acute nature of *S. epidermidis* infections, which may first present many months after surgery and even then, with only subtle signs of infection. Importantly, clinical data has shown that *S. epidermidis* infection is associated with longer treatment and lower cure rates (75%) than equivalent infections caused by *S. aureus* (84%) [109], however, the scientific literature in the field is dominated by *S. aureus.*

This thesis has focused on *S. epidermidis* FRI, with the aim of providing improved understanding of the development and progression of these infections under controlled experimental conditions. A first goal was to establish the first experimental model for *S. epidermidis* FRI. Furthermore, we aimed to investigate the role of features such as implant design, key receptors and cytokines in the progression of FRI and the role played by specific pre-existing immunity to *S. epidermidis* on the development of FRI. The following general summary will place the findings of this thesis into context from a general perspective, covering some discussion points that may not have already appeared in the preceding chapters. This section will also discuss the future studies that would be worthwhile to consider arising from the data generated in this thesis.

## 6.2 Establishment of a *Staphylococcus epidermidis* fracture-related infection model

One of the first aims of this thesis was to develop an *in vivo* model for *S. epidermidis* FRI, as there is a lack of such models in the literature [303, 340]. A model for *S. aureus* FRI was published within the context of this thesis [296], and the *S. epidermidis* model that was successfully established was based on that template. We also compared our S. *epidermidis* results with probably the most widely studied bacteria in the field, *S. aureus* as a means to compare and contrast the infections caused by these two pathogens.

The model presented in this thesis is based on the MouseFix$^{TM}$ system [329, 341], which is a range of commercially available implants and instruments designed to provide standardized fracture

fixation in mice. Historically, most preclinical studies have been performed in large animals, due to the possibility to use the implants and instruments used in human surgery, and the lack of such equipment for small animals. However, the development of the tools required to achieve stable fracture fixation in small animals has led to a significant increase in the use of rodents in bone research in the last 20 years [426, 427]. Although mice and rats lack a Haversian system [428], rodents offer numerous advantages over other animals that makes them attractive models for research. Rodents are easy to handle and to house, are often cheaper to obtain and maintain than other species and have shorter breeding cycles [426, 429]. This makes them especially suitable in exploratory studies where several time-points and/or conditions are to be tested and large numbers of animals are required. In addition, especially for mice, the most common strains are genetically well defined and they offer a large set of technical possibilities (from a broad range of antibodies to the possibility to use genetically modified animals). Amongst the available fixation systems for mice [430], we selected the MouseFix$^{TM}$ system, which offers two fracture fixation plates for femoral fractures, and these two implants provide different mechanical support for healing: a rigid plate used to reproduce a stable fixation and a flexible plate to resemble an unstable fixation. The bone fracture (transverse osteotomy) is generated using a Gigli saw, ensuring that the defects are more consistent between animals and ensuring control over the size of the osteotomy gap. A transverse osteotomy obviously differs from a naturally occurring fracture, which may well involve oblique angles, uneven or jagged fracture ends and possibly may involve multiple fragments. A more naturally occurring fracture may be achieved in a mouse model by, for example, using the 3-point bending system described in other models [431]. Such models are attractive for certain studies, but will inevitably result in greater variability in the precise fracture created and potentially increase the loss of animals who may not develop a fracture that is fixable using a plating system. For the purposes of developing a standardised, reproducible model, the use of an osteotomy therefore provided the most appropriate means to generate a fracture.

When selecting the experimental mice for a bone healing study, several points such as gender, age and strain selection must also be carefully considered. We initially selected C57BL/6 for our studies as the MouseFix$^{TM}$ flexible plate had been previously used in this mouse strain. This allowed us to compare our data with the previously published literature and ensure that the different implant types would result in a mechanics-based difference *in vivo*. As C57BL/6 mice are known to be Th1-skewed (their T cells are more prone to produce Th1 cytokines such as IFN-γ, among other differences in their innate immune system [360, 432, 433]), we selected a second mouse inbred strain to provide a different background against which to compare our data. Therefore, we selected BALB/c mice as they are also widely used and their immune system is known to be Th2-

skewed [360]. BALB/c mice have been used less frequently in bone healing studies than C57BL/6 mice, and we have encountered certain difficulties in using this strain. For reasons that remain unknown to date, the healing of the osteotomy appeared inconsistent in BALB/c mice in our hands. We initially thought that this phenomenon may be due to the on-going infection, however, non-inoculated animals also displayed a similar healing pattern. Based on these observations, the selection of BALB/c mice for FRI studies should be made with caution in the future. With regards to the age of the mice, we have been working with mice more than 20 weeks old, as they are considered to be skeletally mature at this age. Although our main goal was to characterize immune responses towards infection, which may not be as affected by age as skeletal development, we think that the use of adult animals was more appropriate in the context of a study involving bone healing. It has been documented that young, adult and old mice differ with respect to bone healing, being delayed in middle-age but specially in old mice [434, 435]. Since bone healing and fracture mechanics are central factors in FRI, young animals did not seem an appropriate option, despite the time savings this would offer. An additional consideration in animal selection for these studies was the use of specific pathogen free (SPF) mice. Recent publications have highlighted the relevance of adaptive immunity in bone healing [28, 362] and it has been observed that different housing conditions (SPF vs. non-SPF) lead to differences in bone healing, potentially as a result of greater adaptive immune responses in non-SPF mice [369]. In further support of this theory, a paper by Beura *et al.* proposed that non-SPF housing that exposes animals to a more diverse microbial environment, leads to the generation of effector and memory T cells, which more closely resemble those of a human adult [436]. While it seems that the use of non-SPF mice might therefore be the better option, there are certain disadvantages and difficulties. Firstly, standardization might be more difficult, especially between animal facilities, as the environment complexity would be increased. Secondly, it remains unclear exactly which environmental conditions are key in achieving these characteristics. In addition, the use of non-SPF mice may encounter regulatory difficulties in some facilities where the use of SFP mice is preferred to avoid certain diseases outbreak. The final consideration in animal selection in these studies was gender. Females were used throughout the study, although in the latter stages males were also included, following the National Institute of Health recommendations [437]. Males displayed a more aggressive behaviour, requiring single-housing at times, and were more challenging to handle. We did not observe major differences in terms of bacteria clearance and CFU counts between the genders within the same group, although there were slightly different trends in some immune responses (e.g. cytokine production by splenocytes after antigen stimulation was higher in males). In future, it will likely become more commonplace to include both genders in animal studies; however, our data suggests that this may require an increase in total group sizes to account for greater variability between the genders.

With regards to the tested pathogen in these studies, we selected *S. epidermidis* as it is increasingly recognised as a prominent pathogen for all device related infections. Despite this, the literature on *S. epidermidis* FRI is limited [47]. We selected a clinical isolate rather than a laboratory strain for the model, which ensures clinical relevance. Laboratory strains of *S. epidermidis* are available, although as mentioned above, none had been included in an experimental FRI model prior to the start of this thesis. This isolate has since been submitted for whole genome sequencing and the culture has been deposited with the Swiss culture collection and will be available to other researchers in the field in the near future. The number of bacteria inoculated in this model is another crucial feature for discussion. Our infection model is based on a medium-low inoculum ($10^4$ CFU), which we believe more closely resembles what may actually colonise a wound intraoperatively than the higher inocula models described for other pathogens. Whilst high inocula may be more representative of open fractures, this is not likely to occur in all patients. Furthermore, a high inoculum is likely to result in a more significant acute infection which may trigger different immune responses, as observed in some preclinical studies evaluating the effect of infectious dose [348]. In our model, a *S. epidermidis* medium/low inoculum leads to a low-grade infection, similar to clinical manifestation of these bacteria. In addition, this dose allowed some animals to spontaneously clear infection. This indicates that this dose is on the threshold of what is possible for the mice to clear, and represents an ideal starting point for this study. This is because any slight modifications in the local biology (e.g. fracture healing and/or immune response due to changes in stability) may dictate whether the mice gets an infection or is able to clear the inoculum. In other respects, the low-grade infection that develops in this model actually represents a challenge as differences between groups are often minor. For example, results with *S. epidermidis* were strikingly different when compared with *S. aureus*. For *S. aureus*, greater clinical signs (such as higher weight loss) and greater tissue inflammation were observed, which often yields datasets with more pronounced differences, rather than the less virulent *S. epidermidis*. Of course, the increased inflammatory potential of *S. aureus* also leads to more tissue damage and high levels of osteolysis, thus reducing the time of the study for ethical reasons, and also removes the possibility to study the effect of mechanical differences. In general, the fact that *S. epidermidis* inoculation with low numbers of bacteria leads to an infection with few clinical or immunological signs, more closely recapitulate the challenges faced by these infections in real life.

## 6.3 Role of stability in infection

After successfully establishing the *S. epidermidis* FRI model, we subsequently used the model to investigate the role of fracture stability in infection progression. Clinically, it is believed that unstable fractures have a higher infection risk, however, this evidence is not based on large scale

clinical studies, with the only supportive data coming from poorly standardized models of *S. aureus* infection. As described above, a few studies in the past have addressed the role of stability in infections [332-334], however most of those studies presented major drawbacks, such as the lack of a reliable fixation system to determine stability or comparing fixed fractures versus non-fixed ones.

Our study provides the first standardized model that allows controlled conditions. In this first study (Results section 5.1), we evaluated the infection progression in the two different mechanical environments. We demonstrated that fracture stability was associated with a higher *S. epidermidis* infection clearance in C57BL/6N mice, and we observed the same effect in two independent experiments (Results section 5.1 and 5.2). For BALB/c mice, we observed that infection persisted for a longer time (with no clearance up to day 14), and no differences between stable and unstable groups were observed. These results highlight the relevance of host background and suggest that biomechanics are not the single critical feature in infection risk. Other studies with *S. epidermidis* foreign-body infection models have also found that BALB/c mice result in higher CFU counts and/or bigger abscesses compared to C57BL/6 equivalents [354, 355]. A possible reason for these observations, from an immunological perspective, is the fact that C57BL/6 mice are Th1-skewed and, from our data, Th1/Th17 responses may be important for bacteria clearance, as will be discussed below.

We aimed to repeat the study in *S. aureus;* however, we encountered some important limitations that precluded a reliable outcome. Severe osteolysis was observed around the screws of *S. aureus* infected animals, which rendered even the rigid plate unable to provide stability. The osteolysis is considered due to the significant tissue inflammation, the capacity of *S. aureus* to induce osteoclastogenesis [285-288] and its negative impact on osteoblast viability [278, 438, 439]. It remains to be determined therefore, whether stability can influence the progression of *S. aureus* infection. In order to provide a reliable test, alternative technologies would be required to guarantee stability despite ongoing osteolysis.

In future approaches, it would also be interesting to study if changes in mechanical stability within the experimental period (e.g. from flexible fixation to rigid fixation or *vice versa*) has an impact on the infection progression. Such data would be of high clinical relevance as it would provide evidence for the relative merits of the many different fixation options available to the modern trauma surgeon offering different mechanical fixation.

## 6.4 Immune responses associated with bone healing in differing mechanical environments

We used our model to study immune responses associated with fracture healing in different mechanical contexts. Flexible fixation (unstable construct) consistently resulted in higher levels of inflammation when compared to rigid fixation (more stable construct). This was found to be true for both mouse backgrounds and was observed at protein (e.g. IL-6 or G-CSF secretion) and mRNA expression levels (e.g. *Il6, Ccl2*, *Nos2*) at most time-points. Higher levels of inflammatory markers have also been found in the bone marrow of patients at higher risk of developing delayed bone healing or non-union (e.g. patients with autoimmune diseases, cancer) [382]. In combination, this suggests that excessive inflammation can negatively influence the healing process.

In addition, we also observed differences in inflammation between groups in the presence of infection. We observed that the combination of *S. epidermidis* infection and unstable fracture results in a significantly higher level of inflammation compared to the non-inoculated mice with flexible fixation. It could be hypothesized that excessive inflammation can impair immune responses towards bacteria. A possible mechanism could be through the licensing of mesenchymal stem cells (MSC) into an immunosuppressive phenotype, which only occur when MSC are exposed to sufficiently high levels of pro-inflammatory cytokines such as TNF-α or IFN-γ. Proposed mediators of this immunosuppressive role are nitric oxide, prostaglandin E2 or TGF-β, as well as cell-cell interaction [440, 441]. Among the immunosuppressive actions that MSC can exert, one can find: production of IL-10 by numerous cell types, reduction of antigen presentation by dendritic cells, lower proliferation of T cells or induction of Treg and B regulatory cells [441-443]. Although some of the markers associated with MSC immunosuppression function were increased in mice with a flexible implant (e.g. *Tgfb2* or *Nos2*), we did not observe obvious signs of immunosuppression, such as higher levels of IL-10 or lower proliferation of lymphocytes (although reduced proportions of CD8+ T cells in *S. epidermidis* inoculated flexible group and *S. aureus* inoculated groups could be associated to a reduced proliferation of this subset).In addition, some of the genes highly up-regulated in animals with a flexible implant and/or inoculated with *S. epidermidis* (e.g.*Nos2* or *Arg1*) are also associated with myeloid-derived suppressor cells (MDSC).Classically, MDSCs are defined as a heterogeneous population of immature monocytes and granulocytes with immunoregulatory properties [444]. They accumulate during different pathologies that are accompanied by inflammation [445-447]. MDSCs have been shown to contribute to *S. aureus* persistence in a murine model of orthopaedic-device associated infection, through the production of IL-10[300, 448, 449]. The role of MSCs and MDSCs would be an interesting field to explore. Both cell types present similar immunosuppression mechanisms [447], which would be interesting to

explore in future (for example by using IL-10 KO mice). Finally, tissue damage or hypoxia, which based on mRNA expression were increased in animals with a flexible implant (e.g. higher levels of *Il33* or *Hif1a*), may also contribute to the differences observed.

Due to the link between instability and higher inflammation, the model presented here could be used in future to observe the effect of anti-inflammatory drugs in bone healing and/or infection outcome. While inflammation is needed to initiate the healing cascade [450, 451], data suggests that excessive inflammation may have detrimental effects on bone healing [375, 377, 382]. Of note, in our model animals already receive acetaminophen (paracetamol) for 5 days in the drinking water; however this was equivalent for all groups. In addition, in a previous publication with rats, no delay in bone healing was observed after treating animals with acetaminophen for 10 days [452]. In humans, the prolonged use of non-steroidal anti-inflammatory drugs (NSAIDs) and COX-2 specific inhibitors has often been associated with delayed bone healing [453, 454] while the effect of short term usage is less clear [325, 455]. In preclinical studies, contradictory findings have also been reported [456]. Interestingly, Goodman *et al.* compared a short period (2 weeks) of COX-2 selective NSAID consumption versus long term consumption (6 weeks) in rabbits and observed that only the long term consumption impaired bone healing [457]. In general, there is still a need to understand the ideal inflammation timing and intensity for bone healing, which could be addressed in out model. Moreover, our data might suggest that excessive inflammation can be linked to lower bacterial clearance, which would be an interesting research question to pursue in future.

Another point to be discussed in the context of our studies is the role of IL-17A. IL-17A producing lymphocytes have been proposed to contribute to bone healing [32, 389]. In our experiments, IL-17A producing lymphocytes levels and *Il17a* mRNA expression were very low in the non-inoculated mice, suggesting no significant involvement for this cytokine in bone healing. However, we only studied animals from day 3, whereas many cytokines are secreted during the first 24 hours [18, 458], and so, a role for IL-17A in the immediate post-fracture period would still be possible. However, we performed histology in non-inoculated IL-17A KO mice and we did not observe major differences in terms of bone healing when comparing to WT. In both strains, osteotomies were closed at day 14, although techniques allowing quantification of bone formation (such as micro CT) should be used to confirm this histological observation. The exact role of IL-17A in bone healing is a matter of controversy also in the published literature: while some studies have shown a positive effect of this cytokine in supporting bone healing, contrasting data has shown that blocking of IL-17A in osteoporotic bone actually improved healing [459]. Further studies are required to more clearly define the role of IL-17A in bone healing, which could be pursued with the MouseFix$^{TM}$ system.

Finally, it would be interesting to combine mouse models with co-morbid conditions (such as obesity, diabetes, nicotine intake) in this FRI model, in order to evaluate if host condition and fracture instability may have a synergistic effect. This could elucidate if instability may lead to a worse prognosis in certain groups of patients, which are already at higher risk of infection [319, 460].

## 6.5 Immune responses associated with infection

Throughout our study, we observed that IL-17A was often up-regulated due to *S. epidermidis* infection (at mRNA and protein level). IL-17A is a cytokine from the IL-17 family, alongside IL-17B, IL-17C, IL-17D and IL-17F [396]. IL-17A, as a homodimer or as a heterodimer with IL-17F, signals through the IL-17A receptor. IL-17A is produced by Th17 lymphocytes, but also by γδ T cells, NK cells or neutrophils. In our model, upon infection, the main producers of IL-17A were found to be Th17 and γδ T cells. Among its main functions, IL-17A will recruit neutrophils and will induce the secretion of pro-inflammatory cytokines, orchestrating immune responses particularly in tissues with high bacterial exposure [461]. Upregulation of IL-17A has also been observed in a *S. aureus* FRI [296] and there is data suggesting that Th17 responses are important for *S. aureus* clearance in infection models of peritonitis or soft tissue infection [388, 392, 393, 462]. Much less is known regarding the role of IL-17A in *S. epidermidis* infections. In these studies, we have provided the first evidence that IL-17A contributes to the clearance of *S. epidermidis* infection, with higher percentage of culture negative animals in wild-type (WT) than IL-17A knock-out (KO) groups at all time-points studied. However, the lack of complete reversal in infection rate suggests that other mechanisms also contribute to infection resolution. A possible explanation may be that IL-17F would have compensated for the lack of IL-17A, suggesting that the use of an IL-17A/IL-17F double KO should be considered in future studies. Such double KO models have shown to result in greater differences (e.g. lower clearance in KO vs. the WT) than single KO in *S. aureus* nasal colonization models [394]. We were not able to detect IL-17F in the infected bone tissues, even in the KO mice, which suggest that in our system IL-17F may not play an important role. IL-22, which is also often secreted by IL-17A secreting cells, was also not detected. Interestingly, IFN-γ (Th1 responses) was significantly increased in KO mice compared to non-inoculated controls, suggesting that could compensate for IL-17A lack. In addition, IFN-γ administration has been shown by others to reduce bacterial load in a *S. epidermidis* foreign-body infection model [230]. Overall, it seems therefore that both Th17 and Th1 responses are required for infection clearance, although this should be confirmed in future studies by, for example, the use of double KO (e.g. IL-17A and IFN-γ KO) or blocking antibodies. Additionally, the therapeutic potential of cytokines, like IL-17A or IFN-γ, would also be of great interest to address. For example, IFN-γ has been

shown to increase *S. epidermidis* clearance in a subcutaneous DRI model [230]. However, due to the osteolytic potential of these cytokines, their therapeutic use in bone infections should be considered carefully.

The IL-17A KO study was only performed with rigid fixation. It remains an open question if bigger differences would be observed between WT and KO using the flexible implant, as a different inflammatory environment may influence the relative effect of IL-17A.In addition, it would be of interest to see if these observations can be also translated in humans. If the specific increased presence of IL-17A in bone marrow or infected tissues would hold true in patients, it could be used as a complementary tool, for example, to diagnose patients from whom bacteria cannot be isolated and have no obvious clinical signs (e.g. subclinical type of infections as often caused by *S. epidermidis*). Culture techniques are still the gold standard for diagnosis of trauma or arthroplasty infections. However, these techniques are time consuming (with some specimens taking several days to grow) and sometimes yield negative results due to non-cultivable bacteria, previous antibiotic therapy or samples collected where bacteria are not located. The detection of *IL17A* expression, together with other markers, may serve as an additional diagnostic tool that could be tested in humans. A similar proposal has already been used recently, to intraoperatively diagnose prosthetic joint infection patients, using an array of 12 genes [463]. The test, which included several immune markers such as TLRs or IFN-γ, was proven specific and quick to intraoperatively diagnose PJI patients, allowing the surgeon to take relevant decision regarding surgery and treatment. IL-17A was not included in this panel, but would be an interesting candidate to supplement the chosen genes. In addition, *S. epidermidis* is a usual contaminant of clinical samples due to its widespread presence, for this reason, at least 2culture positive biopsies are required for a more certain diagnostic [98]. Thus, molecular techniques addressing host parameters may complement tissue culture techniques in cases where contamination is suspected.

## 6.6 Role of Histamine 2 Receptor

In our initial studies investigating immune responses in the *S. epidermidis* FRI model, increased histamine 2 receptor ($H_2R$) mRNA expression was observed in *S. epidermidis* inoculated mice compared to non-inoculated. The role of $H_2R$ in infection is controversial. Cimetidine (a $H_2R$ antagonist) treatment reduced mortality in diabetic mice in a sepsis model (induced by cecum ligation and puncture) and histamine administration lead to a lower survival rate [401]. Contrasting with this, the same antagonist led to an increased mortality in a *Yersinia enterocolitica* infection model [402] and lead to higher morbidity in a peritonitis model [403]. Finally, the use of antihistamines (specifically $H_2R$ agonists) has been linked to an increased risk of *Clostridium*

infections or infection complications in severely injured patients [464, 465]. In the FRI model developed in this work, different immune responses were observed between WT and KO mouse strains, with higher pro-inflammatory cytokine levels (e.g. TNF-α) or anti-inflammatory cytokines (e.g. IL-10) and higher antibody levels in the $H_2R$ KO groups. This was not exclusively associated with the presence of bacteria, as this was also observed for non-inoculated mice. However, these differences did not lead to differences in terms of bacterial clearance. The earlier studies described in this thesis revealed that BALB/c mice display a slower clearance of infection, and so later time-points may provide further insight as to the exact role of $H_2R$. As it stands, our data suggest that $H_2R$ does not play a role in bacteria clearance in this model of FRI.

## 6.7 Impact of previous immunity in infection resolution

Arising from its status as a commensal microorganism, *S. epidermidis* is expected to elicit adaptive immune responses in humans from early in life. This has been proposed to be largely triggered by a pattern of transient self-resolving infections due to micro-invasions, rather than resulting from local responses due to colonization [246], but the latter cannot be excluded as shown in skin-colonization mouse models [188, 189]. These life-long interactions will lead to the generation of an antibody repertoire and a set of memory T and B cells that may be expected to confer partial protection from infection by *S. epidermidis*. Antibodies recognizing *S. epidermidis* proteins are present in healthy individuals, and in higher titres in infected patients [251, 255].

We induced adaptive immunity against *S. epidermidis* in mice, to study whether it influenced infection in our FRI model. In terms of clearance, we did not observe significant differences between saline and *S. epidermidis* pre-exposed mice, although there was a trend for lower CFU counts in the pre-exposed group. Of note, we did not observe as much clearance in WT C57BL/6 mice as in previously performed studies at the same time-point (Results section 5.1 and 5.2). The only significant difference was the subcutaneous injections and blood collection performed before surgery. In theory, this may also have influenced the results by increasing stress levels in animals. Is important to note that we used inactivated bacteria instead of live bacteria, which would have been a more potent stimulus. Non-viable bacteria were used due to ethical requirements as the animals had to undergo a surgical procedure after exposure and the combination of both procedures with live bacteria was considered too burdensome. The method used to prepare non-viable bacteria can also influence the type of immune responses induced, potentially by affecting protein structures and thus the recognition by pattern recognition receptors [466]. Thus, we preferred UV-inactivation in comparison to heat-inactivation, although we did not address the differences that may arise between this or other methods. Another point of discussion would be the administration route. As described

before, *S. epidermidis* immunity in humans is thought to arise from micro-invasions which most likely happen in the skin and superficial tissues, and that is why we chose to inject bacteria subcutaneously. Intradermal administration would be also an interesting approach, as will deliver bacteria to a site rich in antigen presenting cells (e.g. Langerhans cells) [467]. In future, longer-term exposure should be considered, ideally from early stages in life, in young mice [188]. In addition, live microbes, instead of UV-treated microbes, would be desirable as metabolically active bacteria may trigger different responses in the host. Finally, topical application has been shown useful to study the effect of *S. epidermidis* when colonizing the skin, in health or in diseases like atopic dermatitis [189, 468], and would be another interesting approach to understand how previous colonization may influence the results of our pre-clinical models when aiming to simulate clinical scenarios.

Finally, we have searched for the presence of *S. epidermidis* in mouse skin by means of culturing techniques using staphylococcal selective medium. However, it is known that such techniques tend to over-represent the most prevalent strains and/or strains with the faster growth rate. A more comprehensive analysis of murine skin with more specimens and combining different techniques such as 16s sequencing would be needed in other to achieve a better characterization of mouse microbiota. In addition, infection models with common mouse-skin colonizers (such as *S. xylosus* or *S. cohnii* based on our isolates) could represent an alternative approach to understand the impact of commensal strains in further infections occurring in the host.

Interestingly, as discussed above, it has been described that non-SPF mice can display slower fracture healing. This is believed to be due to the negative effect that some components of adaptive immunity (described at least for CD8+ T cells) have in bone healing. We did not observe differences in our pre-exposed animals compared to saline; although we did not perform measurements (such as micro CT or high resolution radiographs) to quantitatively evaluate bone healing. That would be something interesting to assess in addition to infection responses, and a study for which the model used in the present study would be particularly suitable.

## 6.8 Conclusion

In summary, this thesis presents a *S. epidermidis* fracture-related infection model, which results in a subclinical type of infection. Although this often leads to small differences (as observed when comparing cytokine secretion or mRNA expression in non-inoculated versus *S. epidermidis* inoculated mice), this matches the real-life clinical presentation of *S. epidermidis* infections. In any case, the model has been proven useful to evaluate the role of different parameters in infection clearance. Specifically, the role of fracture fixation, IL-17A, $H_2R$ and previous exposure to bacteria were addressed in our model. The data presented has provided some of the first data on FRI with this pathogen, and has opened up a wide range of experimental possibilities for future studies, as described above. The understanding of *S. epidermidis* FRI arising from this thesis has both clarified the clinical reality, providing some answers to long-held clinical beliefs, and further challenged our understanding of how infection can complicate the healing of fracture bones fixed with modern fracture fixation devices.

# 7. Acknowledgments

In the last years I had the pleasure to perform my PhD studies between the AO Research Institute Davos and the Swiss Institute of Allergy and Asthma Research. Although it was challenging sometimes, working between the two institutes gave me the chance to meet a lot of great people, offered me a lot of different experiences and was a good chance to be introduced to a broad range of techniques and fields.

In first place I would like to thank my supervisors, Dr. Fintan Moriarty (ARI) and Dr. Liam O'Mahony (SIAF) for giving me this opportunity 4 years and a half ago and for all the teaching and support through this journey. I am really thankful to Fintan for his dedication and patience with me; he was always encouraging me and ready to discuss anything. And also to Liam for his optimism and his interesting inputs through my PhD.

I also want to thank all the people in ARI and SIAF that helped me through the years. I think it was very valuable to work in such multidisciplinary and multicultural environments, in both institutes, and I appreciate the good atmosphere and the kindness of so many people around me. I would like to name some of them who specially contributed so that I can write these lines today. The Musculoskeletal Infection group with Iris (the pink "lab dragon", who makes fantastic Hugos but also teached me a lot in the lab), Pamela (and her patience to look for bacteria hours and hours!), Virginia, Barbara, Keith, Willemijn and all the fellows that joined us through the years (Christoph, Simon, Julian, Eri, Willem, Jan and Alejo).I learned a lot from all of them and I am very grateful. Also the team in my second house, the Molecular Immunology group in SIAF. A very special thanks to Mario, for being my co-pilot at the beginning and helping me to find my way. I enjoyed and also learnt a lot from the whole team: Remo, Ruth, David, Elisa, Noelia, Benoit, Marcin and… Wero <3.I also need to dedicate very special words to the Preclinical Facility team. I am very grateful to Katha and Corina, who were by my side all these years and worked very hard for the project. Also Zeiti, Tanja and Iska, for hundreds of surgeries and so many hours in the OR. And Dani, Linda, Karin, Patrizia, Fabian, Moni, Broneck, Nico, Christian, Phillip and all the students that came and went… the list is so long that I cannot name all of them! I also want to recognize the indispensable work of Urban and the animal caretakers: Andrea, Domi, Peter, Reto, Pierina and all others who helped me. And also a big thanks to the tissue morphology people: to Dirk for teaching me so much behind the microscope and to Nora and Mauro for introducing me to a histology lab. I always had so much fun there (despite the paraffin blocks)! I also want to thank people like Hide, Beate, Marietta or Milena for their advices and technical help.

I would like to thank Prof. Cezmi Akdis and Prof. Geoff Richards for their support, and also the other members in my PhD committee: Prof. Roland Wenger and Prof. Georgios Belibasakis for meaningful discussions in our committee meetings.

Last but not least, living in Davos was much more than working in the laboratory. I met a lot of nice people that made my life in Davos more enjoyable. Friends with who I spent hours in the slopes (non-properly skiing or learning to snowboard), running or even climbing. Friends with who I spent even more hours in the bar, learning/dancing tango in Ella's or doing barbecue in Budag (it all starts with a good barbecue, right?). Friends with who I travelled around the world. Friends like Janek (thanks for always helping!), Adriano, Fabian, Alexandra, Ugo (il mio ballerino) and Fatemeh, lovely couples like Ryan and Sarah or Lukas and IngIng with who I shared one of the most important day of their lives; and many other friends like Steph, Yabin, Kerstin, Walter, Gaston, Fabri and Gil (the duo dinamico), Ivan, Matteo, Rihanne, Stijn, Fede (the best guy in Torino), Koen, Leti, Lisanne, Bettina, all the adventure drinkers from SIAF…

And I loved being member of the lunch group. It was always a nice feeling to have a delicious, ready-made meal on the table, and some friends around to relax. A lot of them appeared already, but we were so many through the years: Ying, Tino, Shan, Marta, Adrian, Silvia, Felix, Rose, Inesa, Mitko, Robert, Edu, Zahira, Mike, Anna, Simona, Marc and even some others.

There are some people that became my special ones. Arturo and Weronika, my SIAF dream team, always full of emotions and adrenaline. And my AO family: Ana, Dalila and GJ. From the beginning the 4 of us. Without you I would have not made it!

Last but not least, the worst think of going abroad is that you need to leave people behind. But despite that, they were and are always there. I had some very good friends back home that were always ready to have a Skype call or to exchange some messages when the day was not so good. Also my wonderful family, an example to me and a support that is always there. Isaac, my partner in life, who decided to be with me even if 1000 km would be between us. And my parents, who gave me everything in this life.

Moltes gràcies
Muchas gracias
Thanks a lot
Danke viel mal

# 8. References


1. Court-Brown, C.M. and B. Caesar, *Epidemiology of adult fractures: A review.* Injury, 2006. **37**(8): p. 691-7.
2. W.H.O., *The burden of musculoskeletal conditions at the start of the new millennium.* World Health Organ Tech Rep Ser, 2003. **919**: p. i-x, 1-218, back cover.
3. Mock, C. and M.N. Cherian, *The global burden of musculoskeletal injuries: challenges and solutions.* Clin Orthop Relat Res, 2008. **466**(10): p. 2306-16.
4. Beveridge, M. and A. Howard, *The burden of orthopaedic disease in developing countries.* J Bone Joint Surg Am, 2004. **86-A**(8): p. 1819-22.
5. Sumner-Smith, G., *Bone in Clinical Orthopedics - Second enhanced edition*. 2 ed. 2002, Stuttgart: AO Publishing / Thieme.
6. Smith, G.E., *The Most Ancient Splints.* Br Med J, 1908. **1**(2465): p. 732-736 2.
7. Bartonicek, J., *Early history of operative treatment of fractures.* Arch Orthop Trauma Surg, 2010. **130**(11): p. 1385-96.
8. Browner, B.D., et al., *Skeletal Trauma E-Book: 2-Volume Set*. 2008: Elsevier Health Sciences.
9. Rüedi, T.P., Buckley, Richard E., Moran, Christopher G. , *AO Principles of Fracture Management*. 2nd Edition ed. 2007: AO Publishing.
10. Schell, H., et al., *The haematoma and its role in bone healing.* J Exp Orthop, 2017. **4**(1): p. 5.
11. Marsell, R. and T.A. Einhorn, *The biology of fracture healing.* Injury, 2011. **42**(6): p. 551-5.
12. Rahn, B.A., et al., *Primary bone healing. An experimental study in the rabbit.* J Bone Joint Surg Am, 1971. **53**(4): p. 783-6.
13. Kolar, P., et al., *The early fracture hematoma and its potential role in fracture healing.* Tissue Eng Part B Rev, 2010. **16**(4): p. 427-34.
14. Park, S.H., et al., *Effect of repeated irrigation and debridement on fracture healing in an animal model.* J Orthop Res, 2002. **20**(6): p. 1197-204.
15. Kolaczkowska, E. and P. Kubes, *Neutrophil recruitment and function in health and inflammation.* Nat Rev Immunol, 2013. **13**(3): p. 159-75.
16. Bastian, O.W., et al., *Neutrophils contribute to fracture healing by synthesizing fibronectin+ extracellular matrix rapidly after injury.* Clin Immunol, 2016. **164**: p. 78-84.
17. Gerstenfeld, L.C., et al., *Fracture healing as a post-natal developmental process: molecular, spatial, and temporal aspects of its regulation.* J Cell Biochem, 2003. **88**(5): p. 873-84.
18. Schmidt-Bleek, K., et al., *Boon and Bane of Inflammation in Bone Tissue Regeneration and Its Link with Angiogenesis.* Tissue Eng Part B Rev, 2015.
19. Lorenzo, J., *Osteoimmunology : interactions of the immune and skeletal systems*. 1st ed. 2011, Amsterdam ; Boston: Academic. xiii, 453 p., 20 p. of plates.
20. Einhorn, T.A. and L.C. Gerstenfeld, *Fracture healing: mechanisms and interventions.* Nat Rev Rheumatol, 2015. **11**(1): p. 45-54.
21. Giannoudis, P.V., T.A. Einhorn, and D. Marsh, *Fracture healing: a harmony of optimal biology and optimal fixation?* Injury, 2007. **38 Suppl 4**: p. S1-S2.
22. Giannoudis, P.V., et al., *The diamond concept--open questions.* Injury, 2008. **39 Suppl 2**: p. S5-8.
23. Alford, A.I., K.M. Kozloff, and K.D. Hankenson, *Extracellular matrix networks in bone remodeling.* Int J Biochem Cell Biol, 2015. **65**: p. 20-31.
24. Caetano-Lopes, J., H. Canhao, and J.E. Fonseca, *Osteoblasts and bone formation.* Acta Reumatol Port, 2007. **32**(2): p. 103-10.
25. Khurana, J.S., *Bone pathology*. 2nd ed. 2009, Dordrecht ; New York: Humana Press. xiii, 416 p.
26. Schlundt, C., et al., *Macrophages in bone fracture healing: Their essential role in endochondral ossification.* Bone, 2015.
27. Raggatt, L.J., et al., *Fracture healing via periosteal callus formation requires macrophages for both initiation and progression of early endochondral ossification.* Am J Pathol, 2014. **184**(12): p. 3192-204.
28. Toben, D., et al., *Fracture healing is accelerated in the absence of the adaptive immune system.* J Bone Miner Res, 2011. **26**(1): p. 113-24.
29. Nam, D., et al., *T-lymphocytes enable osteoblast maturation via IL-17F during the early phase of fracture repair.* PLoS One, 2012. **7**(6): p. e40044.
30. Reinke, S., et al., *Terminally differentiated CD8(+) T cells negatively affect bone regeneration in humans.* Sci Transl Med, 2013. **5**(177): p. 177ra36.
31. Sun, G., et al., *Regulatory B cell is critical in bone union process through suppressing proinflammatory cytokines and stimulating Foxp3 in Treg cells.*Clin Exp Pharmacol Physiol, 2017. **44**(4): p. 455-462.

32. Ono, T., et al., *IL-17-producing gammadelta T cells enhance bone regeneration.*Nat Commun, 2016. **7**: p. 10928.
33. Colburn, N.T., et al., *A role for gamma/delta T cells in a mouse model of fracture healing.* Arthritis Rheum, 2009. **60**(6): p. 1694-703.
34. Giannoudis, P.V., T.A. Einhorn, and D. Marsh, *Fracture healing: the diamond concept.* Injury, 2007. **38 Suppl 4**: p. S3-S6.
35. Ono, T. and H. Takayanagi, *Osteoimmunology in Bone Fracture Healing.* Curr Osteoporos Rep, 2017.
36. Claes, L., S. Recknagel, and A. Ignatius, *Fracture healing under healthy and inflammatory conditions.* Nat Rev Rheumatol, 2012. **8**(3): p. 133-43.
37. El-Jawhari, J.J., E. Jones, and P.V. Giannoudis, *The roles of immune cells in bone healing; what we know, do not know and future perspectives.* Injury, 2016. **47**(11): p. 2399-2406.
38. Tsiridis, E., N. Upadhyay, and P. Giannoudis, *Molecular aspects of fracture healing: which are the important molecules?* Injury, 2007. **38 Suppl 1**: p. S11-25.
39. Lacroix, D. and P.J. Prendergast, *A mechano-regulation model for tissue differentiation during fracture healing: analysis of gap size and loading.* J.Biomech., 2002. **35**(9): p. 1163-1171.
40. Klein-Nulend, J., R.G. Bacabac, and M.G. Mullender, *Mechanobiology of bone tissue.* Pathol Biol (Paris), 2005. **53**(10): p. 576-80.
41. Lacroix, D., et al., *Biomechanical model to simulate tissue differentiation and bone regeneration: application to fracture healing.* Med Biol Eng Comput, 2002. **40**(1): p. 14-21.
42. Willie, B.M., et al., *Cancellous bone osseointegration is enhanced by in vivo loading.* Tissue Eng Part C Methods, 2010. **16**(6): p. 1399-406.
43. Bastian, O., et al., *Systemic inflammation and fracture healing.* J.Leukoc.Biol., 2011. **89**(5): p. 669-673.
44. Dimitriou, R., E. Tsiridis, and P.V. Giannoudis, *Current concepts of molecular aspects of bone healing.* Injury, 2005. **36**(12): p. 1392-1404.
45. Moriarty, T.F., et al., *Orthopaedic device-related infection: current and future interventions for improved prevention and treatment.* EFORT Open Rev, 2016. **1**(4): p. 89-99.
46. Morgenstern, M., et al., *Antibiotic Resistance of Commensal Staphylococcus aureus and Coagulase-Negative Staphylococci in an International Cohort of Surgeons: A Prospective Point-Prevalence Study.* PLoS One, 2016. **11**(2): p. e0148437.
47. Widerstrom, M., *Significance of Staphylococcus epidermidis in Health Care-Associated Infections, from Contaminant to Clinically Relevant Pathogen: This Is a Wake-Up Call!* J Clin Microbiol, 2016. **54**(7): p. 1679-81.
48. Otto, M., *Staphylococcus epidermidis--the 'accidental' pathogen.* Nat Rev Microbiol, 2009. **7**(8): p. 555-67.
49. Montanaro, L., et al., *Scenery of Staphylococcus implant infections in orthopedics.* Future Microbiol, 2011. **6**(11): p. 1329-49.
50. Hogan, S., et al., *Current and future approaches to the prevention and treatment of staphylococcal medical device-related infections.* Curr Pharm Des, 2015. **21**(1): p. 100-13.
51. Rogers, K.L., P.D. Fey, and M.E. Rupp, *Coagulase-negative staphylococcal infections.* Infect Dis Clin North Am, 2009. **23**(1): p. 73-98.
52. Darouiche, R.O., *Treatment of infections associated with surgical implants.* N Engl J Med, 2004. **350**(14): p. 1422-9.
53. Brown, R.L. and T.B. Clarke, *The regulation of host defences to infection by the microbiota.* Immunology, 2017. **150**(1): p. 1-6.
54. Collado, M.C., et al., *Human gut colonisation may be initiated in utero by distinct microbial communities in the placenta and amniotic fluid.* Sci Rep, 2016. **6**: p. 23129.
55. Jimenez, E., et al., *Is meconium from healthy newborns actually sterile?* Res Microbiol, 2008. **159**(3): p. 187-93.
56. Dominguez-Bello, M.G., et al., *Delivery mode shapes the acquisition and structure of the initial microbiota across multiple body habitats in newborns.* Proc Natl Acad Sci U S A, 2010. **107**(26): p. 11971-5.
57. Grice, E.A., et al., *Topographical and temporal diversity of the human skin microbiome.* Science, 2009. **324**(5931): p. 1190-2.
58. Majchrzak, K., et al., *Comparison of Staphylococcal Flora in Denture Plaque and the Surface of the Pharyngeal Mucous Membrane in Kidney Transplant Recipients.* Transplant Proc, 2016. **48**(5): p. 1590-7.
59. Sharon, I., et al., *Time series community genomics analysis reveals rapid shifts in bacterial species, strains, and phage during infant gut colonization.* Genome Res, 2013. **23**(1): p. 111-20.
60. Coates, R., J. Moran, and M.J. Horsburgh, *Staphylococci: colonizers and pathogens of human skin.* Future Microbiol, 2014. **9**(1): p. 75-91.
61. N'Diaye, A.R., et al., *Skin-bacteria communication: Involvement of the neurohormone Calcitonin Gene Related Peptide (CGRP) in the regulation of Staphylococcus epidermidis virulence.* Sci Rep, 2016. **6**: p. 35379.

62. Li, M., et al., *Gram-positive three-component antimicrobial peptide-sensing system.* Proc Natl Acad Sci U S A, 2007. **104**(22): p. 9469-74.
63. Joo, H.S. and M. Otto, *Mechanisms of resistance to antimicrobial peptides in staphylococci.* Biochim Biophys Acta, 2015. **1848**(11 Pt B): p. 3055-61.
64. Lai, Y., et al., *The human anionic antimicrobial peptide dermcidin induces proteolytic defence mechanisms in staphylococci.* Mol Microbiol, 2007. **63**(2): p. 497-506.
65. Hirai, Y., *Survival of bacteria under dry conditions; from a viewpoint of nosocomial infection.* J Hosp Infect, 1991. **19**(3): p. 191-200.
66. Amin, U.S., T.D. Lash, and B.J. Wilkinson, *Proline betaine is a highly effective osmoprotectant for Staphylococcus aureus.* Arch Microbiol, 1995. **163**(2): p. 138-42.
67. Park, B., T. Iwase, and G.Y. Liu, *Intranasal application of S. epidermidis prevents colonization by methicillin-resistant Staphylococcus aureus in mice.* PLoS One, 2011. **6**(10): p. e25880.
68. Iwase, T., et al., *Staphylococcus epidermidis Esp inhibits Staphylococcus aureus biofilm formation and nasal colonization.* Nature, 2010. **465**(7296): p. 346-9.
69. Frank, D.N., et al., *The human nasal microbiota and Staphylococcus aureus carriage.* PLoS One, 2010. **5**(5): p. e10598.
70. Sullivan, S.B., et al., *Staphylococcus epidermidis Protection Against Staphylococcus aureus Colonization in People Living With Human Immunodeficiency Virus in an Inner-City Outpatient Population: A Cross-Sectional Study.* Open Forum Infect Dis, 2016. **3**(4): p. ofw234.
71. Christensen, G.J., et al., *Antagonism between Staphylococcus epidermidis and Propionibacterium acnes and its genomic basis.* BMC Genomics, 2016. **17**: p. 152.
72. Janek, D., et al., *High Frequency and Diversity of Antimicrobial Activities Produced by Nasal Staphylococcus Strains against Bacterial Competitors.* PLoS Pathog, 2016. **12**(8): p. e1005812.
73. Otto, M., *Phenol-soluble modulins.* Int J Med Microbiol, 2014. **304**(2): p. 164-9.
74. Wang, R., et al., *Staphylococcus epidermidis surfactant peptides promote biofilm maturation and dissemination of biofilm-associated infection in mice.* J Clin Invest, 2011. **121**(1): p. 238-48.
75. Cogen, A.L., et al., *Staphylococcus epidermidis antimicrobial delta-toxin (phenol-soluble modulin-gamma) cooperates with host antimicrobial peptides to kill group A Streptococcus.* PLoS One, 2010. **5**(1): p. e8557.
76. Cogen, A.L., et al., *Selective antimicrobial action is provided by phenol-soluble modulins derived from Staphylococcus epidermidis, a normal resident of the skin.* J Invest Dermatol, 2010. **130**(1): p. 192-200.
77. Dhople, V.M. and R. Nagaraj, *Conformation and activity of delta-lysin and its analogs.* Peptides, 2005. **26**(2): p. 217-25.
78. Dhople, V.M. and R. Nagaraj, *Delta-toxin, unlike melittin, has only hemolytic activity and no antimicrobial activity: rationalization of this specific biological activity.* Biosci Rep, 1993. **13**(4): p. 245-50.
79. Bastos, M.C., et al., *Staphylococcal antimicrobial peptides: relevant properties and potential biotechnological applications.* Curr Pharm Biotechnol, 2009. **10**(1): p. 38-61.
80. Hassan, M., et al., *Natural antimicrobial peptides from bacteria: characteristics and potential applications to fight against antibiotic resistance.* J Appl Microbiol, 2012. **113**(4): p. 723-36.
81. Allgaier, H., et al., *Epidermin: sequencing of a heterodetic tetracyclic 21-peptide amide antibiotic.* Eur J Biochem, 1986. **160**(1): p. 9-22.
82. van de Kamp, M., et al., *Sequence analysis by NMR spectroscopy of the peptide lantibiotic epilancin K7 from Staphylococcus epidermidis K7.* Eur J Biochem, 1995. **227**(3): p. 757-71.
83. Ekkelenkamp, M.B., et al., *Isolation and structural characterization of epilancin 15X, a novel lantibiotic from a clinical strain of Staphylococcus epidermidis.* FEBS Lett, 2005. **579**(9): p. 1917-22.
84. Sandiford, S. and M. Upton, *Identification, characterization, and recombinant expression of epidermicin NI01, a novel unmodified bacteriocin produced by Staphylococcus epidermidis that displays potent activity against Staphylococci.* Antimicrob Agents Chemother, 2012. **56**(3): p. 1539-47.
85. Bennallack, P.R., et al., *Characterization of a novel plasmid-borne thiopeptide gene cluster in Staphylococcus epidermidis strain 115.* J Bacteriol, 2014. **196**(24): p. 4344-50.
86. Sugimoto, S., et al., *Staphylococcus epidermidis Esp degrades specific proteins associated with Staphylococcus aureus biofilm formation and host-pathogen interaction.* J Bacteriol, 2013. **195**(8): p. 1645-55.
87. Wang, Y., et al., *Staphylococcus epidermidis in the human skin microbiome mediates fermentation to inhibit the growth of Propionibacterium acnes: implications of probiotics in acne vulgaris.* Appl Microbiol Biotechnol, 2014. **98**(1): p. 411-24.
88. Bjorkqvist, M., et al., *Colonization pattern of coagulase-negative staphylococci in preterm neonates and the relation to bacteremia.* Eur J Clin Microbiol Infect Dis, 2010. **29**(9): p. 1085-93.
89. Dong, Y. and C.P. Speer, *The role of Staphylococcus epidermidis in neonatal sepsis: guarding angel or pathogenic devil?* Int J Med Microbiol, 2014. **304**(5-6): p. 513-20.

90. Gill, S.R., et al., *Insights on evolution of virulence and resistance from the complete genome analysis of an early methicillin-resistant Staphylococcus aureus strain and a biofilm-producing methicillin-resistant Staphylococcus epidermidis strain.* J Bacteriol, 2005. **187**(7): p. 2426-38.
91. Heilmann, C. and F. Gotz, *Staphylococcal Viruelnce Factors*. Biomaterials Associated Infections: Immunological Aspects and Antimicrobial Strategies. 2013, New York: Springer. 57-86.
92. Trampuz, A. and W. Zimmerli, *Prosthetic joint infections: update in diagnosis and treatment.* Swiss Med Wkly, 2005. **135**(17-18): p. 243-51.
93. Trampuz, A. and W. Zimmerli, *Diagnosis and treatment of infections associated with fracture-fixation devices.* Injury, 2006. **37 Suppl 2**: p. S59-66.
94. Schafer, P., et al., *Prolonged bacterial culture to identify late periprosthetic joint infection: a promising strategy.* Clin Infect Dis, 2008. **47**(11): p. 1403-9.
95. Melzer, M., et al., *Is methicillin-resistant Staphylococcus aureus more virulent than methicillin-susceptible S. aureus? A comparative cohort study of British patients with nosocomial infection and bacteremia.* Clin Infect Dis, 2003. **37**(11): p. 1453-60.
96. Shurland, S., et al., *Comparison of mortality risk associated with bacteremia due to methicillin-resistant and methicillin-susceptible Staphylococcus aureus.* Infect Control Hosp Epidemiol, 2007. **28**(3): p. 273-9.
97. Zimmerli, W., A. Trampuz, and P.E. Ochsner, *Prosthetic-joint infections.* N Engl J Med, 2004. **351**(16): p. 1645-54.
98. Metsemakers, W.J., et al., *Infection after fracture fixation: Current surgical and microbiological concepts.* Injury, 2016.
99. Costerton, J.W., et al., *New methods for the detection of orthopedic and other biofilm infections.* Fems Immunology and Medical Microbiology, 2011. **61**(2): p. 133-140.
100. Xu, Y., et al., *Microbiological diagnosis of device-related biofilm infections.* APMIS, 2017. **125**(4): p. 289-303.
101. Trampuz, A., et al., *Sonication of removed hip and knee prostheses for diagnosis of infection.* New England Journal of Medicine, 2007. **357**(7): p. 654-663.
102. Puig-Verdie, L., et al., *Implant sonication increases the diagnostic accuracy of infection in patients with delayed, but not early, orthopaedic implant failure.* Bone & Joint Journal, 2013. **95B**(2): p. 244-249.
103. Yano, M.H., et al., *Improved Diagnosis of Infection Associated with Osteosynthesis by Use of Sonication of Fracture Fixation Implants.* Journal of Clinical Microbiology, 2014. **52**(12): p. 4176-4182.
104. Dapunt, U., et al., *Are atrophic long-bone nonunions associated with low-grade infections?* Ther Clin Risk Manag, 2015. **11**: p. 1843-52.
105. Osmon, D.R., et al., *Diagnosis and management of prosthetic joint infection: clinical practice guidelines by the Infectious Diseases Society of America.* Clin Infect Dis, 2013. **56**(1): p. e1-e25.
106. Patzakis, M.J. and C.G. Zalavras, *Chronic posttraumatic osteomyelitis and infected nonunion of the tibia: current management concepts.* J Am Acad Orthop Surg, 2005. **13**(6): p. 417-27.
107. Teterycz, D., et al., *Outcome of orthopedic implant infections due to different staphylococci.* Int J Infect Dis, 2010. **14**(10): p. e913-8.
108. Salgado, C.D., et al., *Higher risk of failure of methicillin-resistant Staphylococcus aureus prosthetic joint infections.* Clin Orthop Relat Res, 2007. **461**: p. 48-53.
109. Morgenstern, M., et al., *Staphylococcal orthopaedic device-related infections in older patients.* Injury, 2016. **47**(7): p. 1427-34.
110. Morgenstern, M., et al., *Biofilm formation increases treatment failure in Staphylococcus epidermidis device-related osteomyelitis of the lower extremity in human patients.* J Orthop Res, 2016.
111. Gristina, A., *Biomaterial-centered infection: microbial adhesion versus tissue integration.* Science, 1987. **237**: p. 1588-1595.
112. Heilmann, C., et al., *Evidence for autolysin-mediated primary attachment of Staphylococcus epidermidis to a polystyrene surface.* Mol. Microbiol., 1997. **24**(5): p. 1013-1024.
113. Qin, Z., et al., *Role of autolysin-mediated DNA release in biofilm formation of Staphylococcus epidermidis.* Microbiology, 2007. **153**(7): p. 2083-2092.
114. Izano, E.A., et al., *Differential roles of poly-N-acetylglucosamine surface polysaccharide and extracellular DNA in Staphylococcus aureus and Staphylococcus epidermidis biofilms.* Appl. Environ. Microbiol., 2008. **74**(2): p. 470-476.
115. Veenstra, G., et al., *Ultrastructural organization and regulation of a biomaterial adhesin of Staphylococcus epidermidis.* J. Bacteriol., 1996. **178**(2): p. 537-541.
116. Baier, R.E., et al., *Surface properties determine bioadhesive outcomes: methods and results.* J. Biomed. Mater. Res., 1984. **18**(4): p. 327-355.
117. Foster, T.J. and M. Hook, *Surface protein adhesins of Staphylococcus aureus.* Trend Microbiol, 1998. **6**(12): p. 484-488.

118. Brennan, M.P., et al., *Elucidating the role of Staphylococcus epidermidis serine-aspartate repeat protein G in platelet activation.* J Thromb Haemost, 2009. **7**(8): p. 1364-72.
119. Hartford, O., et al., *The Fbe (SdrG) protein of Staphylococcus epidermidis HB promotes bacterial adherence to fibrinogen.* Microbiology, 2001. **147**(9): p. 2545-2552.
120. Arciola, C.R., et al., *Staphylococcus epidermidis-fibronectin binding and its inhibition by heparin.* Biomaterials, 2003. **24**(18): p. 3013-9.
121. Bowden, M.G., et al., *Is the GehD Lipase from Staphylococcus epidermidis a Collagen Binding Adhesin?* J. Biol. Chem., 2002. **277**(45): p. 43017-43023.
122. Arrecubieta, C., et al., *SdrF, a Staphylococcus epidermidis Surface Protein, Binds Type I Collagen.* J. Biol. Chem., 2007. **282**(26): p. 18767-18776.
123. Heilmann, C., et al., *Identification and characterization of a novel autolysin (Aae) with adhesive properties from Staphylococcus epidermidis.* Microbiology, 2003. **149**(10): p. 2769-2778.
124. Hussain, M., et al., *Teichoic acid enhances adhesion of Staphylococcus epidermidis to immobilized fibronectin.* Microbial Pathogenesis, 2001. **31**(6): p. 261-270.
125. Chugh, T.D., et al., *Adherence of Staphylococcus epidermidis to fibrin-platelet clots in vitro mediated by lipoteichoic acid.* Infect Immun, 1990. **58**(2): p. 315-9.
126. Myrvik, Q.N., et al., *Effects of extracellular slime produced by Staphylococcus epidermidis on oxidative responses of rabbit alveolar macrophages.* J Invest Surg, 1989. **2**(4): p. 381-9.
127. Kristian, S.A., et al., *Biofilm formation induces C3a release and protects Staphylococcus epidermidis from IgG and complement deposition and from neutrophil-dependent killing.* J Infect Dis, 2008. **197**(7): p. 1028-35.
128. Cerca, F., et al., *Staphylococcus epidermidis biofilms with higher proportions of dormant bacteria induce a lower activation of murine macrophages.* J Med Microbiol, 2011. **60**(Pt 12): p. 1717-24.
129. Schommer, N.N., et al., *Staphylococcus epidermidis uses distinct mechanisms of biofilm formation to interfere with phagocytosis and activation of mouse macrophage-like cells 774A.1.* Infect Immun, 2011. **79**(6): p. 2267-76.
130. Mack, D., et al., *Biofilm formation in medical device-related infection.* Int J Artif Organs, 2006. **29**: p. 343 -359.
131. Cerca, N., et al., *Comparative antibody-mediated phagocytosis of Staphylococcus epidermidis cells grown in a biofilm or in the planktonic state.* Infect Immun, 2006. **74**(8): p. 4849-55.
132. Moriarty, T.F., et al., *4.407 - Bacterial Adhesion and Biomaterial Surfaces A2 - Ducheyne, Paul*, in *Comprehensive Biomaterials*. 2011, Elsevier: Oxford. p. 75-100.
133. Costerton, J.W., et al., *Microbial biofilms.* Annu Rev Microbiol, 1995. **49**: p. 711-745.
134. Heilmann, C., et al., *Molecular basis of intercellular adhesion in the biofilm-forming Staphylococcus epidermidis.* Mol. Microbiol., 1996. **20**(5): p. 1083-1091.
135. Mack, D., et al., *The intercellular adhesin involved in biofilm accumulation of Staphylococcus epidermidis is a linear beta-1,6-linked glucosaminoglycan: purification and structural analysis.* J. Bacteriol., 1996. **178**(1): p. 175-183.
136. Mack, D., et al., *Association of biofilm production of coagulase-negative staphylococci with expression of a specific polysaccharide intercellular adhesin.* J Infect Dis, 1996. **174**(4): p. 881-4.
137. Chokr, A., et al., *Neither the presence of ica locus, nor in vitro-biofilm formation ability is a crucial parameter for some Staphylococcus epidermidis strains to maintain an infection in a guinea pig tissue cage model.* Microb Pathog, 2007. **42**(2-3): p. 94-7.
138. Zhang, Y.-Q., et al., *Genome-based analysis of virulence genes in a non-biofilm-forming Staphylococcus epidermidis strain (ATCC 12228).* Molecular Microbiology, 2003. **49**(6): p. 1577-1593.
139. Harris, L.G., et al., *Biofilm Morphotypes and Population Structure among Staphylococcus epidermidis from Commensal and Clinical Samples.* PLoS One, 2016. **11**(3): p. e0151240.
140. Rohde, H., et al., *Induction of Staphylococcus epidermidis biofilm formation via proteolytic processing of the accumulation-associated protein by staphylococcal and host proteases.* Mol. Microbiol., 2005. **55**(6): p. 1883-1895.
141. Gill, S.R., et al., *Insights on evolution of virulence and resistance from the complete genome analysis of an early methicillin-resistant Staphylococcus aureus strain and a biofilm-producing methicillin-resistant Staphylococcus epidermidis strain.* J. Bacteriol., 2005. **187**(7): p. 2426-2438.
142. Los, R., et al., *A comparative analysis of phenotypic and genotypic methods for the determination of the biofilm-forming abilities of Staphylococcus epidermidis.* FEMS Microbiol Lett, 2010. **310**(2): p. 97-103.
143. Bowden, M.G., et al., *Identification and preliminary characterization of cell-wall-anchored proteins of Staphylococcus epidermidis.* Microbiology, 2005. **151**(Pt 5): p. 1453-64.
144. Tormo, M.A., et al., *Bap-dependent biofilm formation by pathogenic species of Staphylococcus: evidence of horizontal gene transfer?* Microbiology, 2005. **151**(Pt 7): p. 2465-75.
145. Christner, M., et al., *The giant extracellular matrix-binding protein of Staphylococcus epidermidis mediates biofilm accumulation and attachment to fibronectin.* Mol. Microbiol., 2010. **75**(1): p. 187-207.

146. Williams, R.J., et al., *Identification of a Fibronectin-Binding Protein from Staphylococcus epidermidis.* Infect. Immun., 2002. **70**(12): p. 6805-6810.
147. Shahrooei, M., et al., *Inhibition of Staphylococcus epidermidis Biofilm Formation by Rabbit Polyclonal Antibodies against the SesC Protein.* Infect. Immun., 2009. **77**(9): p. 3670-3678.
148. Rohde, H., et al., *Polysaccharide intercellular adhesin or protein factors in biofilm accumulation of Staphylococcus epidermidis and Staphylococcus aureus isolated from prosthetic hip and knee joint infections.* Biomaterials, 2007. **28**(9): p. 1711-1720.
149. Holland, L.M., B. Conlon, and J.P. O'Gara, *Mutation of tagO reveals an essential role for wall teichoic acids in Staphylococcus epidermidis biofilm development.* Microbiology, 2011. **157**(Pt 2): p. 408-18.
150. Xu, L., et al., *Role of the luxS Quorum-Sensing System in Biofilm Formation and Virulence of Staphylococcus epidermidis.* Infect. Immun., 2006. **74**(1): p. 488-496.
151. Knobloch, J.K.-M., et al., *RsbU-dependent regulation of Staphylococcus epidermidis biofilm formation is mediated via the alternative sigma factor sigmaB by repression of the negative regulator gene icaR.* Infect. Immun., 2004. **72**(7): p. 3838-3848.
152. Christner, M., et al., *sarA negatively regulates Staphylococcus epidermidis biofilm formation by modulating expression of 1 MDa extracellular matrix binding protein and autolysis-dependent release of eDNA.* Mol Microbiol, 2012. **86**(2): p. 394-410.
153. Vuong, C., et al., *Quorum-sensing control of biofilm factors in Staphylococcus epidermidis.* J. Infect. Dis., 2003. **188**: p. 706-718.
154. Al-Ishaq, R., et al., *Effects of polysaccharide intercellular adhesin (PIA) in an ex vivo model of whole blood killing and in prosthetic joint infection (PJI): A role for C5a.* Int J Med Microbiol, 2015. **305**(8): p. 948-56.
155. Satorius, A.E., et al., *Complement c5a generation by staphylococcal biofilms.* Shock, 2013. **39**(4): p. 336-42.
156. Vuong, C., et al., *A crucial role for exopolysaccharide modification in bacterial biofilm formation, immune evasion, and virulence.* J. Biol. Chem., 2004. **279**(52): p. 54881-54886.
157. Vuong, C., et al., *Polysaccharide intercellular adhesin (PIA) protects Staphylococcus epidermidis against major components of the human innate immune system.* Cell Microbiol., 2004. **6**(3): p. 269-275.
158. Otto, M., *Bacterial evasion of antimicrobial peptides by biofilm formation.* Curr Top Microbiol Immunol, 2006. **306**: p. 251-8.
159. Ferreirinha, P., et al., *Poly-N-Acetylglucosamine Production by Staphylococcus epidermidis Cells Increases Their In Vivo Proinflammatory Effect.* Infect Immun, 2016. **84**(10): p. 2933-43.
160. Spiliopoulou, A.I., et al., *Bacterial adhesion, intracellular survival and cytokine induction upon stimulation of mononuclear cells with planktonic or biofilm phase Staphylococcus epidermidis.* FEMS Microbiol Lett, 2012. **330**(1): p. 56-65.
161. Nguyen, T.H., M.D. Park, and M. Otto, *Host Response to Staphylococcus epidermidis Colonization and Infections.* Front Cell Infect Microbiol, 2017. **7**: p. 90.
162. Kocianova, S., et al., *Key role of poly-gamma-DL-glutamic acid in immune evasion and virulence of Staphylococcus epidermidis.* J.Clin.Invest, 2005. **115**(3): p. 688-694.
163. Peschel, A., et al., *Inactivation of the dlt operon in Staphylococcus aureus confers sensitivity to defensins, protegrins, and other antimicrobial peptides.* J.Biol.Chem., 1999. **274**(13): p. 8405-8410.
164. Pinheiro, L., et al., *Susceptibility Profile of Staphylococcus epidermidis and Staphylococcus haemolyticus Isolated from Blood Cultures to Vancomycin and Novel Antimicrobial Drugs over a Period of 12 Years.* Microb Drug Resist, 2016. **22**(4): p. 283-93.
165. Hellmark, B., et al., *Antibiotic susceptibility among Staphylococcus epidermidis isolated from prosthetic joint infections with special focus on rifampicin and variability of the rpoB gene.* Clin Microbiol Infect, 2009. **15**(3): p. 238-44.
166. Diekema, D.J., et al., *Survey of infections due to Staphylococcus species: frequency of occurrence and antimicrobial susceptibility of isolates collected in the United States, Canada, Latin America, Europe, and the Western Pacific region for the SENTRY Antimicrobial Surveillance Program, 1997-1999.* Clin Infect Dis, 2001. **32 Suppl 2**: p. S114-32.
167. Cherifi, S., et al., *Comparative epidemiology of Staphylococcus epidermidis isolates from patients with catheter-related bacteremia and from healthy volunteers.* J Clin Microbiol, 2013. **51**(5): p. 1541-7.
168. Chambers, H.F., B.J. Hartman, and A. Tomasz, *Increased amounts of a novel penicillin-binding protein in a strain of methicillin-resistant Staphylococcus aureus exposed to nafcillin.* J Clin Invest, 1985. **76**(1): p. 325-31.
169. Miragaia, M., I. Couto, and H. de Lencastre, *Genetic diversity among methicillin-resistant Staphylococcus epidermidis (MRSE).* Microb Drug Resist, 2005. **11**(2): p. 83-93.
170. Farina, N., et al., *Methicillin resistance and biofilm production of Staphylococcus epidermidis isolates from infectious and normal flora conjunctiva.* Int Ophthalmol, 2016.
171. Salgueiro, V.C., et al., *Methicillin resistance and virulence genes in invasive and nasal Staphylococcus epidermidis isolates from neonates.* BMC Microbiol, 2017. **17**(1): p. 15.

172. Rolo, J., H. de Lencastre, and M. Miragaia, *Strategies of adaptation of Staphylococcus epidermidis to hospital and community: amplification and diversification of SCCmec.* J Antimicrob Chemother, 2012. **67**(6): p. 1333-41.
173. Widerstrom, M., et al., *Colonization of patients, healthcare workers, and the environment with healthcare-associated Staphylococcus epidermidis genotypes in an intensive care unit: a prospective observational cohort study.* BMC Infect Dis, 2016. **16**(1): p. 743.
174. Rohde, H., et al., *Detection of virulence-associated genes not useful for discriminating between invasive and commensal Staphylococcus epidermidis strains from a bone marrow transplant unit.* J Clin Microbiol, 2004. **42**(12): p. 5614-9.
175. Mehlin, C., C.M. Headley, and S.J. Klebanoff, *An inflammatory polypeptide complex from Staphylococcus epidermidis: isolation and characterization.* J Exp Med, 1999. **189**(6): p. 907-18.
176. Vuong, C., et al., *Regulated expression of pathogen-associated molecular pattern molecules in Staphylococcus epidermidis: quorum-sensing determines pro-inflammatory capacity and production of phenol-soluble modulins.* Cell Microbiol, 2004. **6**(8): p. 753-9.
177. Yao, Y., DanielÂ E. Sturdevant, and M. Otto, *Genomewide Analysis of Gene Expression in Staphylococcus epidermidis Biofilms: Insights into the Pathophysiology of S. epidermidis Biofilms and the Role of Phenol Soluble Modulins in Formation of Biofilms.* The Journal of Infectious Diseases, 2005. **191**(2): p. 289-298.
178. Cheung, G.Y., et al., *Staphylococcus epidermidis strategies to avoid killing by human neutrophils.* PLoS Pathog, 2010. **6**(10): p. e1001133.
179. Qin, L., et al., *PSM-Mec-A Virulence Determinant that Connects Transcriptional Regulation, Virulence, and Antibiotic Resistance in Staphylococci.* Front Microbiol, 2016. **7**: p. 1293.
180. Qin, L., et al., *Toxin Mediates Sepsis Caused by Methicillin-Resistant Staphylococcus epidermidis.* PLoS Pathog, 2017. **13**(2): p. e1006153.
181. Johns, B.E., et al., *Phenotypic and Genotypic Characteristics of Small Colony Variants and Their Role in Chronic Infection.* Microbiol Insights, 2015. **8**: p. 15-23.
182. Kahl, B.C., K. Becker, and B. Loffler, *Clinical Significance and Pathogenesis of Staphylococcal Small Colony Variants in Persistent Infections.* Clin Microbiol Rev, 2016. **29**(2): p. 401-27.
183. Magrys, A., et al., *The role of programmed death ligand 1 pathway in persistent biomaterial-associated infections.* J Microbiol, 2015. **53**(8): p. 544-52.
184. Mempel, M., et al., *Invasion of human keratinocytes by Staphylococcus aureus and intracellular bacterial persistence represent haemolysin-independent virulence mechanisms that are followed by features of necrotic and apoptotic keratinocyte cell death.* Br J Dermatol, 2002. **146**(6): p. 943-51.
185. Hamza, T. and B. Li, *Differential responses of osteoblasts and macrophages upon Staphylococcus aureus infection.* BMC Microbiol, 2014. **14**: p. 207.
186. Hirschhausen, N., et al., *A novel staphylococcal internalization mechanism involves the major autolysin Atl and heat shock cognate protein Hsc70 as host cell receptor.* Cell Microbiol, 2010. **12**(12): p. 1746-64.
187. Claro, T., et al., *Staphylococcus epidermidis serine--aspartate repeat protein G (SdrG) binds to osteoblast integrin alpha V beta 3.* Microbes Infect, 2015. **17**(6): p. 395-401.
188. Scharschmidt, T.C., et al., *A Wave of Regulatory T Cells into Neonatal Skin Mediates Tolerance to Commensal Microbes.* Immunity, 2015. **43**(5): p. 1011-21.
189. Naik, S., et al., *Commensal-dendritic-cell interaction specifies a unique protective skin immune signature.* Nature, 2015. **520**(7545): p. 104-8.
190. Tavakkol, Z., et al., *Resident bacterial flora in the skin of C57BL/6 mice housed under SPF conditions.* J Am Assoc Lab Anim Sci, 2010. **49**(5): p. 588-91.
191. Lai, Y., et al., *Commensal bacteria regulate Toll-like receptor 3-dependent inflammation after skin injury.* Nat Med, 2009. **15**(12): p. 1377-82.
192. Xia, X., et al., *Staphylococcal LTA-Induced miR-143 Inhibits Propionibacterium acnes-Mediated Inflammatory Response in Skin.* J Invest Dermatol, 2016. **136**(3): p. 621-30.
193. Laborel-Preneron, E., et al., *Effects of the Staphylococcus aureus and Staphylococcus epidermidis Secretomes Isolated from the Skin Microbiota of Atopic Children on CD4+ T Cell Activation.* PLoS One, 2015. **10**(10): p. e0141067.
194. Akira, S. and H. Hemmi, *Recognition of pathogen-associated molecular patterns by TLR family.* Immunol Lett, 2003. **85**(2): p. 85-95.
195. Fournier, B., *The function of TLR2 during staphylococcal diseases.* Front Cell Infect Microbiol, 2012. **2**: p. 167.
196. Yoshimura, A., et al., *Cutting edge: recognition of Gram-positive bacterial cell wall components by the innate immune system occurs via Toll-like receptor 2.* J Immunol, 1999. **163**(1): p. 1-5.
197. Morath, S., et al., *Synthetic lipoteichoic acid from Staphylococcus aureus is a potent stimulus of cytokine release.* J Exp Med, 2002. **195**(12): p. 1635-40.

198. Akira, S., S. Uematsu, and O. Takeuchi, *Pathogen recognition and innate immunity.* Cell, 2006. **124**(4): p. 783-801.
199. van Bergenhenegouwen, J., et al., *TLR2 & Co: a critical analysis of the complex interactions between TLR2 and coreceptors.* J Leukoc Biol, 2013. **94**(5): p. 885-902.
200. Hajjar, A.M., et al., *Cutting edge: functional interactions between toll-like receptor (TLR) 2 and TLR1 or TLR6 in response to phenol-soluble modulin.* J Immunol, 2001. **166**(1): p. 15-9.
201. Wanke, I., et al., *Skin commensals amplify the innate immune response to pathogens by activation of distinct signaling pathways.* J Invest Dermatol, 2011. **131**(2): p. 382-90.
202. Ommori, R., et al., *Selective induction of antimicrobial peptides from keratinocytes by staphylococcal bacteria.* Microb Pathog, 2013. **56**: p. 35-9.
203. Robertson, J., et al., *Peptidoglycan derived from Staphylococcus epidermidis induces Connexin43 hemichannel activity with consequences on the innate immune response in endothelial cells.* Biochem J, 2010. **432**(1): p. 133-43.
204. Hatakeyama, J., et al., *Contrasting responses of human gingival and periodontal ligament fibroblasts to bacterial cell-surface components through the CD14/Toll-like receptor system.* Oral Microbiol Immunol, 2003. **18**(1): p. 14-23.
205. Strunk, T., et al., *TLR2 mediates recognition of live Staphylococcus epidermidis and clearance of bacteremia.* PLoS One, 2010. **5**(4): p. e10111.
206. Kronforst, K.D., et al., *A neonatal model of intravenous Staphylococcus epidermidis infection in mice <24 h old enables characterization of early innate immune responses.* PLoS One, 2012. **7**(9): p. e43897.
207. Svensson, S., et al., *A novel soft tissue model for biomaterial-associated infection and inflammation - bacteriological, morphological and molecular observations.* Biomaterials, 2015. **41**: p. 106-21.
208. Svensson, S., et al., *Site-specific gene expression analysis of implant-near cells in a soft tissue infection model - application of laser microdissection to study biomaterial-associated infection.* J Biomed Mater Res A, 2017.
209. Bi, D., et al., *Staphylococcus epidermidis Bacteremia Induces Brain Injury in Neonatal Mice via Toll-like Receptor 2-Dependent and -Independent Pathways.* J Infect Dis, 2015. **212**(9): p. 1480-90.
210. Cole, L.E., et al., *Limitations of Murine Models for Assessment of Antibody-Mediated Therapies or Vaccine Candidates against Staphylococcus epidermidis Bloodstream Infection.* Infect Immun, 2016. **84**(4): p. 1143-9.
211. Natsuka, M., et al., *A polymer-type water-soluble peptidoglycan exhibited both Toll-like receptor 2- and NOD2-agonistic activities, resulting in synergistic activation of human monocytic cells.* Innate Immun, 2008. **14**(5): p. 298-308.
212. Kretschmer, D., et al., *Peptide length and folding state govern the capacity of staphylococcal beta-type phenol-soluble modulins to activate human formyl-peptide receptors 1 or 2.* J Leukoc Biol, 2015. **97**(4): p. 689-97.
213. Kretschmer, D., et al., *The virulence regulator Agr controls the staphylococcal capacity to activate human neutrophils via the formyl peptide receptor 2.* J Innate Immun, 2012. **4**(2): p. 201-12.
214. Rautenberg, M., et al., *Neutrophil responses to staphylococcal pathogens and commensals via the formyl peptide receptor 2 relates to phenol-soluble modulin release and virulence.* FASEB J, 2011. **25**(4): p. 1254-63.
215. Park, K., et al., *Epidermal growth factor receptor inhibitors selectively inhibit the expressions of human beta-defensins induced by Staphylococcus epidermidis.* J Dermatol Sci, 2014. **75**(2): p. 94-9.
216. Percoco, G., et al., *Antimicrobial peptides and pro-inflammatory cytokines are differentially regulated across epidermal layers following bacterial stimuli.* Exp Dermatol, 2013. **22**(12): p. 800-6.
217. Lai, Y., et al., *Activation of TLR2 by a small molecule produced by Staphylococcus epidermidis increases antimicrobial defense against bacterial skin infections.* J Invest Dermatol, 2010. **130**(9): p. 2211-21.
218. Li, D., et al., *A novel lipopeptide from skin commensal activates TLR2/CD36-p38 MAPK signaling to increase antibacterial defense against bacterial infection.* PLoS One, 2013. **8**(3): p. e58288.
219. Burgey, C., et al., *Differential induction of innate defense antimicrobial peptides in primary nasal epithelial cells upon stimulation with inflammatory cytokines, Th17 cytokines or bacterial conditioned medium from Staphylococcus aureus isolates.* Microb Pathog, 2016. **90**: p. 69-77.
220. Turner, J., et al., *Activities of LL-37, a cathelin-associated antimicrobial peptide of human neutrophils.* Antimicrob Agents Chemother, 1998. **42**(9): p. 2206-14.
221. Gordon, Y.J., et al., *Human cathelicidin (LL-37), a multifunctional peptide, is expressed by ocular surface epithelia and has potent antibacterial and antiviral activity.* Curr Eye Res, 2005. **30**(5): p. 385-94.
222. Huang, L.C., et al., *Ocular surface expression and in vitro activity of antimicrobial peptides*. Curr Eye Res, 2007. **32**(7-8): p. 595-609.
223. Dapunt, U., et al., *The osteoblast as an inflammatory cell: production of cytokines in response to bacteria and components of bacterial biofilms.* BMC Musculoskelet Disord, 2016. **17**(1): p. 243.
224. Hell, E., et al., *Human cathelicidin peptide LL37 inhibits both attachment capability and biofilm formation of Staphylococcus epidermidis.* Lett Appl Microbiol, 2010. **50**(2): p. 211-5.

225. Brancatisano, F.L., et al., *Inhibitory effect of the human liver-derived antimicrobial peptide hepcidin 20 on biofilms of polysaccharide intercellular adhesin (PIA)-positive and PIA-negative strains of Staphylococcus epidermidis.* Biofouling, 2014. **30**(4): p. 435-46.
226. Zhu, C., et al., *Human beta-defensin 3 inhibits antibiotic-resistant Staphylococcus biofilm formation.* J Surg Res, 2013. **183**(1): p. 204-13.
227. Dapunt, U., et al., *Activation of phagocytic cells by Staphylococcus epidermidis biofilms: effects of extracellular matrix proteins and the bacterial stress protein GroEL on netosis and MRP-14 release.* Pathog Dis, 2016. **74**(5).
228. Meyle, E., et al., *Immune defense against S. epidermidis biofilms: components of the extracellular polymeric substance activate distinct bactericidal mechanisms of phagocytic cells.* Int J Artif Organs, 2012. **35**(10): p. 700-12.
229. Riool, M., et al., *Staphylococcus epidermidis originating from titanium implants infects surrounding tissue and immune cells.* Acta Biomater, 2014. **10**(12): p. 5202-12.
230. Boelens, J.J., et al., *Interferon-gamma protects against biomaterial-associated Staphylococcus epidermidis infection in mice.* J Infect Dis, 2000. **181**(3): p. 1167-71.
231. Guenther, F., et al., *Phagocytosis of staphylococci biofilms by polymorphonuclear neutrophils: S. aureus and S. epidermidis differ with regard to their susceptibility towards the host defense.* Int J Artif Organs, 2009. **32**(9): p. 565-73.
232. Foster, T.J., *Immune evasion by staphylococci.* Nat Rev Microbiol, 2005. **3**(12): p. 948-58.
233. Nilsdotter-Augustinsson, A., et al., *Staphylococcus aureus, but not Staphylococcus epidermidis, modulates the oxidative response and induces apoptosis in human neutrophils.* APMIS, 2004. **112**(2): p. 109-18.
234. Megyeri, K., et al., *Induction of cytokine production by different Staphylococcal strains.* Cytokine, 2002. **19**(4): p. 206-12.
235. Strunk, T., et al., *Responsiveness of human monocytes to the commensal bacterium Staphylococcus epidermidis develops late in gestation.* Pediatr Res, 2012. **72**(1): p. 10-8.
236. Wilsson, A., et al., *Apoptotic neutrophils containing Staphylococcus epidermidis stimulate macrophages to release the proinflammatory cytokines tumor necrosis factor-alpha and interleukin-6.* FEMS Immunol Med Microbiol, 2008. **53**(1): p. 126-35.
237. Simojoki, H., et al., *Innate immune response in experimentally induced bovine intramammary infection with Staphylococcus simulans and S. epidermidis.* Vet Res, 2011. **42**: p. 49.
238. Wakabayashi, G., et al., *Staphylococcus epidermidis induces complement activation, tumor necrosis factor and interleukin-1, a shock-like state and tissue injury in rabbits without endotoxemia. Comparison to Escherichia coli.* J Clin Invest, 1991. **87**(6): p. 1925-35.
239. Boelens, J.J., et al., *Interleukin-1 receptor type I gene-deficient mice are less susceptible to Staphylococcus epidermidis biomaterial-associated infection than are wild-type mice.* Infect Immun, 2000. **68**(12): p. 6924-31.
240. Bialecka, A., et al., *Different pro-inflammatory and immunogenic potentials of Propionibacterium acnes and Staphylococcus epidermidis: implications for chronic inflammatory acne.* Arch Immunol Ther Exp (Warsz), 2005. **53**(1): p. 79-85.
241. Gutierrez-Murgas, Y.M., et al., *IL-10 plays an important role in the control of inflammation but not in the bacterial burden in S. epidermidis CNS catheter infection.* J Neuroinflammation, 2016. **13**(1): p. 271.
242. Perks, W.V., et al., *Death Receptor 3 Promotes Chemokine-Directed Leukocyte Recruitment in Acute Resolving Inflammation and Is Essential for Pathological Development of Mesothelial Fibrosis in Chronic Disease.* Am J Pathol, 2016. **186**(11): p. 2813-2823.
243. Usui, Y., et al., *Platelet aggregation induced by strains of various species of coagulase-negative staphylococci.* Microbiol Immunol, 1991. **35**(1): p. 15-26.
244. Hamzeh-Cognasse, H., et al., *Platelets and infections - complex interactions with bacteria.* Front Immunol, 2015. **6**: p. 82.
245. Vuong, C., et al., *Development of real-time in vivo imaging of device-related Staphylococcus epidermidis infection in mice and influence of animal immune status on susceptibility to infection.* J Infect Dis, 2008. **198**(2): p. 258-61.
246. Brown, A.F., et al., *Staphylococcus aureus Colonization: Modulation of Host Immune Response and Impact on Human Vaccine Design.* Front Immunol, 2014. **4**: p. 507.
247. Cerca, F., et al., *Dormant bacteria within Staphylococcus epidermidis biofilms have low inflammatory properties and maintain tolerance to vancomycin and penicillin after entering planktonic growth.* J Med Microbiol, 2014. **63**(Pt 10): p. 1274-83.
248. Franca, A., et al., *Staphylococcus epidermidis Biofilm-Released Cells Induce a Prompt and More Marked In vivo Inflammatory-Type Response than Planktonic or Biofilm Cells.* Front Microbiol, 2016. **7**: p. 1530.
249. Stanislawska, J., et al., *The response of spleen dendritic cell-enriched population to bacterial and allogeneic antigens.* Ann Transplant, 2005. **10**(4): p. 17-23.

250. Durantez, M., et al., *Tumor therapy in mice by using a tumor antigen linked to modulin peptides from Staphylococcus epidermidis.* Vaccine, 2010. **28**(44): p. 7146-54.
251. Carvalhais, V., et al., *Immunoreactive pattern of Staphylococcus epidermidis biofilm against human whole saliva.* Electrophoresis, 2015. **36**(9-10): p. 1228-33.
252. Sadovskaya, I., et al., *Potential use of poly-N-acetyl-beta-(1,6)-glucosamine as an antigen for diagnosis of staphylococcal orthopedic-prosthesis-related infections.* Clin Vaccine Immunol, 2007. **14**(12): p. 1609-15.
253. Marmor, S., et al., *Multiplex Antibody Detection for Noninvasive Genus-Level Diagnosis of Prosthetic Joint Infection.* J Clin Microbiol, 2016. **54**(4): p. 1065-73.
254. Sellman, B.R., et al., *Identification of immunogenic and serum binding proteins of Staphylococcus epidermidis.* Infect Immun, 2005. **73**(10): p. 6591-600.
255. Pourmand, M.R., et al., *Identification of antigenic components of Staphylococcus epidermidis expressed during human infection.* Infect Immun, 2006. **74**(8): p. 4644-54.
256. Vernachio, J.H., et al., *Human immunoglobulin G recognizing fibrinogen-binding surface proteins is protective against both Staphylococcus aureus and Staphylococcus epidermidis infections in vivo.* Antimicrob Agents Chemother, 2006. **50**(2): p. 511-8.
257. Schaffer, A.C. and J.C. Lee, *Staphylococcal vaccines and immunotherapies.* Infect Dis Clin North Am, 2009. **23**(1): p. 153-71.
258. Nair, N., et al., *Amidase, a cell wall hydrolase, elicits protective immunity against Staphylococcus aureus and S. epidermidis.* Int J Biol Macromol, 2015. **77**: p. 314-21.
259. Shahrooei, M., et al., *Vaccination with SesC decreases Staphylococcus epidermidis biofilm formation.* Infect Immun, 2012. **80**(10): p. 3660-8.
260. Yan, L., et al., *A Single B-repeat of Staphylococcus epidermidis accumulation-associated protein induces protective immune responses in an experimental biomaterial-associated infection mouse model.* Clin Vaccine Immunol, 2014. **21**(9): p. 1206-14.
261. Franca, A., et al., *Monoclonal antibody raised against PNAG has variable effects on static S. epidermidis biofilm accumulation in vitro.* Int J Biol Sci, 2013. **9**(5): p. 518-20.
262. Lam, H., et al., *Antibodies to PhnD inhibit staphylococcal biofilms.* Infect Immun, 2014. **82**(9): p. 3764-74.
263. Hazenbos, W.L., et al., *Novel staphylococcal glycosyltransferases SdgA and SdgB mediate immunogenicity and protection of virulence-associated cell wall proteins.* PLoS Pathog, 2013. **9**(10): p. e1003653.
264. Patel, M. and D.A. Kaufman, *Anti-lipoteichoic acid monoclonal antibody (pagibaximab) studies for the prevention of staphylococcal bloodstream infections in preterm infants.* Expert Opin Biol Ther, 2015. **15**(4): p. 595-600.
265. den Dunnen, J., et al., *IgG opsonization of bacteria promotes Th17 responses via synergy between TLRs and FcgammaRIIa in human dendritic cells.* Blood, 2012. **120**(1): p. 112-21.
266. Redlich, K. and J.S. Smolen, *Inflammatory bone loss: pathogenesis and therapeutic intervention.* Nat Rev Drug Discov, 2012. **11**(3): p. 234-50.
267. Raisz, L.G., *Physiology and pathophysiology of bone remodeling.* Clin Chem, 1999. **45**(8 Pt 2): p. 1353-8.
268. Lam, J., et al., *TNF-alpha induces osteoclastogenesis by direct stimulation of macrophages exposed to permissive levels of RANK ligand.* J Clin Invest, 2000. **106**(12): p. 1481-8.
269. Kobayashi, K., et al., *Tumor necrosis factor alpha stimulates osteoclast differentiation by a mechanism independent of the ODF/RANKL-RANK interaction.* J Exp Med, 2000. **191**(2): p. 275-86.
270. Gilbert, L., et al., *Inhibition of osteoblast differentiation by tumor necrosis factor-alpha.* Endocrinology, 2000. **141**(11): p. 3956-64.
271. Gilbert, L., et al., *Expression of the osteoblast differentiation factor RUNX2 (Cbfa1/AML3/Pebp2alpha A) is inhibited by tumor necrosis factor-alpha.* J Biol Chem, 2002. **277**(4): p. 2695-701.
272. Jilka, R.L., et al., *Osteoblast programmed cell death (apoptosis): modulation by growth factors and cytokines.* J Bone Miner Res, 1998. **13**(5): p. 793-802.
273. Stashenko, P., et al., *Interleukin-1 beta is a potent inhibitor of bone formation in vitro.* J Bone Miner Res, 1987. **2**(6): p. 559-65.
274. Nair, S.P., et al., *Bacterially induced bone destruction: mechanisms and misconceptions.* Infect Immun, 1996. **64**(7): p. 2371-80.
275. Lee, J.H., et al., *Effects of Staphylococcus epidermidis on osteoblast cell adhesion and viability on a Ti alloy surface in a microfluidic co-culture environment.* Acta Biomater, 2010. **6**(11): p. 4422-9.
276. Zaatreh, S., et al., *Co-Culture of S. epidermidis and Human Osteoblasts on Implant Surfaces: An Advanced In Vitro Model for Implant-Associated Infections.* PLoS One, 2016. **11**(3): p. e0151534.
277. Meghji, S., et al., *Staphylococcus epidermidis produces a cell-associated proteinaceous fraction which causes bone resorption by a prostanoid-independent mechanism: relevance to the treatment of infected orthopaedic implants.* Br J Rheumatol, 1997. **36**(9): p. 957-63.

278. Tucker, K.A., et al., *Intracellular Staphylococcus aureus induces apoptosis in mouse osteoblasts.* FEMS Microbiol Lett, 2000. **186**(2): p. 151-6.
279. Alexander, E.H., et al., *Staphylococcus aureus - induced tumor necrosis factor - related apoptosis - inducing ligand expression mediates apoptosis and caspase-8 activation in infected osteoblasts.* BMC Microbiol, 2003. **3**: p. 5.
280. Alexander, E.H., et al., *Staphylococcus aureus and Salmonella enterica serovar Dublin induce tumor necrosis factor-related apoptosis-inducing ligand expression by normal mouse and human osteoblasts.* Infect Immun, 2001. **69**(3): p. 1581-6.
281. Young, A.B., et al., *Causative agents of osteomyelitis induce death domain-containing TNF-related apoptosis-inducing ligand receptor expression on osteoblasts.* Bone, 2011. **48**(4): p. 857-63.
282. Somayaji, S.N., et al., *Staphylococcus aureus induces expression of receptor activator of NF-kappaB ligand and prostaglandin E2 in infected murine osteoblasts.* Infect Immun, 2008. **76**(11): p. 5120-6.
283. Claro, T., et al., *Staphylococcus aureus protein A binding to osteoblast tumour necrosis factor receptor 1 results in activation of nuclear factor kappa B and release of interleukin-6 in bone infection.* Microbiology, 2013. **159**(Pt 1): p. 147-54.
284. Claro, T., et al., *Staphylococcus aureus protein A binds to osteoblasts and triggers signals that weaken bone in osteomyelitis.* PLoS One, 2011. **6**(4): p. e18748.
285. Yang, J., et al., *Impaired osteoclastogenesis by staphylococcal lipoteichoic acid through Toll-like receptor 2 with partial involvement of MyD88.* J Leukoc Biol, 2009. **86**(4): p. 823-31.
286. Kim, J., et al., *Lipoproteins are an important bacterial component responsible for bone destruction through the induction of osteoclast differentiation and activation.* J Bone Miner Res, 2013. **28**(11): p. 2381-91.
287. Pietrocola, G., et al., *Toll-like receptors (TLRs) in innate immune defense against Staphylococcus aureus.* Int J Artif Organs, 2011. **34**(9): p. 799-810.
288. Kishimoto, T., et al., *Peptidoglycan and lipopolysaccharide synergistically enhance bone resorption and osteoclastogenesis.* J Periodontal Res, 2012. **47**(4): p. 446-54.
289. Trouillet-Assant, S., et al., *Dual impact of live Staphylococcus aureus on the osteoclast lineage, leading to increased bone resorption.* J Infect Dis, 2015. **211**(4): p. 571-81.
290. Ahmed, S., et al., *Staphylococcus aureus fibronectin binding proteins are essential for internalization by osteoblasts but do not account for differences in intracellular levels of bacteria.* Infect Immun, 2001. **69**(5): p. 2872-7.
291. Khalil, H., et al., *Invasion of bone cells by Staphylococcus epidermidis.* Microbes Infect, 2007. **9**(4): p. 460-5.
292. Sinha, B., et al., *Fibronectin-binding protein acts as Staphylococcus aureus invasin via fibronectin bridging to integrin alpha5beta1.* Cell Microbiol, 1999. **1**(2): p. 101-17.
293. Valour, F., et al., *Staphylococcus epidermidis in orthopedic device infections: the role of bacterial internalization in human osteoblasts and biofilm formation.* PLoS One, 2013. **8**(6): p. e67240.
294. Campoccia, D., et al., *Orthopedic implant-infections. Incompetence of Staphylococcus epidermidis, Staphylococcus lugdunensis and Enterococcus faecalis to invade osteoblasts.* J Biomed Mater Res A, 2015.
295. Quinn, J.M., N.A. Athanasou, and J.O. McGee, *Extracellular matrix receptor and platelet antigens on osteoclasts and foreign body giant cells.* Histochemistry, 1991. **96**(2): p. 169-76.
296. Rochford, E.T., et al., *Monitoring immune responses in a mouse model of fracture fixation with and without Staphylococcus aureus osteomyelitis.* Bone, 2016. **83**: p. 82-92.
297. Prabhakara, R., et al., *Murine immune response to a chronic Staphylococcus aureus biofilm infection.* Infect Immun, 2011. **79**(4): p. 1789-96.
298. Jensen, L.K., et al., *Specific Antibodies to Staphylococcus aureus Biofilm Are Present in Serum from Pigs with Osteomyelitis.* In Vivo, 2015. **29**(5): p. 555-60.
299. Prabhakara, R., et al., *Suppression of the inflammatory immune response prevents the development of chronic biofilm infection due to methicillin-resistant Staphylococcus aureus.* Infect Immun, 2011. **79**(12): p. 5010-8.
300. Heim, C.E., et al., *IL-12 promotes myeloid-derived suppressor cell recruitment and bacterial persistence during Staphylococcus aureus orthopedic implant infection.* J Immunol, 2015. **194**(8): p. 3861-72.
301. Scherr, T.D., et al., *Mouse model of post-arthroplasty Staphylococcus epidermidis joint infection.* Methods Mol Biol, 2014. **1106**: p. 173-81.
302. Park, K.H., et al., *Activity of Tedizolid in Methicillin-Resistant Staphylococcus epidermidis Experimental Foreign Body-Associated Osteomyelitis.* Antimicrob Agents Chemother, 2016.
303. Lovati, A.B., et al., *Modeling Staphylococcus epidermidis-Induced Non-Unions: Subclinical and Clinical Evidence in Rats.* PLoS One, 2016. **11**(1): p. e0147447.
304. Lovati, A.B., et al., *Systemic and Local Administration of Antimicrobial and Cell Therapies to Prevent Methicillin-Resistant Staphylococcus epidermidis-Induced Femoral Nonunions in a Rat Model.* Mediators Inflamm, 2016. **2016**: p. 9595706.

305. Webster, T.J., et al., *Anti-infective and osteointegration properties of silicon nitride, poly(ether ether ketone), and titanium implants.* Acta Biomater, 2012. **8**(12): p. 4447-54.
306. Ahtinen, H., et al., *(68)Ga-DOTA-Siglec-9 PET/CT imaging of peri-implant tissue responses and staphylococcal infections.* EJNMMI Res, 2014. **4**: p. 45.
307. Zhai, H., et al., *Lavage with allicin in combination with vancomycin inhibits biofilm formation by Staphylococcus epidermidis in a rabbit model of prosthetic joint infection.* PLoS One, 2014. **9**(7): p. e102760.
308. Tan, H.L., et al., *In vivo effect of quaternized chitosan-loaded polymethylmethacrylate bone cement on methicillin-resistant Staphylococcus epidermidis infection of the tibial metaphysis in a rabbit model.* Antimicrob Agents Chemother, 2014. **58**(10): p. 6016-23.
309. Lankinen, P., et al., *A comparative 18F-FDG PET/CT imaging of experimental Staphylococcus aureus osteomyelitis and Staphylococcus epidermidis foreign-body-associated infection in the rabbit tibia.* EJNMMI Res, 2012. **2**(1): p. 41.
310. Del Pozo, J.L., et al., *The electricidal effect is active in an experimental model of Staphylococcus epidermidis chronic foreign body osteomyelitis.* Antimicrob Agents Chemother, 2009. **53**(10): p. 4064-8.
311. An, Y.H., et al., *The prevention of prosthetic infection using a cross-linked albumin coating in a rabbit model.* J Bone Joint Surg Br, 1997. **79**(5): p. 816-9.
312. Isiklar, Z.U., et al., *Efficacy of antibiotics alone for orthopaedic device related infections.* Clin Orthop Relat Res, 1996(332): p. 184-9.
313. Mayberry-Carson, K.J., et al., *Osteomyelitis experimentally induced with Bacteroides thetaiotaomicron and Staphylococcus epidermidis. Influence of a foreign-body implant.* Clin Orthop Relat Res, 1992(280): p. 289-99.
314. Lambe, D.W., Jr., et al., *Foreign-body-associated experimental osteomyelitis induced with Bacteroides fragilis and Staphylococcus epidermidis in rabbits.* Clin Orthop Relat Res, 1991(266): p. 285-94.
315. Mayberry-Carson, K.J., et al., *Effect of ciprofloxacin on experimental osteomyelitis in the rabbit tibia, induced with a mixed infection of Staphylococcus epidermidis and Bacteroides thetaiotaomicron.* Microbios, 1990. **64**(258): p. 49-66.
316. Petty, W., et al., *The influence of skeletal implants on incidence of infection. Experiments in a canine model.* J Bone Joint Surg Am, 1985. **67**(8): p. 1236-44.
317. van der Borden, A.J., et al., *Prevention of pin tract infection in external stainless steel fixator frames using electric current in a goat model.* Biomaterials, 2007. **28**(12): p. 2122-6.
318. Laure, B., et al., *Effect of hydroxyapatite coating and polymethylmethacrylate on stainless steel implant-site infection with Staphylococcus epidermidis in a sheep model.* J Biomed Mater Res A, 2008. **84**(1): p. 92-8.
319. Willey, M. and M. Karam, *Impact of Infection on Fracture Fixation.* Orthop Clin North Am, 2016. **47**(2): p. 357-64.
320. Uckay, I., et al., *Prevention of surgical site infections in orthopaedic surgery and bone trauma: state-of-the-art update.* J Hosp Infect, 2013. **84**(1): p. 5-12.
321. Montanaro, L., et al., *Scenery of Staphylococcus implant infections in orthopedics.* Future.Microbiol., 2011. **6**(11): p. 1329-1349.
322. Elek, S.D. and P.E. Conen, *The virulence of Staphylococcus pyogenes for man; a study of the problems of wound infection.* Br J Exp Pathol, 1957. **38**(6): p. 573-86.
323. James, R.C. and C.J. Macleod, *Induction of staphylococcal infections in mice with small inocula introduced on sutures.* Br J Exp Pathol, 1961. **42**: p. 266-77.
324. Moucha, C.S., et al., *Modifiable risk factors for surgical site infection.* J Bone Joint Surg Am, 2011. **93**(4): p. 398-404.
325. Jeffcoach, D.R., et al., *Nonsteroidal anti-inflammatory drugs' impact on nonunion and infection rates in long-bone fractures.* J Trauma Acute Care Surg, 2014. **76**(3): p. 779-83.
326. Augat, P., et al., *Mechanics and mechano-biology of fracture healing in normal and osteoporotic bone.* Osteoporos Int, 2005. **16 Suppl 2**: p. S36-43.
327. Glatt, V., C.H. Evans, and K. Tetsworth, *A Concert between Biology and Biomechanics: The Influence of the Mechanical Environment on Bone Healing.* Front Physiol, 2016. **7**: p. 678.
328. Lacroix, D. and P.J. Prendergast, *A mechano-regulation model for tissue differentiation during fracture healing: analysis of gap size and loading.* J Biomech, 2002. **35**(9): p. 1163-71.
329. Grongroft, I., et al., *Fixation compliance in a mouse osteotomy model induces two different processes of bone healing but does not lead to delayed union.* J Biomech, 2009. **42**(13): p. 2089-96.
330. Mouzopoulos, G., et al., *Management of bone infections in adults: the surgeon's and microbiologist's perspectives.* Injury, 2011. **42 Suppl 5**: p. S18-23.
331. Rittman, W.W. and S. Perren, *Cortical Bone Healing after Internal Fixation and Infection*. 1st ed. 1974: Springer-Verlag Berlin Heidelberg.
332. Friedrich, B. and P. Klaue, *Mechanical stability and post-traumatic osteitis: an experimental evaluation of the relation between infection of bone and internal fixation.* Injury, 1977. **9**(1): p. 23-9.

333. Merritt, K. and J.D. Dowd, *Role of internal fixation in infection of open fractures: studies with Staphylococcus aureus and Proteus mirabilis.* J.Orthop.Res., 1987. **5**(1): p. 23-28.
334. Worlock, P., et al., *The prevention of infection in open fractures: an experimental study of the effect of fracture stability.* Injury, 1994. **25**(1): p. 31-8.
335. Windolf, C.D., et al., *Implant-associated localized osteitis in murine femur fracture by biofilm forming Staphylococcus aureus: a novel experimental model.* J Orthop Res, 2013. **31**(12): p. 2013-20.
336. Worlock, P., et al., *An experimental model of post-traumatic osteomyelitis in rabbits.* Br J Exp Pathol, 1988. **69**(2): p. 235-44.
337. Lindsey, B.A., et al., *An animal model for open femur fracture and osteomyelitis: Part I.* J Orthop Res, 2010. **28**(1): p. 38-42.
338. Robinson, D.A., et al., *Development of a fracture osteomyelitis model in the rat femur.* J Orthop Res, 2011. **29**(1): p. 131-7.
339. Arens, D., et al., *A rabbit humerus model of plating and nailing osteosynthesis with and without Staphylococcus aureus osteomyelitis.* Eur Cell Mater, 2015. **30**: p. 148-61; discussion 161-2.
340. Lovati, A.B., et al., *Animal Models of Implant-Related Low-Grade Infections. A Twenty-Year Review.* Adv Exp Med Biol, 2016.
341. Matthys, R. and S.M. Perren, *Internal fixator for use in the mouse.* Injury, 2009. **40 Suppl 4**: p. S103-9.
342. Steck, R., et al., *Influence of internal fixator flexibility on murine fracture healing as characterized by mechanical testing and microCT imaging.* J Orthop Res, 2011. **29**(8): p. 1245-50.
343. Stepanovic, S., et al., *A modified microtiter-plate test for quantification of staphylococcal biofilm formation.* J Microbiol Methods, 2000. **40**(2): p. 175-9.
344. Campoccia, D., et al., *The selection of appropriate bacterial strains in preclinical evaluation of infection-resistant biomaterials.* Int J Artif Organs, 2008. **31**(9): p. 841-7.
345. Moriarty, T.F., et al., *Influence of material and microtopography on the development of local infection in vivo: experimental investigation in rabbits.* Int J Artif Organs, 2009. **32**(9): p. 663-70.
346. Hamers, F.P., et al., *Automated quantitative gait analysis during overground locomotion in the rat: its application to spinal cord contusion and transection injuries.* J Neurotrauma, 2001. **18**(2): p. 187-201.
347. Versalovic, J., T. Koeuth, and J.R. Lupski, *Distribution of repetitive DNA sequences in eubacteria and application to fingerprinting of bacterial genomes.* Nucleic Acids Res, 1991. **19**(24): p. 6823-31.
348. Vidlak, D. and T. Kielian, *Infectious Dose Dictates the Host Response during Staphylococcus aureus Orthopedic-Implant Biofilm Infection.* Infect Immun, 2016. **84**(7): p. 1957-65.
349. Ueno, M., et al., *Influence of internal fixator stiffness on murine fracture healing: two types of fracture healing lead to two distinct cellular events and FGF-2 expressions.* Exp Anim, 2011. **60**(1): p. 79-87.
350. Montjovent, M.O., et al., *Expression of antagonists of WNT and BMP signaling after non-rigid fixation of osteotomies.* Bone, 2013. **53**(1): p. 79-86.
351. Stadelmann, V.A., et al., *In Vivo MicroCT Monitoring of Osteomyelitis in a Rat Model.* Biomed Res Int, 2015. **2015**: p. 587857.
352. Marmor, S. and Y. Kerroumi, *Patient-specific risk factors for infection in arthroplasty procedure.* Orthop Traumatol Surg Res, 2016. **102**(1 Suppl): p. S113-9.
353. Forsberg, J.A., et al., *Diagnosis and management of chronic infection.* J Am Acad Orthop Surg, 2011. **19 Suppl 1**: p. S8-S19.
354. Sander, G., et al., *Catheter colonization and abscess formation due to Staphylococcus epidermidis with normal and small-colony-variant phenotype is mouse strain dependent.* PLoS One, 2012. **7**(5): p. e36602.
355. Broekhuizen, C.A., et al., *Peri-implant tissue is an important niche for Staphylococcus epidermidis in experimental biomaterial-associated infection in mice.* Infect Immun, 2007. **75**(3): p. 1129-36.
356. Chan, L.C., et al., *Innate Immune Memory Contributes to Host Defense Against Recurrent Skin and Skin Structure Infections Caused by Methicillin-Resistant Staphylococcus aureus.* Infect Immun, 2016.
357. von Kockritz-Blickwede, M., et al., *Immunological mechanisms underlying the genetic predisposition to severe Staphylococcus aureus infection in the mouse model.* Am J Pathol, 2008. **173**(6): p. 1657-68.
358. Nippe, N., et al., *Subcutaneous infection with S. aureus in mice reveals association of resistance with influx of neutrophils and Th2 response.* J Invest Dermatol, 2011. **131**(1): p. 125-32.
359. Nishitani, K., et al., *Quantifying the natural history of biofilm formation in vivo during the establishment of chronic implant-associated Staphylococcus aureus osteomyelitis in mice to identify critical pathogen and host factors.* J Orthop Res, 2015. **33**(9): p. 1311-9.
360. Sellers, R.S., et al., *Immunological variation between inbred laboratory mouse strains: points to consider in phenotyping genetically immunomodified mice.* Vet Pathol, 2012. **49**(1): p. 32-43.
361. Claes, L., S. Recknagel, and A. Ignatius, *Fracture healing under healthy and inflammatory conditions.* Nat.Rev.Rheumatol., 2012. **8**(3): p. 133-143.

362. El Khassawna, T., et al., *T Lymphocytes Influence the Mineralization Process of Bone.* Front Immunol, 2017. **8**: p. 562.
363. Kalyan, S., *It May Seem Inflammatory, but Some T Cells Are Innately Healing to the Bone.* J Bone Miner Res, 2016. **31**(11): p. 1997-2000.
364. Lu, L.Y., et al., *Pro-inflammatory M1 macrophages promote Osteogenesis by mesenchymal stem cells via the COX-2-prostaglandin E2 pathway.* J Orthop Res, 2017.
365. Ogle, M.E., et al., *Monocytes and macrophages in tissue repair: Implications for immunoregenerative biomaterial design.* Exp Biol Med (Maywood), 2016. **241**(10): p. 1084-97.
366. Ramirez-GarciaLuna, J.L., et al., *Defective bone repair in mast cell-deficient Cpa3Cre/+ mice.* PLoS One, 2017. **12**(3): p. e0174396.
367. Sun, G., et al., *STAT3 promotes bone fracture healing by enhancing the FOXP3 expression and the suppressive function of regulatory T cells.* APMIS, 2017.
368. Edderkaoui, B., *Potential Role of Chemokines in Fracture Repair.* Front Endocrinol (Lausanne), 2017. **8**: p. 39.
369. Schlundt, C., et al., *Immune modulation as a therapeutic strategy in bone regeneration.* J Exp Orthop, 2015. **2**(1): p. 1.
370. Godwin, J.W., A.R. Pinto, and N.A. Rosenthal, *Chasing the recipe for a pro-regenerative immune system.* Semin Cell Dev Biol, 2017. **61**: p. 71-79.
371. Vuong, C., et al., *Polysaccharide intercellular adhesin (PIA) protects Staphylococcus epidermidis against major components of the human innate immune system.* Cell Microbiol, 2004. **6**(3): p. 269-75.
372. Vuong, C., et al., *A crucial role for exopolysaccharide modification in bacterial biofilm formation, immune evasion, and virulence.* J Biol Chem, 2004. **279**(52): p. 54881-6.
373. Sabate Bresco, M., et al., *Influence of fracture stability on Staphylococcus epidermidis and S. aureus infection in a murine femoral fracture model.* Eur Cell Mater, 2017.
374. Schmidt-Bleek, K., et al., *Inflammatory phase of bone healing initiates the regenerative healing cascade.* Cell Tissue Res, 2012. **347**(3): p. 567-73.
375. Alblowi, J., et al., *High levels of tumor necrosis factor-alpha contribute to accelerated loss of cartilage in diabetic fracture healing.* Am J Pathol, 2009. **175**(4): p. 1574-85.
376. Abou-Khalil, R., et al., *Delayed bone regeneration is linked to chronic inflammation in murine muscular dystrophy.* J Bone Miner Res, 2014. **29**(2): p. 304-15.
377. Reikeras, O., et al., *Lipopolysaccharide impairs fracture healing: an experimental study in rats.* Acta Orthop, 2005. **76**(6): p. 749-53.
378. Recknagel, S., et al., *Experimental blunt chest trauma impairs fracture healing in rats.* J Orthop Res, 2011. **29**(5): p. 734-9.
379. Claes, L., et al., *The effect of a combined thoracic and soft-tissue trauma on blood flow and tissue formation in fracture healing in rats.* Arch Orthop Trauma Surg, 2017. **137**(7): p. 945-952.
380. Hurtgen, B.J., et al., *Severe muscle trauma triggers heightened and prolonged local musculoskeletal inflammation and impairs adjacent tibia fracture healing.* J Musculoskelet Neuronal Interact, 2016. **16**(2): p. 122-34.
381. Hildebrand, F., et al., *Is There an Impact of Concomitant Injuries and Timing of Fixation of Major Fractures on Fracture Healing? A Focused Review of Clinical and Experimental Evidence.* J Orthop Trauma, 2016. **30**(3): p. 104-12.
382. Hoff, P., et al., *A Pronounced Inflammatory Activity Characterizes the Early Fracture Healing Phase in Immunologically Restricted Patients.* Int J Mol Sci, 2017. **18**(3).
383. Dapunt, U., et al., *The osteoblast as an inflammatory cell: production of cytokines in response to bacteria and components of bacterial biofilms.* BMC Musculoskelet Disord, 2016. **17**: p. 243.
384. Hoff, P., et al., *Immunologically restricted patients exhibit a pronounced inflammation and inadequate response to hypoxia in fracture hematomas.* Immunol Res, 2011. **51**(1): p. 116-22.
385. Konnecke, I., et al., *T and B cells participate in bone repair by infiltrating the fracture callus in a two-wave fashion.* Bone, 2014. **64**: p. 155-65.
386. Hayday, A.C., *[gamma][delta] cells: a right time and a right place for a conserved third way of protection.* Annu Rev Immunol, 2000. **18**: p. 975-1026.
387. Murphy, A.G., et al., *Staphylococcus aureus infection of mice expands a population of memory gammadelta T cells that are protective against subsequent infection.* J Immunol, 2014. **192**(8): p. 3697-708.
388. Maher, B.M., et al., *Nlrp-3-driven interleukin 17 production by gammadeltaT cells controls infection outcomes during Staphylococcus aureus surgical site infection.* Infect Immun, 2013. **81**(12): p. 4478-89.
389. Croes, M., et al., *Proinflammatory T cells and IL-17 stimulate osteoblast differentiation.* Bone, 2016. **84**: p. 262-70.
390. Uluckan, O., et al., *Chronic skin inflammation leads to bone loss by IL-17-mediated inhibition of Wnt signaling in osteoblasts.* Sci Transl Med, 2016. **8**(330): p. 330ra37.

391. Kim, Y.G., et al., *IL-17 inhibits osteoblast differentiation and bone regeneration in rat.* Arch Oral Biol, 2014. **59**(9): p. 897-905.
392. Montgomery, C.P., et al., *Protective immunity against recurrent Staphylococcus aureus skin infection requires antibody and interleukin-17A.* Infect Immun, 2014. **82**(5): p. 2125-34.
393. Vidlak, D. and T. Kielian, *Differential effects of interleukin-17 receptor signaling on innate and adaptive immunity during central nervous system bacterial infection.* J Neuroinflammation, 2012. **9**: p. 128.
394. Archer, N.K., et al., *Interleukin-17A (IL-17A) and IL-17F Are Critical for Antimicrobial Peptide Production and Clearance of Staphylococcus aureus Nasal Colonization.* Infect Immun, 2016. **84**(12): p. 3575-3583.
395. Roark, C.L., et al., *Exacerbation of collagen-induced arthritis by oligoclonal, IL-17-producing gamma delta T cells.* J Immunol, 2007. **179**(8): p. 5576-83.
396. Akdis, M., et al., *Interleukins (from IL-1 to IL-38), interferons, transforming growth factor beta, and TNF-alpha: Receptors, functions, and roles in diseases.* J Allergy Clin Immunol, 2016. **138**(4): p. 984-1010.
397. O'Mahony, L., M. Akdis, and C.A. Akdis, *Regulation of the immune response and inflammation by histamine and histamine receptors.* J Allergy Clin Immunol, 2011. **128**(6): p. 1153-62.
398. Ferstl, R., C.A. Akdis, and L. O'Mahony, *Histamine regulation of innate and adaptive immunity.* Front Biosci (Landmark Ed), 2012. **17**: p. 40-53.
399. Mazzoni, A., et al., *Histamine regulates cytokine production in maturing dendritic cells, resulting in altered T cell polarization.* J Clin Invest, 2001. **108**(12): p. 1865-73.
400. Frei, R., et al., *Histamine receptor 2 modifies dendritic cell responses to microbial ligands.* J Allergy Clin Immunol, 2013. **132**(1): p. 194-204.
401. Carlos, D., et al., *Histamine h2 receptor signaling in the pathogenesis of sepsis: studies in a murine diabetes model.* J Immunol, 2013. **191**(3): p. 1373-82.
402. Handley, S.A., P.H. Dube, and V.L. Miller, *Histamine signaling through the H(2) receptor in the Peyer's patch is important for controlling Yersinia enterocolitica infection.* Proc Natl Acad Sci U S A, 2006. **103**(24): p. 9268-73.
403. Metz, M., et al., *Effects of antihistamines on innate immune responses to severe bacterial infection in mice.* Int Arch Allergy Immunol, 2011. **155**(4): p. 355-60.
404. Werner, K., D. Neumann, and R. Seifert, *Analysis of the histamine H2-receptor in human monocytes.* Biochem Pharmacol, 2014. **92**(2): p. 369-79.
405. Vasicek, O., et al., *Role of histamine receptors in the effects of histamine on the production of reactive oxygen species by whole blood phagocytes.* Life Sci, 2014. **100**(1): p. 67-72.
406. Ciz, M. and A. Lojek, *Modulation of neutrophil oxidative burst via histamine receptors.* Br J Pharmacol, 2013. **170**(1): p. 17-22.
407. Dawicki, W., et al., *Mast cells, histamine, and IL-6 regulate the selective influx of dendritic cell subsets into an inflamed lymph node.* J Immunol, 2010. **184**(4): p. 2116-23.
408. Anderson, J.M., A. Rodriguez, and D.T. Chang, *Foreign body reaction to biomaterials.* Semin Immunol, 2008. **20**(2): p. 86-100.
409. Higgins, D.M., et al., *Localized immunosuppressive environment in the foreign body response to implanted biomaterials.* Am J Pathol, 2009. **175**(1): p. 161-70.
410. Ando, T., et al., *Stimulation of the synthesis of histamine and putrescine in mice by a peptidoglycan of gram-positive bacteria.* Microbiol Immunol, 1994. **38**(3): p. 209-15.
411. Urb, M. and D.C. Sheppard, *The role of mast cells in the defence against pathogens.* PLoS Pathog, 2012. **8**(4): p. e1002619.
412. Barcik, W., et al., *Histamine-secreting microbes are increased in the gut of adult asthma patients.* J Allergy Clin Immunol, 2016. **138**(5): p. 1491-1494 e7.
413. Yokoi, K.J., et al., *Characterization of the histidine decarboxylase gene of Staphylococcus epidermidis TYH1 coded on the staphylococcal cassette chromosome.* Gene, 2011. **477**(1-2): p. 32-41.
414. Maslinska, D., et al., *Subcellular localization of histamine in articular cartilage chondrocytes of rheumatoid arthritis patients.* Inflamm Res, 2004. **53 Suppl 1**: p. S35-6.
415. Kim, K.W., et al., *Histamine and Histamine H4 Receptor Promotes Osteoclastogenesis in Rheumatoid Arthritis.* Sci Rep, 2017. **7**(1): p. 1197.
416. de Oliveira, P.A., et al., *Cimetidine Reduces Interleukin-6, Matrix Metalloproteinases-1 and -9 Immunoexpression in the Gingival Mucosa of Rat Molars With Induced Periodontal Disease.* J Periodontol, 2017. **88**(1): p. 100-111.
417. Biosse-Duplan, M., et al., *Histamine promotes osteoclastogenesis through the differential expression of histamine receptors on osteoclasts and osteoblasts.* Am J Pathol, 2009. **174**(4): p. 1426-34.
418. Wang, J., S. Kuenzel, and J.F. Baines, *Draft Genome Sequences of 11 Staphylococcus epidermidis Strains Isolated from Wild Mouse Species.* Genome Announc, 2014. **2**(1).
419. Garcia-Garcera, M., et al., *Staphylococcus prevails in the skin microbiota of long-term immunodeficient mice.* Environ Microbiol, 2012. **14**(8): p. 2087-98.

420. Zuo, Q.F., et al., *Identification of the immunodominant regions of Staphylococcus aureus fibronectin-binding protein A.* PLoS One, 2014. **9**(4): p. e95338.
421. den Reijer, P.M., et al., *Characterization of the humoral immune response during Staphylococcus aureus bacteremia and global gene expression by Staphylococcus aureus in human blood.* PLoS One, 2013. **8**(1): p. e53391.
422. Verkaik, N.J., et al., *Heterogeneity of the humoral immune response following Staphylococcus aureus bacteremia.* Eur J Clin Microbiol Infect Dis, 2010. **29**(5): p. 509-18.
423. Verkaik, N.J., et al., *Immunogenicity of toxins during Staphylococcus aureus infection*. Clin Infect Dis, 2010. **50**(1): p. 61-8.
424. Holtfreter, S., J. Kolata, and B.M. Broker, *Towards the immune proteome of Staphylococcus aureus - The anti-S. aureus antibody response.* Int J Med Microbiol, 2010. **300**(2-3): p. 176-92.
425. Broker, B.M. and A. van Belkum, *Immune proteomics of Staphylococcus aureus.* Proteomics, 2011. **11**(15): p. 3221-31.
426. Histing, T., et al., *Small animal bone healing models: standards, tips, and pitfalls results of a consensus meeting.* Bone, 2011. **49**(4): p. 591-9.
427. Garcia, P., et al., *Rodent animal models of delayed bone healing and non-union formation: a comprehensive review.* Eur Cell Mater, 2013. **26**: p. 1-12; discussion 12-4.
428. Nunamaker, D.M., *Experimental models of fracture repair.* Clin Orthop Relat Res, 1998(355 Suppl): p. S56-65.
429. Ning, B., et al., *Surgicallyinduced mouse models in the study of bone regeneration: Current models and future directions (Review).* Mol Med Rep, 2017. **15**(3): p. 1017-1023.
430. Holstein, J.H., et al., *Advances in the establishment of defined mouse models for the study of fracture healing and bone regeneration.* J Orthop Trauma, 2009. **23**(5 Suppl): p. S31-8.
431. De Giacomo, A., E.F. Morgan, and L.C. Gerstenfeld, *Generation of closed transverse fractures in small animals.* Methods Mol Biol, 2014. **1130**: p. 35-44.
432. Mills, C.D., et al., *M-1/M-2 macrophages and the Th1/Th2 paradigm.* J Immunol, 2000. **164**(12): p. 6166-73.
433. Watanabe, H., et al., *Innate immune response in Th1- and Th2-dominant mouse strains.* Shock, 2004. **22**(5): p. 460-6.
434. Lu, C., et al., *Cellular basis for age-related changes in fracture repair.* J Orthop Res, 2005. **23**(6): p. 1300-7.
435. Lu, C., et al., *Effect of age on vascularization during fracture repair.* J Orthop Res, 2008. **26**(10): p. 1384-9.
436. Beura, L.K., et al., *Normalizing the environment recapitulates adult human immune traits in laboratory mice.* Nature, 2016. **532**(7600): p. 512-6.
437. Clayton, J.A. and F.S. Collins, *Policy: NIH to balance sex in cell and animal studies.* Nature, 2014. **509**(7500): p. 282-3.
438. Josse, J., F. Velard, and S.C. Gangloff, *Staphylococcus aureus vs. Osteoblast: Relationship and Consequences in Osteomyelitis.* Front Cell Infect Microbiol, 2015. **5**: p. 85.
439. Sanchez, C.J., Jr., et al., *Staphylococcus aureus biofilms decrease osteoblast viability, inhibits osteogenic differentiation, and increases bone resorption in vitro.* BMC Musculoskelet Disord, 2013. **14**: p. 187.
440. Szabo, E., et al., *Licensing by Inflammatory Cytokines Abolishes Heterogeneity of Immunosuppressive Function of Mesenchymal Stem Cell Population.* Stem Cells Dev, 2015. **24**(18): p. 2171-80.
441. Glenn, J.D. and K.A. Whartenby, *Mesenchymal stem cells: Emerging mechanisms of immunomodulation and therapy.* World J Stem Cells, 2014. **6**(5): p. 526-39.
442. Najar, M., et al., *Mesenchymal stromal cells and immunomodulation: A gathering of regulatory immune cells.* Cytotherapy, 2016. **18**(2): p. 160-71.
443. Cao, W., et al., *Mesenchymal stem cells and adaptive immune responses.* Immunol Lett, 2015. **168**(2): p. 147-53.
444. Millrud, C.R., C. Bergenfelz, and K. Leandersson, *On the origin of myeloid-derived suppressor cells.* Oncotarget, 2017. **8**(2): p. 3649-3665.
445. Ray, A., K. Chakraborty, and P. Ray, *Immunosuppressive MDSCs induced by TLR signaling during infection and role in resolution of inflammation.* Front Cell Infect Microbiol, 2013. **3**: p. 52.
446. Atretkhany, K.N. and M.S. Drutskaya, *Myeloid-Derived Suppressor Cells and Proinflammatory Cytokines as Targets for Cancer Therapy.* Biochemistry (Mosc), 2016. **81**(11): p. 1274-1283.
447. Vladimirovna, I.L., et al., *Mesenchymal Stem Cells and Myeloid Derived Suppressor Cells: Common Traits in Immune Regulation.* J Immunol Res, 2016. **2016**: p. 7121580.
448. Heim, C.E., et al., *Myeloid-derived suppressor cells contribute to Staphylococcus aureus orthopedic biofilm infection.* J Immunol, 2014. **192**(8): p. 3778-92.
449. Heim, C.E., D. Vidlak, and T. Kielian, *Interleukin-10 production by myeloid-derived suppressor cells contributes to bacterial persistence during Staphylococcus aureus orthopedic biofilm infection.* J Leukoc Biol, 2015. **98**(6): p. 1003-13.

450. Soehnlein, O. and L. Lindbom, *Phagocyte partnership during the onset and resolution of inflammation.* Nat Rev Immunol, 2010. **10**(6): p. 427-39.
451. Chan, J.K., et al., *Low-dose TNF augments fracture healing in normal and osteoporotic bone by up-regulating the innate immune response.* EMBO Mol Med, 2015. **7**(5): p. 547-61.
452. Bergenstock, M., et al., *A comparison between the effects of acetaminophen and celecoxib on bone fracture healing in rats.* J Orthop Trauma, 2005. **19**(10): p. 717-23.
453. Vuolteenaho, K., T. Moilanen, and E. Moilanen, *Non-steroidal anti-inflammatory drugs, cyclooxygenase-2 and the bone healing process.* Basic Clin Pharmacol Toxicol, 2008. **102**(1): p. 10-4.
454. Gerstenfeld, L.C., et al., *Differential inhibition of fracture healing by non-selective and cyclooxygenase-2 selective non-steroidal anti-inflammatory drugs.* J Orthop Res, 2003. **21**(4): p. 670-5.
455. Sivaganesan, A., et al., *The effect of NSAIDs on spinal fusion: a cross-disciplinary review of biochemical, animal, and human studies.* Eur Spine J, 2017.
456. Geusens, P., et al., *NSAIDs and fracture healing.* Curr Opin Rheumatol, 2013. **25**(4): p. 524-31.
457. Goodman, S.B., et al., *Temporal effects of a COX-2-selective NSAID on bone ingrowth.* J Biomed Mater Res A, 2005. **72**(3): p. 279-87.
458. Mountziaris, P.M., et al., *Harnessing and modulating inflammation in strategies for bone regeneration.* Tissue Eng Part B Rev, 2011. **17**(6): p. 393-402.
459. Dixit, M., et al., *Functional block of IL-17 cytokine promotes bone healing by augmenting FOXO1 and ATF4 activity in cortical bone defect model.* Osteoporos Int, 2017. **28**(7): p. 2207-2220.
460. Zhu, Y., et al., *Incidence and risks for surgical site infection after adult tibial plateau fractures treated by ORIF: a prospective multicentre study.* Int Wound J, 2017.
461. Veldhoen, M., *Interleukin 17 is a chief orchestrator of immunity.* Nat Immunol, 2017. **18**(6): p. 612-621.
462. Mancini, F., et al., *One Dose of Staphylococcus aureus 4C-Staph Vaccine Formulated with a Novel TLR7-Dependent Adjuvant Rapidly Protects Mice through Antibodies, Effector CD4+ T Cells, and IL-17A.* PLoS One, 2016. **11**(1): p. e0147767.
463. Fillerova, R., et al., *Excellent diagnostic characteristics for ultra-fast gene profiling of DEFA1-IL1B-LTF in the detection of prosthetic joint infections.* J Clin Microbiol, 2017.
464. Tleyjeh, I.M., et al., *The association between histamine 2 receptor antagonist use and Clostridium difficile infection: a systematic review and meta-analysis.* PLoS One, 2013. **8**(3): p. e56498.
465. O'Keefe, G.E., L.M. Gentilello, and R.V. Maier, *Incidence of infectious complications associated with the use of histamine2-receptor antagonists in critically ill trauma patients.* Ann Surg, 1998. **227**(1): p. 120-5.
466. Strunk, T., et al., *Method of bacterial killing differentially affects the human innate immune response to Staphylococcus epidermidis.* Innate Immun, 2011. **17**(6): p. 508-16.
467. Johansen, P., et al., *Lympho-geographical concepts in vaccine delivery.* J Control Release, 2010. **148**(1): p. 56-62.
468. Byrd, A.L., et al., *Staphylococcus aureus and Staphylococcus epidermidis strain diversity underlying pediatric atopic dermatitis.* Sci Transl Med, 2017. **9**(397).

# 9. Curriculum Vitae

Family name, name: SABATÉ BRESCÓ, Marina
Date of birth: 2nd October 1986
Nationality: Spanish

**Education**

| | |
|---|---|
| 2013 – 2017 | ***PhD student*** at AO Research Institute Davos (ARI) and Swiss Institute of Allergy and Asthma Research (SIAF), Davos, University of Zürich, CH<br>PhD project: Role of Implant Stability and Local Inflammatory Responses on the Development and Progression of Infection Associated with Internal Fixation Devices.<br>Supervisors: Dr. T. Fintan Moriarty (ARI) and Dr. Liam O'Mahony (SIAF) |
| 2011 – 2012 | ***Master of Science*** in Immunology (Immunomedicine) at Universitat de Barcelona and Universitat Autònoma de Barcelona. Graduated with Honours.<br>Master thesis project: Study of CD4+ T lymphocyte subsets involved in chronic rejection of heart transplanted patients.<br>Supervisor: Prof. Carme Gelpí Sabater. Institut de Recerca Sant Pau, Barcelona, SP |
| 2004 – 2009 | ***Bachelor*** in Biology (Biomedical speciality) at Universitat de Barcelona<br>Course 2007-2008 in Aarhus Universitet (DK) with an Erasmus Mundus Scholarship. Internship in Dr. Thomas Vorup-Jensen laboratory. |

**Professional experience**

| | |
|---|---|
| 10/2009 – 10/2010 | ***Superior Lab Technician*** at IMIM-Hospital del Mar, Barcelona, SP<br>1-year contract as a superior lab technician in the research group of "Molecular mechanisms of lung cancer predisposition" lead by Dr. Esther Barreiro Portela. |

**Courses and workshops**

- **Immunology Lectures**
  Fall semester 2013 – Spring semester 2014
  Swiss Institute of Allergy and Asthma Research, Davos

- **Workshop: Animal models in bone regeneration research**
  26th – 27th September 2013
  AO Research Institute Davos, Davos

- **Bacterial biofilms and their role in chronic infections**
  November 2013.
  University of Copenhagen. On-line course

- **MIM Introductory Course**
  13th – 17th January 2014
  MIM PhD Programm (UZH/ETH), Zürich

- **Scanning Electron Microscopy Course**
  15th – 16th September 2014
  AO Research Institute Davos and University of Wales, Davos

- **Scientific Writing in the Sciences and Medicine**
  October 2014
  LSZGS, Zürich

- **Time and Self-Management**
  March 2015
  LSZGS, Zürich

- **Practical Statistics for Biology/Medical Research**
  6th – 7th June 2016
  Swiss Institute of Allergy and Asthma Research, Davos

---

| **Journal Clubs in SIAF/AO:** | **Progress Reports in SIAF/AO:** |
|---|---|
| 11.11.2013 (SIAF) | 11.12.2013 (SIAF) |
| 05.06.2014 (AO) | 28.01.2014 (AO) |
| 17.12.2014 (SIAF) | 20.05.2014 (SIAF) |
| 04.06.2015 (AO) | 23.09.2014 (SIAF) |
| 23.06.2015 (SIAF) | 03.03.2015 (AO) |
| 14.07.2015 (AO) | 31.03.2015 (SIAF) |
| 06.10.2015 (SIAF) | 01.09.2015 (SIAF) |
| 20.04.2016 (SIAF) | 01.03.2016 (SIAF) |
| 25.10.2016 (SIAF) | 27.09.2016 (SIAF) |
| 11.04.2017 (SIAF) | 05.04.2017 (AO) |
| | 28.02.2017 (SIAF) |

---

**Retreats and winter schools**

**7th MIM Retreat**
4th – 6th September 2014
Wildhaus, CH

**Immunology Winter School**
26th – 29th January 2017
Sierra Nevada, SP

**Conferences**

Sabaté Brescó, Marina, Berset, Corina, Zeiter, Stephan, Richards, R. Geoff, O'Mahony, Liam, Moriarty, T. Fintan
*Staphylococcus epidermidis* infection progression and associated immune response in a murine fracture model: role of biomechanical stability (oral presentation)
40th Congress of the Spanish Society of Immunology, 25th – 27th May 2017, Zaragoza (SP)

Sabaté Brescó, Marina; Berset, Corina; Kluge, Katharina; Richards, Geoff; O'Mahony, Liam; Moriarty, Fintan
Immune responses in a murine device-related infection model: role of IL-17A (oral presentation)
X Catalan Society of Immunology Congress, 17th–18th November 2016, Barcelona (SP)

Sabaté Brescó, M.; Berset, C.; Kluge, K.; Richards, R.G.; O'Mahony, L.; Moriarty, T.F.
Immune responses in a murine device-related infection model (poster)
Graubünden Forscht: Young scientist in contest, 14th – 15th September 2014, Davos (CH)

Sabaté Brescó, M.; Kluge, K.; Ziegler, M.; Richards, R.G.; Moriarty, T.F.; O' Mahony, L.
Immune response during bone healing in a murine fracture model with osteomyelitis: role of biomechanical stability (poster)
World Immune Regulation Meeting X, 16th – 19th March 2016, Davos (CH)

Sabaté Brescó, M., Kluge, K., Ziegler. M., Richards, R.G., O'Mahony, L., Moriarty, T.F.
The role of biomechanical stability on *Staphylococcus epidermidis* osteomyelitis in a murine fracture model (oral)
eCM 2015; 30(suppl. 2): 30

Sabaté Brescó, M.; Kluge, K.; Ziegler, M.; Nowicki, B.; Richards, R.G.; O'Mahony, L.; Moriarty, T.F.
*Staphylococcus epidermidis* infection progression and associated immune response in a murine fracture model: role of biomechanical stability (poster)
16th EFORT Congress, 17th– 19th May 2015, Prague (CZ)

Sabaté Brescó, M.; Kluge, K.; Ziegler, M.; Richards, R.G.; Moriarty, T.F.; O' Mahony, L.
Immune response during bone healing in a murine fracture model with osteomyelitis: role of biomechanical stability (oral)
World Immune Regulation Meeting IX, 18th – 21st March 2015, Davos (CH)

Sabaté Brescó, M., Kluge, K., Ziegler, M., Richards, R.G., O'Mahony, L., Moriarty, T.F.
Assessing the role of implant stability on the development of staphylococcal osteomyelitis in a murine fracture model (oral)
Graubünden Forscht: Young scientist in contest, 10th – 11th September 2014, Davos (CH)

Sabaté Brescó, M., Kluge, K., Ziegler, M., Richards, R.G., O'Mahony, L., Moriarty, T.F.
Immune response during bone healing in a murine fracture model with osteomyelitis: role of biomechanical stability (poster)
5th International Conference on Osteoimmunology, 15th – 20th June 2014, Kos (GR)

Rochford, E.T., Sabaté Brescó, M., Ziegler, M., O'Mahoney, L., Moriarty, T.F.
Assessing the role of implant associated immune responses on the development of infection (oral)
Bone Joint J. 2014; 96B (suppl.11): 282

---

**Awards and grants**

Student travel award for poster presentation
5th International Conference on Osteoimmunology, 15th – 20th June 2014, Kos (GR)

Award for best oral presentation in Clinical Sciences category
Graubünden Forscht: Young scientist in contest, 10th – 11th September 2014, Davos (CH)

Award for best poster presentation in Clinical Sciences category
Graubünden Forscht: Young scientist in contest, 14th – 15th September 2014, Davos (CH)

Student travel grant
40th Congress of the Spanish Society of Immunology, 25th – 27th May 2017, Zaragoza (SP)

**Publications**

Sabaté Brescó M, O'Mahony L, Zeiter S, Kluge K, Ziegler M, Berset C, Nehrbass D, Richards RG, Moriarty TF. Influence of Fracture Stability on *Staphylococcus epidermidis* and *S. aureus* Infection in a Murine Femoral Fracture Model.
**Eur Cell Mater.**, 2017 Nov 21; 34:321-340. PMID: 29160896

Sabaté Brescó M, Harris LL, Thompson K, Stanic B, Morgenstern M,O'Mahony L, Richards RG, Moriarty TF. Pathogenic Mechanisms and Host Interactions in *Staphylococcus epidermidis* Device-Related Infection.
**Frontiers in Microbiology**. 2017 Aug 2, 8:1401. PMID: 28824556

Ausín P, Martínez-Llorens J, Sabaté-Bresco M, Casadevall C, Barreiro E, Gea J. Sex differences in function and structure of the quadriceps muscle in chronic obstructive pulmonary disease patients.
**Chron Respir Dis.** 2017 May; 14(2):127-139. PMID: 27923983

Rochford ET, Sabaté Brescó M, Zeiter S, Kluge K, Poulsson A, Ziegler M, Richards RG, O'Mahony L, Moriarty TF. Monitoring immune responses in a mouse model of fracture fixation with and without *Staphylococcus aureus* osteomyelitis.
**Bone.** 2016 Feb; 83:82-92. PMID: 26525592

Domínguez-Álvarez M, Sabaté-Brescó M, Vilà-Ubach M, Gáldiz JB, Alvarez FJ, Casadevall C, Gea J, Barreiro E. Molecular and physiological events in respiratory muscles and blood of rats exposed to inspiratory threshold loading.
**Transl. Res.** 2014 May; 163(5):478-93. PMID: 24373863